

Distribution Category:  
Physics--General  
(UC-34)

ANL--86-22

DE87 002350

ANL-86-22

ARGONNE NATIONAL LABORATORY  
9700 South Cass Avenue  
Argonne, Illinois 60439

**PHYSICS DIVISION ANNUAL REVIEW**

1 April 1985--31 March 1986

Donald S. Gemmell  
Division Director

September 1986

Preceding Annual Reviews

ANL-83-25	1982--1983
ANL-84-24	1983--1984
ANL-85-22	1984--1985

This report was prepared as an account of work sponsored by an agency of the United States Government. Neither the United States Government nor any agency thereof, nor any of their employees, makes any warranty, express or implied, or assumes any legal liability or responsibility for the accuracy, completeness, or usefulness of any information, apparatus, product, or process disclosed, or represents that its use would not infringe privately owned rights. Reference herein to any specific commercial product, process, or service by trade name, trademark, manufacturer, or otherwise does not necessarily constitute or imply its endorsement, recommendation, or favoring by the United States Government or any agency thereof. The views and opinions of authors expressed herein do not necessarily state or reflect those of the United States Government or any agency thereof.

**DISCLAIMER**

**MASTER**

# **LEGIBILITY NOTICE**

A major purpose of the Technical Information Center is to provide the broadest dissemination possible of information contained in DOE's Research and Development Reports to business, industry, the academic community, and federal, state and local governments.

Although a small portion of this report is not reproducible, it is being made available to expedite the availability of information on the research discussed herein.

## FOREWORD

The Physics Division Annual Review presents a broad but necessarily incomplete view of the research activities within the Division for the year ending in March 1986.

At the back of this report a complete list of publications along with the Division roster can be found.

# NUCLEAR PHYSICS RESEARCH

	<u>Page</u>
Introduction.....	1
<b>I. <u>MEDIUM-ENERGY PHYSICS RESEARCH</u>.....</b>	<b>3</b>
<b>A. NON-NUCLEONIC EFFECTS IN NUCLEI.....</b>	<b>5</b>
a. Deep Inelastic Muon Scattering from Nuclei with Hadron Detection.....	6
b. Electron-Deuteron Scattering with a Polarized Deuterium Gas Target in and Electron Storage Ring.....	10
c. Electroproduction of the Delta Isobar in Nuclei.....	12
d. Pion Electroproduction in Deuterium.....	13
e. Study of Pion Absorption in $^3\text{He}$ through the $(\pi^+, 2p)$ and $(\pi^-, pn)$ Reactions.....	14
f. The A-Dependence of the $(e, e'p)$ Reaction in the Quasifree Region.....	16
g. Study of Correlations Between Light Nuclear Fragments and the Scattered Projectile with 300-MeV Protons.....	17
h. Light Fragment Emission in Pion-Nucleus Reactions.....	18
i. Focal-Plane Detector for 1.6-GeV Spectrometer at SLAC.....	19
j. Data-Acquisition System for SLAC Experiments.....	20
k. Review Article on Pion Absorption.....	20
<b>B. INTERMEDIATE AND RELATIVISTIC HEAVY ION PHYSICS.....</b>	<b>21</b>
a. Fission and Charged Particle Emission in Nucleus-Nucleus Collisions at Intermediate Energy.....	22
<b>C. WEAK INTERACTIONS.....</b>	<b>23</b>
a. Neutrino Oscillations at LAMPF.....	24
b. Neutron Beta Decay.....	28
c. The Vector Weak Coupling and $^{10}\text{C}$ Superallowed Beta Decay.....	30

d.	Beta Decay of Polarized Nuclei and the Decay Asymmetry of $^8\text{Li}$ .....	31
e.	The $\beta$ -decay Spectrum in the $A=8$ System and the Solar Neutrino Problem.....	32
f.	Weak Magnetism Effects in Beta Spectra.....	34
g.	Beta Spectra Following the Spontaneous Fission of $^{252}\text{Cf}$ ....	34
h.	Search for a Light-Scalar Boson Emitted in Nuclear Decay...	35
i.	Measurement of the Electric Dipole Moment of the Neutron...	36
D.	NUCLEAR STRUCTURE STUDIES	
a.	Inelastic Scattering of Pions by $^{10}\text{B}$ and $^{11}\text{B}$ .....	40
b.	Isoscalar Quenching in the Excitation of $8^-$ States in $^{52}\text{Cr}$ .....	40
c.	Excitation of $8^-$ States in $^{52}\text{Cr}$ .....	41
II.	<u>RESEARCH AT ATLAS</u> .....	43
A.	QUASIELASTIC PROCESSES AND STRONGLY DAMPED COLLISIONS.....	45
a.	Quasielastic Processes in Si-Induced Reactions on Pb.....	46
b.	Quasielastic Processes in the $^{28}\text{Si} + ^{40}\text{Ca}$ Reaction at 225 MeV.....	47
c.	Study of Transfer Reactions in the System $^{58}\text{Ni} + ^{208}\text{Pb}$ at High Incident Energies.....	48
d.	Quasi- and Deep-Inelastic Reactions Studied in the System $^{80}\text{Se} + ^{208}\text{Pb}$ .....	50
e.	Study of Neutron Transfer Cross Sections for Ni + Ni Systems Below the Coulomb Barrier.....	50
f.	Elastic Scattering, Quasielastic and Total Reaction Cross Sections Near the Barrier for $^{58}\text{Ni} + \text{Sn}$ .....	52
g.	Quasielastic Transfer for $^{58,64}\text{Ni}$ -Induced Reactions on Even-A Tin Isotopes Well Above the Barrier.....	53
h.	A Random-Walk Model for the Transition from Quasielastic to Deep-inelastic Collisions.....	55

i.	Proximity Effects in Deep-Inelastic Collisions in the Reactions of $^{32}\text{S}$ with $^{58}\text{Ni}$ .....	57
j.	Systematics of Neutron Transfer Cross Sections in Heavy Systems.....	58
B.	FUSION AND FISSION OF HEAVY IONS.....	61
a.	Fusion Evaporation Residues and the Distribution of Reaction Strength in $^{16}\text{O} + ^{40}\text{Ca}$ and $^{28}\text{Si} + ^{28}\text{Si}$ Reactions.....	63
b.	Time-of-Flight Measurements of Evaporation Residues from $^{32}\text{S} + ^{24}\text{Mg}$ .....	64
c.	Incomplete Fusion at 10 MeV/Nucleon in Heavy Asymmetric System: $^{12}\text{C} + \text{A}(100-200)$ .....	65
d.	Light Particle Emission in Reactions Induced by $E/A > 10$ MeV/Nucleon.....	67
e.	Production of Very High Energy Light Particles in Heavy-ion Collisions at Zero Degrees.....	71
f.	Fusion of $^{78}\text{Se} + ^{78}\text{Se}$ and $^{82}\text{Se} + ^{82}\text{Se}$ .....	72
g.	Evaporation Residue Cross Sections in Fusion of $^{64}\text{Ni} + ^{92}\text{Zr}$ and $^{12}\text{C} + ^{144}\text{Sm}$ .....	73
h.	Total Fusion Cross Sections for $\text{Ni} + \text{Sn}$ .....	76
i.	Status Report on $^{24}\text{Mg} + ^{24}\text{Mg}$ Fusion.....	78
j.	Fission-like Yields in the $^{16}\text{O} + ^{40,44}\text{Ca}$ Reactions.....	79
k.	Evidence for Asymmetric Fission in the $^{32}\text{S} + ^{24}\text{Mg}$ Reaction.....	81
l.	Study of Fission Fragments from the Reaction $^{32}\text{S} + ^{182}\text{W}$ .....	83
m.	Experimental Study of the Reaction $^{60}\text{Ni} + ^{154}\text{Sm}$ .....	85
n.	Kinematic Coincidence Studies of the $^{127}\text{I} + ^{87}\text{Rb}$ Reaction.....	85
o.	Characteristic Time for Mass Asymmetry Relaxation in Quasifission Reactions.....	86
p.	Complete Fusion of $^{238}\text{U}$ and $^{48}\text{Ca}$ ; Prospects for Superheavy Element Synthesis.....	88

C.	HIGH ANGULAR MOMENTUM STATES IN NUCLEI.....	91
a.	Entrance-channel Dependence in the Decay of $^{156}\text{Er}$ .....	92
b.	Total $\gamma$ -Spectrum from $^{153}\text{Ho}$ Measured with BGO Compton-Suppressed Spectrometers.....	95
c.	Lifetimes of Very High Spin States in $^{147}\text{Gd}$ .....	97
d.	The Study of High Spin States in $^{155}\text{Ho}$ .....	98
e.	Recoil Distance Lifetime Measurements in $^{184}\text{Pt}$ .....	100
f.	Shell-Model States Around $N=82$ .....	103
g.	Feasibility Studies on Using Multiple Compton- Suppressed Ge Detectors to Search for Neutrinoless Double- $\beta$ Decay in $^{76}\text{Ge}$ .....	105
h.	High-Spin Structure of $^{153,154}\text{Dy}$ --First Experiment with the BGO $\gamma$ -Ray Facility.....	106
i.	Lifetimes of Very High Spin States in $^{156}\text{Dy}$ Through DSAM.....	108
j.	Structure and Lifetimes of Continuum States in $^{152}\text{Dy}$ .....	109
D.	HEAVY-ION RESONANCES.....	113
a.	Analysis of the $E_{\text{cm}} = 45.65\text{-MeV}$ $^{24}\text{Mg} + ^{24}\text{Mg}$ .....	114
b.	Search for Shape Isomers in $^{56}\text{Ni}$ .....	116
c.	Elastic and Inelastic Scattering of the $^{28}\text{Si} + ^{28}\text{Si}$ System.....	118
E.	ACCELERATOR MASS SPECTROMETRY (AMS).....	119
a.	AMS of $^{60}\text{Fe}$ at Low Concentrations.....	120
b.	Accelerator Mass Spectrometry of $^{205}\text{Pb}$ and Its Application of Solar Neutrino Detection.....	122
c.	$^{41}\text{Ca}$ -radioisotope Concentration in Natural Samples of Terrestrial Origin.....	124
F.	OTHER TOPICS.....	127
a.	Cluster Decay of $^{241}\text{Am}$ .....	128

b.	Electron-Capture Decay Branching Ratio of $^{81m}\text{Kr}$ .....	130
c.	El Matrix Elements and the Test of the Octupole Deformation Model in $^{225}\text{Ra}$ .....	132
d.	Measurement of Rates of Fast El Transitions in Ac-Ra Nuclei.....	133
e.	Exploration of the Possibility of a Condensed Crystalline State in Heavy-Ion Beams.....	135
f.	Search for Positron Resonances in the Interaction of Positrons with Electrons.....	137
G.	EQUIPMENT DEVELOPMENT AT THE ATLAS FACILITY.....	139
a.	Detector Development Laboratory.....	140
b.	Development of Large-Area Position-Sensitive Timing Detectors.....	141
c.	Development Work on a Large Bragg-Curve Spectrometer.....	142
d.	Development of a Position Sensitive Timing Detector for the Split-Pole Magnetic Spectrograph.....	144
e.	Development of NaI(Tl) Charged Particle Detectors.....	144
f.	Room Temperature Electron Detector.....	148
g.	Superconducting Solenoid Lens Electron Spectrometer.....	150
h.	Development and Testing of an Air-Core Superconducting Solenoid for Measurements on the Linac.....	151
i.	The Split-Pole Spectrograph in the New ATLAS Target Room.....	152
j.	Nuclear Charge and Isobar Separation in the Gas-Filled Enge Split-Pole Magnetic Spectrograph.....	153
k.	Construction of a Gamma-Ray Facility for ATLAS.....	1545
l.	Results from the BGO Compton-Suppression Shields for the $\gamma$ -ray Facility at ATLAS.....	157
m.	Tests of Prototype Hexagon BGO Detectors for the Inner Array of the $\gamma$ -ray Facility for ATLAS.....	158
n.	Design and Construction of a Scattering Chamber Facility for ATLAS.....	159



o.	Process Control System for the Scattering Facility at ATLAS.....	160
p.	Nuclear Target Making and Development.....	161
q.	Physics Division Computer Facilities.....	162
r.	The Data-Acquisition System DAPHNE.....	164
<b>III.</b>	<b><u>THEORETICAL NUCLEAR PHYSICS</u></b> .....	<b>165</b>
<b>A.</b>	<b>NUCLEAR FORCES AND SUBNUCLEON DEGREES OF FREEDOM</b> .....	<b>166</b>
a.	Nuclear Effects in Deep-Inelastic Lepton Scattering.....	168
b.	Variational Monte Carlo Calculations of Few-Body Nuclei...169	
c.	Coupled Cluster and Variational Calculations of Nuclear Matter.....	172
d.	Electromagnetic Form Factors of the Deuteron.....	174
e.	Relativistic Effects in Three-Body Nuclei.....	175
f.	Relativistic Effects in Nuclear Many-Body Systems.....	176
g.	Implications of Dirac Nucleon Dynamics for the Binding of Light Nuclei.....	177
h.	Quark Models of Hadron Interactions.....	178
<b>B.</b>	<b>INTERMEDIATE ENERGY PHYSICS</b> .....	<b>179</b>
a.	Theory of Mesonic and Dibaryonic Excitations in the $\pi NN$ System.....	180
b.	Unitary Study of $NN$ and $\pi d$ Scattering Based on Meson-Exchange Model.....	181
c.	Unitary Calculation of $NN \rightarrow NN\pi$ .....	184
d.	Study of Quark Dynamics in $NN \rightarrow N\Delta$ Transition.....	186
e.	Electromagnetic Interaction with the Deuteron Above the Pion Production Threshold.....	187
f.	Effects of $\pi\pi$ Correlations in $\pi N$ Scattering.....	188
g.	The Strange Quark Mass in a Chiral $SU(3)$ Bag Model.....	190

h.	Study of the Two-Nucleon Mechanism of Pion Absorption in Nuclei.....	192
i.	Mechanism of ${}^3\text{He}(\pi^-, pn)$ Reaction.....	193
j.	Calculation of Landau Parameters for the $\Delta$ -hole Interaction.....	194
k.	Nuclear Structure in the $(p, \pi^+)$ Reaction.....	195
l.	Quasielastic Proton-Nucleus Scattering at 300-800 MeV.....	196
m.	Delta Excitations in Heavy Nuclei Induced by Charge Exchange Reactions.....	198
n.	Continuum Polarization Transfer in Proton-Nucleus Scattering.....	200
o.	The $(p, n)$ Reaction and the Nucleon-Nucleon Force.....	202
p.	The Classical Limit of the Surface Response in Fermi Liquids.....	202
C.	HEAVY-ION INTERACTIONS	
a.	A Coupled-Channels Analysis of Silicon-Nickel Fusion Reactions.....	204
b.	On the Nuclear Polarization Potential for Heavy-Ion Scattering.....	206
c.	Coupled-Channel Approach to Heavy-ion Reactions Near the Coulomb Barrier.....	208
d.	Conversion of Ptolemy to the ER Cray.....	208
D.	QUANTUM-MECHANICAL VARIATIONAL CALCULATIONS OF FINITE MANY-BODY SYSTEMS.....	209
a.	Elementary Excitations of Liquid ${}^4\text{He}$ Drops.....	210
b.	Variational Monte Carlo Calculations of ${}^3\text{He}$ Drops.....	213

E.	NUCLEAR STRUCTURE STUDIES IN DEFORMED TRANSITIONAL NUCLIDES.....	217
a.	$\gamma$ -Deformation in a Reflection Asymmetric Single-Particle Potential.....	218
b.	Many-Body Treatment of Quadrupole and Octupole Correlations in Nuclei.....	218
c.	Incipient Octupole and $2^6$ -Pole Deformation in the Mass Region $220 < A < 230$ .....	219
d.	Octupole Correlations in $^{227}\text{Ac}$ .....	220
e.	Spectroscopic Studies of $^{225}\text{Ra}$ .....	220
F.	BINDING ENERGIES OF HYPERNUCLEI AND $A$ -NUCLEAR INTERACTIONS.....	221
a.	Binding Energies of Hypernuclei and 3-body $\text{ANN}$ Forces.....	222
b.	Coulomb Effects and Charge Symmetry Breaking for the $A=4$ Hypernuclei.....	223
c.	Alpha-Cluster Calculations of $^9_{\Lambda}\text{Be}$ .....	223
G.	OTHER THEORETICAL PHYSICS.....	225
a.	Magnetic Monopoles and Dipoles in Quantum Mechanics.....	225
b.	The Spins of Cyons and Dyons.....	226
c.	Saddle-Point Variational Method for the Dirac Equation.....	228
d.	High-Spin States in $^{97}_{45}\text{Rh}$ .....	229
IV.	<u>SUPERCONDUCTING LINAC DEVELOPMENT</u> .....	231
A.	THE ATLAS PROJECT.....	231
	1. Completion of ATLAS.....	231
	2. Refinement of ATLAS Technology.....	231
B.	THE POSITIVE-ION INJECTOR.....	233
	1. Description of the Positive-Ion Injector.....	233
	2. Tests of the 4-gap 10-cm Accelerating Structure.....	236
	3. Estimates of Performance.....	238
C.	SUPERCONDUCTING MAGNETS.....	241
	1. Dual-beam Capability.....	241
	2. Superconducting Switch Magnet.....	241

V. <u>ACCELERATOR OPERATIONS</u> .....	243
A. OPERATION OF ATLAS.....	245
1. Summary of Operations.....	245
2. Completion of the ATLAS Project.....	248
3. Status of ATLAS.....	249
4. Plans for 1987.....	251
5. Plans for 1988.....	253
6. Assistance to Outside Users of ATLAS.....	254
B. OPERATION OF THE DYNAMITRON FACILITY.....	264
1. Future Developments at the Dynamitron.....	266
2. Operational Experience of the Dynamitron.....	267
3. University Use of the Dynamitron.....	270

# ATOMIC AND MOLECULAR PHYSICS RESEARCH

	<u>Page</u>
Introduction .....	273
<b>VI.     <u>PHOTOIONIZATION-PHOTOELECTRON RESEARCH</u></b> .....	<b>275</b>
a.   Photoionization of the NH <sub>2</sub> Radical.....	276
b.   Photoionization Mass Spectrometric Study and ab initio Calculations of Ionization and Bonding in P-H Compounds; Heats of Formation, Bond Energies, and the <sup>3</sup> B <sub>1</sub> - <sup>1</sup> A <sub>1</sub> Separation in PH <sub>2</sub> <sup>+</sup> .....	278
c.   Bond energies of Nitrogen and Phosphorus Hydrides and Fluorides.....	279
d.   Autoionization in Molecules-a Path Toward Better Understanding.....	280
e.   Photoionization of Atomic Sulfur.....	281
f.   Photoionization of Atomic Selenium.....	283
g.   UV Laser Photodissociation of Molecular Ions.....	283
<b>VII.    <u>HIGH-RESOLUTION LASER-rf SPECTROSCOPY WITH ATOMIC AND           MOLECULAR BEAMS</u></b> .....	<b>285</b>
a.   Electric-dipole Moments in CaI and CaF by Molecular-beam Laser-rf Double-resonance Study of Stark Splittings.....	286
b.   Hyperfine Structure of Excited 4f <sup>11</sup> 5d6s <sup>2</sup> Levels in <sup>167</sup> Er I: Measurements and MCDF Calculations.....	286
c.   High-precision Laser and rf Spectroscopy of the Spin-rotation and hfs Interactions in the X <sup>2</sup> Σ <sup>+</sup> and B <sup>2</sup> Σ States of LaO.....	287
d.   Extension of Molecular-beam hfs Studies into Rare-earth Monohalides: Hfs of PrO.....	290
e.   Hfs of Even-parity Levels in <sup>139</sup> La: Theory and Experiment.....	290
f.   Apparatus for Collinear Laser Spectroscopy of Slow Atomic and Molecular Ions.....	291

<b>VIII.</b>	<b><u>BEAM-FOIL RESEARCH, ION-BEAM/LASER RESEARCH, AND COLLISION DYNAMICS OF HEAVY IONS</u></b> .....	293
	a. Fast Ion-Beam Laser Interactions.....	294
	b. Alignment and Orientation Production in Hydrogenic States.....	295
	c. Precision Measurements of the $1s2s^3S - 1s2p^3P$ Transitions.....	296
	d. Autoionization of Helium Following Excitation by Fast, Multiply-Charged Ions.....	296
	e. Accurate Transition Probabilities for the Resonance Transitions in Na- and Mg-like Ar.....	297
	f. Extended Analysis of the $2p^53s, 3p$ and $3d$ Configurations in Ne-like Argon (Ar IX).....	299
	g. Lamb Shifts and Fine Structures of $n = 2$ in Helium-like Ions.....	301
<b>IX.</b>	<b><u>INTERACTIONS OF FAST-ATOMIC AND MOLECULAR IONS WITH SOLID AND GASEOUS TARGETS</u></b> .....	303
	a. Development of a Multiparticle Imaging Detector.....	304
	b. Enhanced Electron Capture by Fast Heavy Di-clusters Exiting Solids.....	306
	c. Charge-state-distributions of Foil-excited Heavy Rydberg Atoms.....	310
	d. Observation of Electron Density Fluctuations Induced in Solids.....	311
<b>X.</b>	<b><u>THEORETICAL ATOMIC PHYSICS</u></b> .....	313
<b>XI.</b>	<b><u>ATOMIC PHYSICS AT ATLAS</u></b> .....	315
	a. Doppler-free Auger Electron Spectroscopy from Ne-like and Na-like High-Z Atoms.....	316
	b. Recoil Gas Spectroscopy.....	317
	c. Heavy-ion-induced Desorption of Molecules.....	320

d. Resonant Transfer and Excitation for  
Highly-charged Ions.....322

e. Radiation Chemistry Studies with Heavy Ions.....324

f. Accelerator Development.....326

**STAFF MEMBERS OF THE PHYSICS DIVISION.....327**

**PUBLICATIONS FROM 1 APRIL 1985 TO 31 MARCH 1986.....337**

# NUCLEAR PHYSICS RESEARCH

## Introduction

The highlight of the Argonne Physics Division during the past year (1985/86) has been the completion and dedication of the final superconducting linac stages of the ATLAS system and the beginning of the research program that utilizes the full capabilities of that system. The transition to using the full ATLAS and the new experimental area has been a smooth one and the research program is beginning to bear fruit.

The experimental facilities have also come into operation with three major components, consisting of the first stage of a gamma detection system incorporating an array of Compton-suppressed germanium detectors and BGO total energy detectors, a magnetic spectrograph of the Enge split-pole design, with a focal-plane detector system adapted to heavy ions, and a new scattering facility with a number of features. Interesting new data are emerging on quasi-elastic processes, on the transition between fission and quasi-fission and the study of nuclear structure at high spin.

The past year has also seen the merging of the nuclear research in the Argonne Chemistry Division, mostly in heavy-ion and medium-energy nuclear physics, with the Physics Division. The merger is leading to full cooperation within the larger group and will help broaden and strengthen the total effort in nuclear physics.

In medium-energy physics the year has seen the successful execution of an experiment at the SLAC NPAS station to study the delta resonance in nuclei. Progress is being made in the effort at Fermilab on deep inelastic muon scattering, on the development of a tensor polarized gas deuterium target for use with storage rings, and on the LAMPF neutrino oscillation experiment.

In theoretical nuclear physics an effort is continuing on investigating the relevant degrees of freedom in the microscopic dynamics of nuclei and the importance of three-body forces. Work has focussed especially on investigating the pionic and delta degrees of freedom in describing the dynamics of intermediate energy processes. And in the heavy-ion field the effects of coupled channels in heavy-ion reactions, especially near the Coulomb barrier, are being investigated.



## I. MEDIUM-ENERGY PHYSICS RESEARCH

### INTRODUCTION

The major components of the medium-energy physics program center around (i) the use of leptonic probes to study nuclei beyond the nucleons-only regime, and (ii) weak-interaction physics studied both in nuclei and with the neutrino beam at LAMPF. A substantial fraction of available resources and manpower was devoted to the development of new instrumentation required to pursue new directions in this area. Members of the Argonne group in a collaborative effort at Fermilab moved the deep-inelastic muon experiment closer to fruition. The Argonne group played a key role in tests of approximately 70% of the detectors and of the new muon beam line by managing the development of the data-acquisition system. In addition, great strides were made in detector development for the experiment at the new Nuclear Physics Injector at SLAC to study the delta resonance in nuclei being carried out during the last year. Moreover, progress was made towards the test of the spin-exchange optical-pumping scheme as a means for providing polarized gas targets for electron-scattering studies in storage rings. The experiment at LAMPF designed to detect neutrino oscillations should begin during the next LAMPF cycle. The active shield, Argonne's primary responsibility, has been completed and is undergoing tests. During the past year the Medium-Energy Programs in the Physics and Chemistry Divisions at ANL were consolidated into one group in the Physics Division. This merger has brought to the Medium-Energy Group in the Physics Division an interest in the issues of relativistic heavy-ion physics. The program is severely limited at present by the availability of technical manpower and the sharply-reduced number of postdoctoral research associates, (the latter caused by a combination of attrition and the extremely tight budget.) Experiments which have been especially undermanned are the muon scattering work and the polarized target development. During the next two years we plan to correct this and propose to increase the number of postdoctorals, add a new person for the internal-target project and one for software development for the Fermilab experiment.

## A. NON-NUCLEONIC EFFECTS IN NUCLEI

The primary intent of these studies is to characterize, as completely as possible, non-nucleonic effects--pion propagation, delta formation and quark degrees of freedom in the nuclear medium. The experiment to observe deep-inelastic muon scattering in coincidence with leading hadrons from both light and heavy nuclei addresses a central issue in nuclear physics, the EMC effect. For this experiment the ANL group has assumed a major responsibility for the on-line data-acquisition software. The most stringent test for QCD effects in nuclei would be a measurement of the polarization in electron-deuteron elastic scattering at high momentum transfer. Here the Argonne medium-energy group in collaboration with members of the atomic physics group is actively engaged in developing a polarized deuterium jet target suitable for use in an electron storage ring. Electroproduction of the delta in nuclei is the only way to produce delta-hole excitations uniformly throughout the nucleus to investigate delta isobar dynamics in the nuclear medium. The ANL group has initiated the first experiment to provide longitudinal and transverse separations of the electro-excitation cross section in the delta region. This experiment will be performed at the Nuclear Physics Facility at SLAC. Pion and delta propagation are also the primary focus of the ( $\pi NN$ ) experiments in  $^3\text{He}$ . These experiments provide crucial information on the pion-absorption mechanism, including the three-body pion-absorption process. An issue important in nuclear physics and closely related to the pion-absorption studies is the question of the nucleon mean free path in nuclei, the subject of a quasifree electron scattering experiment to be performed at the MIT-Bates laboratory.

a. Deep Inelastic Muon Scattering from Nuclei with Hadron Detection

D. F. Geesaman, M. C. Green, M. Adams,\*\* H. Braun,¶¶ H. Brueck,¶¶  
 T. H. Burnett,§§ W. Busza,## G. Coutrakon,|| I. Derado,||| S. Dhawan,\*\*\*  
 V. Eckardt,||| A. Eskreys,‡ W. R. Francis,\* J. Haas,§ C. Halliwell,\*\*  
 V. Hughes,\*\*\* T. B. W. Kirk,||, V. Kistiakowsky,## H.G.E. Kobrak,\*  
 W. Krasny,‡ S. Krzywdzinski,§§ S. Kunori,†† J. J. Lord,§§  
 H. J. Lubatti,§§ P. Malecki,‡ A. Manz,||| S. McHugh,\* D. McLeod,\*\*  
 H. Melanson,|| W. Mohr,§ H. Montgomery,|| J. Morfin,|| K. Moriyasu,§§  
 R. Nickerson,¶ R. Oppenheim,\*\*\* L. Osborne,## A. M. Osborne,† B. Pawlik,‡  
 F. M. Pipkin,¶ R. Pitt,## P. Rapp,†† N. Schmitz,||| P. Schuler,\*\*\*  
 A. Skuja,†† J. Shiers,||| G. Snow,†† P. Steinberg,†† H. E. Stier,§  
 R. W. Swanson,\* A. Weidemann,\* J. Wilkes,§§ R. Wilson,¶ S. Wolbers,|| and  
 G. Wolf,||

Deep inelastic muon scattering from nuclei provided the first convincing evidence that the structure of nucleons is modified in the nuclear medium. This has profound implications on the understanding of nuclear dynamics. Many low-energy nuclear measurements have previously suggested interpretations involving modification of the nucleon structure. However the muon scattering data which are sensitive to the incoherent scattering from the quarks in nuclei can indicate the difference between the quark distribution functions in the free nucleon and in nuclei. The conclusion of these studies was that the distribution of the fraction of the momentum carried by the quarks,  $F(x)$ , is shifted to lower fractional momenta,  $x$ . Theoretical interpretations include a possible rescaling of the nucleon size in nuclear matter or the effect of an enhanced meson field in the nuclear interior.

A new experiment, E665, using the Tevatron II at Fermi National Accelerator Laboratory (Fig. I-1) will provide new information on the nuclear effects on nucleon properties by studying deep inelastic muon scattering with coincident hadron detection. The key features of this experiment are: 1) an

---

\*University of California, San Diego, CA.

†CERN,

‡Institute of Nuclear Physics, Cracow, Poland.

§University of Freiburg, W. Germany.

||Fermi National Accelerator Laboratory, Batavia, IL.

¶Harvard University, Cambridge, MA.

\*\*University of Illinois, Chicago, IL.

††University of Maryland, College Park, Md.

##Massachusetts Institute of Technology, Cambridge, MA.

|||Max-Planck-Institute, Munich, W. Germany.

§§University of Washington, Seattle, WA.

¶¶University of Wuppertal,

\*\*\*Yale University, New Brunswick, N.J.

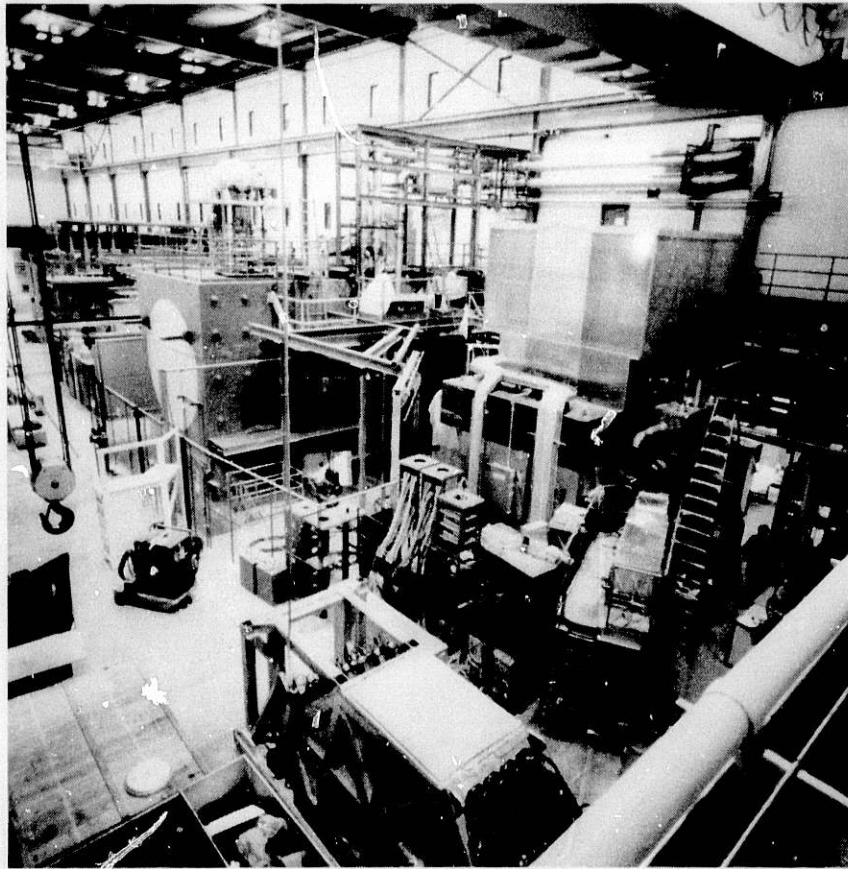


Figure I-1. The spectrometer of the E665 experiment using the Tevatron muon beam which enters from the bottom right. The first major component is the superconducting vertex magnet from the European Muon Collaboration experiment at CERN, and further back the superconducting spectrometer magnet using steel from the old Chicago Cyclotron.

open geometry allowing essentially  $4\pi$ -hadron detection. 2) A streamer chamber vertex detector for low-energy fragments. 3) Two large-field-volume superconducting magnets, with field strengths of 4 T-m and 7 T-m to provide accurate measurements of the muon and hadron momenta. 4) A particle identification system including a ring-imaging Cerenkov counter which can separate pions, kaons and protons from 7.0 GeV/c to 150 GeV/c. 5) A muon beam energy of 600 to 800 GeV, a factor-of-two higher than was previously available. This high beam energy makes the experiment particularly suited to the study of the region of  $x < 0.1$ , where there is little or no data from other measurements.

The hadron detection provides several important new directions for this research. With the excellent particle identification, the flavor dependence of the fragmentation properties of nucleons in nuclei can be studied. This allows the isolation of features of the quark sea from the valence quark distributions. Furthermore, the time required for the struck quarks to form hadrons is sufficiently long that hadronization takes place both inside and outside the nucleus. This permits the study of the propagation of quarks through the nucleus and the effects of the nucleus on the hadronization process.

Argonne is responsible for the management of the on-line software for the experiment. The recent Argonne efforts have concentrated on systematic tests of the system concepts and developing and implementing monitoring strategies and techniques. The most serious issues involve the flow of data between the various machines, including the ability of stand-alone monitoring tasks to communicate with the data stream. A centralized message and error reporting facility is being developed by Argonne. During the year, most of the effort was directed into establishing overall run control for the experiment and in preparing the on-line data analysis. Data will be read in through three front-end PDP 11/34's which will be linked to a micro-VAX II for data concentration and logging to magnetic tape. On-line event analysis will be performed on a VAX 11/780. The data-acquisition software will be based on the FNAL-DA system on the front-end machines and the FNAL VAX-ONLINE system on the concatenation and analysis machines.

During the summer of 1985, the muon beam line was commissioned and the first beam present in the new experimental hall was used for detector

tests. Roughly 70% of the experimental equipment was in place at this time. During the fall of 1985, and the winter and spring of 1986, the rest of the experimental equipment will be brought into operation.

It is expected that limited test beams will be available beginning in September 1986. The experiment is scheduled for 5 months of beam time beginning in December 1986 with a second five-month period beginning in the fall of 1987.

Measurements are planned on targets of hydrogen, deuterium, nitrogen and xenon.

b. Electron-Deuteron Scattering with a Polarized Deuterium Gas Target in an Electron Storage Ring

(R. J. Holt, M. C. Green, L. Young, D. F. Geesaman, L. S. Goodman, R. Kowalczyk, and B. Zeidman)

An estimate of the luminosity that could be achieved for an internal target in the PEP storage ring at SLAC indicates that the internal target method is potentially the most powerful method for the study of electron-deuteron scattering. If this method is indeed feasible, it appears possible to extend the present limit of polarization measurements in e-d scattering from a momentum transfer of  $q^2 = 4.1 \text{ fm}^{-2}$  to  $\sim 40 \text{ fm}^{-2}$ . Polarization measurements in this high-momentum-transfer region are extremely interesting since there has been speculation that QCD effects may be important because helicities are conserved in the QCD picture of the nucleus, but not constrained within the framework of a hadronic model.

To perform these polarization measurements at high momentum transfer it is essential to develop a highly polarized deuterium gas target with a thickness in excess of  $10^{14} \text{ nuclei/cm}^2$ . This target thickness could be maintained in a storage ring provided that a high-flux polarized source could be developed. Tests of a prototype tensor-polarized deuterium gas source, shown in Fig. I-2, are underway. Specifically, the feasibility of employing a spin-exchange optical-pumping method to produce a high flux of polarized deuterium nuclei is being tested. The selection of this technology is based upon the following criteria: (i) potential for very high flux of polarized nuclei ( $>10^{17} \text{ s}^{-1}$ ), (ii) minimum vacuum-pumping load to the electron storage ring and (iii) low magnetic fields ( $\lesssim 10$  gauss) in the target region.

During 1985 the prototype target was installed in the Dynamitron experimental area so that the tensor polarization of a deuterium gas jet from the source could be measured directly with the well-known  $\vec{D}({}^3\text{He}, p){}^4\text{He}$  reaction. The profile of the gas jet is shown in the lower part of the figure and was measured by observing the K atoms with the scanning Re hot wire. During this period the signal-to-background ratio for this analyzing reaction was improved dramatically by modifications to the Dynamitron beam line and increasing the vacuum-pumping speed. In preliminary tests of the prototype we achieved 80 mW of laser power absorbed, which contributed to the spin-exchange process with deuterium. This laser-power absorption would correspond to a

## PROTOTYPE POLARIZED TARGET TEST ASSEMBLY

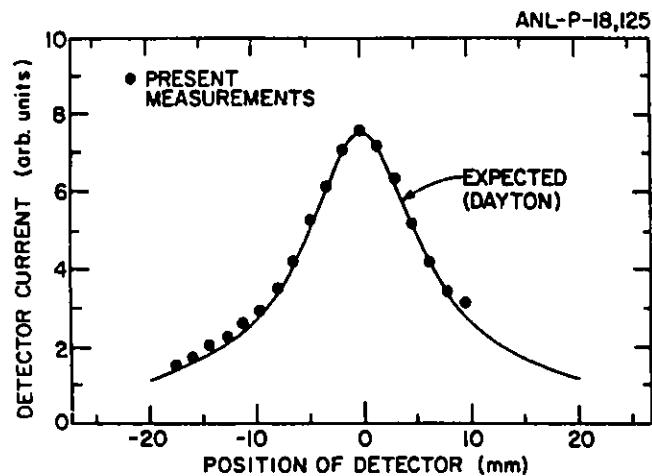
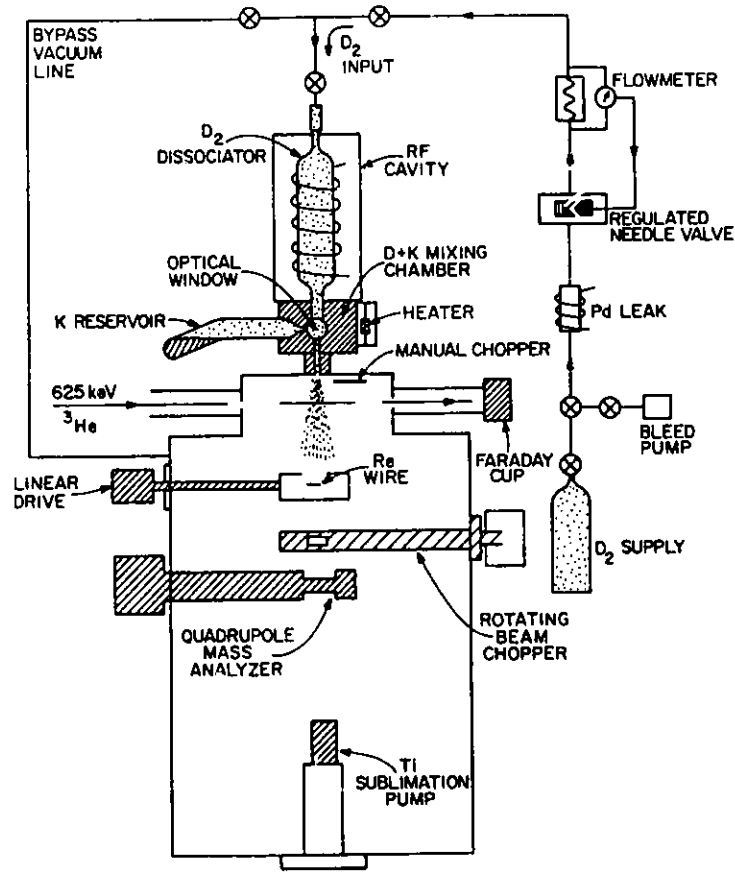


Figure I-2. (a) Schematic diagram of prototype polarized target assembly. The laser beam, not shown, enters the mixing cell through the optical window. The hot Re wire was used to detect the relative density of K atoms as well as the profile of the emerging atomic jet. (b) Measured profile of the K atomic beam emerging from the mixing cell. It is expected that the deuterium atoms will emerge with the same profile from the cell.



flux of  $2 \times 10^{16} \text{s}^{-1}$  of polarized deuterium nuclei, the approximate yield available from the most intense conventional atomic beam sources. Since this preliminary test, the following steps were taken to improve the stability and flux of the polarized deuterium source so that tests with the Dynamitron beam could be performed: (i) Modifications were made to the laser cavity to permit stable operation of the CW laser up to a power level of 300 mW; (ii) the efficiency of dissociation of molecular deuterium was improved by a factor of three and now ranges between 60 and 80%; and (iii) a surface coating was found which inhibits spin-relaxation of K atoms in collisions with the walls in the exchange cell. The present goal is to obtain a stable flow of highly-polarized, optically-pumped potassium vapor through the target system. This goal should be met during 1986 and a full test of the target would proceed immediately thereafter.

c. Electroproduction of the Delta Isobar in Nuclei

H. E. Jackson, D. F. Geesaman, M. C. Green, R. J. Holt, R. S. Kowalczyk, T.-S. H. Lee, P. Seidl, B. Zeidman, D. Baran,\* and R. E. Segel\*

A study of the electroproduction of the delta isobar in complex nuclei has been proposed and approved at the Stanford Linear Accelerator (SLAC). The 1.6-GeV and 8-GeV spectrometers will be used to investigate the scattering of medium-energy electrons ( $T_e = 0.5$  to  $2.0$  GeV) by targets of  $^{12}\text{C}$  and  $^{56}\text{Fe}$ . The particular feature to be studied in this experiment will be the separation of the longitudinal and transverse cross sections at relatively low four-momentum transfer,  $q^2 \approx 0.1 (\text{GeV}/c)^2$ , where the kinematic conditions correspond to those obtained in pion excitation of the delta. Since the excitation of the (3,3) resonance is the dominant feature of both pion and electron interactions at medium energies, an understanding of the nuclear response function requires a detailed knowledge of delta propagation in nuclei. Inasmuch as there are distortions and strong absorption present in pion-induced excitation of the delta, electroproduction is the only way to produce delta-hole excitations uniformly throughout the nucleus and investigate delta isobar dynamics in the nuclear medium. The experiment is scheduled to run in February 1986.

---

\*Northwestern University, Evanston, Illinois.

- d. Pion Electroproduction in Deuterium H. E. Jackson, M. Bernheim,\*  
G. Fournier,\* A. Gerárd,\* J. Julien,\* J. M. Laget,\* A. Magnon,\*  
C. Marchand,\* J. Morgenstern,\* J. Mougey,\* J. Picard,\* D. Reffay,\*  
B. Saghai,\* S. Turck-Chieze,\* and P. Vernin\*

Pion electroproduction on nucleons bound in nuclear matter may be significantly different from production on free nucleons because of the contributions of higher-order processes involving neighboring nucleons. Such multi-nucleon processes are a basic feature of nuclear matter and their study can provide useful insights into the properties of nuclear forces. To explore the use of electroproduction as a probe of such processes we have begun a series of experiments at the Saclay electron linac (CEN) to study the reaction in simple nuclear systems. The deuteron has been chosen for the first measurement because it is a simple benchmark nucleus for which theoretical calculations can be made. The Saclay high-energy, high-resolution coincidence spectrometer (HE3), will be used to observe pions emitted in the direction of the virtual photon in coincidence with the scattered electron. Measurements will be made for two values of the nucleon invariant mass. The first will be in the region of the peak of the delta (1232 MeV). The second will be for an invariant mass near 1160 MeV. In this region electroproduction on the proton is predominately longitudinal and the "photo electric" or pion pole term provides the largest contribution to the cross section. If there are significant deviations in total yields from the free nucleon values the shape of the energy spectrum of the pions may provide clues as to their origin. Measurements will be made using deuterium and hydrogen in a single cryogenic target with identical spectrometer geometry. Thus, a direct comparison will be possible without the systematic errors common in absolute measurements.

---

\*CEN Saclay, France.

e. Study of Pion Absorption in  $^3\text{He}$  through the  $(\pi^+, 2p)$  and  $(\pi^-, pn)$

Reactions D. Ashery,\* D. F. Geesaman, G. S. F. Stephans,† J. P. Schiffer, B. Zeidman, B. D. Anderson,‡ R. Madey,§ R. C. Minehart, S. Mukhopadhyay,|| E. Piazzetsky,¶ R. E. Segel,|| C. Smith, and J. Watson‡

Measurements at 165, 250 and 500 MeV pion energy were completed during the past year at the LAMPF P<sup>3</sup> area. Data have been obtained both for two-nucleon absorption, where the pion's momentum and energy are essentially taken up by two nucleons, and for three-nucleon absorption in which the momentum is shared among all three nucleons. A typical proton spectrum measured in the region of the two-nucleon peak is shown in Fig. I-3.

A combination of the LAS spectrometer and two  $\text{lm}^2$  scintillator arrays were used to provide information on these reactions. Angular distributions for the two-body process allow the determination of the partial waves for absorption on two nucleons in an initial  $S=0$ ,  $T=1$  state as a function of pion energy. The analysis of these data is in progress, and will provide a rather complete picture of pion absorption on  $^3\text{He}$  and the  $^3\text{S}_0$  nucleon pair, from stopped and low-energy pions (already in the literature) up to 500 MeV. Preliminary analyses indicate that the three-body absorption mode accounts for  $30 \pm 10\%$  of the total absorption at 165 MeV.

---

\*Tel Aviv University, Tel Aviv, Israel.

†Massachusetts Institute of Technology, Cambridge, Massachusetts.

‡Kent State University, Kent, Ohio.

§University of Virginia, Charlottesville, Virginia.

||Northwestern University, Evanston, Illinois.

¶Los Alamos National Laboratory, Los Alamos, New Mexico.

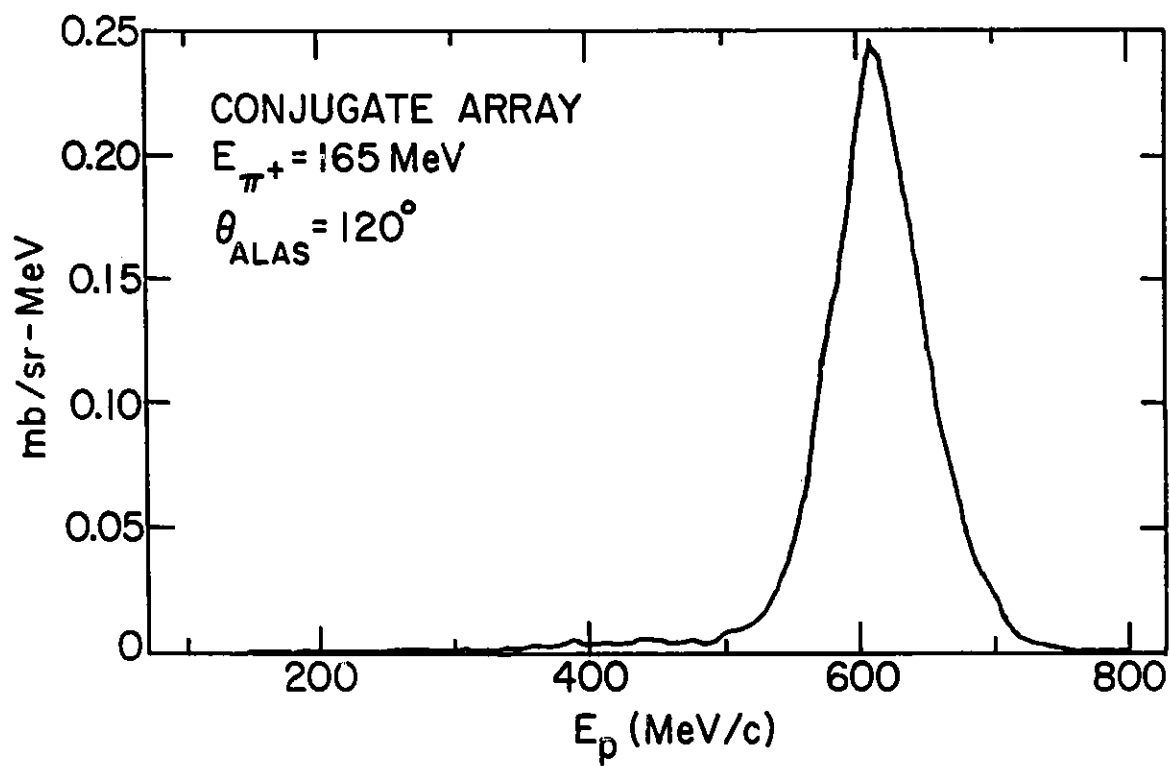


Figure I-3. Proton spectrum measured over the region of the conjugate angle (i.e., the angle for  $\pi^+_{d+2p}$ ) in coincidence with 120° protons from the absorption of 165-MeV  $\pi^+$  by  $^3\text{He}$ .

- f. The A-Dependence of the (e,e'p) Reaction in the Quasifree Region (D. F. Geesaman, M. C. Green, R. J. Holt, J. P. Schiffer, B. Zeidman, B. Beise,§ M. Deady,|| G. Garino,† N. S. Chant,\* X. K. Maruyama,‡ R. P. Redwine,§ P. Roos, W. W. Sapp,§ R. E. Segel,† R. H. Siemssen, and C. F. Williamson,§)

Information on proton propagation in nuclei is essential for the analysis of many processes, including pion absorption and inclusive proton-induced reactions. At the present time, proton-elastic-scattering data support a long mean free path ( $\sim 5$  fm). The electron-knockout reactions appear to be the cleanest technique to provide macroscopic and microscopic measures of this fundamental nuclear parameter property. Thus, the Argonne Medium-Energy group is leading an experiment at the MIT-Bates Laboratory to study the A-dependence of the (e,e'p) reaction at  $|q| = 540$  MeV/c. From the A-dependence of the ratio of (e,e'p) coincidence to (e,e') singles events, the macroscopic attenuation of  $140 \pm 20$  MeV nucleons in nuclei will be deduced.

During 1985, a final shakedown run of the BIGBITE spectrometer was completed to test the detector stack and magnetic optics. A gas Cerenkov counter for electron identification in OHIPS was constructed and then tested during the short OHIPS-BIGBITE coincidence test. Beam time for the experimental measurements is expected in 1986.

---

\*National Bureau of Standards, Washington, D.C.

†Northwestern University, Evanston, Illinois.

‡University of Maryland, College Park Maryland.

§Massachusetts Institute of Technology, Cambridge, Massachusetts.

||Mt. Holyoke College, South Hadley, MA.

- g. Study of Correlations Between Light Nuclear Fragments and the Scattered Projectile with 300-MeV Protons (S. B. Kaufman, B. D. Wilkins, R. G. Korteling,\* R. E. L. Green,\* J. M. D'Auria,\* R. L. Helmer,† and K. P. Jackson†)

The emission of light fragments ( $A \leq 4$ ) in coincidence with an energetic proton observed at forward angles (presumably the scattered projectile) has been studied using 300-MeV protons and targets of Be and Ag in an experiment at the TRIUMF Cyclotron. The objective was to place constraints on the various models suggested to account for inclusive spectra of these fragments, and in particular to determine the importance of single-scattering models. Earlier studies of the relatively simple (p, 2p) and (p, pd) reactions on Be had indicated a direct interaction component in the coincidence data not observed in the inclusive data. Of course, the results of (e,e'p) experiment at Bates described in section A.f. is crucial to the interpretation of these data. Preliminary data analysis reveals a direct component is also present for  $^3\text{He}$  and  $^4\text{He}$  emission from Be, and also for the high-energy (non-evaporative) portion of the spectra from the Ag target. This is most clearly seen in the increased coincidence rates at or near the correlation angle between the fragment and the scattered proton for which the momentum transfer to the rest of the system is a minimum. A detailed analysis of the different correlations between angle, energy, and type of particle, and their dependence is underway.

---

\*Simon Fraser University, Burnaby, British Columbia, Canada.

†TRIUMF, Vancouver, British Columbia, Canada.

- h. Light Fragment Emission in Pion-Nucleus Reactions (S. B. Kaufman, F. Videbaek, B. D. Wilkins, D. J. Henderson, S. J. Sanders, R. G. Korteling,\* and G. W. Butler†)

In a previous study of pion-induced nuclear reactions, we measured the inclusive energy spectra of  $^3\text{He}$  and  $^4\text{He}$  emitted in reactions of positive and negative pions with Ag, as a function of laboratory angle. These spectra were similar in shape and magnitude to those of the same fragments emitted at  $90^\circ$  to the beam in medium-energy proton-induced reactions, but were almost independent of angle, in sharp contrast to the strong forward-peaked distributions observed with incident protons. These data were interpreted in terms of a mechanism in which the pion is absorbed inside the nucleus, resulting in two or more fast nucleons moving apart, which then lead to the emission of the more complex fragments. This work complements the program of pion-absorption studies which were led by the ANL Medium-Energy group at LAMPF. A detailed study of the reaction mechanism itself was performed for  $^3\text{He}$  and is the subject of section A.e. Because of the relatively low momentum transferred by the pion, there is little net forward motion of the nucleons, and the resulting final-state fragments do not have the typical forward peaking observed with other projectiles. A proposal to study the correlations between coincident light fragments following pion-nucleus reactions at LAMPF has been approved, and the experiment is expected to be carried out during this year. The aim is to detect coincident protons, deuterons, tritons,  $^3\text{He}$ , and  $^4\text{He}$  particles, and to measure the correlations in angle and energy between them. A comparison between positive and negative pions is especially important, since the emission of two charged particles following negative pion absorption must necessarily involve participation of a multinucleon cluster or of substantial final-state interactions among the nucleons involved. We plan to construct a new scatter chamber with thin walls, in order to mount scintillator telescopes outside the chamber to detect the hydrogen isotopes, while using conventional silicon detector telescopes inside to detect helium isotopes.

---

\*Simon Fraser University, Burnaby, British Columbia, Canada.

†Los Alamos National Laboratory, Los Alamos, NM.

- i. Focal-Plane Detector for 1.6-GeV Spectrometer at SLAC (D. F. Geesaman, M. C. Green, R. J. Holt, H. E. Jackson, R. S. Kowalczyk, B. Zeidman, S. T. Thornton,\* D. Baran,† and P. Siedl)

A new focal-plane detector assembly for the 1.6-GeV spectrometer has been constructed in order to perform experiments NE-1 [item A.b.(2)] and NE-5 at SLAC. This is a general-purpose system suitable for detection of either electrons or hadrons and consists of scintillation hodoscopes, multi-wire drift chambers, Cerenkov counters and a segmented shower counter. The particular ANL responsibilities are the hodoscopes, composed of 18 segments which form two x-y grids about 80 cm apart, and three sections of double x-y drift chambers for precise position measurements. The data-acquisition electronic system utilizes emitter-coupled logic (ECL) extensively, thereby permitting individual time-to-digital converters on each wire of the drift chambers, computer-controlled logic and delays, and a rudimentary trajectory selection in the hardware trigger. The system has been installed in the 1.6-GeV spectrometer and preliminary tests indicate satisfactory performance, particularly for background rejection at high instantaneous count rates.

---

\*University of Virginia, Charlottesville, VA.

†Northwestern University, Evanston, Illinois.



j. Data-Acquisition System for SLAC Experiments

(M. C. Green, P. Seidl, B. Zeidman, D. Baran,\* D. Day,† O. Rondon,† and Z. E. Mezzian†)

As a result of constraints imposed by the schedule of experiments at SLAC, a new data-acquisition system was required for experiments that use the 1.6-GeV/c spectrometer. The ANL group assumed responsibility for this task and has developed a VAX-based data-acquisition system using a CAMAC Serial Highway; this system being adapted from the MUPDAS program used with the MUPPATS detector, a fast 2-dimensional detector developed in the ANL Physics Division's Atomic Physics program. The system is capable of recording more than 180 events per second (the maximum repetition rate at SLAC) with about 100 parameters per event. At this rate a substantial fraction of the events can be analyzed on line to provide continuous monitoring of the experiment during the run. At the expected rate of 120 events/s nearly all events will be analyzed. Inasmuch as the End Station A VAX computer was occupied for the six months preceding the present experiment, it was absolutely essential to employ the VAX-based computer system on board the ANL trailer in order to develop the data-acquisition system. The data will be processed by the VAX in the ANL trailer.

In addition, experiment monitoring of beam rate, magnet settings, etc., will utilize the End Station A VAX which will also be used with existing software for data acquisition in those parts of experiments involving the 8-GeV/c spectrometer. Information will be transferred between the ESA VAX and the ANL VAX via an Ethernet communication link thereby allowing data acquisition with either spectrometer or simultaneous acquisition from both spectrometers.

---

\*Northwestern University, Evanston, Illinois.

†University of Virginia, Charlottesville, VA.

k. Review Article on Pion Absorption (J. P. Schiffer and D. Ashery)

A review article summarizing the present state of information on pion absorption in nuclei was completed during the past year for Annual Reviews of Nuclear Science.

## B. INTERMEDIATE AND RELATIVISTIC HEAVY ION PHYSICS

The aim of this program is to characterize the interaction between heavy ions and complex nuclei, and to study how the particle-particle interactions are affected by the nuclear medium. The energy region between 40-200 MeV/A constitutes a transition regime and has hitherto not been well studied. At the lower energies the interactions can be described in terms of nucleus-nucleus potential and collective variables for the system. At the higher relativistic energies nucleon-nucleon interactions dominate and the central collisions eventually lead to fragmentation. The intermediate nuclear system is highly excited and compressed and could undergo phase transitions.

Aspects of the problem in the transition regime are addressed in an experiment at the low-energy beamline at the BEVALAC. The question of momentum and energy deposition in the composite system is studied, and the measurements should provide information on the limits to compound-like nucleus formation.

The group plans to join the E802 experiment at BNL-AGS and assume responsibility for the event trigger. The experiment focuses on particle-production systematics with 15-GeV/A  $^{32}\text{S}$  and  $^{16}\text{O}$  beams, on two-particle interferometry and a search for strange particles. The beam energy is such that the intermediate nuclear system is expected to have maximum possible baryon density. The experimental setup is well underway and beam time is expected towards the end of 1986.

- a. Fission and Charged Particle Emission in Nucleus-Nucleus Collisions at Intermediate Energy (F. Videbaek, S. B. Kaufman, B. K. Dichter, O. Hansen,\* M. J. LeVine,\* C. E. Thorn,\* A. Pfoh,\* W. Trautman,† R. L. Ferguson,‡ H. C. Britt,§ A. Gavron,§ B. Jacak,§ J. Wilhelmy,§ J. Boissevain,§ M. Fowler,§ G. Mamane,|| and Z. Fraenkel||)

The reactions of 100-MeV/a.m.u.  $^{56}\text{Fe}$  on a target of  $^{197}\text{Au}$  have been studied at the low-energy beam line at the BEVALAC. The objective is to study the momentum and energy transfer in nucleus-nucleus collisions in the energy regime 50-100 MeV/a.m.u. (between the low-energy regime describable in terms of potentials and macroscopic variables and the high-energy regime where the nucleon-nucleon interaction dominates.) This is achieved in part by detecting fission-like fragments in a scattering chamber with eight gas detectors, each recording energy, position and time-of-flight. Coincident light particles are detected and identified in dE-E phoswich detectors. These measurements will assist in determining the amount of energy deposited in the reaction. High multiplicity light-particle events are also recorded. A first data run was done in December 1985. The coverage with light-particle detectors was less than will be the case in the final setup. The analysis of the data from the experiment has started and we expect to submit a proposal for further experiments when it has progressed further.

---

\*Brookhaven National Laboratory, Upton, New York.

†GSI, Darmstadt, West Germany.

‡Oak Ridge National Laboratory, Oak Ridge, Tennessee.

§Los Alamos National Laboratory, New Mexico.

||Weizmann Institute, Israel.

### C. WEAK INTERACTIONS

The goals of the weak-interactions program are to verify the implications of the standard model and to discover its inadequacies.

The search for massive neutrinos with a neutrino-oscillation experiment at LAMPF is ready to begin operation with the next beam cycle in the spring. The ANL hardware responsibility for this experiment, to provide the passive and active cosmic-ray shield, is now satisfied. The ANL effort will now shift to the operation of the experiment, but we expect our primary role will be off-line data evaluation. This experiment will test an important possible extension of the standard model in a region where there are already experimental hints of new physics.

An important thrust of the program in the last few years has been an experiment to study neutron beta decay at the Institut Laue-Langevin. The result of a precision measurement of the neutron beta asymmetry is now being published. This work now provides the best available determination of the ratio of the neutron axial-vector to vector weak-interaction coupling constants. This new knowledge has important implications for cosmology, for astrophysics, and for the standard model. One surprise is that our result implies a value for the neutron lifetime that is inconsistent with all precise direct lifetime measurements. This year's work at Grenoble is concentrating on a new measurement of the neutron lifetime using the spectrograph built originally to measure the beta asymmetry. With accurate measures of both the asymmetry and the lifetime we will be able to determine both  $g_A$  and  $g_V$  directly from experiments with neutrons. While this work should clear up the experimental discrepancy, the expected error is not yet capable of determining  $g_V$  as precisely as  $0^+ \rightarrow 0^+$  superallowed beta decay experiments.

There is now a hint that the experimental values of the elements of the Kobayashi-Moskawa mixing matrix may fail to satisfy the unitarity condition, indicating the existence of a new generation of quarks and leptons. This exciting possibility is being investigated in a new experiment to measure the weak vector coupling constant for the lowest-Z  $0^+ \rightarrow 0^+$  superallowed nuclear beta decay possible,  $^{10}\text{C} \rightarrow ^{10}\text{B} + \bar{e} + \nu$ . This work is the first step toward obtaining the smallest possible error for the Cabbibo angle from the light nuclei. If present indications hold up, the experiments will establish the existence of quarks at the hundred-GeV scale by studying low-energy beta decay.

Experiments to study the implications of the conserved vector current hypothesis and the absence of second-class currents continue with the magnetic spectrograph at Argonne and with polarized-beam experiments at the Wisconsin tandem accelerator. The Argonne beta spectrograph has also been used to measure delayed beta spectra following fission important for the interpretation of reactor neutrino-oscillation experiments. Recently, the beta spectra of  $^8\text{Li}$  and  $^8\text{B}$  were measured to help put the prediction of the flux of solar neutrinos on a firmer foundation.

Finally, our interest in searching for new particles whenever opportunities arise continues to drive an important component of the program. In recent years we have searched for light Higgs particles and magnetic monopoles. New experiments in this direction are under development.

- a. Neutrino Oscillations at LAMPF (S. J. Freedman, M. Green, J. Napolitano, R. Carlini,\* C. Choi,† J. Donohue,\* A. Fazely,†, B. Fujikawa,‡ G. T. Garvey,\* R. Harper,§ R. Imlay,† K. Lesko,|| T. Y. Ling,§ R. D. McKeown,‡ W. Metcalf,† J. Mitchell,§ E. Norman,|| T. Romanowski,§ V. Sandberg,\* E. Smith,§ and M. Timko§)

The apparatus for the neutrino-oscillation experiment (LAMPF experiment 645) is now completely constructed. Work is proceeding to insure that the detector and shield will be fully operational for the beginning of the next LAMPF beam cycle in the spring.

The active 20-ton internal  $\bar{\nu}_e$ -detector consisting of 40 modules of liquid scintillators and proportional drift tubes tracking is now undergoing checkout and calibration with cosmic-ray muons. The electronic shakedown for the detector is proving to be the most time consuming job, but the OSU-LSU group is confident that the few remaining bugs will be corrected before the beam time begins.

All major construction necessary for operation of the experiment has been completed. The tunnel is now complete and most of the overburden is in place. In the worst case the overburden will be only 2000 g/cm<sup>2</sup> instead of the desired 2500 for the first part of the running period. This may, in fact, turn out to make a differential shielding test possible. The water-tank plug to seal the tunnel after installation of the detector is constructed and tested. The electrical and air-conditioning work necessary for operation in the tunnel is all complete.

The cosmic-ray active and passive shields are the principal hardware responsibilities of the ANL group. All construction is complete. The plumbing necessary to fill and empty the 25 tons of liquid scintillator in the active shield is in operation. The system for filling and emptying works well and the entire shield can be filled in less than a day by two people. The 360 photomultipliers and cables are installed and tested. The shield electronics is completely debugged and now operates routinely. The shield is now undergoing extensive testing and calibration with cosmic rays. A problem has

---

\*Los Alamos National Laboratory, Los Alamos, New Mexico.

†Louisiana State University, Baton Rouge, Louisiana.

‡California Institute of Technology, Pasadena, California.

§Ohio State University, Columbus, Ohio.

||Lawrence Berkeley Laboratory, Berkeley California.

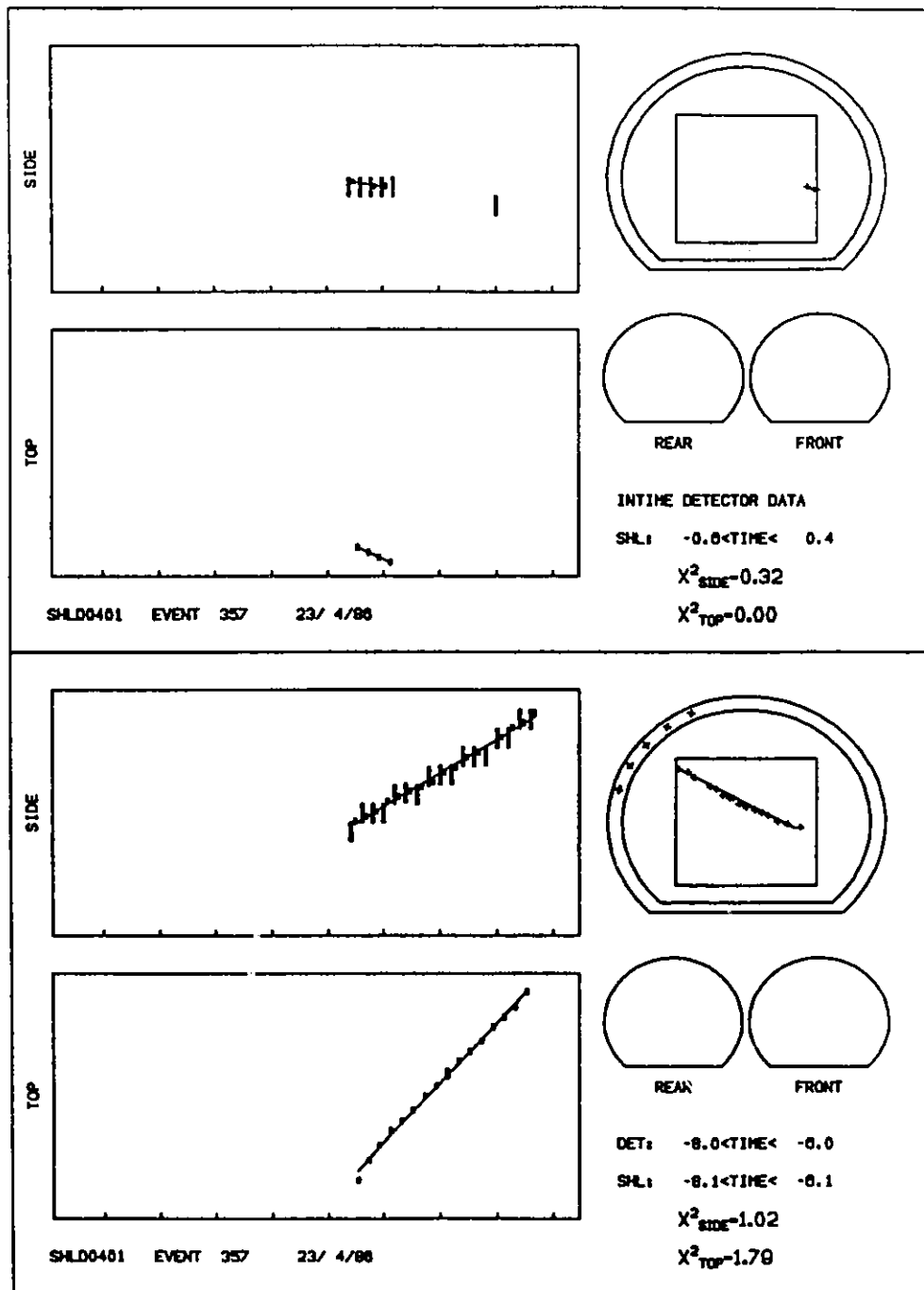


Figure I-4. A muon decay in the LAMPF neutrino oscillation apparatus. The upper half shows side, top, and axial views in the detector and shield for the triggering data, presumably an electron or positron. The lower half shows the same views for the entering muon data which occurs roughly  $7 \mu\text{s}$  in the past.

arisen with the EMI photomultipliers used in the shield. Some of the phototubes developed cracks in the feedthrough section of the tube and about 10% of the tubes have failed. Fortunately the shield is designed to operate with only 70-80% of the phototubes, but we are working toward a more permanent solution to the phototube problem. In general, however, the active shield performs extraordinarily well.

With the routine operation of the cosmic-ray shield we expect the efforts of the ANL group will shift toward operating the detector and off-line data evaluation. A paper describing the construction and operation of the shield is being prepared.

One of the first tests of the detector and shield as a single unit consists of setting a  $\sim$  few  $\mu$  veto time from the shield and looking for muon decay products in the detector. This not only tests many fundamental aspects of the apparatus, but also provides a sample of  $e^+$  and  $e^-$  from muon decay with which we can study the detector response to events closely resembling neutrino oscillations. Figure I-4 shows such an event. The triggering signals indicate an electron (or positron) from muon decay. The incoming muon which stops and subsequently decays is found approximately 7  $\mu$ s in the past. (The experiment electronics is capable of recording a "time history" of what happens in the apparatus.) Figure I-5 shows a histogram of the measured delay time for a sample of selected events using a 2  $\mu$ s veto time. The data is clearly consistent with the muon lifetime of 2.2  $\mu$ s.

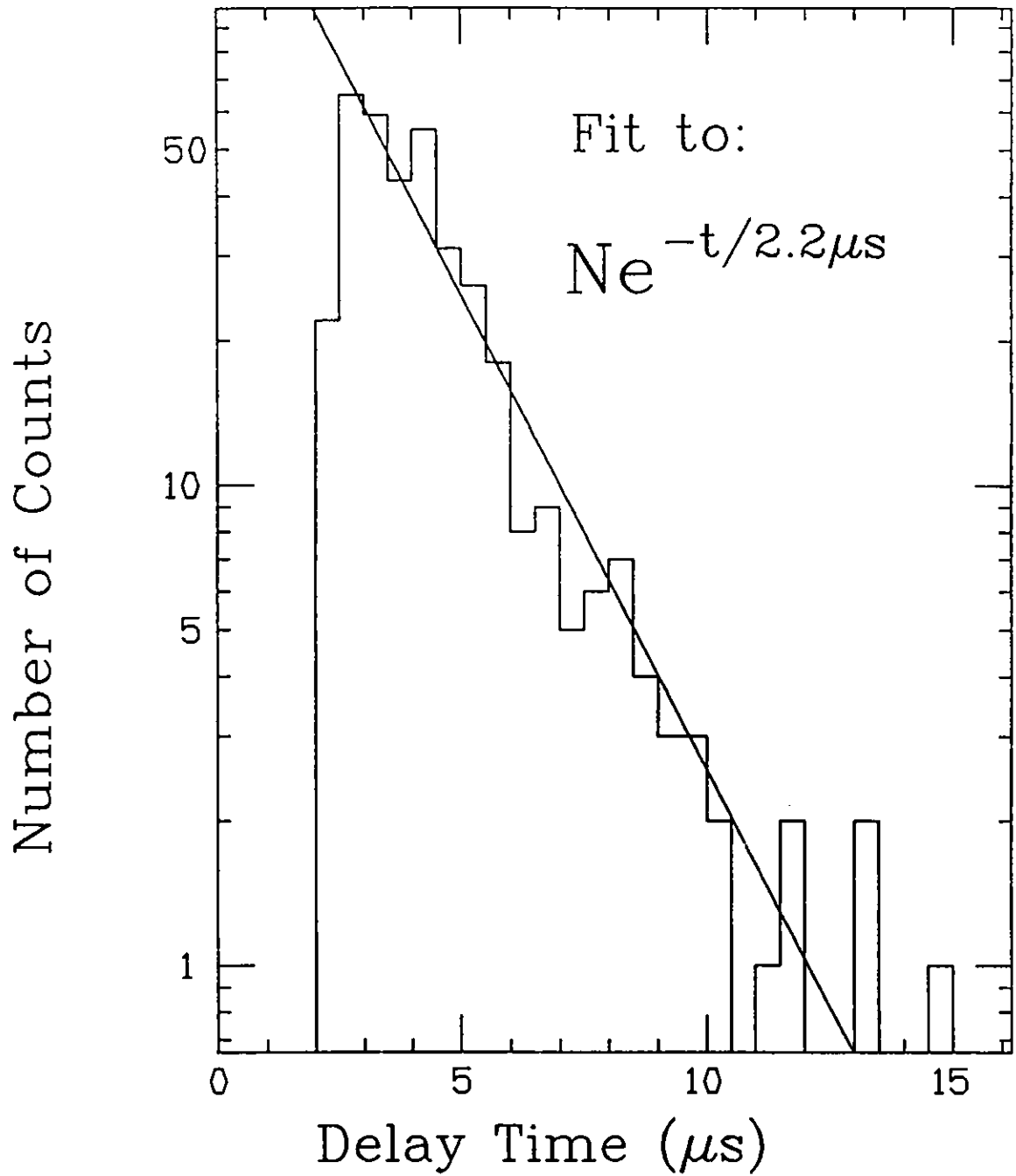


Figure I-5. Time of the "entering-muon" data relative to the experiment trigger for selected muon decay events in the LAMPF neutrino oscillation experiment. The active shield was used to generate a 2  $\mu\text{s}$  veto in hardware to acquire this data.



b. Neutron Beta Decay (S. J. Freedman, M. Arnold,\* J. Doehner,\*  
D. Dubbers† and J. Last\*)

The final runs to measure the beta asymmetry of the neutron were completed last year. The experiment now provides the most precise available value for  $g_A/g_V$ . We find  $g_A/g_V = -1.262 \pm 0.005$ . This result is consistent with our preliminary result of  $g_A/g_V = -1.27 \pm 0.01$  and with previous results from correlation experiments, but it is inconsistent with the results of all precise neutron lifetime measurements. The experiment also obtains a value for the weak-magnetism parameter, although the uncertainty is still too large to provide a meaningful test of the conserved current hypothesis and the absence of second-class currents. A paper reporting the experiment was submitted to Physical Review Letters.

A cosmological argument based on the Big Bang Theory using the new value for  $g_A/g_V$  along with other experimental data now implies that there should be no more than four types of light neutrinos. Thus, within the context of the Standard Model we expect no more than four generations of quarks and leptons. This is particularly interesting because of the evidence that more than four generations may be required (see section C.c.).

The predicted flux of solar neutrinos is also modified by the new determination of  $g_A/g_V$ . The flux is changed from  $7.6 \pm 3.3$  to  $5.8 \pm 2.2$  SNU. The predicted neutrino flux is closer to the measured value of  $2.1 \pm 0.3$  SNU, but the reduced error in the prediction, a reflection of our more precise knowledge of  $g_A/g_V$ , slightly increases the discord between theory and experiment.

To better understand the experimental discrepancy between the asymmetry and direct lifetime experiments we have begun some lifetime experiments using the PERKEO spectrometer. The lifetime is measured by a variety of techniques and we expect to provide a  $\approx 1\%$  determination. This precision is as good as any previous lifetime experiments. We believe the  $1\%$  uncertainty is about the limit of any neutron-beam technique. In our experiment we measure the absolute rate of beta decay with PERKEO. In one version of the experiment we use a continuous beam and measure the neutron

---

\*Physikalisches Institut, Heidelberg, Germany.

†Institut Laue-Langevin, Grenoble, France.

capture flux with a  $^3\text{He}$  counter (a gold foil is used as a crosscheck). In another experiment we use a pulsed neutron beam and measure the total neutron flux with a cobalt or gold beamstop. The measurements are well underway and initial tests indicate that a result from both methods will be possible this year. The experiment is scheduled to run at Grenoble until April 1986.

The work on the neutron lifetime has delayed some of our plans for future neutron decay experiments. However, we are still considering a better asymmetry measurement and a new test of time reversal invariance in neutron beta decay.

c. The Vector Weak Coupling and  $^{10}\text{C}$  Superaligned Beta Decay

(S. J. Freedman, R. Holzmann, M. Kroupa\*, J. Napolitano, and J. Nelson)

In principle both the vector and axial vector weak-interaction coupling constants can be determined from neutron beta decay, but as yet experiments are not good enough to provide the best value for the vector coupling. Meanwhile the vector coupling is critical to the basic phenomenology of the weak interaction. Recently, it has been noted that the experimental values of the elements of the Kobayashi-Moskawa mixing matrix do not satisfy the unitarity condition. The obvious explanation (if the present two- $\sigma$  effect holds up) is that there are at least four generations of quarks and leptons instead of three. The principal experimental error leading to this exciting conclusion is the experimental value of the weak vector coupling strength for the nucleon.

The best value now comes from  $0^+ \rightarrow 0^+$  superallowed nuclear beta decay. The best experiment is the  $\beta$ -decay of  $^{14}\text{O}$ . Most of the error now comes from radiative corrections, so it does not help much to improve the  $^{14}\text{O}$  experiment. The smallest-Z system which has the appropriate  $\beta$ -decay is mass-10; this system has the smallest radiative corrections. To extract the vector coupling one needs the partial lifetime for the  $0^+ \rightarrow 0^+$  decay and the energy released. The biggest error by about a factor of ten, is from the branching ratio of the ground state of  $^{12}\text{C}$  to the  $0^+$  excited state of  $^{10}\text{B}$ . We are proceeding to measure the branching ratio.

The experimental challenge reduces to measuring the ratio of two  $\gamma$ -rays, at 1.1 MeV and 0.7 MeV, to the 0.1% level. The main experimental problem is to calibrate Ge-detectors to this level. Our method is to calibrate with inelastic proton scattering to the excited  $0^+$  level and tagging the excited state with coincidence proton counting. This method determines the relative detection efficiencies directly using the same  $\gamma$ -rays that make up the experimental signal for the branching-ratio measurement. An initial run at the Argonne FN Tandem indicated that the method is sound, but in order to measure the small  $\gamma$ -ray branch from  $^{10}\text{C}$  produced in the  $^{10}\text{B}(p,n)^{10}\text{C}$  reaction a  $\approx 1 \mu\text{A}$  beam current of 7.5-MeV protons is required. This beam is difficult to obtain with the Argonne Tandem in its present configuration as an

---

\*Thesis Student, University of Chicago, Chicago, Illinois.

injector for ATLAS. The experiment is now proceeding at the EN Tandem accelerator at the University of Western Michigan at Kalamazoo. Present indications are good that the measurement can be accomplished in only a week of beam time.

d. Beta Decay of Polarized Nuclei and the Decay Asymmetry of  $^8\text{Li}$   
(S. J. Freedman, J. Napolitano, R. Bigelow,\* and P. A. Quin\*)

Under favorable conditions, it is possible to produce polarized radioactive nuclei using nuclear reactions with polarized projectiles where the polarization relaxation time is comparable to, or longer than, the  $\beta$ -decay lifetime. This makes possible a variety of experiments on the allowed  $\beta$ -decay of polarized low-A nuclei. Such experiments bear on tests of CVC, sensitive searches for second-class weak currents, and measurements of the weak vector-coupling constant. In addition, the values of a variety of forbidden nuclear matrix elements may also be determined.

At the present time we are concentrating on completing our initial experiment on the  $\beta$ -decay of polarized  $^8\text{Li}$ . With the aid of the intense polarized beams available at the University of Wisconsin, we produce  $^8\text{Li}^\uparrow$  via  $^7\text{Li}(\uparrow, p)^8\text{Li}^\uparrow$  using a cold  $^7\text{Li}$  metal target in a weak magnetic field. The parity-violating  $\beta$ -decay asymmetry is measured as a function of  $\beta$  energy using  $\Delta E$ -E plastic scintillator telescopes at  $0^\circ$  and  $180^\circ$  to the polarization direction. Our first run using the new data-acquisition computers at the University of Wisconsin yielded approximately 10% of the amount of data needed for this measurement. Preliminary results show good agreement with expectations at the present level of statistics. A method of taking singles histograms at high rate using an intelligent CAMAC crate controller is presently being developed at Argonne.

---

\*University of Wisconsin, Madison, WI.

e. The  $\beta$ -decay Spectrum in the A=8 System and the Solar Neutrino Problem  
(J. Camp,\* J. Napolitano, and S. J. Freedman)

The only available experimental result for the flux of solar neutrinos is from Davis et al. who report a value some three standard deviations smaller than the expected theoretical result. The measured flux is essentially entirely due to high-energy neutrinos from the  $\beta$ -decay of  $^8\text{B}$ . Consequently, the spectrum of neutrinos from this  $\beta$ -decay is crucial to the calculation of the expected flux, particularly since the final state in  $^8\text{Be}$  does not have a definite energy. This final state, however, is unstable to  $2\alpha$  decay. The neutrino spectrum is therefore derived from the  $\alpha$ -energy spectrum using certain reasonable assumptions. However, there is reason to believe that the measured  $\alpha$ -spectra at low energies (corresponding to high neutrino energies) are in error. Indeed, various measurements of this spectrum show discrepancies with each other.

Using the Argonne high-energy  $\beta$  spectrograph we have measured the beta spectrum of  $^8\text{B}$ .  $^8\text{B}$  was produced using the Physics Division Dynamitron via  $^6\text{Li}(^3\text{He},n)^8\text{B}$ . Figure I-6 shows the allowed spectrum of  $^{12}\text{B}$  (used for calibration) and the beta spectrum of  $^8\text{B}$ . The data are completely consistent with a prediction based on a recently published  $\alpha$  spectrum. This work is being prepared for publication.

---

\*Thesis Student, University of Chicago, Chicago, Illinois.

ANL-P-18,372

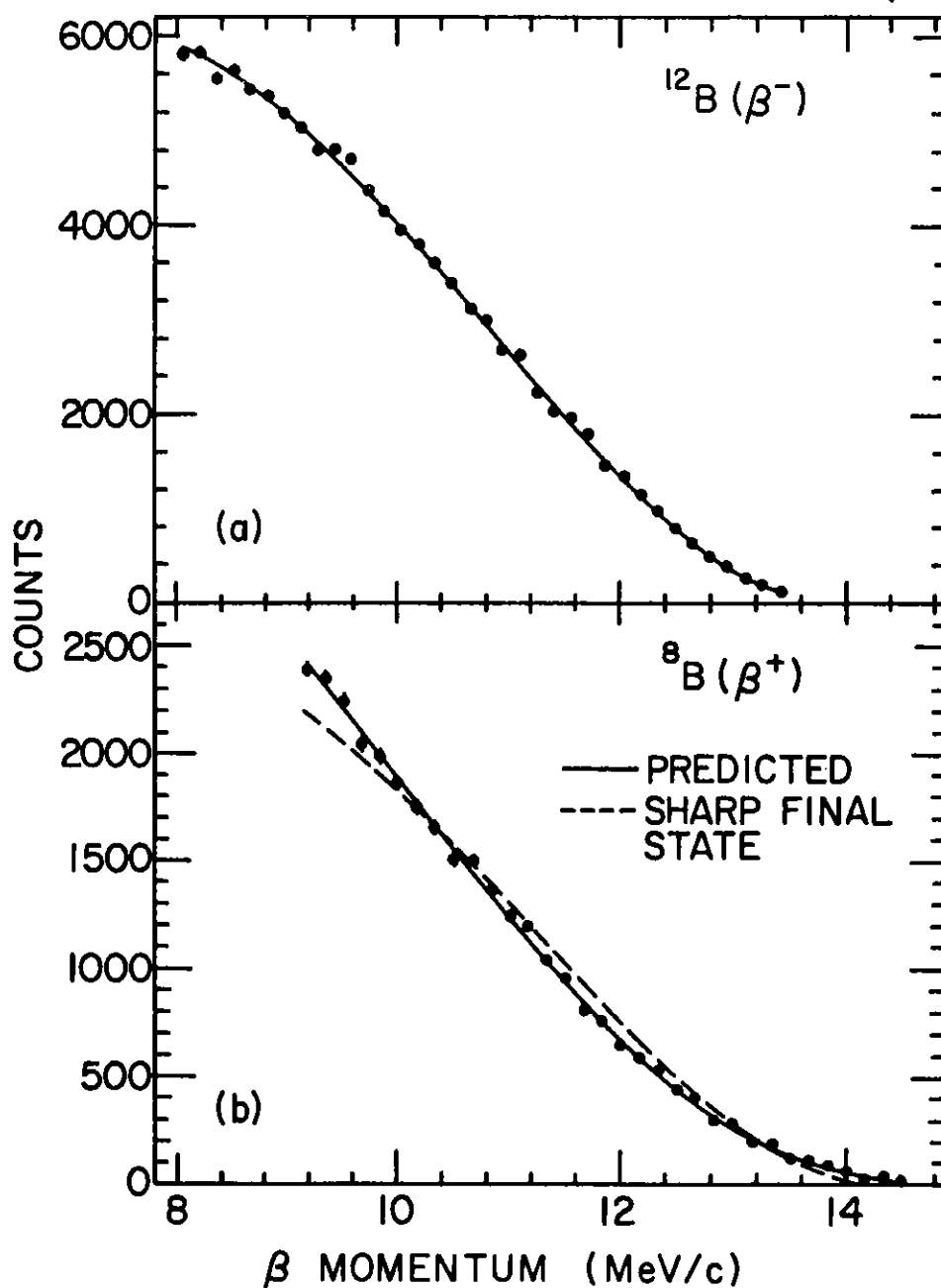


Figure I-6. Beta spectra measured using the Argonne high-energy beta spectrometer at the Physics Division Dynamitron accelerator. Top: the allowed spectrum of  $^{12}\text{B}(\beta^-)$  used to calibrate the spectrometer. Bottom: the spectrum of  $^8\text{B}(\beta^+)$  compared to an allowed spectrum assuming a sharp final state (dashed line) and the predicted spectrum based on a recently published alpha spectrum from  $^8\text{B}(\beta^+)^8\text{Be}(2\alpha)$ .

f. Weak Magnetism Effects in Beta Spectra (J. Camp,\* G. T. Garvey,† and D. Wark‡)

We have developed a high-energy beta spectrograph to make precision measurements of beta spectra. The system is now stable over long counting times and has been calibrated to better than 1% in momentum and efficiency.

Initial measurements of  $^{12}\text{N}$  and  $^{12}\text{B}$  beta decays have indicated the presence of weak magnetism effects. We expect this year to quantify systematic instrumental errors to the level necessary to complete the investigation of weak magnetism in mass 12.

---

\*Thesis Student, University of Chicago, Chicago, Illinois.

†Los Alamos National Laboratory, Los Alamos, N.M.

‡California Institute of Technology, Pasadena, California.

g. Beta Spectra Following the Spontaneous Fission of  $^{252}\text{Cf}$  (D. Wark,\* G. Garvey, F. Boehm,\* and J. Camp†)

Neutrino-oscillation studies using reactor sources can be made much more sensitive if the  $\nu$  spectrum from the reactor is known. The fission of a heavy nucleus such as Cf or U creates neutron-rich nuclei so far from the valley of stability that their beta-decay spectra are not known. Thus a model must be employed to predict the overall beta-decay spectrum and the attendant  $\nu$  spectrum. In order to test the reliability of the procedure in use the beta spectrum of the fission fragments following  $^{252}\text{Cf}$  fission is being measured to an accuracy of 3% in shape and 5% in total yield. An actively-collimated, flat-field beta spectrometer is used. Its acceptance has been calibrated to much better than 5% and its momentum resolution is  $\Delta p/p = 4 \times 10^{-3}$ . A spectrum has been obtained in the last year from 2 to 8 MeV using a 180- $\mu\text{c}$   $^{252}\text{Cf}$  source and a spectrum from  $^{96}\text{Yr}$  for absolute acceptance calibration. This data is currently being analyzed and a final publication will soon be written.

---

\*California Institute of Technology, Pasadena, California.

h. Search for a Light-Scalar Boson Emitted in Nuclear Decay  
(J. Napolitano, S. J. Freedman, and J. Nelson)

Using the Physics Division Dynamitron to produce  ${}^4\text{He}$  ( $0^+$ , 20 MeV) via radiative capture of protons on a tritium target, we performed a sensitive search for Higgs-like scalar particles with masses between 3 and 14 MeV/c<sup>2</sup>. This work has been published. As pointed out in that publication, uncertainties in the theoretical interpretation strongly suggest that a more sensitive experiment be performed.

A number of straightforward modifications to the last experiment would increase the sensitivity by as much as an order of magnitude. However, much greater sensitivity would be achieved if the cosmic-ray background in the detector system were reduced. Using a segmented detector for the  $e^+e^-$  pair (emitted in the decay of the scalar) it appears to be possible to minimize the cosmic-ray background problem by enhancing the signature for the signal relative to that of residual cosmic rays. The Dynamitron remains the optimum accelerator on which to perform this experiment. Consequently we are in the process of securing the necessary components needed to mount this experiment at Argonne.



i. Measurement of the Electric Dipole Moment of the Neutron

(M. S. Freedman, G. R. Ringo, T. W. Dombeck,\* J. M. Carpenter,†  
N. Jarmie,\* J. W. Lynn‡, and J. D. Moses\*)

The purpose of this project is to measure the electric dipole moment (EDM) of the neutron. Such a measurement would probably constitute the most sensitive test of time-reversal symmetry now available. The present situation is that with about a factor-of-10 improvement in sensitivity, a whole class of gauge theories--those which explain CP failure by introducing a new scalar field--can be given a definitive test.

Since the measurement of the neutron EDM is fundamentally a frequency measurement, its statistical uncertainty is inversely proportional to the duration of the measurement. It is therefore natural to try the measurement on ultracold neutrons (UCN). These neutrons with  $v < 7$  m/s can be kept in a bottle for hundreds of seconds. We propose to do this using two unique features. First, we propose to use a pulsed neutron source and keep the inlet to the bottle open only when the pulsed source is on, thus allowing a buildup to an asymptotic density determined by the peak flux of the source instead of the average. This has the advantage that pulsed sources have peak fluxes that are much higher than the average fluxes of steady-state sources of the same average power. Second, we propose to produce the UCN by Bragg reflection of considerably faster (400-m/s vs 7-m/s) neutrons from a moving crystal designed so that the reflected neutrons are almost stationary in the laboratory system. The advantage of this is that it avoids the problems of extracting the very delicate UCN from the hard-to-control environment in a high-flux source. The present state of the project is that both of these ideas have been tested and shown to be practical, as have several other ideas for enhancing the production of UCN, such as the use of reflectors around the moving crystal and funnels to concentrate the UCN in real space at the expense of their concentration in velocity space.

---

\*Los Alamos National Laboratory, Los Alamos, NM.

†Intense Pulsed Neutron Source, ANL.

‡University of Maryland, College Park, MD.

Since the LAMPF accelerator at Los Alamos has the highest pulsed-current proton beams available anywhere at energies  $>200$  MeV, it can produce and indeed we have produced the highest peak neutron fluxes that are available. These will not be produced on a regular basis until late 1986 or 1987, but it is proposed to set up the EDM experiment at this source, which is now called LANSCE. In the meantime we have built an improved moderator using solid methane at  $15^{\circ}\text{K}$ , which should produce several times as high a flux of the relevant neutrons (100 to 400 m/sec) as any sources hitherto available. We are also developing an improved system for converting cold to ultracold neutrons using an artificial crystal (multilayer). In addition, we plan to do further work on the magnetic fields and shields needed for the EDM experiment aiming at a sensitivity of  $10^{-26}$  e  $\cdot$  cm about 1/20 the present limit on the neutron EDM.

#### D. NUCLEAR STRUCTURE STUDIES

Pion scattering is a particularly good probe of isoscalar and isovector spin-flip modes in nuclei because of the isospin-dependence of the pion-nuclear interaction. In recent years the mechanism for quenching of spin-flip transitions in nuclei has been an important question and the intent of this work is to further characterize the quenching mechanism, in particular, the isospin dependence of the quenching effect.

- a. Inelastic Scattering of Pions by  $^{10}\text{B}$  and  $^{11}\text{B}$  (B. Zeidman, D. F. Geesaman, C. Olmer,\* G. C. Morrison,† G. R. Burleson,‡ J. S. Greene,§ C. L. Morris,§ R. L. Boudrie,§ R. E. Segel,|| L. W. Swenson,¶ G. S. Blanpied,\*\* B. R. Ritchie,\*\* C. Harvey,†† and P. Zupranski||)

Elastic and inelastic scattering of  $\pi^+$  and  $\pi^-$  by  $^{10}\text{B}$  and  $^{11}\text{B}$  were previously studied at  $T_\pi = 162$  MeV with the EPICS system at LAMPF. For nuclei with  $T \neq 0$  the isospin dependence, the energy dependence, and the angular distributions of the cross sections allow separate multipole decompositions of mixed electric and magnetic transitions for neutrons and protons. A number of states strongly excited at high excitation energy, can be compared with theoretical shell-model predictions. A paper is in preparation.

---

\*Indiana University, Bloomington, Indiana.

†University of Birmingham, Birmingham, England.

‡New Mexico State University, Las Cruces, New Mexico.

§Los Alamos National Laboratory, Los Alamos, New Mexico.

||Northwestern University, Evanston, Illinois.

¶Oregon State University, Corvallis, Oregon.

\*\*University of South Carolina, Columbia, South Carolina.

††University of Texas, Austin, Texas.

- b. Isoscalar Quenching in the Excitation of  $8^-$  States in  $^{52}\text{Cr}$   
(D. F. Geesaman, B. Zeidman, G. C. Morrison,\* R. L. Boudrie,† C. L. Morris,† G. R. Burleson,‡ S. J. Greene,‡ and L. W. Swenson§)

The properties of  $8^-$  states in  $^{52}\text{Cr}$  excited by the scattering of 162-MeV  $\pi^+$  and  $\pi^-$  were studied with the EPICS system at LAMPF. The data, in conjunction with experiments utilizing other probes, should indicate whether or not quenching of isoscalar transitions relative to isovector transitions is merely an artifact of inadequate structure calculations or requires a new quenching mechanism. Because of the substantial fragmentation, identification of the  $8^-$  strength is critically dependent upon precise knowledge of the excitation energies and possible background states, and final analysis of the data awaits completion of analysis of electron scattering by  $^{52}\text{Cr}$ .

---

\*University of Birmingham, Birmingham, England.

†Los Alamos National Laboratory, Los Alamos, New Mexico.

‡New Mexico State University, Las Cruces, New Mexico.

§Oregon State University, Corvallis, Oregon.

- c. Excitation of  $8^-$  States in  $^{52}\text{Cr}$  (B. Zeidman, D. Geesaman, O. Karbon,\*  
G. C. Morrison,\*<sup>†</sup>, L. W. Fagg,<sup>†</sup> D. I. Sober,<sup>†</sup> X. K. Maruyama,<sup>‡</sup>  
R. A. Lindgren,<sup>§</sup> H. deVries,<sup>||</sup> and J. F. K. van Hienen<sup>¶</sup>)

Scattering of electrons with kinetic energies ranging from 170 MeV to 260 MeV by  $^{52}\text{Cr}$  have been studied at NIKHEF, Amsterdam. Inasmuch as these  $8^-$  states are found at excitation energies above 8 MeV where the density of states is exceedingly high, unambiguous identification of  $8^-$  states requires detailed analyses of both backgrounds and contaminant states. This analysis has been hampered by a relatively low peak-to-background ratio caused by the unusually high fragmentation of the T=2, M8 strength so that approximately ten states are  $8^-$  candidates as seen in Fig. I-7. The T=3, M8 strength, however, does not appear to be fragmented, is observed at 15.47-MeV excitation, and provides a valuable reference for calibrations.

---

\*University of Birmingham, Birmingham, England.

<sup>†</sup>Catholic University, Washington, D.C.

<sup>‡</sup>National Bureau of Standards, Gaithersburg, Maryland.

<sup>§</sup>University of Massachusetts, Amherst, Massachusetts.

<sup>||</sup>NIKHEF, Amsterdam.

<sup>¶</sup>Free University, Amsterdam.

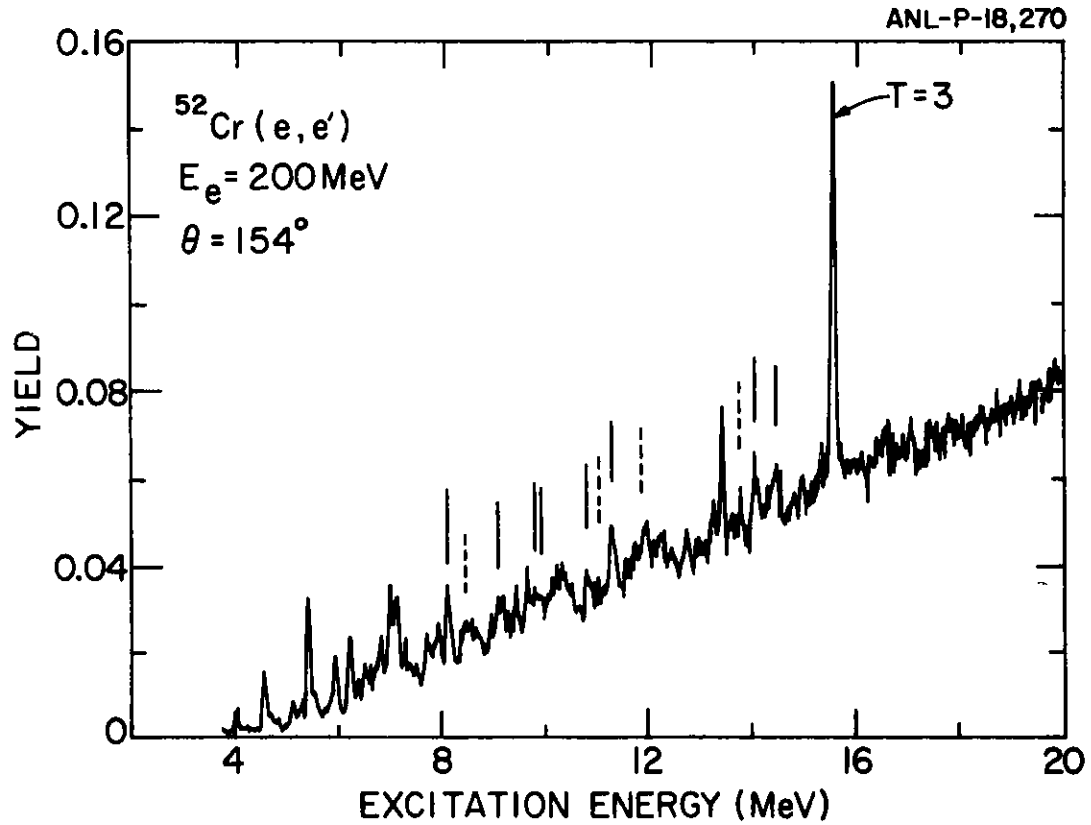


Figure I-7. Spectrum for inelastic scattering of 200-MeV electrons by  $^{52}\text{Cr}$  at an angle of  $154^\circ$ . The solid lines indicate the positions of  $T = 2$  states that probably involve  $8^-$  excitations, while the dashed lines denote other, less certain candidates. The yrast  $T = 3, 8^-$  state is also labeled.

## II. RESEARCH AT ATLAS

### Introduction

The highlight for heavy-ion physics research was the completion of the full ATLAS system. There was a concomitant transfer of effort from equipment and beam-line construction to research at ATLAS. The main themes of research are on reaction mechanisms of interacting heavy ions, nuclear structure at high spin and the interplay between the two. The areas of investigation are on quasielastic scattering, many aspects of complete and incomplete fusion, fission, structure of nuclei at high temperature and spin, resonances in heavy-ion reactions, accelerator mass spectrometry, and a broad range of other topics.

In heavy ion reactions we have found that a large fraction of the cross-section is in quasielastic processes, including few-nucleon transfer. A large body of data makes apparent a systematic dependence of neutron transfer cross section on ground-state Q values, which can be understood in terms of a random walk process within a potential energy surface in the N-Z plane. The coupling of the quasielastic process to other reaction channels, has been studied and found to be important, particularly near the barrier where it may account for some of the enhancement in sub-barrier fusion cross sections. A substantial fraction of the overall effort is directed towards studying many aspects of fusion, including dynamics of fusion near the barrier, compound nucleus decay, with emphasis on shape relaxation and fission and the possible influence of shell effects on these processes, the transition from fission to quasifission with increasing Coulomb repulsion, and the change from complete to incomplete fusion with increasing energy. The evolution of nuclear structure with spin, neutron number and temperature is being probed and progress has been made in understanding the transition from the oblate coupling scheme near the yrast line (in certain nuclei) to a rotational one with increasing temperature and spin. The origin of resonances in the interaction of heavy ions is being studied, including the possible connection to shell effects at high spin. Several important advances in accelerator mass spectrometry have been made with the use of the full tandem-linac accelerator and the gas-filled spectrograph, making it possible to detect heavy isotopes, e.g.  $^{41}\text{Ca}$  and  $^{60}\text{Fe}$ . Several other topics outside the above classification were also investigated. Among these are the investigation of static octupole deformation in nuclei, condensed crystalline state in cooled heavy-ion beams, and the emission of heavy clusters such as  $^{14}\text{C}$  and  $^{34}\text{Si}$  from heavy nuclei.

A major fraction of our effort was devoted to building up the ATLAS experimental area. In addition to installing beam lines, with the requisite controls and diagnostics, several major facilities were prepared: a general-purpose scattering chamber; Phase I of the Argonne-Notre Dame gamma facility, consisting of 7 Compton-suppressed Ge detectors and 14 BGO hexagons as a multiplicity filter; an Enge split-pole spectrometer; two general-purpose beam lines for mounting temporary setups; and an atomic physics beam line. A sophisticated data-acquisition system, DAPHNE, was developed, based on multiple microprocessors, to handle data from a new generation of experiments. Considering that the equipment, acquisition system and accelerator were all new, it was very gratifying that all functioned well for the first ATLAS beams, resulting in completely successful experiments.

### A. QUASIELASTIC PROCESSES AND STRONGLY DAMPED COLLISIONS

The study of quasielastic processes in heavy systems has been further actively pursued. These processes had generally been overlooked in reaction studies because they are difficult to resolve from the elastic-scattering contribution unless excellent experimental conditions are available. This has also led to the belief that the contributions of these processes are small compared to the total reaction cross section. The present studies clearly reveal that these quasielastic processes constitute a major fraction of the total reaction cross section. At ATLAS the availability of high-quality beams with masses  $A \gtrsim 40-80$  and with energies sufficient to overcome the Coulomb barrier for even the heaviest target nuclei, and the availability of high-resolution spectrometers in the form of the split-pole magnetic spectrographs with sophisticated focal-plane gas detectors, have allowed such measurements. A detailed study of quasielastic reaction strength in the Ni + Sn system indicates the importance of these channels on the average nucleus-nucleus potential. At subbarrier energies, the importance of transfer channels for fusion enhancement has been investigated. Some of the experiments performed over the last year were aimed at getting a better understanding of the mass and energy dependence of transfer reactions induced by medium-weight projectiles. In several systems (Ni + Sn, Ni + Pb) it was tentatively concluded that the cross sections for neutron transfer reactions stay constant over a large range of energy (up to 160 MeV (for  $^{58}\text{Ni} + ^{208}\text{Pb}$ ), while the cross sections for charge transfer increase strongly with higher bombarding energies. For all neutron transfer processes a systematic behavior has been found which depends on the ground-state Q-values  $Q_{gg}$ . From these systematics, neutron transfer cross sections for the heaviest systems can be predicted. A model has been developed to understand the distribution of the reaction strength, quasi-elastic and strongly damped, using a random walk description in the potential energy surface of the N-Z plane. For the system Ni + Sn it was observed that at incident energies very close to the barrier ( $E - V_c \approx 10$  MeV), strongly-damped processes with energy losses exceeding 30 MeV seem to occur with a surprisingly large fraction, about 1/3, of the total reaction cross section.



- a. Quasielastic Processes in Si-Induced Reactions on Pb (R. J. Vojtech,\* J. J. Kolata,\* K. E. Rehm, D. G. Kovar, G. S. F. Stephans, G. Rosner, and H. Ikezoe)

The previous study of  $^{28}\text{Si} + ^{208}\text{Pb}$  quasielastic reaction products at  $E_{\text{lab}} = 225$  MeV was extended by measurements performed at  $E_{\text{lab}} = 166$  MeV. Also, to study the influence of Q values and nuclear structure, the reactions  $^{28}\text{Si}$ ,  $^{30}\text{Si} + ^{208}\text{Pb}$  and  $^{30}\text{Si} + ^{208}\text{Pb}$  at  $E_{\text{lab}} = 122$  MeV were measured. These measurements, performed with the split-pole magnetic spectrograph, are characterized by energy resolutions of 400 keV, allowing studies of transitions to resolved final states in the nucleus. The elastic and inelastic scattering analysis of  $^{28}\text{Si} + ^{208}\text{Pb}$  at 166 MeV was performed using a coupled-channels treatment, as dictated by the earlier analysis of the same reaction at  $E_{\text{lab}} = 225$  MeV, where the inelastic scattering was found to be dominated by the Coulomb excitation of the 1.778-MeV  $2^+$  level in  $^{28}\text{Si}$ . The CCBA calculations reproduce the strengths and angular distributions of the elastic,  $^{28}\text{Si} (2^+)$ , and a multiplet of unresolved states at 4.5 MeV, and do poorly on the  $^{208}\text{Pb} (3^-)$  state. The failure of the CCBA to reproduce the  $^{208}\text{Pb}(3^-)$  behavior may be due to strong coupling of the  $3^-$  to one of the other reaction channels at this bombarding energy. The total quasielastic transfer cross section was also measured and found to account for a significant part of the total reaction cross section at this energy. Quasielastic one-neutron transfer in particular, is found to make up 15% of the 1083-mb total reaction cross section. This compares to 9% observed at 225 MeV. Further analysis of the data is proceeding.

---

\*University of Notre Dame, South Bend, Indiana.

b. Quasielastic Processes in the  $^{28}\text{Si} + ^{40}\text{Ca}$  Reaction at 225 MeV  
(M. F. Vineyard, D. G. Kovar, G. S. F. Stephans, K. E. Rehm,  
G. Rosner, H. Ikezoe, J. J. Kolata,\* and R. Vojtech\*)

In the past year, we have completed a study of the quasielastic processes in the  $^{28}\text{Si} + ^{40}\text{Ca}$  reaction at 8 MeV/A. This study was performed to investigate the applicability of the distorted-wave Born-approximation (DWBA) in describing one-nucleon transfer reactions to discrete final states induced by heavier projectiles and at higher energies than have previously been studied. Data for the elastic and inelastic scattering, and for single-nucleon transfer reactions to discrete final states were taken in the Enge split-pole magnetic spectrograph using a position-sensitive ionization chamber in the focal plane. The inelastic scattering and transfer data were analyzed in the framework of the DWBA with considerable success showing that this simple first-order theory remains a valuable tool for predicting direct reaction behaviors for medium-mass heavy-ion systems.

---

\*University of Notre Dame, South Bend, Indiana.

c. Study of Transfer Reactions in the System  $^{58}\text{Ni} + ^{208}\text{Pb}$  at High Incident Energies (K. E. Rehm, F. L. H. Wolfs, W. Phillips, F. Videbaek, M. Vineyard, and J. L. Yntema)

We have studied the energy dependence of the transfer channels in the system  $^{58}\text{Ni} + ^{208}\text{Pb}$  with beams from ATLAS. In our previous studies of the transfer strength in the system  $^{58}\text{Ni} + ^{208}\text{Pb}$  at energies in the vicinity of the Coulomb barrier ( $E/V < 1.25$ ) it was observed that the cross sections for charge transfer reactions increase with increasing incident energy, whereas the cross sections for neutron transfer processes stay constant. We have therefore extended our measurements to energies of about twice the Coulomb barrier using the full ATLAS accelerator. The experiment was performed in the new split-pole spectrograph in target area III (Fig. II-1). The data analysis for this experiment is still in progress. From the results obtained so far it can be concluded that increasing the bombarding energy from 345 MeV to 550 MeV has no influence on the strength of the neutron transfer reactions. The cross sections for charge transfer reactions on the other hand are still increasing and are even stronger than for the neutron transfer channels. An analysis of the data in the framework of a random walk model is in progress.

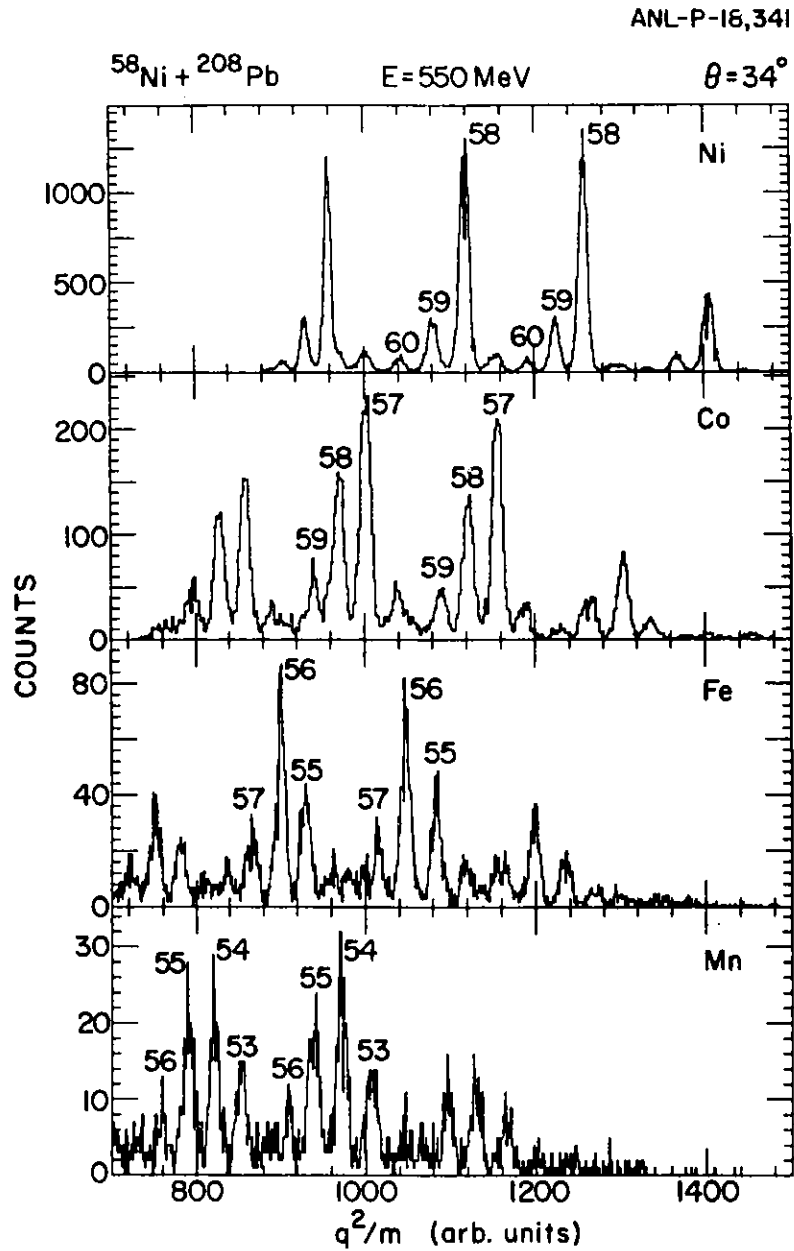


Figure II-1. Mass spectra for several elements between  $Z = 25 - 28$ .

- d. Quasi- and Deep-Inelastic Reactions Studied in the System  
 $^{80}\text{Se} + ^{208}\text{Pb}$  (K. E. Rehm, Ch. Beck, D. G. Kovar, W. C. Ma,  
 F. Videbaek, M. Vineyard and T. F. Wang)

In continuation of our studies of the interaction between medium-weight projectiles and heavy target nuclei, we have investigated the system  $^{80}\text{Se} + ^{208}\text{Pb}$  at  $E_{\text{Lab}} = 525$  MeV. The experiment was performed at the new spectrograph in the ATLAS experimental area. Angular distributions were measured in the angle range  $\theta_{\text{Lab}} = 20^\circ - 55^\circ$  covering the excitation energy range from elastic to deep-inelastic scattering. The data analysis for this experiment is still in progress.

- e. Study of Neutron Transfer Cross Sections for Ni + Ni Systems Below the Coulomb Barrier (F. Videbaek, B. B. Back, W. Henning, K. E. Rehm, and S. J. Sanders)

A study to extend the few-nucleon transfer reactions of  $^{58}\text{Ni} + ^{64}\text{Ni}$  to energies well below the Coulomb barrier is underway at ATLAS. This scattering system has an unusually large subbarrier fusion cross section and it has been suggested that this enhancement may be related to the details of the couplings between elastic and transfer channels. The transfer cross sections have been measured at and above the barrier (see Sec. c). Our measurement will extend these cross sections to lower energies where the anomalous fusion cross sections are observed. The split-pole spectrometer is used to identify the reaction products by measuring magnetic rigidity, residual energy and time-of-flight. The measurement at  $E_{\text{cm}} = 93.4$  MeV has been completed. The data for this energy is displayed with the data from Sec. c. in Fig. II-2. Further measurements at lower energies, which require good time resolution are scheduled for the summer.

ANL-P-18,213

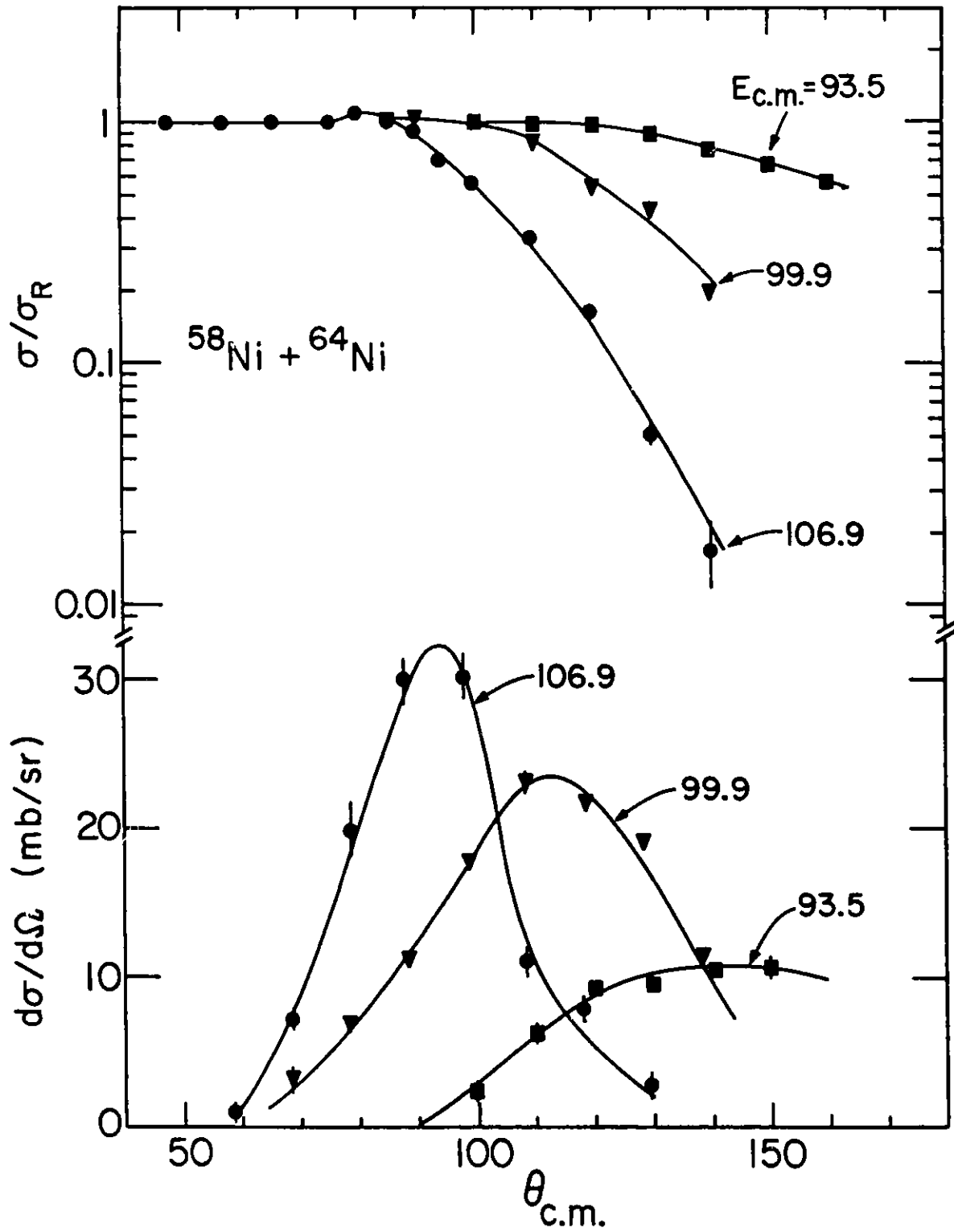


Figure II-2. Angular distributions for elastic scattering (top) and one-nucleon transfer reactions (bottom).

f. Elastic Scattering, Quasielastic and Total Reaction Cross Sections Near the Barrier for  $^{58}\text{Ni} + \text{Sn}$  (F. L. H. Wolfs,\* A. M. van den Berg, W. S. Freeman,† W. Henning, K. E. Rehm, J. P. Schiffer and R. H. Siemssen)

Very limited information exists on the distribution of the reaction strength in heavy-ion collisions at energies close to the Coulomb barrier. In continuation of our systematic studies of reactions in the Ni + Sn systems, we have measured the elastic scattering (not resolving inelastic scattering) and transfer yields at the same center-of-mass energy for  $^{58}\text{Ni} + ^{112}\text{Sn}$  and for  $^{58}\text{Ni} + ^{124}\text{Sn}$  ( $E_{\text{lab}} = 253.7$  MeV and 245.8 MeV, respectively). The measurements were performed with the split-pole magnetic spectrograph. The quasielastic transfer cross sections change from 75 mb for  $^{58}\text{Ni} + ^{112}\text{Sn}$  to 245 mb for  $^{58}\text{Ni} + ^{124}\text{Sn}$ . The total reaction cross sections, obtained from the analyses of the elastic scattering yields, including inelastic yields up to  $E_x = 5$  MeV, change from 320 mb for  $^{58}\text{Ni} + ^{112}\text{Sn}$  to 570 mb for  $^{58}\text{Ni} + ^{124}\text{Sn}$ . Comparing the total reaction cross sections with the sum of the quasielastic cross sections and the previously measured fusion cross sections, a deficit of 180 mb is observed for both systems, possibly due to a process that may be related to deep inelastic scattering. In a forthcoming experiment we will try to establish whether this is the case. It would be quite surprising if there are indeed substantial contributions from such processes to the total reaction cross sections at energies around the barrier. This would imply di-nuclear composite systems of very large deformation.

---

\*Graduate Student, University of Chicago, Chicago, Illinois.

†Fermi National Accelerator Laboratory, Batavia, IL.

- g. Quasielastic Transfer for  $^{58,64}\text{Ni}$  Induced Reactions on Even-A Tin Isotopes Well Above the Barrier (A. M. van den Berg, W. S. Freeman,\* W. Henning, L. L. Lee,† K. T. Lesko, K. E. Rehm, J. P. Schiffer, G. S. F. Stephans, F. L. H. Wolfs)

We have completed<sup>1</sup> a study of quasielastic transfer reactions induced by  $^{58}\text{Ni}$  beams at 330 MeV and  $^{64}\text{Ni}$  beams at 341 and 380 MeV, respectively, on  $^{112,116,120,124}\text{Sn}$ . Angular distributions for elastic (+ inelastic) scattering were analyzed using the coupled-channels reaction code PTOLEMY, from which the total reaction cross sections were obtained. The angular distributions for quasielastic neutron-transfer reactions are bell-shaped and peak at angles roughly 10 degrees smaller than the grazing angle for elastic scattering. The angle-integrated cross sections for one- and two-neutron pickup (stripping) reactions increase (decrease) smoothly as a function of neutron excess of the composite system and, consequently, as a function of Q value or neutron binding-energy difference.

The mean behavior observed in the total neutron-transfer strengths, as well as the behavior of the overall quasielastic nucleon-transfer strength (Fig. II-3) suggests that it is reasonable to discuss the effects of these reaction channels on the interaction potential in an average way. From the measured cross-section magnitude and the angular distributions, and using semi-classical trajectory calculations, we find that altogether for the grazing partial waves transfers and inelastic excitations amount to a total quasielastic cross section of 830 mb or more than 95% of the elastic flux entering the collision zone.

The surface nature of the quasielastic processes in these heavy systems is, of course, not unexpected. What appears surprising, though, is the quantitative extent of the nearly-complete exhaustion of the elastic flux by these processes over a certain region in distance of closest approach. We suspect that the quasielastic reaction channels have a dominant influence on the average macroscopic scattering potential at these interaction distances.

---

<sup>1</sup>A. M. van den Berg et al., Phys. Rev. Lett. 56, 572 (1986).

\*Fermi National Accelerator Laboratory, Batavia, IL.

†State University of New York, Stony Brook, NY.



ANL-P-17,716

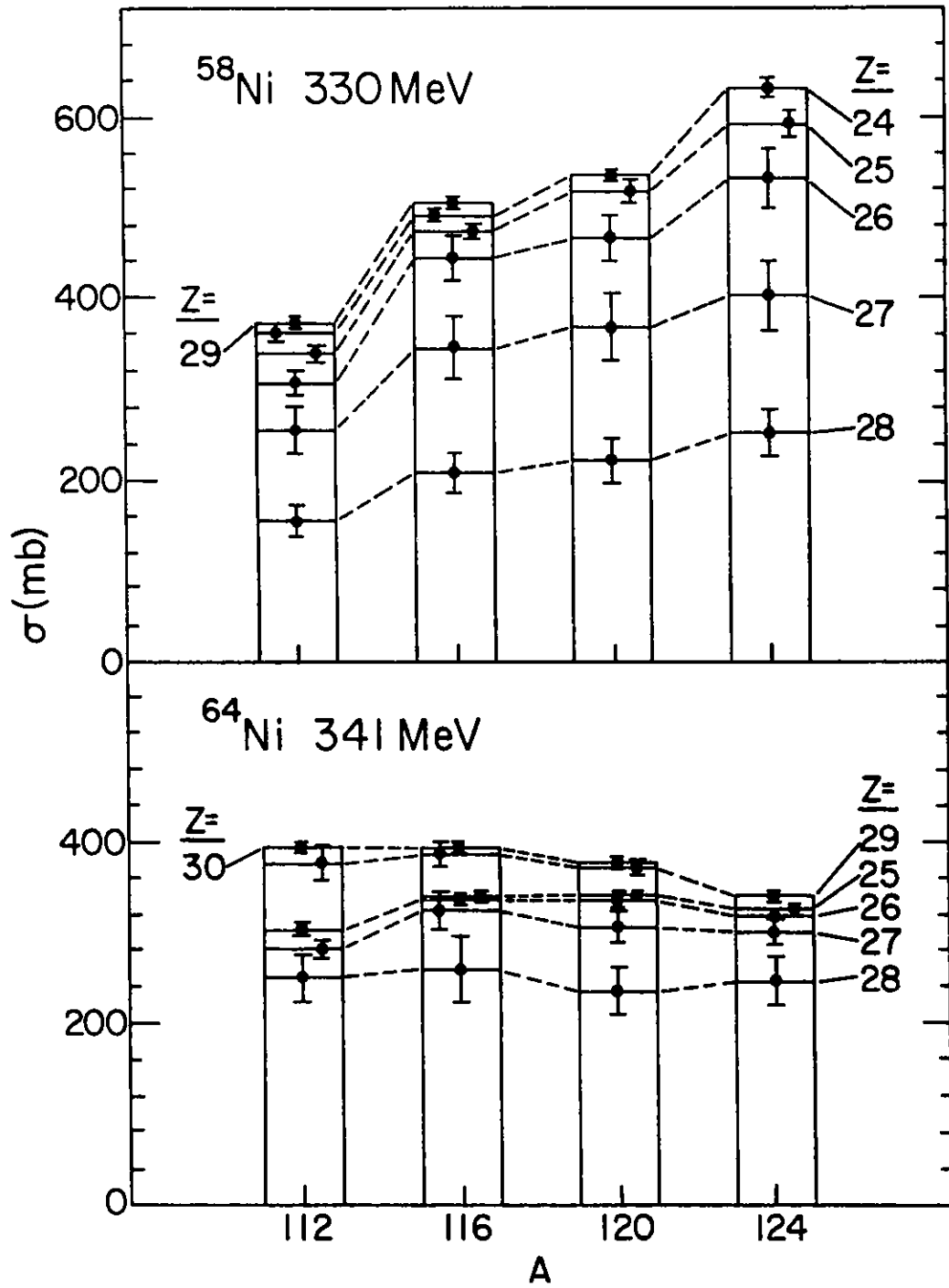


Figure II-3. Mean behavior in total neutron-transfer strengths and overall quasielastic nucleon-transfer strength.

h. A Random Walk Model for The Transition from Quasielastic to Deep-inelastic Collisions (K. E. Rehm)

The good mass and charge resolution achieved in our studies of transfer reactions induced by medium weight projectiles allows a detailed study of the transition from quasi-elastic to deep inelastic processes. Previous studies in that field concentrated mainly on the deep inelastic part of the cross section, mainly because of limitations in the particle identification of medium-weight projectiles. In our experiments with  $^{48}\text{Ti} + ^{208}\text{Pb}$  at  $E_{\text{lab}} = 300$  MeV Wilczynski plots for a variety of fully-resolved reaction products (in A and Z) near  $^{48}\text{Ti}$  could be produced. In order to get a better understanding of the important reaction channels a model has been developed which is based on a random walk in the two-dimensional N-Z-plane. The main ingredients of the model are the underlying driving potential and the energy loss per transfer step which was taken from experimental data. With this model a quantitative description of the Q-value-spectra for the reaction products measured in the system  $^{48}\text{Ti} + ^{208}\text{Pb}$  was achieved. Figure II-4 shows a comparison of the experimental data and the random-walk predictions for the integrated cross sections and the average Q-values for several reaction channels from the reaction  $^{48}\text{Ti} + ^{208}\text{Pb}$ . The results obtained so far indicate that there is a continuous transition from quasi-elastic to deep-inelastic reactions. A comparison with data from other systems is in progress.

ANL-P-18,015

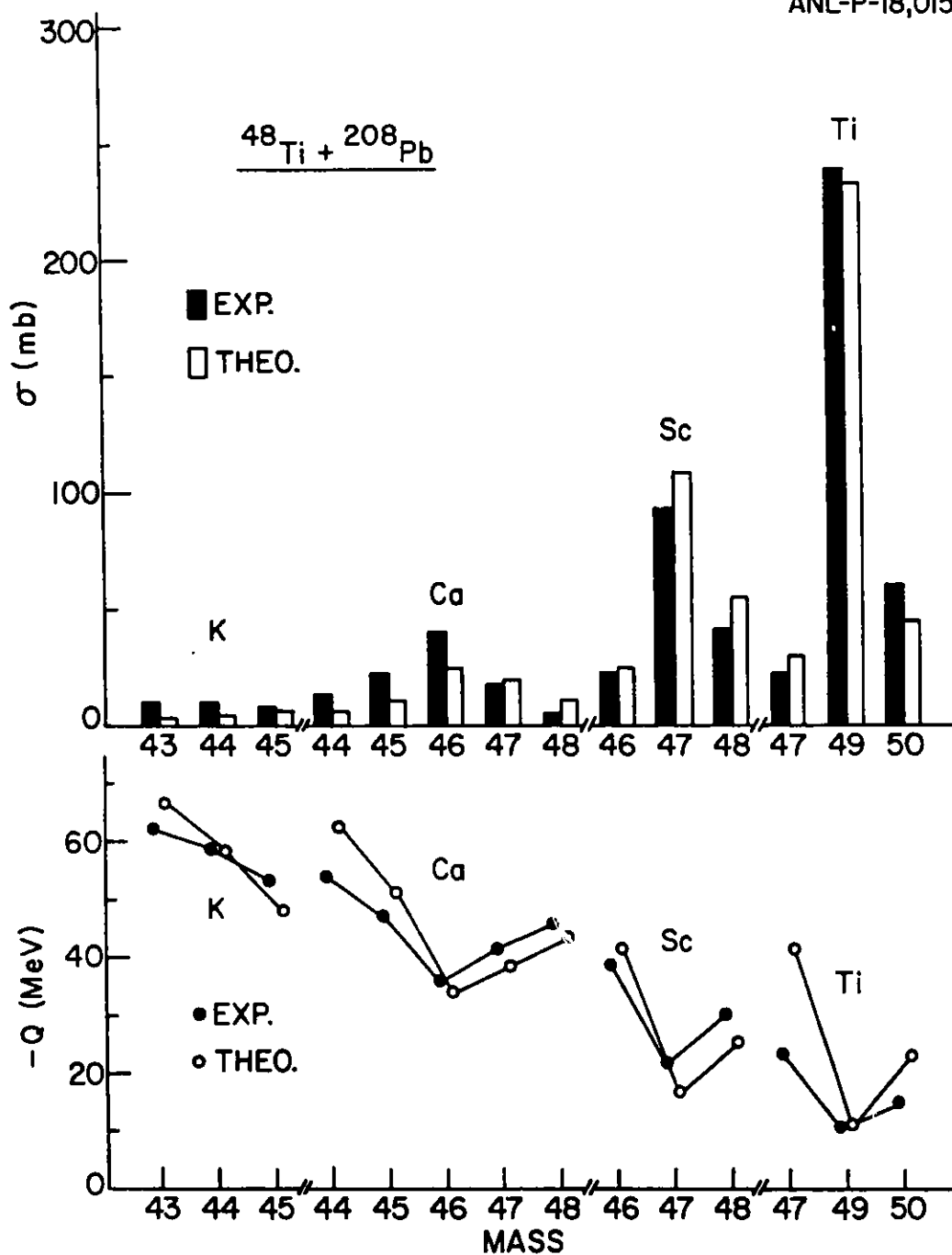


Figure II-4. Comparison of experimental data since theoretical predictions for integrated cross sections and average Q-values for several reactions channels from the reaction  $^{48}\text{Ti} + ^{208}\text{Pb}$ .

1. Proximity Effects in Deep-Inelastic Collisions in the Reactions of  $^{32}\text{S}$  with  $^{58}\text{Ni}$  (P. L. Gonthier\*, R. Ramaker\*, D. Mogdrige\*, D. G. Kovar, G. S. F. Stephans, A. van de Berg, B. Wilkins, M. Vineyard)

An experiment was performed to measure proximity effects in the deep-inelastic reactions of 280-MeV  $^{32}\text{S}$  with  $^{58}\text{Ni}$  by measuring  $\alpha$  particles in coincidence with projectile-like fragments detected at  $\pm 40^\circ$ . The data were analyzed in terms of the sequential emission of  $\alpha$  particles from both projectile-like (PLF) and target-like fragments (TLF). The comparison of the coincidence data with the three-body Coulomb trajectory calculations indicate the shadowing of the  $\alpha$  particles emitted from the TLFs. The shadowing results from the effect on the  $\alpha$  particle trajectory on the proximate Coulomb field of the PLFs. From these comparisons between the calculation and the coincident energy spectra and angular correlations, the average lifetime of target-like fragments was estimated to be  $1-5 \times 10^{-21}$  seconds which is in agreement with the lifetime predicted by the statistical model.

In order to obtain this result with adequate statistics, we had to examine the energy spectra of  $\alpha$  particles in coincidence with PLFs of atomic numbers between 11 and 16. The entire energy distribution of the PLFs was also included. These considerations make it more difficult to make precise comparisons with model calculations. Much more information could have been extracted from the data, if the statistics were such that we could put windows on the energy distribution of the PLFs for a specific atomic number.

There are plans to continue these studies at the ATLAS facility with higher bombarding energies and with larger area detectors to improve the coincidence counting rate. The goals for these future experiments are to study the evolution of light particle emission from the two strongly-interacting nuclei as the lifetime for particle emission decreases to the point at which the two nuclei emit particles while still interacting and to explore the rate of energy dissipation during the interaction.

---

\*Hope College, Holland, MI.

j. Systematics of Neutron Transfer Cross Sections in Heavy Systems

(K. E. Rehm, A. van den Berg, D. G. Kovar, W. Kutschera, and J. L. Yntema)

In the last few years a large number of quasi-elastic neutron transfer cross sections have been measured for systems ranging from  $^{58}\text{Ni} + ^{58}\text{Ni}$  to  $^{64}\text{Ni} + ^{208}\text{Pb}$ . We have started to look for systematic behaviour in these cross sections. Figure II-5 shows as functions of the ground-state Q-value cross sections integrated over all angles and excitation energies for one- and two-neutron pickup reactions measured for a variety of different systems at energies for the one-neutron pickup reactions of about 25% above the Coulomb barrier. In addition to the general trend of increasing cross sections with increasing Q-value, a systematic dependence of the cross sections on the projectile neutron excess is also evident in Fig. II-5(a). Transfer reactions induced by projectiles with a high N/Z ratio (e.g.  $^{37}\text{Cl}$ ,  $^{50}\text{Ti}$ ,  $^{64}\text{Ni}$ ; open symbols in Fig. II-5) show generally larger cross sections as compared to the results obtained from reactions induced by projectiles like  $^{28}\text{Si}$ ,  $^{46}\text{Ti}$ ,  $^{58}\text{Ni}$  (see full symbols). The only case involving an unpaired neutron ( $^{58}\text{Ni} + ^{149}\text{Sm}$  shown as cross Fig. II-5) does not fall into either of these two curves.

The cross sections for two-neutron pickup reactions (e.g.: A( $^{58}\text{Ni}$ ,  $^{60}\text{Ni}$ )B) induced by neutron deficient projectiles are shown in relation to the corresponding one-neutron pickup reactions in Fig. II-5(b). The cross sections at a given Q-value are generally smaller than the corresponding one-neutron transfer cross sections by about a factor of 10 and seem to saturate for very positive Q-values.

The Q-value dependence of the cross sections for different systems can be understood from the underlying Q-matching effects. The dashed lines in Fig. II-5 are obtained from an integration of a Gaussian-shaped Q-bump centered at the optimum Q-value  $Q_{\text{opt}}$  from the ground-state Q-value  $Q_g$  to high excitation energies. From this systematics it is now possible to predict the strengths of neutron transfer cross sections for even heavier systems. The predictions are generally in good agreement with experimental data.

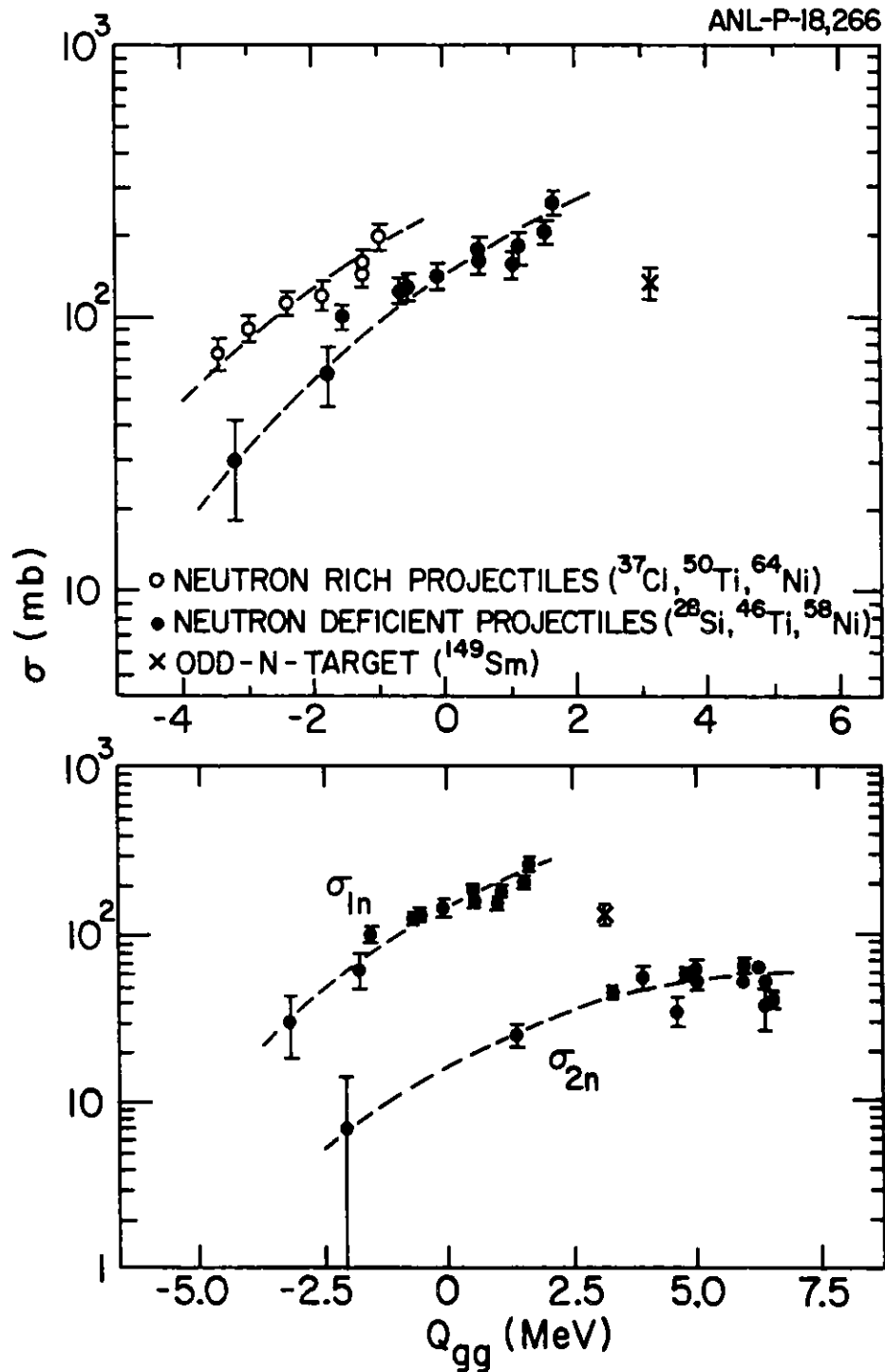


Figure II-5. a) Cross sections for one-neutron pickup reactions measured for various systems as function of the ground state  $Q$ -value  $Q_{gg}$ . The open symbols are the results using neutron-rich projectiles ( $^{64}\text{Ni}$ ,  $^{50}\text{Ti}$ ,  $^{37}\text{Cl}$ ) while the full symbols are from reactions with neutron-deficient projectiles ( $^{58}\text{Ni}$ ,  $^{46}\text{Ti}$ ,  $^{28}\text{Si}$ ). The cross is from the ( $^{58}\text{Ni}$ ,  $^{59}\text{Ni}$ ) reaction on an odd-neutron number target ( $^{149}\text{Sm}$ ). b) Two-neutron pickup reaction induced by neutron-deficient projectiles ( $^{58}\text{Ni}$ ,  $^{46}\text{Ti}$ ,  $^{30}\text{Si}$ ) together with the corresponding one-neutron pickup reactions.

## B. FUSION AND FISSION OF HEAVY IONS

Studies of fusion, both complete and incomplete, represent a major component of research at ATLAS. Many aspects of the process are covered including: dynamics of fusion near and above the barrier; coupling between fusion and inelastic channels; decay of the compound nucleus via particle emission and fission, including defining the physical parameters which govern the decay; shape relaxation following formation and the possible influence of shell effects on this process; fission in both heavy and light nuclei, the transition to quasifusion and quasifission; incomplete fusion, the mechanism responsible for the process and the transition from complete to incomplete fusion; and the onset with increasing bombarding energy of processes with emission of very energetic light particles.

An active field of research is focussed on fusion near and below the barrier. Efforts are directed towards a detailed understanding of the process, in particular the couplings between fusion, inelastic and transfer channels and the influence of these couplings in enhancing fusion near the barrier and in affecting the partial wave cross sections leading to fusion. To gain information on the properties and relaxation processes of nuclei formed in fusion of heavy ions, several experiments have been conducted. The decay through fission and particle evaporation has been investigated for Ni + Sn over a wide range of neutron number and incident energy and the process is well characterized in CASCADE calculations using a single set of model parameters. The energy dependence of the fusion cross sections also provides data for understanding the processes which limit the fusion leading to very heavy compound nuclei. The stage of shape relaxation has been probed through measurements of neutron multiplicity distributions,  $l$  distributions, evaporation residue cross sections, and entrance channel dependence of compound nucleus decay. It appears that the time scale for this process may be influenced by shell effects, resulting in relaxation times about  $10^3$  times slower than usual estimates. The quasi-fission process manifests itself in several ways, one of these being the high angular anisotropies observed in some of our earlier studies. In heavier systems with projectiles of  $A$  larger than 32 we have found experimentally that there is a clear correlation between the scattering angle and the mass of fission-like fragments. From such an analysis we have found the surprising result that the rate of mass transfer is essentially independent of the projectile-target combination, and more important, the temperature of the intermediate system. This latter observation provides strong support for the one-body dissipation mechanism, which, in contrast to two-body dissipation, is expected to show this temperature independence.

Extensive studies were performed to investigate processes of incomplete fusion where breakup and fragmentation of the incident projectile or target lead to fusion of only parts of the collision partners. The studies of incomplete fusion reactions have revealed features in the data which suggest that the mechanism responsible for incomplete fusion may be associated with Fermi motion of the nucleons in the interacting nuclei. When modelled in a simple quantitative way a number of features observed in the experimental data have a natural explanation. If this is indeed the mechanism which is, at least partially, responsible for incomplete fusion our presently held concepts about how one describes reactions as we go to higher bombarding energies ( $E_{\text{Lab}} > 10$  MeV/nucleon) will have to be altered significantly. The first generation

of light particle-evaporation residue coincidence measurements in which the masses of the residues were resolved have shown that there is hope of distinguishing, more quantitatively than had previously been possible, the products of complete and incomplete fusion.



- a. Fusion Evaporation Residues and the Distribution of Reaction Strength in  $^{16}\text{O} + ^{40}\text{Ca}$  and  $^{28}\text{Si} + ^{28}\text{Si}$  Reactions (J. Hinnefeld,\* J. J. Kolata,\* D. G. Kovar, C. Beck, M. F. Vineyard, D. Henderson, R. V. F. Janssens, K. T. Lesko, A. Menchaca-Rocha,† F. W. Prosser,‡ S. J. Sanders, G. S. F. Stephans, and B. Wilkins)

Previous experiments at Argonne involving the systems  $^{16}\text{O} + ^{40}\text{Ca}$  and  $^{28}\text{Si} + ^{28}\text{Si}$ , which form the same compound nucleus ( $^{56}\text{Ni}$ ), have demonstrated that at higher bombarding energies (above about 6 MeV/nucleon) the distributions of reaction strength are significantly different for the two systems. While the total reaction cross sections, as determined by optical-model calculations, are essentially the same for both entrance channels, the  $^{28}\text{Si} + ^{28}\text{Si}$  evaporation residue cross section is found to decrease rapidly with increasing energy, whereas the  $^{16}\text{O} + ^{40}\text{Ca}$  evaporation residue cross section remains essentially constant over the same energy range. This implies that either the fusion cross section or the evaporation-residue/fission competition in the two reactions differs significantly. To investigate this, coincidence measurements were made between  $A > 35$  and  $A > 12$  fragments for both systems at  $E_{\text{lab}} = 9$  MeV/nucleon. The goal was to clearly distinguish between evaporation residues and products of fission or other binary-like reactions. Because of the wide range of possible Q-values for binary reactions (measured Q values for coincident events range from about -40 MeV to about -105 MeV), it was impossible to detect both products of every binary reaction. Analysis of the data is proceeding.

---

\*University of Notre Dame, South Bend, Indiana.

†Universidad de Chile, Chile.

‡University of Kansas, Lawrence, KS.

- b. Time-of-Flight Measurements of Evaporation Residues from  $^{32}\text{S} + ^{24}\text{Mg}$   
 (J. Hinnefeld,\* J. J. Kolata,\* D. G. Kovar, R. V. F. Janssens,  
 K. T. Lesko, G. S. F. Stephans, G. Rosner, B. Wilkins, D. Henderson,  
 P. L. Gonthier,† and F. W. Prosser‡)

Previous experiments<sup>1</sup> at Argonne which looked for incomplete fusion processes in the systems  $^{16}\text{O} + ^{40}\text{Ca}$  and  $^{28}\text{Si} + ^{28}\text{Si}$  provided motivation for performing similar measurements with the system  $^{32}\text{S} + ^{24}\text{Mg}$ , which leads to the same compound nucleus ( $^{56}\text{Ni}$ ) and which is intermediate between these two systems in its degree of mass asymmetry. A time-of-flight detector system was used to measure angular distributions and velocity spectra for resolved evaporation residue masses in reactions induced by beams of  $E_{\text{lab}}(^{32}\text{S}) = 278, 239, \text{ and } 194 \text{ MeV}$ . Especially at the larger angles, the measurement of the differential cross sections was complicated by the overlap in mass between the evaporation residues and products of deep-inelastic reactions. The yield was estimated for each mass for which this ambiguity existed by comparison of the measured velocity spectrum with that predicted by a statistical model calculation. The measured total evaporation residue cross sections at these three energies are  $868 \pm 77, 916 \pm 54, \text{ and } 1013 \pm 46 \text{ nb}$ , respectively.<sup>2</sup> These values are much closer to  $^{28}\text{Si} + ^{28}\text{Si}$  than to  $^{16}\text{O} + ^{40}\text{Ca}$  cross sections at comparable energies above the Coulomb barrier. In addition, the measured centroids of the velocity spectra are consistent, within their uncertainties, with the predictions of complete fusion calculations.

---

\*University of Notre Dame, Notre Dame, Indiana.

†Hope College, Holland, Michigan.

‡University of Kansas, Lawrence, Kansas.

<sup>1</sup>D. G. Kovar, Fundamental Problems in Heavy-Ion Collisions, edited by N. Cindro, W. Greiner, and R. Caplar (World Scientific Publishing, Singapore, 1984), p. 185, and references therein.

<sup>2</sup>J. D. Hinnefeld et al., Bull. Am. Phys. Soc. 29, 1048 (1984).

c. Incomplete Fusion at 10 MeV/Nucleon in Heavy Asymmetric System:  
 $^{12}\text{C} + \text{A}(100-200)$  (I. Tserruya,\* W. Henning, D. G. Kovar, and M. Vineyard)

The cross sections for complete and incomplete fusion in collisions of  $^{12}\text{C}$  with  $^{90}\text{Zr}$ ,  $^{120}\text{Sn}$ , and  $^{197}\text{Au}$  were measured in the energy range  $E_{\text{lab}} = 90-130$  MeV. The measurements were performed using a large-area low-pressure multi-wire proportional counter situated at zero degrees immediately behind a small beam stopper covering  $1^\circ-1.5^\circ$  around the beam axis. The detector covers the angular range  $1.5^\circ-9.5^\circ$  with a nearly  $2\pi$  azimuthal geometry, measuring the position and time-of-flight of the particles detected. The time-of-flight spectra showed evidence of a slower velocity component which is identified with incomplete fusion (see Fig. II-6), and which was found to increase with increasing bombarding energy. The angular range allowed detection of  $\sim 80\%$  of the total evaporation residue yield in a single run and the extraction of an angular distribution adequate for establishing total cross sections. The preliminary results of the analysis imply that incomplete fusion begins at energies near the Coulomb barrier and grows rapidly with bombarding energies. This technique is more sensitive than that using the velocity measurements of evaporation residue centroids or the folding angle measurements of fission fragments. It allows study of incomplete fusion processes in the intermediate mass range ( $60 < A_{\text{CN}} < 200$ ). Future plans include coincidence measurements between evaporation residues and light particles for the systems previously studied in order to extract information on the energy spectra and angular correlation of the pre-equilibrium light particles emitted.

---

\*Weizmann Institute of Science, Rehovot, Israel.

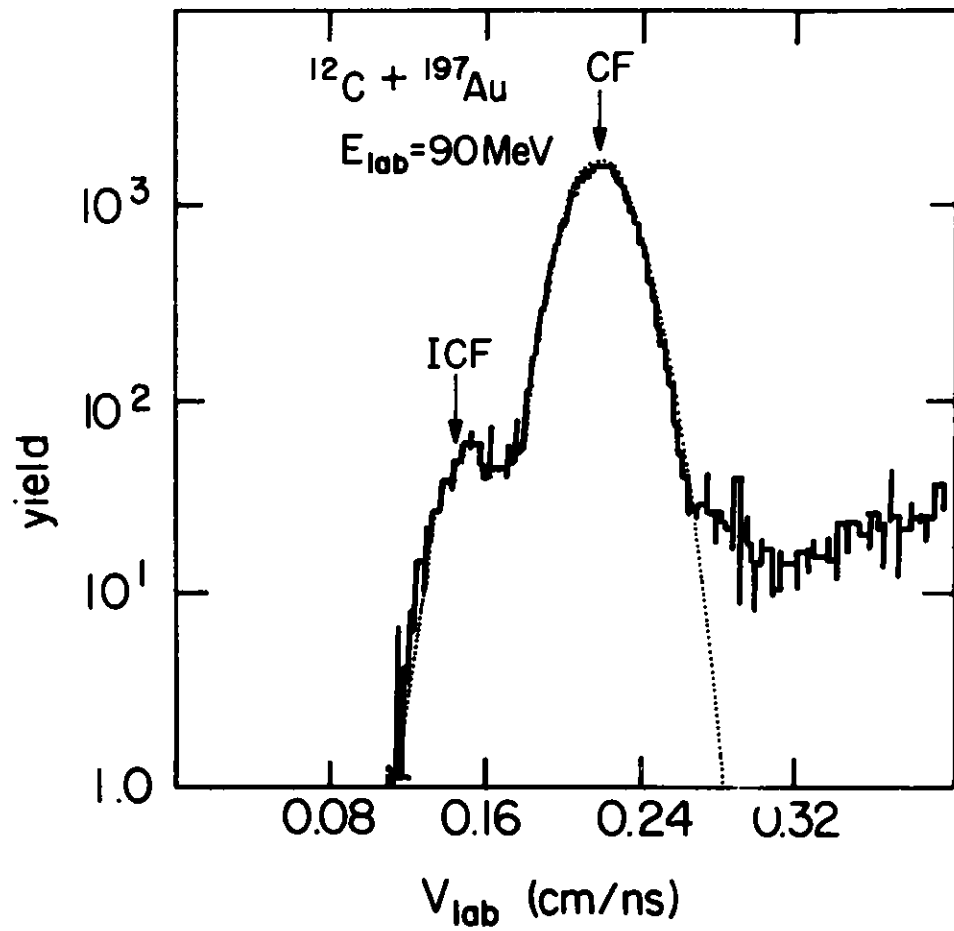


Figure II-6. Velocity spectrum obtained from time-of-flight measurements, showing evidence of a slower velocity component identified as incomplete fusion (ICF).

d. Light Particle Emission in Reactions Induced at  $E/A > 10$  MeV/Nucleon  
 (P. DeYoung,\* R. L. McGrath,† J. Alexander,† J. Gilfoyle,† M. Gordan,†  
 D. G. Kovar, C. Beck, M. Vineyard, K. Kossen,\* and M. Hammond\*)

At an energy of 215 MeV the light particles (p,d,t, $\alpha$  emitted from the  $^{16}\text{O}+^{27}\text{Al}$  reaction are produced via several competing reaction mechanisms. While a significant portion of the light particle cross section is the result of evaporation from a thermally equilibrated compound nucleus, the remainder of the cross section comes from mechanisms (such as hot spots) which are poorly understood. It is expected<sup>1</sup> that exclusive measurements such as correlations between light particles will enable one to distinguish the different components of the interaction. The  $^{16}\text{O}+^{27}\text{Al}$  reaction is of particular interest because past work by Awes et al.<sup>2</sup> has shown that a significant portion of the inclusive cross section is not accounted for by the statistical model.

The experiment consisted of three parts: inclusive light-particle angular distribution measurements, small angle light-particle coincidence measurements, and some preliminary light-particle heavy-fragment coincidence measurements. For the inclusive angular distribution measurement the light particles are detected in seven NaI(Tl) crystals<sup>3</sup> (particle identification from time-of-flight and pulse shape) and two back-angle  $\Delta E$ -E Si telescopes (particle identification from time-of-flight and  $dE/dx$ ). The detector configuration resulted in a large dynamic range and energy thresholds of an  $\sim 3$  MeV for  $Z = 1$  and  $\sim 8$  MeV for alpha particles, significantly better than previous measurements, and covered  $\theta_{\text{lab}} = 6^\circ - 170^\circ$ .

Good light particle identification was maintained down to the lowest energies by projecting the data not only onto the energy pulse-shape plane and energy time-of-flight (TOF) plane, but also utilizing a projection onto the

---

\*Hope College, Holland, Michigan.

†State University of New York, Stony Brook, N.Y.

<sup>1</sup>R. G. Stokstad, Comments Nucl. Part. Phys. 13, 231 (1984).

<sup>2</sup>T. C. Awes, S. Saini, G. Poggi, C. K. Gelbke, D. Cha, R. Legrain, and G. D. Westfall, Phys. Rev. C 25, 2361 (1982).

<sup>3</sup>P. DeYoung, R. L. McGrath, W. F. Piel, Jr., Nucl. Instr. and Meth. 226, 555 (1984).

pulse-shape TOF plane (Fig. II-7). For the small-angle correlation phase of the experiment NaI detectors were clustered in a hexagonal close-packed array centered at 53.5 degrees. This gave 21 pairs of detectors, 12 of which had a separation of 3 degrees to enhance the measurement of small relative momenta. To examine the influence of the light particles on the fragment distributions and the effect of detecting a fragment on the light-particle behavior a triple Si detector telescope was placed at forward angles in order to measure the residue and quasielastic angular distributions, both in singles and coincidence with the light particles.

It was also found that due to the excellent time resolution ( $\sim 120$  ps FWHM), the forward silicon detector could readily distinguish between different heavy residues that stopped in the front section of the telescope. Figure II-8 displays a plot of raw time-of-flight versus energy from that detector. In the lower half of the plot the recoil nuclei were stopped in the silicon so this pulse gives a true energy signal. In the upper half the ions passed through the detector into the second section of the telescope so that front detector registers a  $\Delta E$  pulse. The spectacular separation of the different masses for those ions stopping in this section of the telescope is readily apparent. This powerful technique will surely prove useful in the analysis of the interaction between the two nuclei.

The analysis has been divided between Stony Brook, Hope College, and Argonne and is well underway.

Future plans include increasing the statistics in the small-angle correlation phase, and expanding the range of angles covered in the light-particle, heavy-fragment portion of the experiment.

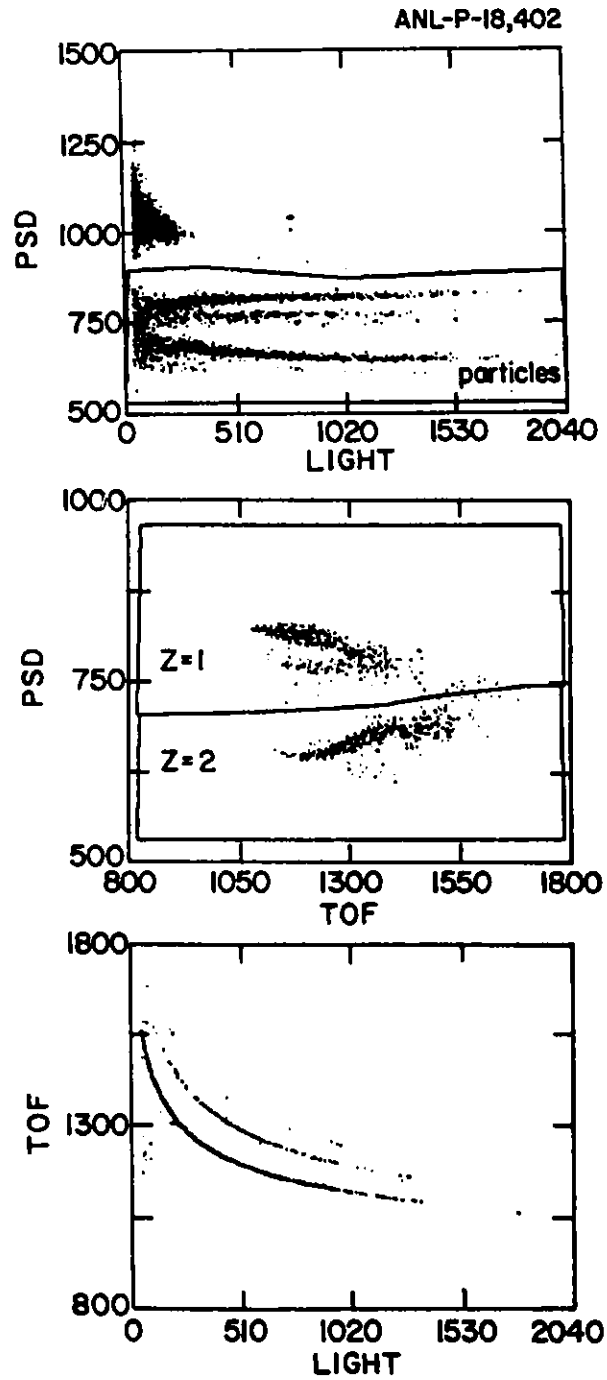


Figure II-7. Scatterplots for a NaI(Tl) detector at  $16^\circ$  and 80 cm from the target. The different light particles are resolved for all energies above  $\sim 3$  MeV.

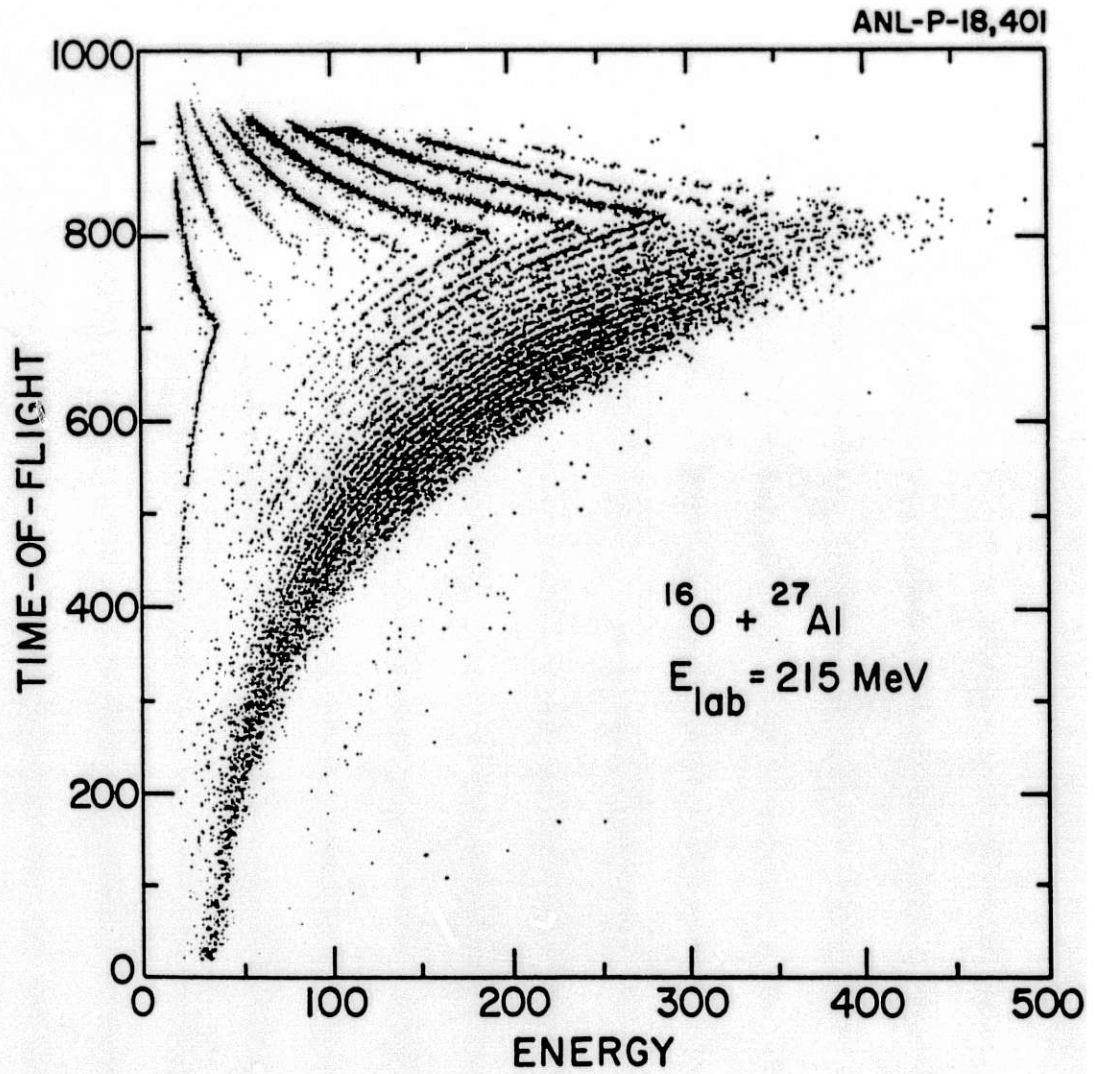


Figure II-8. Scatterplot of energy versus time-of-flight for the forward Si telescope, The mass range is  $A = 3$  to  $A = 37$ .



- e. Production of Very High Energy Light Particles in Heavy-ion Collisions at Zero Degrees (F. D. Becchetti,\* J. Janecke,\* P. Lister,\* R. Stern,\* D. G. Kovar, C. N. Davids, C. Beck, M. Vineyard, C. Maguire,† and J. J. Kolata‡)

Those runs at ATLAS using beams of 300- and 475-MeV  $^{32}\text{S}$  and 600-MeV  $^{58}\text{Ni}$  on thick Ta targets were performed where the energetic light particle production (p,d,t, $\alpha$ ,...) at  $0^\circ$  was measured. A large 5.0 cm  $\times$  15.0 cm long BGO scintillator was used in the initial runs as the fast-particle detector ( $E_p < 400$  MeV,  $E_\alpha < 2$  GeV). Particle identification was obtained using TOF and/or dE-E with the aid of a thin plastic dE detector. In a later run a large 4"  $\times$  4" NaI(Tl) detector was also used, where pulse-shape discrimination provided the particle identification. Very energetic protons ( $E_p > 100$  MeV) and  $\alpha$  particles ( $E_\alpha \approx E_{\text{beam}}$ ) were observed along with smaller numbers of deuterons and tritons. Unlike most observations of light particle production, we are concentrating on the region well above the beam velocity and, surprisingly, find significant light particle emission with  $E > \frac{1}{2} E_{\text{beam}}$ ; with alpha particles often extending out to approximately full beam energy and protons to approximately one half beam energy.<sup>1</sup> Further runs have been approved at ATLAS and the NSCL at Michigan State University to examine this phenomenon in more detail.

The results of the pulse-height and timing response of BGO to light and heavy ions obtained in calibration runs at IUCF and ATLAS have been published.<sup>2</sup>

---

\*University of Michigan, Ann Arbor, Michigan.

†Vanderbilt University, Nashville, Tennessee.

‡University of Notre Dame, Notre Dame, Indiana.

<sup>1</sup>P. Shulman et al., Bull. Am. Phys. Soc. 31, 840 (1986).

<sup>2</sup>F. Becchetti, P. Lister and C. Thorn, Nucl. Instrum. Methods 225, 280 (1984).

- f. Fusion of  $^{78}\text{Se} + ^{78}\text{Se}$  and  $^{82}\text{Se} + ^{82}\text{Se}$  (M. Piiparinen,\* M. Quader,\*  
R. V. F. Janssens, T. L. Khoo, W. Henning, W. Kühn,† K. T. Lesko,  
D. C. Radford, R. M. Ronningen,‡ and A. van den Berg)

These measurements are part of a series directed towards understanding the suppression of neutron emission observed in fusion of  $^{64}\text{Ni} + ^{92}\text{Zr} \rightarrow ^{156}\text{Er}$  and not seen in fusion of  $^{12}\text{C} + ^{144}\text{Sm} \rightarrow ^{156}\text{Er}$ .<sup>1</sup> The initial deformation upon fusion is larger in the former case and we have speculated that in the shape relaxation the compound nucleus may be trapped in a superdeformed potential minimum. This theoretically predicted minimum arises from shell structure effects and is expected to disappear in Er isotopes as the neutron number increases from 88 to 96. In  $^{78}\text{Se} + ^{78}\text{Se} \rightarrow ^{156}\text{Er}$  and  $^{82}\text{Se} + ^{82}\text{Se} \rightarrow ^{164}\text{Er}$  fusion the compound nuclei have these neutron numbers. If trapping in a superdeformed minimum is indeed the cause for neutron suppression, then this suppression should disappear in the latter case.

The channel yields have been measured in the fusion reaction of both systems in order to extract the neutron multiplicity distributions. These can be compared with results from our earlier experiments for  $^{156}\text{Er}$  and with published results for  $^{16}\text{O} + ^{148}\text{Nd} \rightarrow ^{164}\text{Er}$ . Data analysis is still in progress but the major results obtained so far can be summarized as follows: (i) in the  $^{78}\text{Se} + ^{78}\text{Se}$  reaction, the measured neutron multiplicities as a function of the excitation energy of the compound nucleus follow a curve very similar to the one observed in the  $^{64}\text{Ni} + ^{92}\text{Zr}$  reaction. Thus, the measured neutron multiplicities are lower at all energies than those calculated within the framework of the statistical model. (ii) for the  $^{82}\text{Se} + ^{82}\text{Se}$  reaction, severe problems with target impurities have limited the analysis so far and data of better quality will be required.

---

\*Purdue University, West Lafayette, IN.

†Universität Giessen, West Germany.

‡Michigan State University, East Lansing, MI.

<sup>1</sup>R. V. F. Janssens et al., submitted to Physics Letters.

g. Evaporation Residue Cross-Sections in Fusion of  $^{64}\text{Ni} + ^{92}\text{Zr}$  and  $^{12}\text{C} + ^{144}\text{Sm}$  (R. V. F. Janssens, R. Holzmann, W. Henning, T. L. Khoo, K. T. Lesko, G. S. F. Stephans, D. C. Radford, and A. van den Berg)

As part of a study to understand the origin of neutron suppression in  $^{64}\text{Ni} + ^{92}\text{Zr}$  fusion<sup>1</sup>, we have measured evaporation residue cross-sections. These measurements have also a direct bearing on the problem of enhanced sub-barrier fusion. Residue cross-section in fusion of  $^{64}\text{Ni} + ^{92}\text{Zr}$  and  $^{12}\text{C} + ^{144}\text{Sm}$  have been measured over a wide range of bombarding energies, including those below the Coulomb barrier. Using a technique previously developed here at ANL,<sup>2</sup> the residues were separated from the beam by electrostatic deflection and detected at 4 angles including  $0^\circ$ . The analysis has now been completed and the results are summarized in Fig. II-9. For the  $^{12}\text{C} + ^{144}\text{Sm}$  reaction [Fig. II-9(a)], the measured cross section agrees nicely (dashed line) with calculations using the extra push model.<sup>3</sup> These cross sections were then used in statistical-model calculations from which average neutron multiplicities were derived which compare well with experimental data available from a separate experiment.<sup>4</sup> In summary, all data available for the  $^{12}\text{C} + ^{144}\text{Sm}$  reaction can be accounted for consistently in the framework of the existing models.

Figure II-9(b) presents evaporation residues cross sections for the  $^{64}\text{Ni} + ^{92}\text{Zr}$  reaction. The dashed line represents a calculation with the extra push model. Clearly, this calculation does not agree with the data: at energies below the barrier ( $E_{\text{cm}} = 132.7$  MeV) the cross section is much larger than predicted, while above the barrier the measurements fall below the computed values. This comparison suggests that subbarrier enhancement of the fusion cross section is observed for this reaction, a phenomenon found to occur in many reactions with heavy ions. The deviations at higher energies most likely originate from the onset of fission, a process which escapes detection in the present measurement.

<sup>1</sup>W. Kühn et al., Phys. Rev. Lett. 51, 1858 (1983).

<sup>2</sup>W. S. Freeman et al., Phys. Rev. Lett. 51, 1563 (1983).

<sup>3</sup>W. J. Swiatecki, Physica Scripta 24, 113 (1981).

<sup>4</sup>R. V. F. Janssens et al., ANL Report No. ANL-84-24, p. 74.

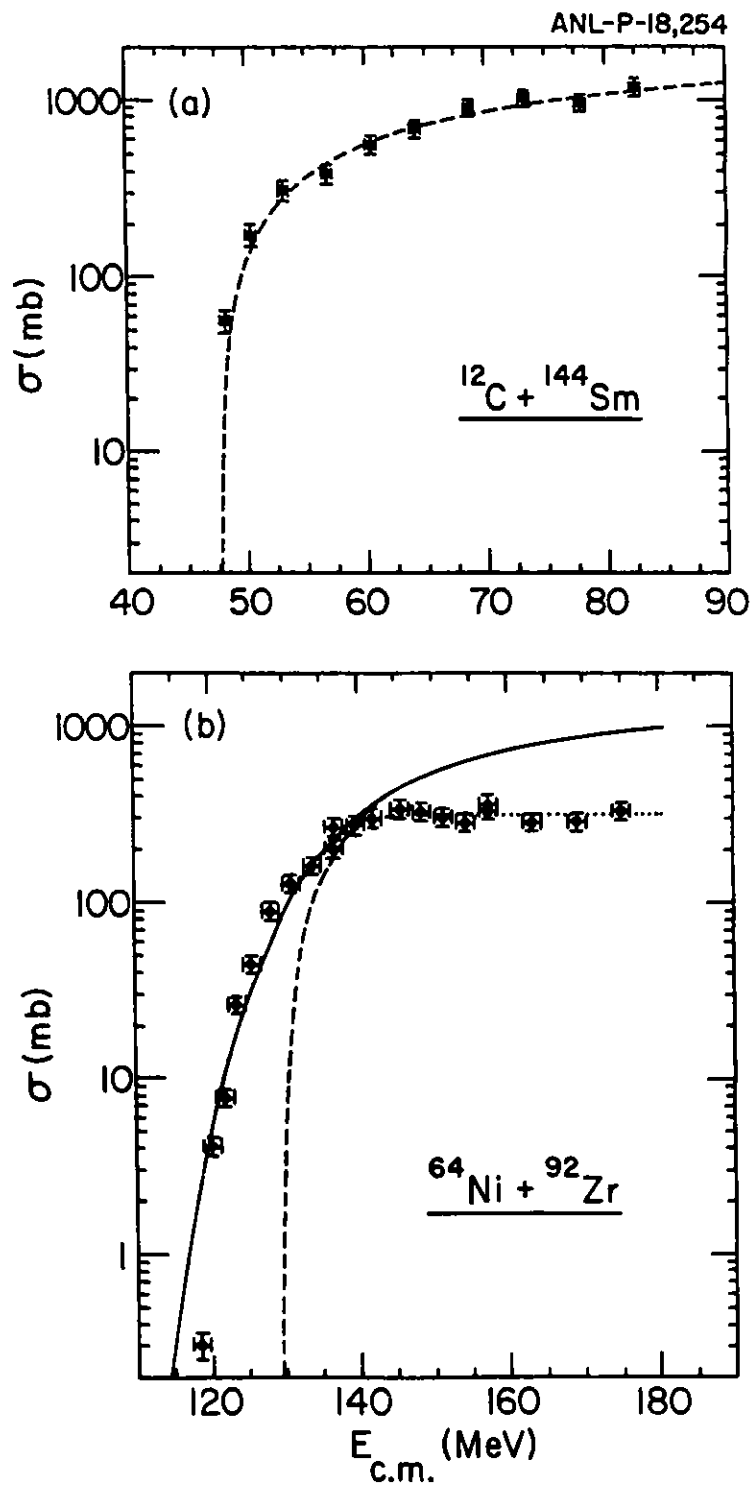


Figure II-9. Average neutron multiplicities for the  $^{12}\text{C} + ^{144}\text{Sm}$  and  $^{64}\text{Ni} + ^{92}\text{Zr}$  reactions as a function of the compound nucleus excitation energy. The solid lines present the statistical-model estimates.

The solid line in Fig. II-9(b) represents a fusion cross section calculation where the extra push model was modified to include the fluctuations in barrier height based on the model of Esbensen.<sup>5</sup> The fusion cross sections obtained in this way have been introduced into statistical-model calculations with the code CASCADE in order to compute fission and evaporation residues cross sections. Use was made of the fission barrier treatment proposed by Sierk<sup>6</sup> and the partial wave distribution of the compound nucleus was altered to reflect the coupling of the quasielastic channels by modifying the diffuseness parameter of the entrance channel transmission coefficients of CASCADE. The dotted line of Fig. II-9(b) presents the calculated evaporation residues cross section. Good agreement with the measurements is obtained. The same statistical calculations were also used to derive average neutron multiplicities for the  $^{64}\text{Ni} + ^{92}\text{Zr}$  reaction. The measured values are found to be lower by 0.5 neutrons on the average than those calculated. Thus the apparent inhibition of neutron emission persists even when high tails in the  $\sigma_\ell$  distribution are taken into account.

---

<sup>5</sup>H. Esbensen, Nucl. Phys. A352, 147 (1981).

<sup>6</sup>A. Sierk, private communication.

#### h. Total Fusion Cross Sections for Ni + Sn

(K. T. Lesko, W. Henning, K. E. Rehm, G. Rosner,\* J. P. Schiffer,  
G. S. F. Stephans, B. Zeidman, and W. S. Freeman†)

We have completed our studies of the fusion-fission cross sections for the reactions Ni + Sn. Excitation functions for fission were measured for  $^{58,64}\text{Ni}$  beams incident on the even  $^{112-124}\text{Sn}$  targets, for energies extending from well below to about 1.5 times the Coulomb barrier. From these and the previously measured cross sections for leaving evaporation residues we obtain the total fusion cross sections for the fission probabilities over the energy range  $130 \text{ MeV} < E_{\text{c.m.}} < 240 \text{ MeV}$ . The competition between particle evaporation and fission in the compound nuclei is compared to statistical-model calculations. A good description of the data for all 14 systems is achieved with the use of a single set of parameters for the model, including fission barriers with finite range and nuclear diffuseness effects as well as fusion partial wave distributions that are qualitatively consistent with microscopic reaction model calculations. The fusion excitation functions are analyzed in terms of the dynamical fusion model of Swiatecki et al. In Fig. II-10 we show the measured total-fusion excitation functions and model calculations without (dashed curves) and with (solid curves) extra push. Within this model we extract new values for the "extra-push" parameters.  $X_{\text{th}} = 0.64 \pm 0.05$ ,  $a = 7.8 \pm 0.6$ , and  $f = 0.55 \pm 0.05$ .

---

\*Technical University of Munich, W. Germany.

†Fermi National Accelerator Laboratory, Batavia, Illinois.

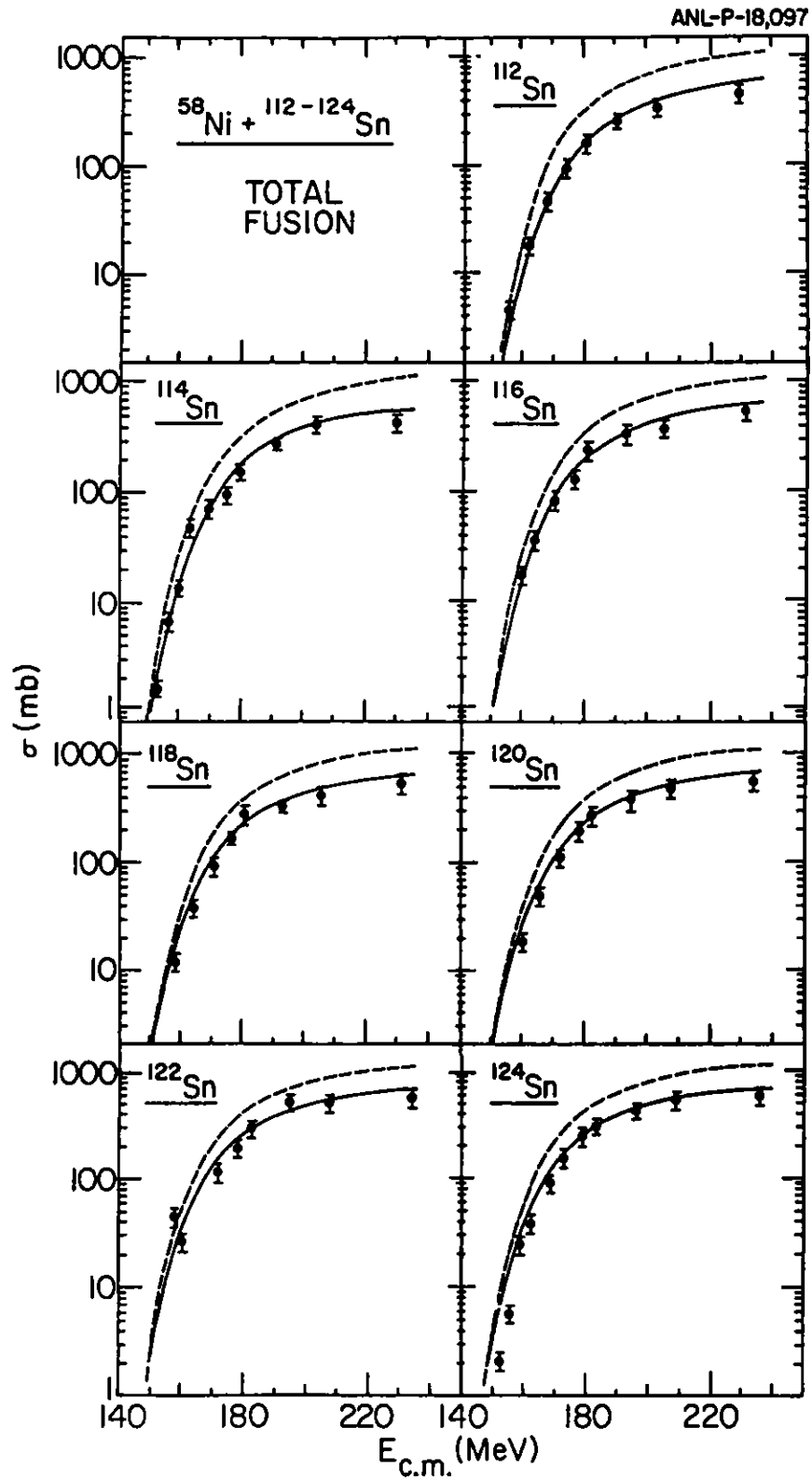


Figure II-10. Total-fusion excitation functions and model calculations without (dashed curves) and with (solid curves) extra push.

1. Status Report on  $^{24}\text{Mg} + ^{24}\text{Mg}$  Fusion (F. W. Prosser,\* S. V. Reinert,\*  
D. G. Kovar, G. Rosner, G. S. F. Stephans, J. J. Kolata,†  
A. Szanto de Toledo,‡ and E. Szanto‡)

Measurements have been made of the cross section for fusion leaving evaporation residues of  $^{24}\text{Mg} + ^{24}\text{Mg}$  at beam energies of 110, 159 and 205 MeV. Complete angular distributions of the fusion residues were taken at each energy with a time-of-flight telescope to obtain residue mass identification and the associated velocity spectra. Analysis of the data has been completed during the past year and a report of the results has been made. At 110 MeV the cross section of  $1078 \pm 43$  mb agrees well with earlier ANL measurements; at 159 and 205 MeV the cross sections were  $971 \pm 68$  and  $767 \pm 77$  mb, respectively. Comparisons with model calculations are being carried out. The calculations using the codes LILITA and PACE reproduce the magnitudes of the cross sections, assuming that fission limits them with a fission barrier of 7 MeV.

For symmetric systems the only possible signal for incomplete fusion in the residue spectra is an anomalous broadening of the velocity distribution. The experimental velocity distributions agree well with the predictions at 110 and 159 MeV, but the distribution at 205 MeV is significantly wider. If this result is confirmed by more detailed exclusive measurements, it will be the first evidence for incomplete fusion in light symmetric systems. Further measurements at the higher bombarding energies of ATLAS are planned.

---

\*University of Kansas, Lawrence, Kansas.

†University of Notre Dame, Notre Dame, Indiana.

‡Universidade de Sao Paulo, Sao Paulo, Brazil.



- j. Fission-like Yields in the  $^{16}\text{O} + ^{40,44}\text{Ca}$  Reactions (S. J. Sanders, R. R. Betts, I. Ahmad, B. K. Dichter, K. T. Lesko, S. Saini, B. D. Wilkins, F. Videbaek)

We have conducted a study of the  $^{16}\text{O} + ^{40}\text{Ca}$  and  $^{16}\text{O} + ^{44}\text{Ca}$  reactions, leading to fragments with masses between 20 and 30 at beam energies approximately twice the Coulomb barrier energy, to determine if a fusion-fission reaction takes place. The presence of such a mechanism in light systems, such as the Ni isotopes, could have a number of consequences. At bombarding energies well above the Coulomb barrier, the total fusion cross section may not be equal to the evaporation residue cross section, as had been previously assumed. The sensitivity of the calculated fission cross sections in these systems to the highest  $\ell$  values that contribute to fusion suggest that fission measurements may be useful in exploring the high- $\ell$  dependence of fusion. Finally, this mechanism may be invoked to explain the narrow resonances seen in  $^{28}\text{Si} + ^{28}\text{Si}$  elastic and inelastic scattering.

The differences in the measured excitation functions of the  $^{16}\text{O} + ^{40}\text{Ca}$  and the  $^{16}\text{O} + ^{44}\text{Ca}$  reactions are well described by the fusion-fission mechanism; in addition, the angular distributions, mass distributions and Q-values of the reactions are consistent with this mechanism. The measured total kinetic energies (TKE) in the outgoing channels corresponding to symmetric fragmentation of the  $^{56}\text{Ni}$  and  $^{60}\text{Ni}$  compound systems, respectively, are shown in Fig. II-11. Compared to these data are predictions of the TKE values (solid curve:  $^{56}\text{Ni}$ , dashed curve:  $^{60}\text{Ni}$ ) obtained by approximating the liquid-drop saddle-point configurations (calculated with finite-range and diffuse-surface corrections) by two deformed spheroids and equating the asymptotic kinetic energy with the potential energy of the spheroids at the saddle point. This schematic model is found to reproduce the data reasonably well. We are continuing these studies of light nucleus fusion-fission with measurements in additional systems.

---

<sup>1</sup>R. R. Betts, Proc. of 5th Adriatic Int. Conf. on Nucl. Phys., Hvar, Yugoslavia, 1984, ed. N. Cindro, W. Greiner, and R. Caplar (World Scientific, Singapore, 1984) p. 33.

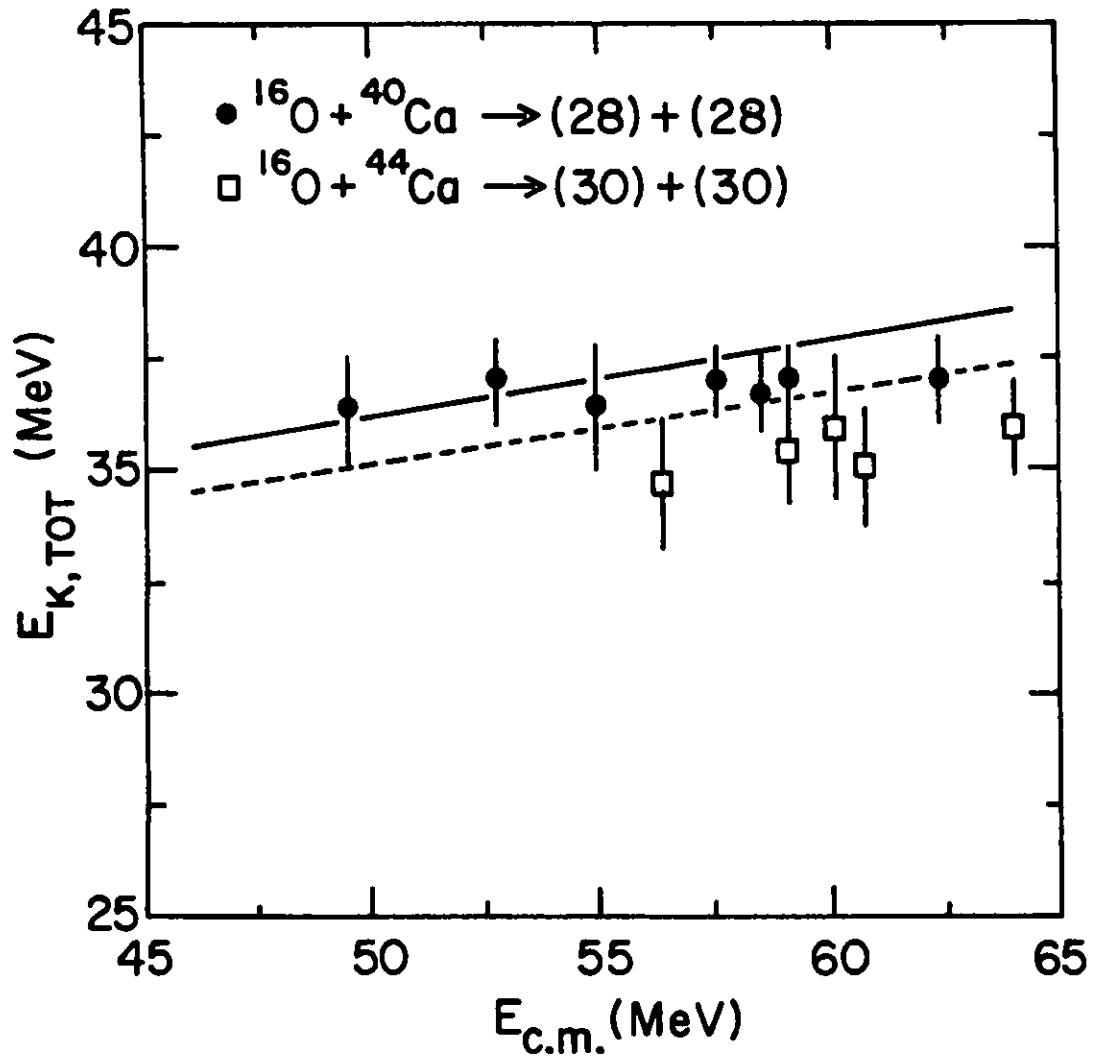


Figure II-11. Average values of the final total kinetic energies measured for the  $^{16}\text{O} + ^{40}\text{Ca} \rightarrow (28) + (28)$  and  $^{16}\text{O} + ^{44}\text{Ca} \rightarrow (30) + (30)$  reactions. The curves indicate the predicted values of these energies based on the liquid-drop saddle-point configuration (see text).

- k. Evidence for Asymmetric Fission in the  $^{32}\text{S} + ^{24}\text{Mg}$  Reaction  
 (S. J. Sanders, B. B. Back, B. K. Dichter, D. Henderson, S. Kaufman,  
 D. G. Kovar, F. Videbaek, and B. D. Wilkins)

As part of a program to study the possible role of the fusion-fission mechanism in the nuclear reactions of light systems, we have measured angular distributions of the fully-damped yields from the  $^{32}\text{S} + ^{24}\text{Mg}$  reaction at  $E_{\text{cm}} = 60$  MeV. This reaction reaches the same  $^{56}\text{Ni}$  compound system as in the  $^{16}\text{O} + ^{40}\text{Ca}$  reaction (also reported on in this Review), but with a more symmetric entrance channel. The angular dependence of the cross sections (following largely a  $1/\sin\theta_{\text{c.m.}}$  dependence, assuming two-body kinematics) and final total kinetic energies (largely angle independent) indicate the formation of a long-lived rotating system. Most significant however, is the observed mass dependence of the fully-damped yields (see Fig. II-12): there is evidence of an increasing yield in going to the more asymmetric mass partitions. This mass dependence might be expected in the asymmetric fission of the  $^{56}\text{Ni}$  system, but would be surprising assuming the alternative explanation of the yields in terms of a deep-inelastic scattering process where memory of the entrance channel is retained. We plan to continue these studies with coincidence measurements of the  $^{32}\text{S} + ^{24}\text{Mg}$  reaction products at a number of beam energies.

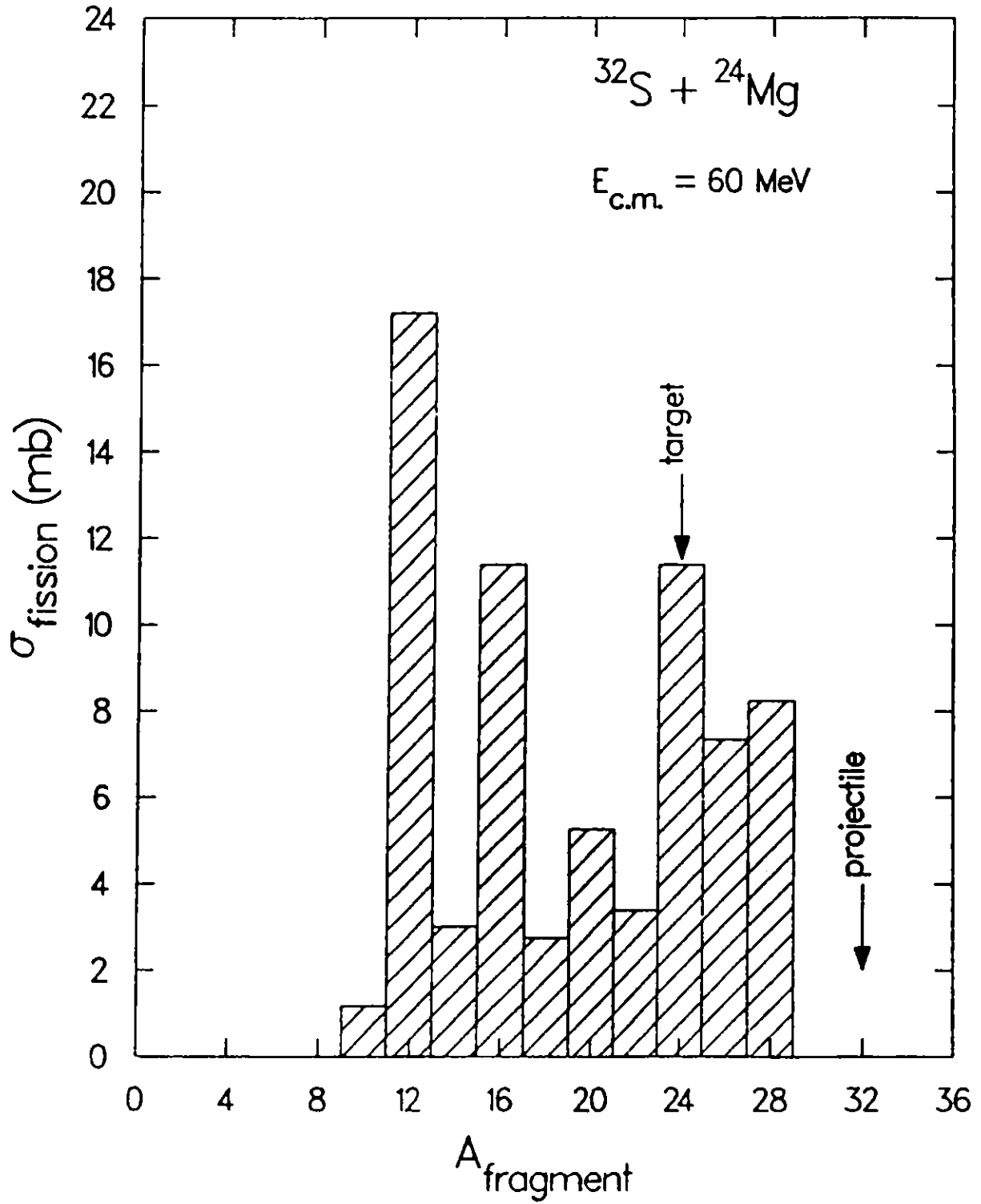


Figure II-12. Mass distribution of the fully-damped yields in the  $^{32}\text{S} + ^{24}\text{Mg}$  reaction.

2. Study of Fission Fragments from the Reaction  $^{32}\text{S} + ^{182}\text{W}$  (B. B. Back, J. G. Keller, A. Worsham, B. G. Glagola, S. J. Sanders, F. Videbaek, S. Kaufman, B. D. Wilkins, D. Henderson and R. Siemssen)

This experiment is part of a program to study the effects of the entrance channel mass asymmetry on the binary reaction channels in systems leading to  $^{214}\text{Th}$ . Reaction products from the  $^{32}\text{S} + ^{182}\text{W}$  reaction were measured in an array of Si detectors over the full angular range from  $10^\circ$  to  $170^\circ$  in the laboratory system. Bombarding energies of 166, 177, 222, and 260 MeV were studied. The product masses were obtained from the combined measurement of energy and velocity of the fragments utilizing the time structure of the beam. A fraction of the coincident fragments is detected in a position-sensitive avalanche detector covering an area of  $8 \times 10 \text{ cm}^2$ . Total reaction cross sections will be derived from an optical-model analysis of the simultaneously measured elastic scattering cross section. The angle-integrated fission cross section is compared with theoretical model predictions based on the proximity potential. The fission anisotropies will be analyzed in terms of the Saddle-Point Model. The mass distributions have been studied with respect to possible contributions from non-compound-nucleus reactions. In Figure II-13 we show the centroid of the mass distributions as a function of center-of-mass scattering angle. At beam energies of  $E_{\text{lab}} = 166, 177 \text{ MeV}$ , angle-independent mass centroids are observed as expected for the fission decay of compound. For the two higher energies, however, we see a small but significant angular dependence of the mass centroids, which indicates a contribution of quasifission processes.<sup>1</sup> Such processes do not proceed via the formation of a compound system and may therefore exhibit such mass-angle correlations.

---

<sup>1</sup>J. Toke et al., Nucl. Phys. A440, 327 (1985).

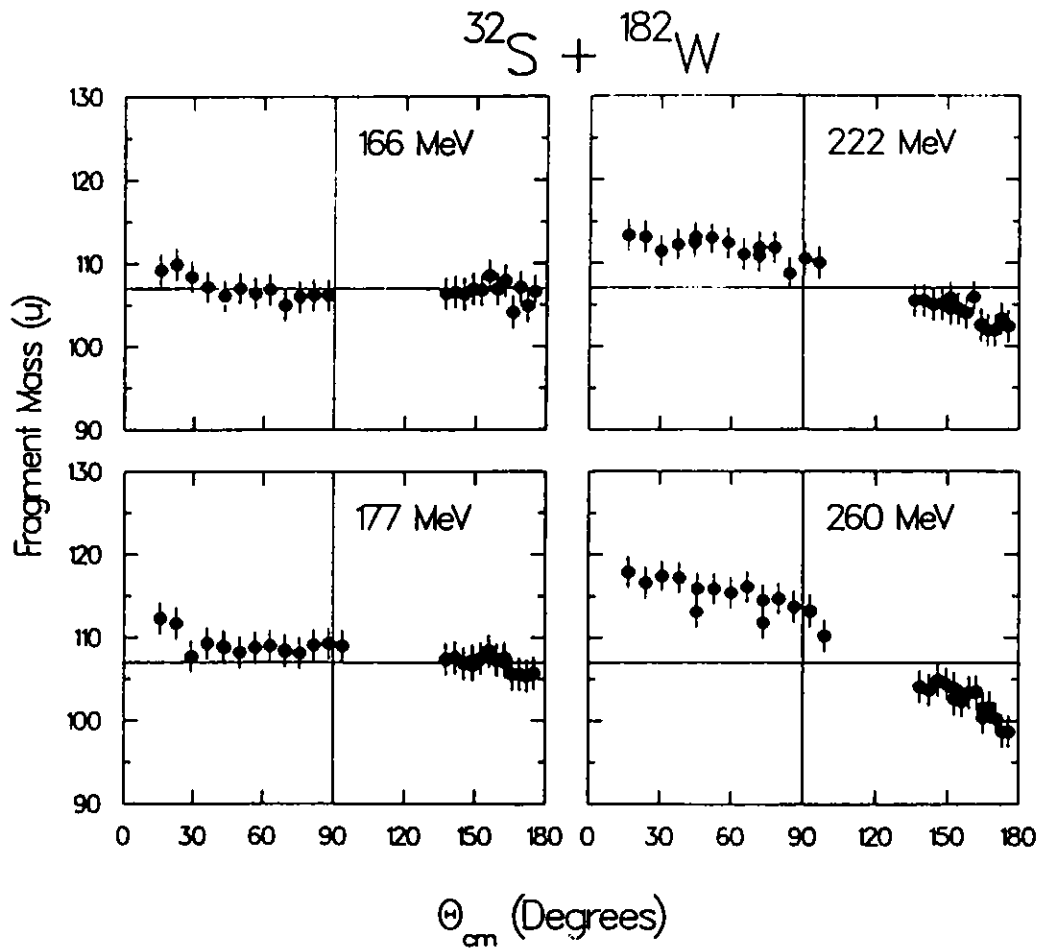


Figure II-13. Mass centroids for fission-like products are shown as a function of center-of-mass scattering angle for the reaction  $^{32}\text{S} + ^{182}\text{W}$  at four different bombarding energies  $E_{lab} = 166, 177, 222, 260$  MeV.

- m. Experimental Study of the Reaction  $^{60}\text{Ni} + ^{154}\text{Sm}$  (B. B. Back, J. G. Keller, A. Worsham, S. J. Sanders, F. Videbaek, S. Kaufman, B. D. Wilkins, D. Henderson and B. G. Glagola)

This experiment represents a continuation of the study of entrance channel effects on binary reaction channels for systems leading to the possible formation of  $^{214}\text{Th}$ . In this less asymmetric system, as compared with the  $^{32}\text{S} + ^{182}\text{W}$  reaction, we may expect non-compound-nucleus reactions to contribute to the fission-like processes at a measurable level, and provide a determination of the onset of such processes as a function of mass asymmetry. Reaction products emitted in the forward hemisphere were measured in an array of 8 Si-detectors for beam energies of 275, 350, 400, 425 MeV. By recording time-of-flight of the reaction products relative to the beam timing, it is possible to determine both mass and energy of the products. From a preliminary analysis of the data it appears that a strong component of deep inelastic scattering occurs for the two highest energies. The elastic scattering, deeply inelastic scattering and fission-like components of the total reaction cross section will be analyzed and compared to the prediction of theoretical models.

- n. Kinematic Coincidence Studies of the  $^{127}\text{I} + ^{87}\text{Rb}$  Reaction  
(B. B. Back, F. L. H. Wolfs, J. G. Keller, B. G. Glagola, D. Henderson, S. Kaufman, F. Videbaek, S. J. Sanders and B. D. Wilkins)

This experiment, scheduled for the spring of 1986, is aimed at studying binary reaction channels by using the kinematic coincidence technique. Again, the target-projectile system is chosen such that  $^{214}\text{Th}$  would be formed in complete fusion reactions, thus extending the study to more symmetric entrance channels. The choice of a heavy beam incident onto a lighter target simplifies the experiment by focussing all the heavy reaction products into the forward hemisphere. Velocity vectors of coincident binary reaction products will be measured in two  $20 \times 20 \text{ cm}^2$  gridded parallel-plate avalanche detectors, which provide both the x-y position and the time of incidence of penetrating particles. The time-of-flight is obtained by utilizing the time structure of the beam. By kinematical reconstruction of each event from the measured quantities one can obtain masses, center-of-mass scattering angles and kinetic energies of the reaction products.

- o. Characteristic Time for Mass Asymmetry Relaxation in Quasifission Reactions (B. B. Back, W. Q. Shen,\* S. Björnholm,† S. P. Sørensen,† J. Albinski,‡ R. Bock,§ A. Gobbi,§ K. D. Hildenbrand,§ W. F. J. Müller,§ H. Stelzer,§ J. Kuzminski,¶ J. Töke,¶ A. Olmi\*\* and G. Guarino††)

Quasifission reactions induced by a beam of  $^{238}\text{U}$  particles on targets of  $^{32}\text{S}$ ,  $^{40}\text{Ca}$ ,  $^{48}\text{Ca}$ , and  $^{\text{nat}}\text{Zn}$  have been studied at GSI (Darmstadt, W. Germany) at several bombarding energies ranging from 4.6 MeV/u to 7.5 MeV/u. The time required for a given drift in mass asymmetry to occur during the reaction is determined from the angular distributions and from the  $l$ -values, which in turn are derived from the cross sections. The results imply a "universal" time constant of  $(5.3 \pm 1) \times 10^{-21}$  s for relaxation of the mass asymmetry degree of freedom, irrespective of target mass and the excitation energy. The nature of the conservative driving forces, the shapes, and the dissipation mechanism that appears to be common for all these reactions are found to strongly support the one-body dissipation picture,<sup>1</sup> in particular due to the temperature independence of the characteristic time for mass drift toward symmetry as illustrated in Fig. II-14.

---

\*Institute of Modern Physics, Lanzhou, Peoples Republic of China.

†Niels Bohr Institute, Copenhagen, Denmark.

‡University of Cracow, Cracow, Poland.

§Gesellschaft für Schwerionenforschung, Darmstadt, West Germany.

¶University of Basel, Basel, Switzerland.

¶Nuclear Structure Research Laboratory, Univ. of Rochester, Rochester, N.Y.

\*\*Istituto Nazionale de Fisica Nucleare, Florence, Italy.

††Istituto Nazionale de Fisica Nucleare, Bari, Italy.

<sup>1</sup>W. Q. Shen et al., *Europhys. Lett* 1, 113 (1986).



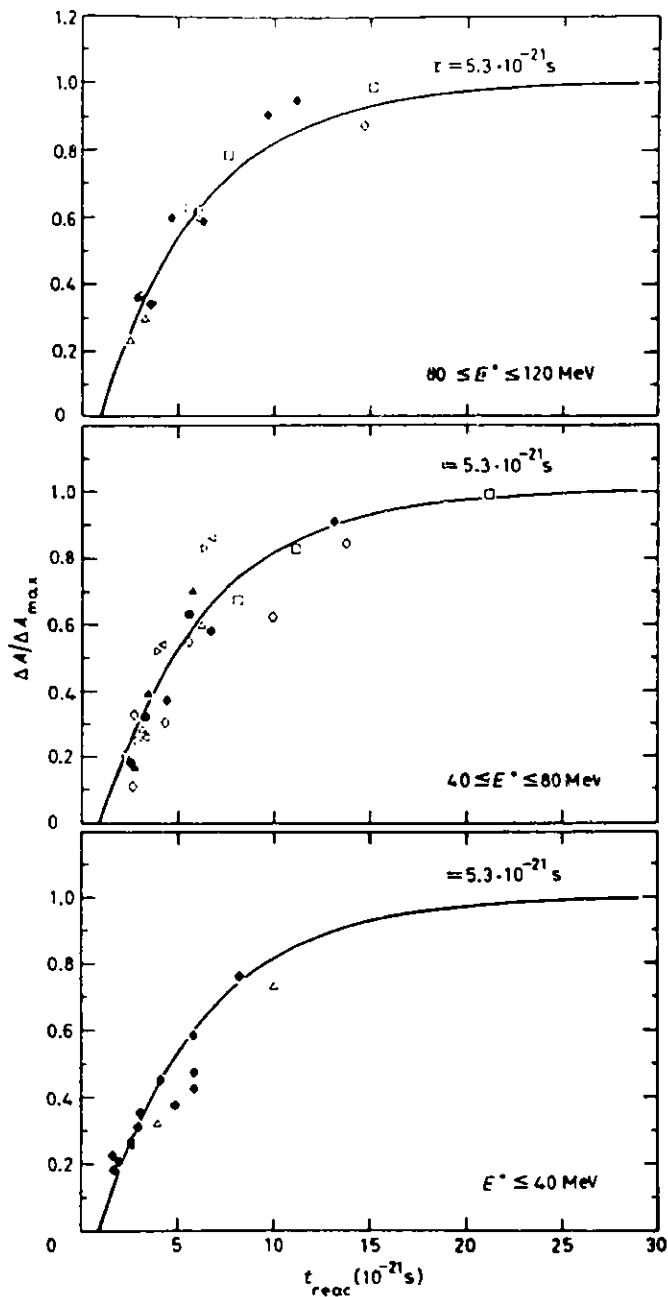


Figure II-14. The normalized drift toward symmetry  $\Delta A / \Delta A_{\max}$  is shown as a function of the reaction time  $t_{\text{reac}}$  for three different intervals of the excitation energy. The solid curves represent an exponential drift toward symmetry with a characteristic time constant of  $\tau = 5.3 \times 10^{-21}$  s.

- p. Complete Fusion of  $^{238}\text{U}$  and  $^{48}\text{Ca}$ ; Prospects for Superheavy Element Synthesis (B. B. Back, W. Q. Shen,\* S. Bjørnholm,† S. P. Sørensen,† J. Albinski,‡ R. Bock,§ A. Gobbi,§ K. D. Hildenbrand,§ W. F. J. Müller,§ H. Stelzer,§ J. Kuzminski,‡ J. Töke,¶ A. Olmi\*\* and G. Guarino††)

Differential cross sections for binary reactions between  $^{238}\text{U}$  and  $^{48}\text{Ca}$  have been measured at energies from 4.6 to 7.5 MeV/u over the full range of fragment energies, scattering angles and masses.<sup>1</sup> This experiment was carried out at Gesellschaft für Schwerionenforschung, Darmstadt, Germany. The cross sections for complete fusion followed by fission are determined from the observed mass-angle correlations. They can be understood within the extra-push model. On this basis, predictions for the complete fusion cross sections for the  $^{48}\text{Ca} + ^{248}\text{Cm}$  and  $^{48}\text{Ca} + ^{254}\text{Es}$  reaction are made, and discussed in terms of the possibilities for super-heavy element synthesis by means of heavy-ion fusion reactions. In Fig. II-15 we show the experimental cross section for capture (solid points) and complete fusion (solid squares) compared to theoretical calculations based on the extra-push model<sup>2</sup> (solid and dotted curves, respectively). An extrapolation of the complete fusion cross section to the  $^{48}\text{Ca} + ^{248}\text{Cm}$  system within this model is represented by the dotted curve in the insert. The cross sections for the various neutron emission channels predicted by a statistical evaporation code using the fission barriers and masses from a Strutinski-type calculation<sup>3</sup> are compared to the experimental upper limits for the production of these elements<sup>4</sup> (open triangles). Note that the predicted lifetime of the elements produced after the evaporation of two or three neutrons are too short to be detected experimentally. It is concluded from this work that although the cross section for complete fusion in the  $^{48}\text{Ca} + ^{248}\text{Cm}$  is strongly hindered by entrance-channel dissipation, it may still be sufficient to produce superheavy elements at detectable levels, if such elements possess sufficient stability.

\*Institute of Modern Physics, Lanzhou, Peoples Republic of China.

†Niels Bohr Institute, Copenhagen, Denmark.

‡University of Cracow, Cracow, Poland.

§Gesellschaft für Schwerionenforschung, Darmstadt, West Germany.

¶University of Basel, Basel, Switzerland.

¶Nuclear Structure Research Laboratory, Univ. of Rochester, Rochester, N.Y.

\*\*Istituto Nazionale de Fisica Nucleare, Florence, Italy.

††Istituto Nazionale de Fisica Nucleare, Bari, Italy.

<sup>1</sup>B. B. Back et al., submitted to Phys. Lett.

<sup>2</sup>S. Bjornholm and W. J. Swiatecki, Nucl. Phys. A391, 471 (1982).

<sup>3</sup>J. Randrup et al., Physica Scripta 10A, 60 (1974).

<sup>4</sup>P. Armbruster et al., Phys. Rev. Lett. 54, 406 (1985).

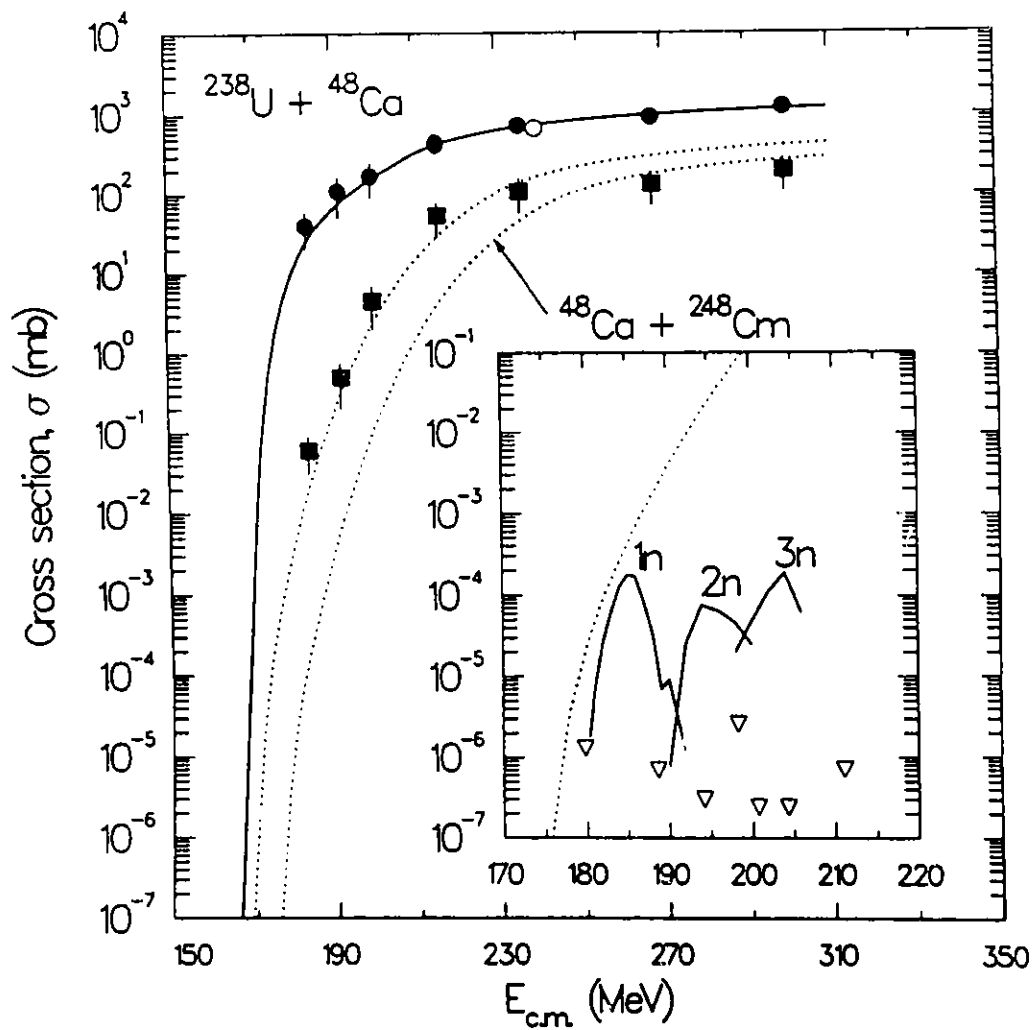


Figure II-15. Experimental capture (solid points) and complete fusion cross sections (solid squares) are shown as a function of center-of-mass energy and compared to extra-push model calculations. See text for further details.

## C. HIGH ANGULAR MOMENTUM STATES IN NUCLEI

The main emphases of our efforts have been on a) construction of the ATLAS  $\gamma$ -ray facility, and b) research on nuclear structure at high spin above the yrast line, on compound-nucleus decay, and on structural evolution of transitional nuclei.

Phase I of the  $\gamma$ -ray facility, consisting of 7 Compton-suppressed Ge (CSG) detectors and a multiplicity filter of 14 hexagonal BGO elements, was completed in time for the earliest beams from ATLAS. The facility is now being upgraded in Phase II, with additional BGO hexagons in 1986 to complete the sum/multiplicity spectrometer.

Research on the evolution of structure above the yrast line was based on studies of the  $\gamma$ -ray continuum with CSG's, which yielded more detailed properties than has previously been possible. We have established that when the yrast states are of single-particle character a region up to 1-2 MeV above the yrast line also has similar character. At higher energy (and spin), these single-particle states give way to collective E2 structures. In general, the time evolution of the  $\gamma$ -deexcitation cascade is being well established. This information was derived from the detailed properties of gamma spectra of the isotopes  $^{153}\text{Ho}$  and  $^{152}\text{Dy}$ , and from the feeding times and yrast structure of  $^{147}\text{Gd}$ , all nuclei with aligned-particle yrast configurations. We have also made progress in understanding the structure of the nucleus in the highly-excited state preceding gamma decay (see Sec. B).

We are also investigating the structural evolution with spin and neutron number of the transitional nuclei. We have found that nuclei with  $N \sim 88$  exhibit both the oblate coupling scheme seen for  $N < 86$  and the prolate rotational scheme seen for  $N > 90$ . The role of individual particle alignment in inducing a prolate-to-oblate transition is being sought in  $^{155}\text{Ho}$ , and experiments on  $^{153},^{154}\text{Dy}$  have been initiated with Phase I of the ATLAS gamma-ray facility. With the high sensitivity of the CSG's it will be possible to determine the lifetimes of states with higher spin ( $\sim 40$ ) than has hitherto been possible, and experiments to measure lifetimes in  $^{154},^{156}\text{Dy}$  have been performed. Another transitional region occurs in the Hg, Pt region and lifetime measurements in  $^{184}\text{Pt}$  suggest coexistence of bands with different deformation. Work on shell-model states around  $N = 82$ , led by Purdue, has continued, with studies on  $^{147}_{66}\text{Dy}_{81}$  directed towards studying the  $\pi$   $\rho$   $\alpha$   $\tau$   $\psi$   $\omega$   $\epsilon$   $\nu$  hole interactions and on the odd-odd  $^{150}\text{Ho}$  and  $^{152}\text{Tm}$  (with  $N = 83$ ) directed towards studying the  $\pi$ - $\nu$  particle interactions.

Several projects are joint ventures with outside user groups including overseas scientists from Copenhagen, GSI, Heidelberg, Giessen and Strasbourg. Active collaborations continue with Prof. P. J. Daly's group at Purdue University as well as with Profs. U. Garg and J. Kolata from the University of Notre Dame.

- a. Entrance-channel Dependence in the Decay of  $^{156}\text{Er}$  (T. L. Khoo, R. V. F. Janssens, W. Kühn,\* V. Metag,\* A. Ruckelhausen,\* D. Habs,† H. Groger,† R. Repnow,† S. Hlavac,‡ R. Simon,‡ G. Duchin,§ R. Freeman,§ B. Haas,§ and F. Haas§)

We have previously observed that in fusion of  $^{64}\text{Ni}$  and  $^{92}\text{Zr}$  there is a suppression of neutron emission,<sup>1</sup> whereas in fusion of  $^{12}\text{C}$  and  $^{144}\text{Sm}$  into the same compound nucleus the observed neutron multiplicity distribution is close to that expected. Possible explanations for the suppression in terms of anomalously energetic neutrons, unusually large gamma-decay widths or an unknown yrast line have been ruled out. Measurements of the  $l$ -distribution of the compound nucleus in the  $^{64}\text{Ni}$ -induced reaction have ruled out the possibility that the explanation lies in a tail which extends to very high  $l$ -values.

The measurements of  $l$ -distributions have been performed with the Darmstadt-Heidelberg crystal ball at the Heidelberg tandem-linac accelerator. Care has been taken to correct for the detector response, to determine the average spin removed per photon, and to convert from multiplicity to spin. The  $l$ -distributions associated with individual channels have been determined in both the  $^{12}\text{C}$ - and  $^{64}\text{Ni}$ -induced reactions which lead to  $^{156}\text{Er}^*$  at the same compound-nucleus excitation energy. It was, therefore, possible to examine the decay of the compound nucleus for the same  $E$  and  $I$  in the two reactions.

If the Bohr hypothesis applied there should be no memory of the entrance channel during particle decay and hence no entrance-channel dependence on the reaction. Instead we find such a dependence. The ratio of cross sections corresponding to emission of 2 and 3 neutrons,  $\sigma(2n)/\sigma(n)$  is almost identical at low spins ( $I \lesssim 22$ ) but becomes significantly larger at high spin for the  $^{64}\text{Ni}$ -induced reaction (see Fig. II-16). Thus there is

---

\*Universität Giessen, W. Germany.

†Max Planck Institute, Heidelberg, W. Germany.

‡GSI, Darmstadt, W. Germany.

§CRN, Strasbourg, France.

<sup>1</sup>W. Kühn et al., Phys. Rev. Lett. 51, 1858 (1983).

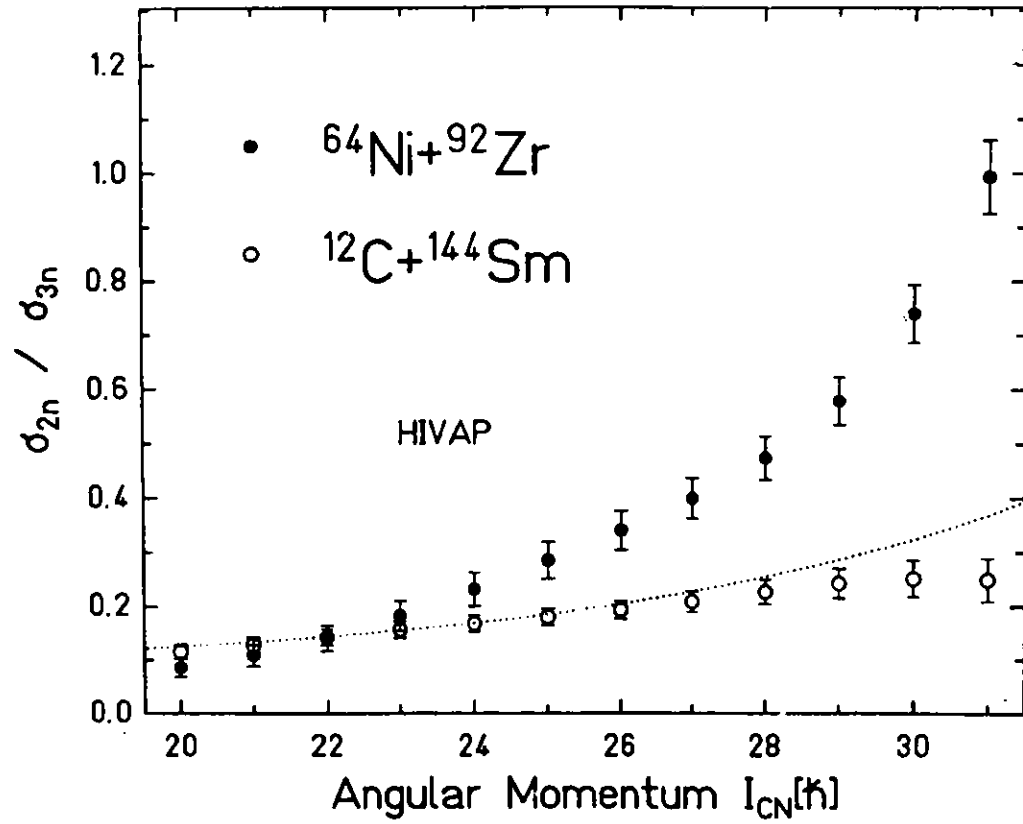


Figure II-16. Ratio of cross sections for 2 and 3 neutron emission.

memory of the entrance channel during particle evaporation. This result would be expected if, during relaxation from the initially deformed shape, the compound nucleus were to be trapped in a superdeformed secondary potential minimum. The initial deformation in the C-induced reaction is not sufficiently large to enable the population of the superdeformed shape.

All of our experimental data to date ( $\ell$ -distributions, neutron multiplicity distributions, their dependence on neutron number and entrance channel and evaporation residue cross sections) are all consistent with a picture of trapping in a superdeformed well during compound nucleus decay. However, there is as yet no unambiguous proof for this picture.

b. Total  $\gamma$ -Spectrum from  $^{153}\text{Ho}$  Measured with BGO Compton-Suppressed Spectrometers (D. C. Radford, T. L. Khoo, I. Ahmad, H. Helppi,\* R. Holzmann, R. V. F. Janssens, M. Driggert,† and U. Garg†)

While there is now a good understanding of the properties of the cold yrast line at high spin, the evolution of nuclear structure with increasing temperature, i.e., increasing excitation energy above the yrast line, remains to be investigated. One probe available for such an investigation is a measurement of the complete  $\gamma$ -spectrum emitted as the nucleus cools towards the yrast line.

We have employed two Compton-suppressed-spectrometers to measure the spectra of the  $\gamma$ -rays emitted at  $0^\circ$  and  $90^\circ$  by  $^{153}\text{Ho}$  formed in the reaction  $165 \text{ MeV } ^{37}\text{Cl} + ^{120}\text{Sn}$ . By tagging on the decay of a 229-ns isomer in this nucleus it was possible to obtain spectra for gammas emitted by this and only this nucleus. The combination of Compton-suppression and selection of a single-channel with delayed coincidence tagging produces a completely clean spectrum. The CSS's, each consisting of a Ge detector with a BGO shield, are prototypes of the larger system being constructed by the Notre Dame-Argonne collaboration. The virtue of using a CSS, as opposed to a NaI detector, is that all features of the spectrum, including sharp lines, can be distinguished in the same detector.

The resultant spectra can be classified into four components: (i) discrete lines which deexcite yrast and near-yrast states and which dominate the spectra; (ii) sharp resolved lines which have not been assigned in the known level scheme and which are normally attributed to the unresolved quasi-continuum in studies with NaI detectors; (iii) the smooth continuum underlying these lines; and (iv) statistical  $\gamma$ -rays, which have been obtained by fitting the spectra between 2.43 and 3.88 MeV by an  $E^3 \cdot e^{-E\gamma/kT}$  functional form.

The gross features are similar to those observed in studies with NaI detectors. However, as an improvement we have now been able to measure the spectrum reliably down to  $\sim 130$  keV, compared to the previous thresholds of  $\sim 350$  keV. The new feature observed is that the so-called quasicontinuum is not continuous but actually consists of sharp lines (in addition to those

---

\*Lappeenranta University of Technology, Finland.

†University of Notre Dame, South Bend, IN.



assigned in the known level scheme), constituting  $\sim 6\%$  of the total  $\gamma$ -multiplicity, superimposed on an underlying smooth background. Anisotropy measurements show these lines to be mainly dipole transitions, while the absence of a Doppler-shift indicates that they occur late in the  $\gamma$ -cascade ( $\sim 5$  ps). On the other hand, the smooth background is dominated by stretched quadrupole transitions and appears to occur very early in the cascade ( $\sim 1$  ps).

These data, the feeding times information, and other available information suggest that the  $\gamma$ -decay starts out with a fast collective E2 cascade and is then funnelled, in a small spin range ( $\Delta I \sim 8$ ), into the aligned-particle configurations of the yrast line through states of similar character. The data suggest a definite paucity of collective excitations in the vicinity ( $\sim 2$  MeV) of the yrast line. The results from this investigation have been published.<sup>1</sup>

---

<sup>1</sup>D. C. Radford et al., Phys. Rev. Lett. 55, 1727 (1985).

- c. Lifetimes of Very High Spin States in  $^{147}\text{Gd}$  (S. Bjornholm,\* J. Borggreen,\* J. Pedersen,\* G. Sletten,\* R. V. F. Janssens, T. L. Khoo, and D. C. Radford†)

Our first results on the spectroscopy of very high spin states in  $^{147}\text{Gd}$  have been published.<sup>1</sup> The main features of these data can be summarized as follows: (a) states up to an excitation energy of  $\approx 17$  MeV and a spin of  $79/2$  were established, (b) the resulting level scheme is characteristic of the single-particle nature of the yrast line up to the highest states, with no evidence of collectivity. This interpretation is supported by shell-model calculations using a deformed potential. These calculations tell us also that within a few more units of angular momentum the nucleus now has to find extraordinary ways of producing spin, either by exciting nucleons from the next major shell or by collective rotation.

In an attempt to distinguish between these two modes, lifetimes and feeding times were measured by the recoil distance method. The analysis initiated last year has now been completed with the following results: (i) Information has been obtained for all states along the yrast line with spins  $I < 75/2$  and  $I > 59/2$ . (ii) The measured lifetimes confirm the single-particle nature of the various states. Hindrances (or enhancements) with respect to the Weisskoff estimates are found to be small. (iii) For levels below 13.5 MeV, a long lived ( $> 5\text{ns}$ ) component is present in the side feeding, suggesting the presence of an isomer above the yrast line. (iv) Short ( $< 1$  ps) and long ( $\geq 10$  ps) feeding lifetimes are found for the states located above 13.5 MeV. The short lifetimes may be interpreted as due to collective transitions and to fast dipole transitions. Thus the occurrence of collective states in the vicinity of the yrast line is suggested by the data. This picture has some similarity with the one emerging from earlier measurements on  $^{154}\text{Dy}$ .<sup>2</sup> A paper summarizing our results is currently in preparation.

---

\*The Niels Bohr Institute, Copenhagen, Denmark.

†Chalk River Nuclear Laboratory, Chalk River, Canada

<sup>1</sup>G. Sletten et al., Phys. Lett. 135B, 33 (1984).

<sup>2</sup>F. Azgüi et al., Nucl. Phys. A439, 573 (1985).

- d. The Study of High Spin States in  $^{155}\text{Ho}$  (H. Helppi,\* D. C. Radford,\*\* R. Holzmann, R. V. F. Janssens, T. L. Khoo, R. Broda,† P. J. Daly,† Z. W. Grabowski,† and J. McNeill†)

The nuclei  $^{153,154}\text{Dy}$  have been extensively studied at this laboratory during the last 2-3 years.<sup>1</sup> In these nuclei a transition from collective rotational behavior to single-particle character is observed for the yrast levels, suggesting a change from prolate to oblate shapes. This transition occurs at different spins in the two isotopes ( $I > 32\hbar$  in  $^{154}\text{Dy}$ ,  $I > 41/2\hbar$  in  $^{153}\text{Dy}$ ).

Such changes in the character of yrast levels are of particular interest since they are a sensitive test of our understanding of the interplay between collective and single-particle modes of excitation. To further extend the systematics of the transition in this mass region we have chosen to study high-spin states in  $^{155}\text{Ho}$ , an isotone of  $^{154}\text{Dy}$ . The analysis of an angular distribution measurement and of a  $\gamma$ - $\gamma$  coincidence experiment has continued and turned out to be rather difficult. This is due to the complexity of the decay scheme which translates into the occurrence of a large number of weak  $\gamma$ -rays difficult to place in a level scheme consistent with all the data. Nevertheless, a level scheme was obtained (see Fig. II-17) which exhibits band structures of two types. First, so-called decoupled bands (corresponding to the rotation of the prolate nucleus around an axis perpendicular to the symmetry axis where the spin of the  $h_{11/2}$  odd proton is aligned with the rotation axis) are observed up to  $61/2^-$  and  $59/2^-$  respectively. A second irregularity in the rotational sequences (backbending) is observed. Secondly, a rather complex structure of levels without marked regularity in the energy spacings is also seen. The latter structure most probably corresponds to states of single-particle nature build on an overall oblate shape. A few levels are also identified for which no connection to the levels placed in the scheme was possible. All the available evidence points however toward their placement on top of the level scheme and more work is required to establish their complex decay paths. The picture emerging from this study is all together rather similar to the one seen in  $^{153}\text{Dy}$ , i.e. that of coexisting

\*Lappeenranta University of Technology, Finland.

\*\*Chalk River Nuclear Laboratory, Chalk River, Canada.

†Purdue University, W. Lafayette, IN.

<sup>1</sup>F. Azgui, Nucl. Phys. A439, 573 (1985).

<sup>2</sup>M. Korhela, Phys. Lett. 131B, 305 (1983).

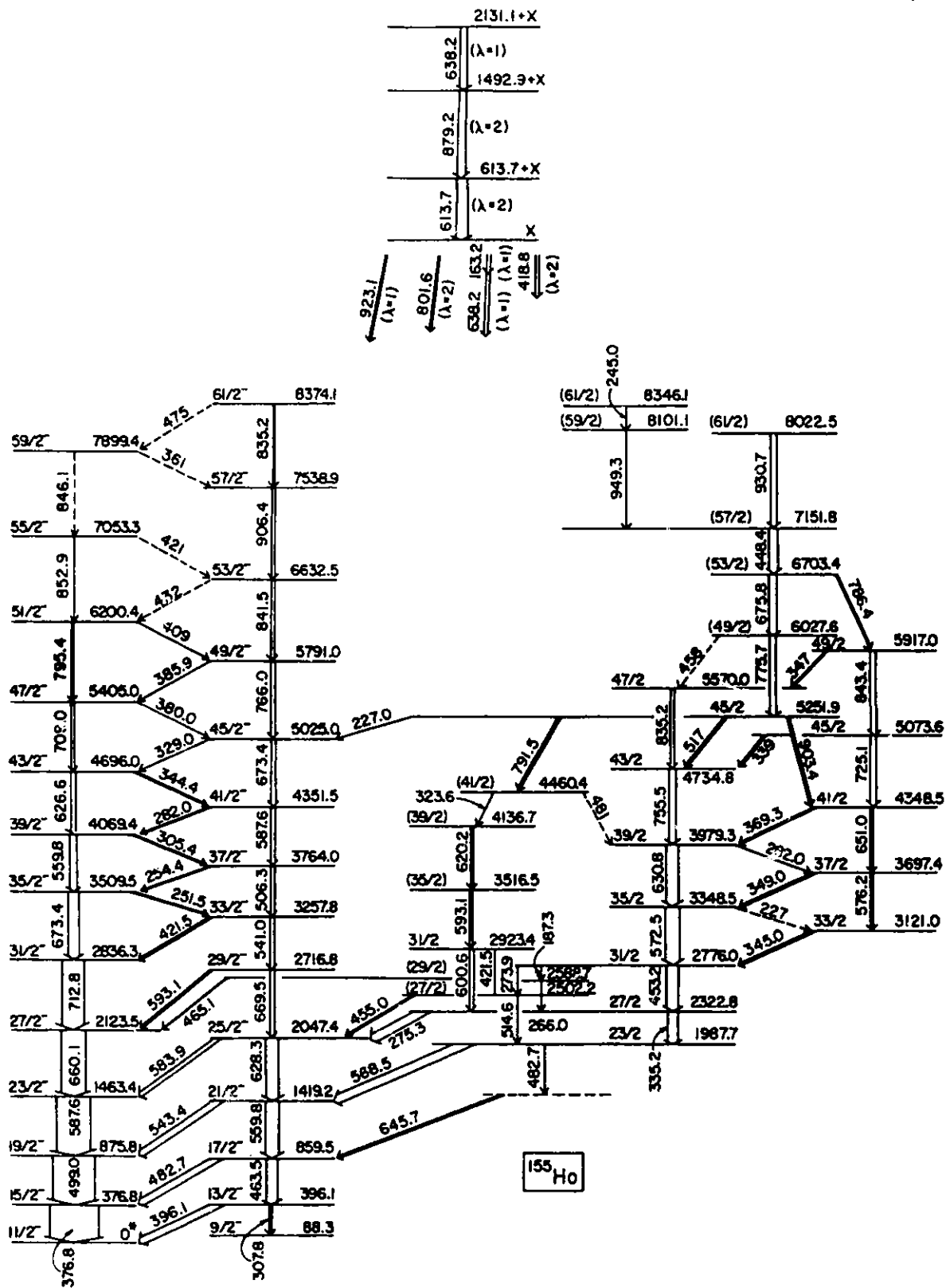


Figure II-17. Proposed level scheme for  $^{155}\text{Ho}$  from the present study with the  $^{125}\text{Sn}(^{35}\text{Cl}, 4n)$  reaction.

structures associated with different nuclear shapes with the states corresponding to the oblate shape dominating at the highest spins. Calculations within the cranked shell model have been performed in order to account for the behavior of the decoupled bands. Good agreement with the data requires the onset of  $\gamma$  deformation. The results of this work are currently being prepared for publication.

- e. Recoil Distance Lifetime Measurements in  $^{184}\text{Pt}$  (U. Garg,\* A. Chaudhury,\* M. W. Drigert,\* E. G. Funk,\* J. W. Mihelich,\* D. C. Radford,\*\* R. Holzmann, R. V. F. Janssens, T. L. Khoo, and H. Helppit†)

The structure of the very neutron-deficient Pt(Z=78) isotopes is most unusual. Moments of inertia deduced from the excitation energies of the first few excited states show a strong odd-even staggering,<sup>1</sup> the odd-mass isotopes showing large deformations ( $h^2/2 \sim 14$  keV). The neighboring Hg(Z=80) isotopes show a closely-related behavior and detailed spectroscopic studies of  $^{184,186,188}\text{Hg}$  (see Ref. 2 and references therein) have revealed the coexistence of complete bands of states with very different deformations. The presence of these different deformations is indicated by energy spacings and B(E2) values. The corresponding even-Pt isotopes do not show a clear coexistence of bands of different deformation. However, they possess low-lying  $0^+$  excited states and a number of  $2^+$  and  $4^+$  states. Further, the energy spacings of the yrast bands reveal<sup>3</sup> a rapid decrease in the rotational parameter,  $h^2/2$ , from (typically) 27 keV for the  $2^+ \rightarrow 0^+$  transition to 14 keV for the  $8^+ \rightarrow 6^+$  transition. It has been argued that these features are indicative of coexisting bands at low energy, albeit masked by band mixing at low spin. The pattern proposed in Ref. 3 places the more-deformed band lower in energy than the less-deformed band.

A simple prediction of the interpretation proposed for the very neutron-deficient Pt isotopes is that the B(E2) values in the yrast bands should undergo a rapid increase with increasing spin (matching the decrease in

---

\*University of Notre Dame, South Bend, IN.

\*\*Chalk River Nuclear Laboratory, Chalk River, Canada

†Lappeenranta University of Technology, Finland.

<sup>1</sup>E. Hagberg et al., Nucl. Phys. A318, 29 (1979).

<sup>2</sup>J. D. Cole et al., Phys. Rev. C 30, 1267 (1984)

<sup>3</sup>J. L. Wood, CERN Report 81-09, 1981, p. 612.

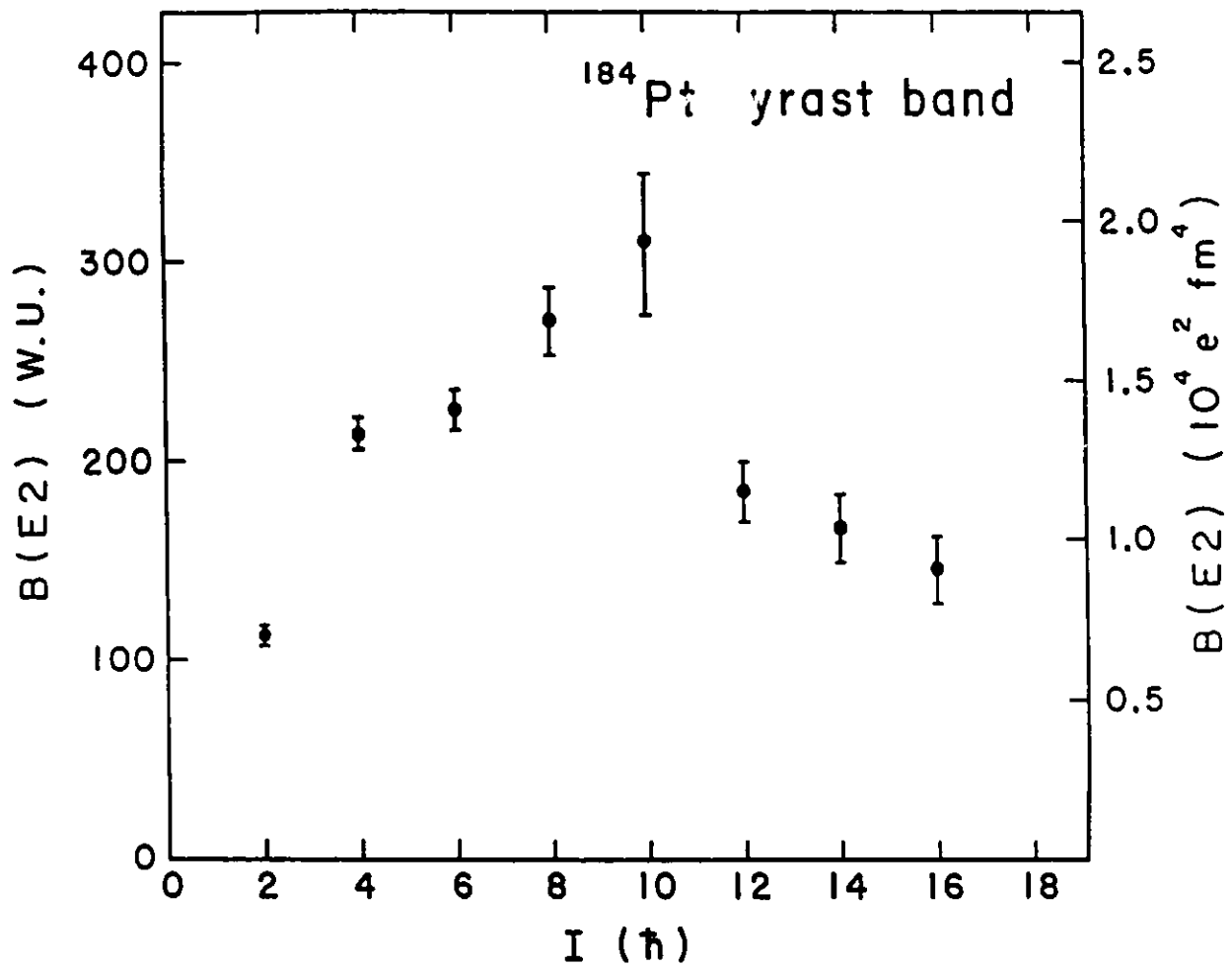


Fig. II-15.  $B(E2)$  values for  $^{184}\text{Pt}$  yrast band vs. spin of the depopulating state.

$h^2/2$  ).<sup>3</sup> This increase would reflect the appearance of the full collective strength of the more-deformed band, which is masked at low spin due to mixing with the less-deformed band. The analysis of the lifetimes of the levels in the yrast band of  $^{184}\text{Pt}$  started last year has now been completed. The data were obtained in a recoil distance measurement where the ANL plunger apparatus was used in conjunction with the sum spectrometer for the  $^{154}\text{Sm}(^{34}\text{S}, 4n)$  reaction at 160 MeV.  $B(E2)$  values were obtained for all yrast levels up to  $18^+$ . A significant increase (by a factor of  $>2.5$ ) is seen in Fig. II-18 between spins  $2^+$  and  $10^+$ . This result is in line with the picture of mixing outlined above. Beyond  $10^+$ , a decline of the  $B(E2)$  values is also observed. The latter effect is similar to that observed in rare earth nuclei after the onset of the "backbending" phenomenon and may be an indication for a change in the structure of the states along the yrast line (possibly a crossing of the g.s. band with a rotational band with an aligned  $i 13/2$  neutron pair). The results have been submitted for publication.

f. Shell-Model States around N=82 (R. Broda,\* P. J. Daly,\*  
Z. W. Grabowski,\* J. McNeill,\* H. Helppi,\* M. Piiparinen,\*  
M. Quader,\* , Z. Trzaska,\* R. Holzmann, R. V. F. Janssens, T. L. Khoo)

The systematic study of very proton-rich nuclei around N=82 has continued in order to test further the applicability of the shell model in this region. Shell model calculations, using  $^{146}\text{Gd}$  as a closed core have been extremely successful previously in describing the level structure of N=82 and N=83 nuclei.

We have completed our study of the level structure of the N=81 nucleus  $^{147}\text{Dy}$  as obtained by  $\gamma$ -ray spectroscopy following the reactions of 230-250 MeV  $^{58,60}\text{Ni}$  beams on  $^{89}\text{Y}$  and  $^{90,92}\text{Zr}$  targets.<sup>1</sup> Yrast and near-yrast levels in  $^{147}\text{Dy}$  above the known  $59\text{-s } 11/2^-$  state have been established up to  $\sim 3.7$  MeV. Guided by the results of the shell model calculations, we interpret most of the observed levels as seniority-three states arising from the coupling of  $s_{1/2}$ ,  $d_{3/2}$  and  $h_{11/2}$  neutron holes with  $(h_{11/2})^2$  protons. Analysis is continuing on data obtained with  $^{58,60}\text{Ni}$  induced reactions for the nuclei  $^{149}\text{Er}$ ,  $^{150}\text{Ho}$ ,  $^{151}\text{Yb}$ , and  $^{152}\text{Tm}$ . A preliminary level scheme for  $^{152}\text{Tm}$  and  $^{150}\text{Ho}$  is given in Fig. II-19. The level spectra in these two nuclei are interpreted using the shell model in terms of the coupling of an  $f_{7/2}$ ,  $h_{9/2}$  or  $i_{13/2}$  valence neutron to the yrast excitations of the neighboring N=82 nuclei.

Finally, another attempt was made to identify the N=82 nucleus  $^{153}\text{Lu}$ . This study follows our earlier investigations of the  $(h_{11/2})^n$  proton configurations in the nuclei  $^{148}\text{Dy}$ ,  $^{149}\text{Er}$ ,  $^{150}\text{Er}$ ,  $^{151}\text{Tm}$ , and  $^{152}\text{Yb}$ . The main emphasis is placed on the  $h_{11/2}$  spectrum. Unfortunately, this nucleus can only be reached with the  $^{96}\text{Ru} (^{58}\text{Ni}, p)$  reaction for which the fusion cross section is very low. We employed the familiar recoil catching technique where the recoiling nuclei are collected downstream from the target on a foil surrounded by the Ge detectors, thereby enlarging the detection sensitivity for delayed  $\gamma$ -rays by shielding the detectors carefully from prompt radiation from the target. The  $(h_{11/2})$  proton configuration of seniority 3 is calculated to be isomeric with a half life on the order of 10-500  $\mu\text{s}$  and the pulsing system of the linac was set accordingly. No evidence for  $^{153}\text{Lu}$  could be found.

\*Purdue University, W. Lafayette, Indiana.

†Lappeenranta University of Technology, Finland.

<sup>1</sup>R. Broda et al., Z. Physik A321, 287 (1985).



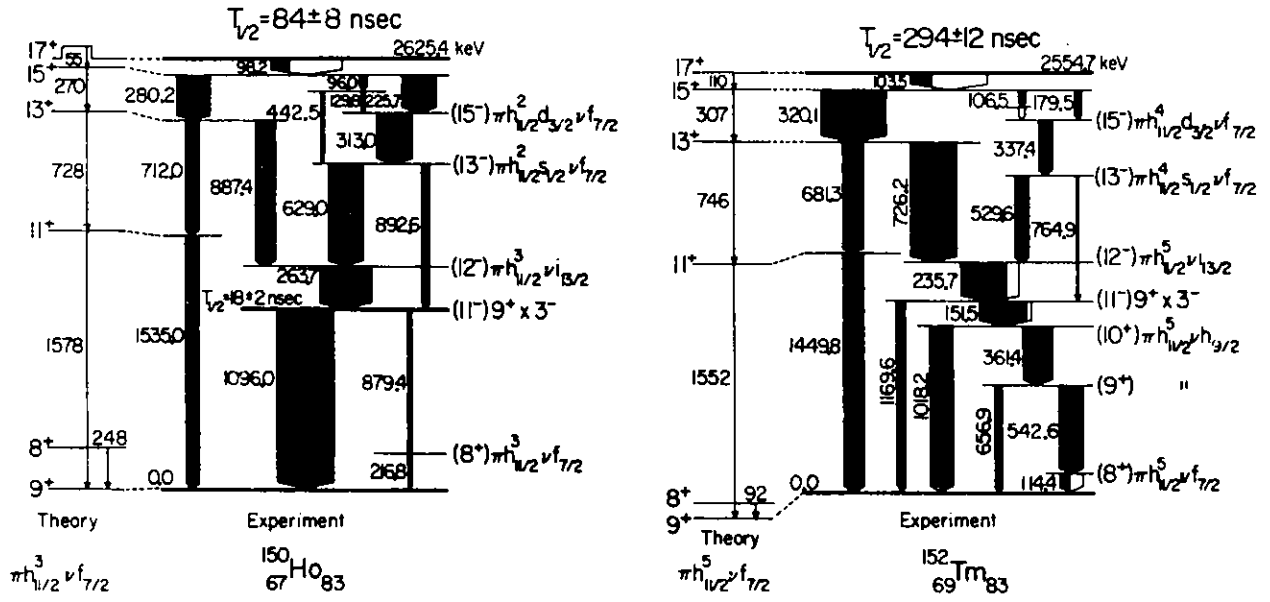


Figure II-19. Preliminary level scheme for  $^{150}\text{Ho}$  and  $^{152}\text{Tm}$ .

g. Feasibility Studies on Using Multiple Compton-Suppressed Ge Detectors to Search for Neutrinoless Double- $\beta$  Decay in  $^{76}\text{Ge}$

(W. R. Phillips, I. Ahmad, R. Holzmann, R. V. F. Janssens, and T. L. Khoo)

The large amount of Ge [ $\sim 90^{\circ} \text{cm}^3$ ] available in the BGO-array counters, and the very efficient Compton suppression provided by the BGO shields, prompted an investigation into the feasibility of their use in a search for the neutrinoless double-beta decay ( $2\beta-0\nu$ ) of  $^{76}\text{Ge}$ . The observation of such a decay would indicate non-conservation of lepton number and have implications for the mass of the neutrino and the nature of the weak interaction. The  $2\beta-0\nu$  decay to the  $^{76}\text{Se}$  ground state, observed in anticoincidence with events in the shields, would provide a sharp line at 2040.7 keV; the decay to the  $2_1^+$  state at 559.1 keV in  $^{76}\text{Se}$  would provide a sharp line at 1481.6 keV in coincidence with 559 keV  $\gamma$  rays observed in the shields. To improve on the most recently published upper limits for the appropriate decay rates, it was necessary to obtain background count rates in the Ge detectors of roughly the same size per unit volume as reported by others. One of the array detectors was extensively tested in and out of its shield in the low background counting area at ANL. The background per keV interval per khour per  $200 \text{cm}^3$  Ge in the region 2.0-2.2 MeV was  $\sim 18$  counts with the Ge detector suppressed inside its shield. The background in the same units in the region 1.4-1.6 MeV with the Ge detector gated on the interval 400-700 keV in the BGO shield was  $\sim 34$  counts. The largest part of the background was determined to arise from radioactive impurities in the materials surrounding the detectors, and in the detectors themselves and it was concluded that even with better cosmic-ray suppression, a significantly improved neutrinoless double beta decay experiment was not feasible with the existing detectors.

- h. High Spin Structure of  $^{153,154}\text{Dy}$ —First Experiment with the BGO  $\gamma$ -Ray Facility (I. Ahmad, B. Dichter, H. Emling, R. Holzmann, R. V. F. Janssens, T. L. Khoo, M. Drigert,\* U. Garg,\* Z. Grabowski,† M. Piiparinen,† M. Quader,† and W. Trzaska†

The first experiment with the BGO  $\gamma$ -ray facility has just been completed using 7 Compton-suppressed Ge detectors (CSG's) and 14 BGO hexagonal elements as a multiplicity filter. Furthermore, the new ATLAS data acquisition system (DAPHNE) was used. Thus the experiment represented a successful coupling of two new systems at ATLAS. The  $^{122}\text{Sn}(^{36}\text{S},\text{xn})$  reactions were used to produce the transitional nuclei  $^{153,154}\text{Dy}$  at high spin. More than  $100 \times 10^6$   $\gamma$ - $\gamma$  coincidences were recorded in the experiment. Excitation function and directional  $\gamma\gamma$  correlation data were also collected. Examples of coincidence spectra are shown in Fig. II-20.

The high resolution and good response (high peak/total ratio) of the CSG's make it possible to address many different aspects of the high spin structure of  $^{153,154}\text{Dy}$ . Among these are: (a) Structure of yrast and near yrast states. (b) Structure of quasi-continuum states as a function of increasing energy above the yrast line. (c) Lifetimes of discrete lines through the Doppler shift attenuation method (DSAM). (d) Lifetimes of continuum states through DSAM. (e)  $\gamma$ - $\gamma$  correlations; the ability to reliably unfold the 2-dimensional spectrum should permit more details to be examined than has hitherto been possible.

---

\*Notre Dame University, Notre Dame, Indiana.

†Purdue University, W. Lafayette, Indiana.

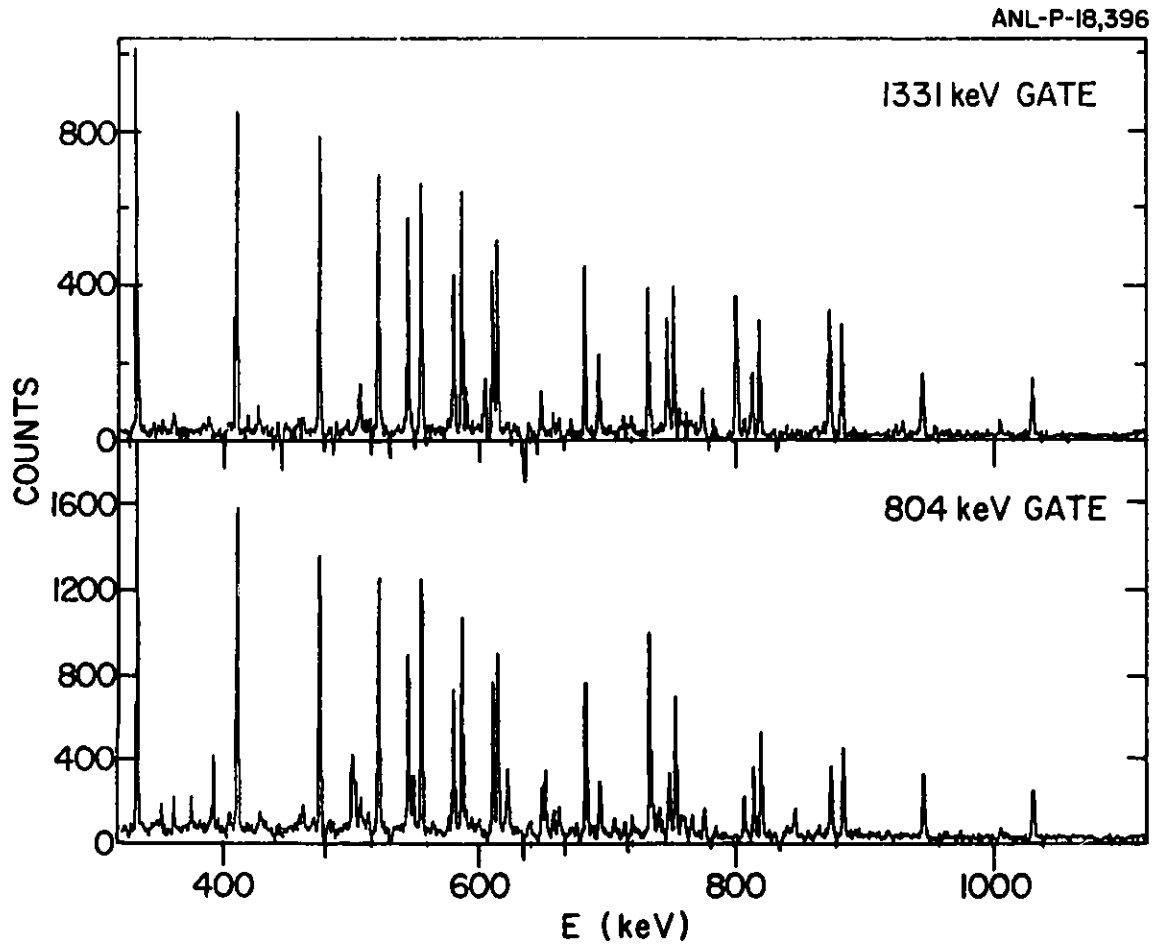


Figure II-20. Spectra in coincidence with ten 1331- ( $42^+ - 40^+$ ) and 804- ( $36^+ - 34^+$ ) keV transitions in  $^{154}\text{Dy}$ .

- i. Lifetimes of Very High Spin States in  $^{156}\text{Dy}$  Through DSAM  
 (H. Emling, I. Ahmad, B. Dichter, R. Holzmann, R. V. F. Janssens,  
 T. L. Khoo, M. Drigert,\* , U. Garg,\* , Z. Grabowski,† M. Piiparinen,†  
 M. Quader,† and W. Trzaska)

Compton-suppressed Ge detectors yield  $\gamma$  spectra with not only high resolution but very low background, particularly when only a single channel is selected, e.g. by coincidence with specific  $\gamma$  rays. The quality is such that the line shapes of individual lines reflect not only the lifetime of the decaying state but also the feeding history. A first attempt to exploit these features to measure lifetimes and feeding times of high spin states in  $^{156}\text{Dy}$  has been performed with the BGO  $\gamma$ -ray facility, where  $\sim 10^7$  coincidences were recorded with the  $^{124}\text{Sn}(^{36}\text{S},4n)$  reaction.  $^{156}\text{Dy}$  with  $N = 90$  is the lightest Dy isotope where deformation becomes well established. Thus it is of interest to establish if the deformation is altered by rapid rotation, e.g. if triaxial and oblate shapes set in. In addition, we would like to study the evolution of the quasi-continuum states with spin internal excitation energy (above the yrast line) and neutron number by examining the total  $\gamma$ -spectra of different Dy isotopes.

---

\*Notre Dame University, Notre Dame, Indiana.

†Purdue University, W. Lafayette, Indiana.

j. Structure and Lifetimes of Continuum States in  $^{152}\text{Dy}$

(R. Holzmann, I. Ahmad, R. V. F. Janssens, T. L. Khoo, M. Drigert,\*  
U. Garg,\* D. C. Radford,† P. J. Daly,‡ Z. Grabowski,‡ H. Helppi,‡  
M. Quader,‡ and W. Trzaska‡)

Our study of the total  $\gamma$  radiation from  $^{153}\text{Ho}$  (see Sec. C.b.) demonstrated the power of Compton-suppressed Ge detectors (CSG's) in unravelling details of the quasicontinuum spectra. We have employed 4 of the CSG's (which were eventually mounted in the BGO  $\gamma$ -facility) to measure the total  $\gamma$  radiation from  $^{152}\text{Dy}$  produced in the  $^{76}\text{Ge}(^{80}\text{Se},4n)$  reaction. Gamma rays from this and only this nucleus could be isolated by tagging on the decay of its 60 ns isomer. The contribution of neutrons in the spectrum were separately measured and removed.

The average angular momentum in the  $^{152}\text{Dy}$  channel was very large ( $\bar{I} = 54$ ) and resulted in a dominant component of stretched E2 cascades. This indicated that the continuum states at the highest spins are decidedly collective although the yrast states up to  $I \sim 40$  are of aligned-particle nature. A component at low energy ( $E_\gamma \lesssim 700$  keV) was found to be of mixed M1-E2 character. The origin of this is not yet understood, but may be associated with transitions between single-particle states above the yrast line. The continuous portion of the  $\gamma$ -ray spectra in  $^{152}\text{Dy}$ --so-called "soil"--are shown in Fig. II-21, and are compared with the spectra from  $^{153}\text{Ho}$ .

Analysis is now being concentrated on extracting lifetime information on the quasicontinuum states by comparing the spectra emitted from nuclei either recoiling in vacuum or stopping in a Au-backing. The excellent gain stability of the CSG's, the ability to reliably extract the primary  $\gamma$  spectrum by correcting for the detector response and to subtract the contribution of slow discrete lines (some very weak) all make it now feasible to be confident that we are determining the lifetimes associated only with the quasicontinuum spectrum and not with near-yrast transitions. The high-energy part of the E2 "soil" bump is fast ( $\tau < 2$  ps, corresponding to  $Q_0 = 3-5$  barns). The M1/E2 "soil" component is emitted later ( $\tau < 2$  ps), followed in turn by the gross transitions ( $\tau < 8$  ps). The time sequence of the different  $\gamma$ -ray components is shown in Fig. II-22. This figure also shows the average  $\gamma$  flow towards the yrast line.

ANL-P-18,217

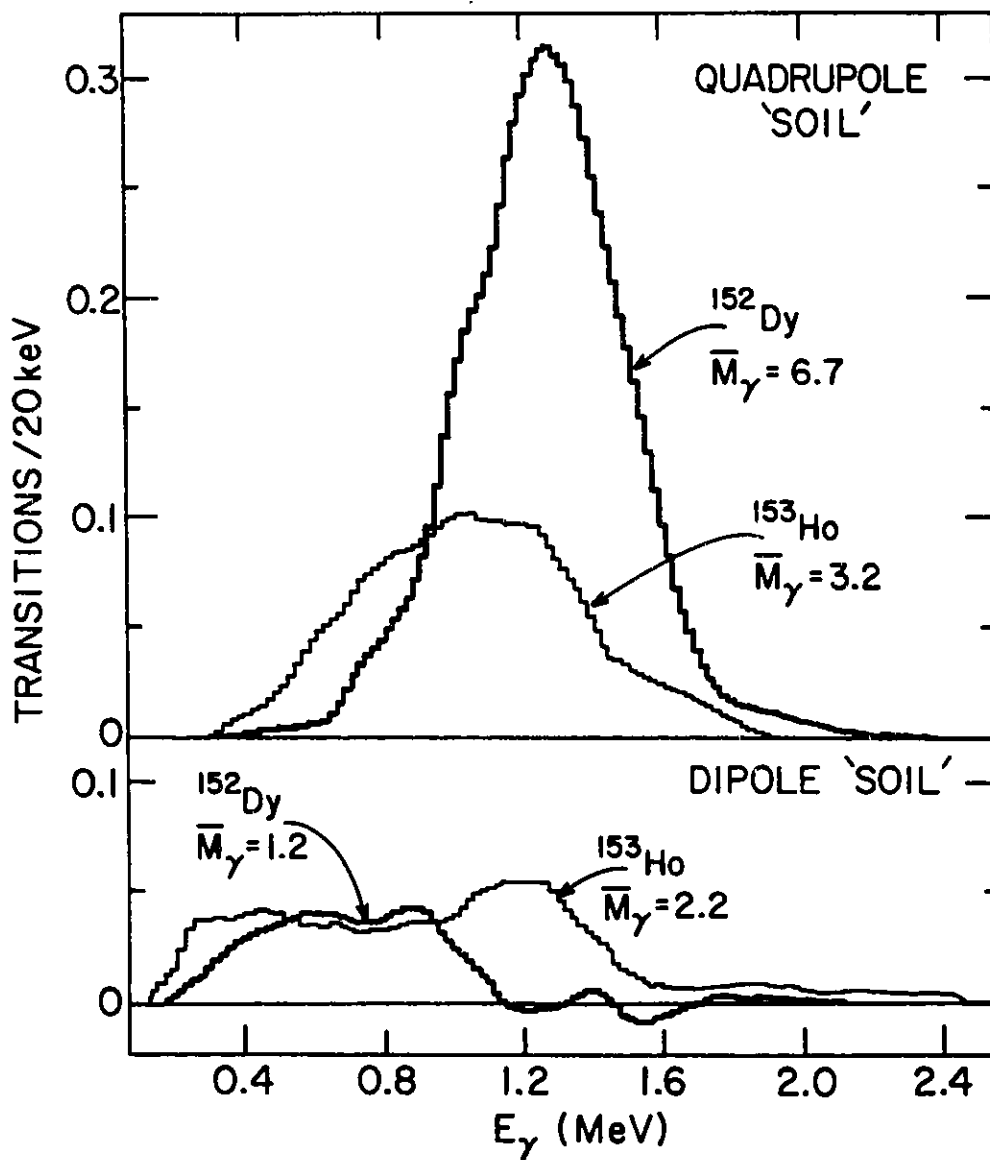


Figure II-21. Quadrupole and dipole 'soil' measured in  $^{152}\text{Dy}$  and  $^{153}\text{Ho}$ .

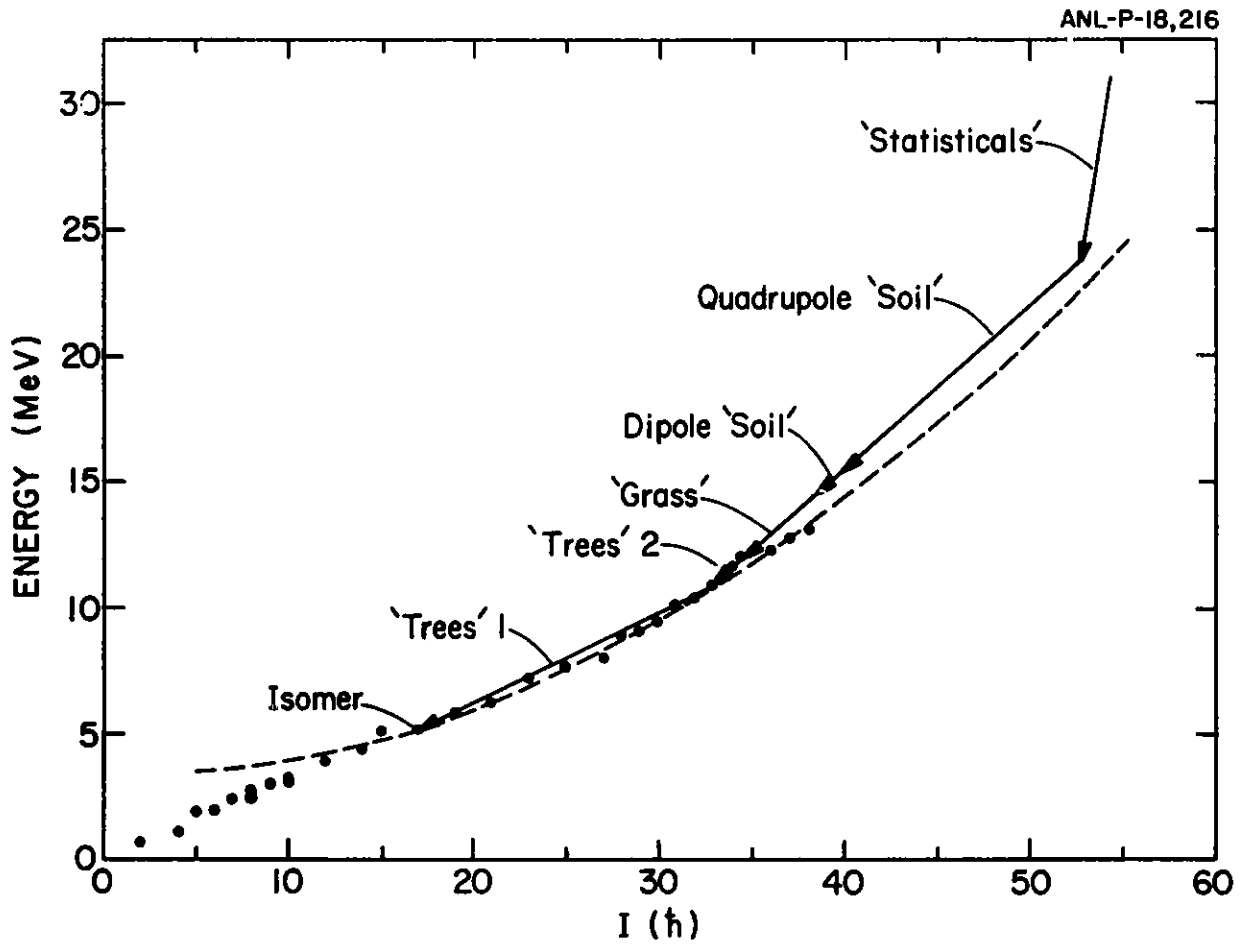


Figure II-22. Average  $\gamma$ -decay path in the E vs. I plane for  $^{152}\text{Dy}$ .



## D. HEAVY-ION RESONANCES

The emphasis of the heavy-ion resonance program has been on understanding the narrow structures observed in elastic and inelastic excitation functions for the  $^{24}\text{Mg} + ^{24}\text{Mg}$  and  $^{28}\text{Si} + ^{28}\text{Si}$  systems, and in exploring the limits on the occurrence of this resonance behavior in even heavier systems. The apparent simplicity of the observed resonance states, as compared to the multitude of compound nuclear states of the same spin and excitation energy, is a remarkable and yet poorly understood feature of nuclear structure. It has been even suggested that the observed structures have a dynamical origin rather than corresponding to true compound-nuclear resonances. In an analysis of elastic and inelastic scattering distributions for the  $^{28}\text{Si} + ^{28}\text{Si}$  system, it has been possible for us to show that these distributions cannot be described by an optical potential without either explicitly, or implicitly, including a resonance origin. In a separate analysis of a number of detailed elastic scattering angular distributions at energies covering one of the narrow  $^{24}\text{Mg} + ^{24}\text{Mg}$  resonances, we were able to determine the parameters for this state with the surprising result that its molecular strength appears to be rather widely spread. It is possible that heavy-ion resonances are a quite general feature of nuclear behavior with the limitations on their observed occurrence related more to experimental restrictions than any aspect of the underlying nuclear structure. We are presently testing new techniques for searching for evidence of resonance behavior in heavier systems where standard large-angle scattering excitation functions are no longer feasible.

a. Analysis of the  $E_{\text{cm}} = 45.65 \text{ MeV}$   $^{24}\text{Mg} + ^{24}\text{Mg}$  Resonance  
 (S. J. Sanders and R. R. Betts)

An analysis of detailed elastic scattering angular distributions at a number of energies over a narrow resonance in the  $^{24}\text{Mg} + ^{24}\text{Mg}$  system indicates that the structure underlying this resonance differs considerably from that of a simple molecular resonance. Seven angular distributions with  $45.5 \text{ MeV} < E_{\text{cm}} < 45.8 \text{ MeV}$  were analyzed together by fitting to the data an energy-independent background to which was added a Breit-Wigner resonance term in one partial wave (see Fig. II-23). The fitting procedure varied the resonance parameters as well as the background  $S_\ell$  values for  $\ell = 26 - 40$ . The resonance was determined to most probably have spin  $J = 34$ , with the ratio of elastic to single-particle reduced widths  $\gamma_{e\ell}^2 / \gamma_{\text{SP}}^2 = 0.008$ . Assuming that the 45.65 MeV resonance and similar nearby resonances are part of the strength function of a spread single particle or molecular resonance, the width of this spread state is found to be  $\Gamma \sim 19 \text{ MeV}$ , at variance with the width of a few MeV that might be expected for a simple molecule.

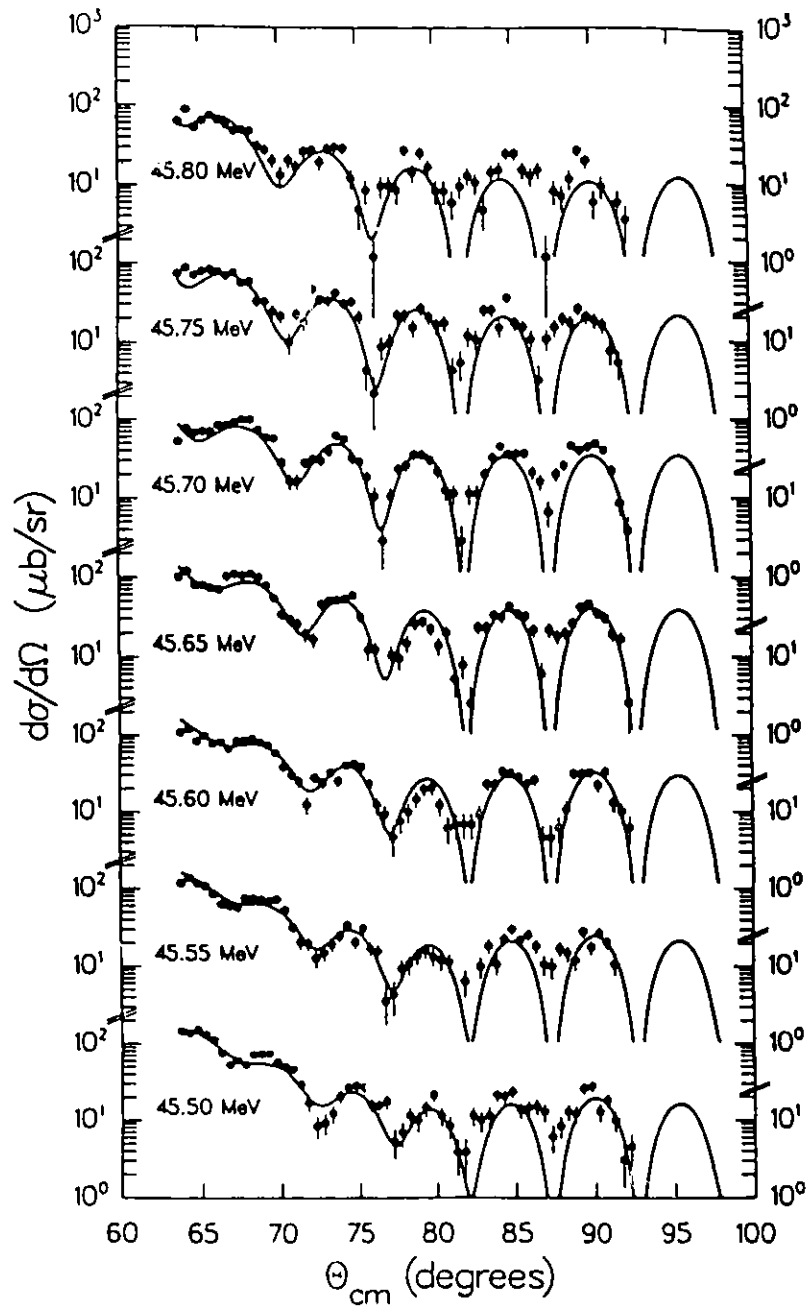


Figure II-23. Angular distributions for  $^{24}\text{Mg} + ^{24}\text{Mg}$  elastic scattering for  $45.5 < E_{\text{cm}} < 45.8$  MeV. The curves are the results of the fitting procedure described in the text with  $J = 34$ .

**b. Search for Shape Isomers in  $^{56}\text{Ni}$**  (B. K. Dichter, S. J. Sanders, R. R. Betts, and P. D. Parker\*)

We have conducted a study of the  $^{40}\text{Ca}(^{16}\text{O}, ^{28}\text{Si}^*)^{28}\text{Si}$  reaction, at approximately twice the Coulomb barrier energy, searching for resonant structures in the excitation function. The presence of resonances in this energy range, which are correlated with the previously observed resonances in  $^{28}\text{Si} + ^{28}\text{Si}$  scattering yields would be evidence for the existence of long-lived states of  $^{56}\text{Ni}$  with spins of the order of  $40\hbar$  and excitation energies of about 70 MeV. Recent theoretical calculations<sup>1</sup> suggest that these states may correspond to super-deformed  $^{56}\text{Ni}$  nuclei (shape isomers), which have a prolate shape and a 3:1 axis ratio. Experimental observation of the shape isomers in Ni is therefore of great importance to our understanding of nuclear structure at high spins and excitation energies.

The excitation function of the  $^{40}\text{Ca}(^{16}\text{O}, ^{28}\text{Si}^*)^{28}\text{Si}^*$  reaction was measured between 74.925 and 77.25 MeV in 75-keV steps for angles between  $30^\circ$  and  $60^\circ$  in the laboratory (Fig. II-24). Q-value distributions and angular distributions at each energy were also measured. Statistical analysis of the data shows that the observed structures in the  $^{40}\text{Ca}(^{16}\text{O}, ^{28}\text{Si}^*)^{28}\text{Si}^*$  reaction are correlated with those in the  $^{28}\text{Si}(^{28}\text{Si}, ^{28}\text{Si}^*)^{28}\text{Si}^*$  reaction at an 80% confidence level. Experiments seeking a signature for the conjectured fission isomers in  $\gamma$  rays from the de-excitation of the  $^{56}\text{Ni}$  compound nucleus are planned for the future.

---

\*Yale University, New Haven, CT.

<sup>1</sup>T. Bengtsson, M. Faber, M. Ploszajczak, I. Ragnarsson and S. Aberg, Lund MPh-84/01, preprint.

<sup>2</sup>R. R. Betts, B. B. Back and B. G. Glagola, Phys. Rev. Lett. 47, 23 (1981).

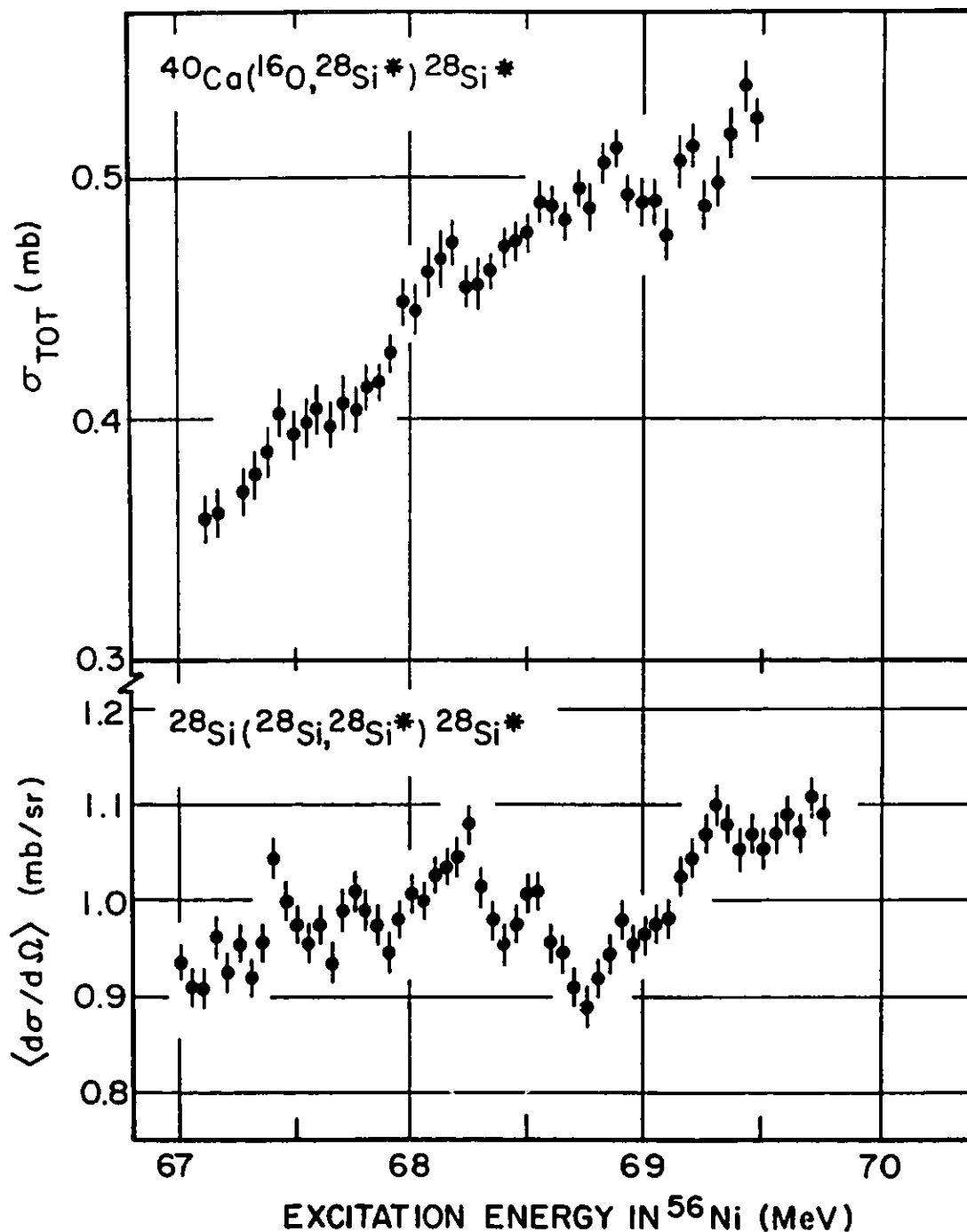


Figure II-24. The  $^{40}\text{Ca}(^{16}\text{O}, ^{28}\text{Si}^*) ^{28}\text{Si}^*$  reaction cross section is plotted together for comparison with the  $^{28}\text{Si}(^{28}\text{Si}, ^{28}\text{Si}^*) ^{28}\text{Si}^*$  reaction cross section as a function of the excitation energy of the  $^{56}\text{Ni}$  compound nucleus. The Q-value range covered in the  $^{16}\text{O} + ^{40}\text{Ca}$  measurement is  $-20 < Q < 0$  MeV and in the  $^{28}\text{Si} + ^{28}\text{Si}$  measurement in  $-22 < Q < 0$  MeV.

c. Elastic and Inelastic Scattering of the  $^{28}\text{Si} + ^{28}\text{Si}$  System

(F. Videbaek, B. B. Back, R. R. Betts, P. D. Bond,\*  
P. R. Christensen,† O. Hansen,\* S. Pieper, S. Saini,‡ S. J. Sanders,  
C. E. Thorn,\* and B. D. Wilkins)

Complete elastic and inelastic scattering angular distributions for the  $^{28}\text{Si} + ^{28}\text{Si}$  system at laboratory energies of 100, 112, 120, 151, and 180 MeV have been analyzed using optical-model and coupled-channel calculations. The forward-angle data and the higher-energy data can be described reasonably well using a normal strongly-absorbing potential. The large-angle scattering at the lowest energies, however, cannot be described using a conventional optical potential even when a surface absorbing imaginary potential is used with a conventional real potential. This result indicates that the large-angle scattering is dominated by a resonance state of the compound  $^{56}\text{Ni}$  nucleus.

---

\*Brookhaven National Laboratory, Upton, New York.

†Niels Bohr Institute, Copenhagen, Denmark.

‡University of Pennsylvania, Philadelphia, Pennsylvania.

## E. ACCELERATOR MASS SPECTROMETRY (AMS)

The technique of AMS has become a powerful tool to measure extremely low concentrations ( $10^{-10}$  to  $10^{-15}$ ) of a variety of long-lived radioisotopes ( $^{10}\text{B}$ ,  $^{14}\text{C}$ ,  $^{26}\text{Al}$ ,  $^{32}\text{Si}$ ,  $^{36}\text{Cl}$ ,  $^{41}\text{Ca}$ ,  $^{44}\text{Ti}$ ,  $^{59}\text{Ni}$ ,  $^{60}\text{Fe}$ ,  $^{129}\text{I}$ ) allowing various applications in a variety of research areas. In the past year, after the measurement on the half-life of  $^{60}\text{Fe}$  was completed, we have utilized the full tandem-linac system to extend quantitative AMS measurements of  $^{60}\text{Fe}$  into the region  $^{60}\text{Fe}/\text{Fe} < 10^{-13}$ . This allowed for the first measurements of  $^{60}\text{Fe}$  in meteoritic samples. The  $^{60}\text{Fe}$  measurement was performed with our new technique of using the gas-filled Enge split-pole spectrograph for isobar separation. The systematic studies of this technique as a function of gas pressure and gas composition, incident beam energy and ion species is also important in connection with our attempts to identify via AMS the very heavy radioisotope  $^{205}\text{Pb}$ . This study is of interest in connection with the possibility of measuring the integrated solar neutrino production of  $^{205}\text{Pb}$  from  $^{205}\text{Tl}$  in a very old thallium mineral. We have also spent some effort on producing pre-enriched  $^{41}\text{Ca}$  samples from natural materials which hopefully will allow us to perform AMS measurements of  $^{41}\text{Ca}$  at natural concentration levels.

a. AMS of  $^{60}\text{Fe}$  at Low Concentrations (W. Kutschera, W. Henning, Z. Liu,\*  
R. Pardo, M. Paul,† K. E. Rehm, R. K. Smither, and J. L. Yntema)

We have recently measured<sup>1</sup> through AMS the half-life of  $^{60}\text{Fe}$  to be  $T_{1/2} = (1.49 \pm 0.27) \times 10^6$  y, significantly longer than previously reported.  $^{60}\text{Fe}$  has recently gained renewed interest for a number of astrophysical reasons. 1) After the discovery of live  $^{26}\text{Al}$  ( $T_{1/2} = 7.2 \times 10^5$  y) in the interstellar medium,  $^{60}\text{Fe}$  appears to be another nuclide which could be used to trace ongoing nucleosynthesis in our galaxy. 2) There are measurements underway to find extinct  $^{60}\text{Fe}$  in meteorites through the measurement of  $^{60}\text{Ni}$  isotopic anomalies, which would provide information on the early history of the solar system, similarly to  $^{26}\text{Al}$  which was found through  $^{26}\text{Mg}$  isotopic anomalies. 3) Related to the question of primordial  $^{60}\text{Fe}$  abundance in meteorites is the role of  $^{60}\text{Fe}$  in the early heating of planetary bodies. 4) Another field of interest is the production of  $^{60}\text{Fe}$  through cosmic-ray interaction in meteorites. Due to the expected low concentration ( $^{60}\text{Fe}/\text{Fe} \approx 10^{-14}$ ) and the long half-life,  $^{60}\text{Fe}$  has not been detected with certainty in meteoritic samples. We have therefore embarked on AMS measurements of  $^{60}\text{Fe}$  in meteorites. Using our newly developed technique of isobar separation in a gas-filled magnetic spectrograph we have been able to increase our  $^{60}\text{Fe}$  sensitivity into the region where  $^{60}\text{Fe}$  is expected to occur in meteorites. This is illustrated in Fig. II-25 where we show the total energy vs. focal-plane position in the spectrograph for  $^{60}\text{Fe}$  ions from ion source samples with  $^{60}\text{Fe}/\text{Fe} \approx 10^{-8}$  (upper half) and  $^{60}\text{Fe}/\text{Fe} < 10^{-13}$  (lower half). The  $^{60}\text{Ni}$  peak (about  $10^6$  times as intense) is blocked off by a tantalum shield mounted in front of the focal-plane detector, with only a tail reaching into the focal-plane acceptance window. The technique seems to work particularly well in a situation like the present one where the interfering stable isobar is of higher Z such that low-energy tails in the magnetic rigidity spectrum (focal-plane position) are directed away from the region where the radioisotope is situated. This is not obvious from Fig. II-25 where the low-energy portion of the spectrum (left side) is blocked by the tantalum shield. However, comparison with systems with inverted Z sequence (like  $^{41}\text{Ca}$ - $^{41}\text{K}$ ) show this very clearly.

\*Institute of Atomic Energy, Beijing, The People's Republic of China.

†The Hebrew University of Jerusalem, Jerusalem, Israel.

<sup>1</sup>W. Kutschera et al., Nucl. Instrum. Methods B5, 430 (1984).



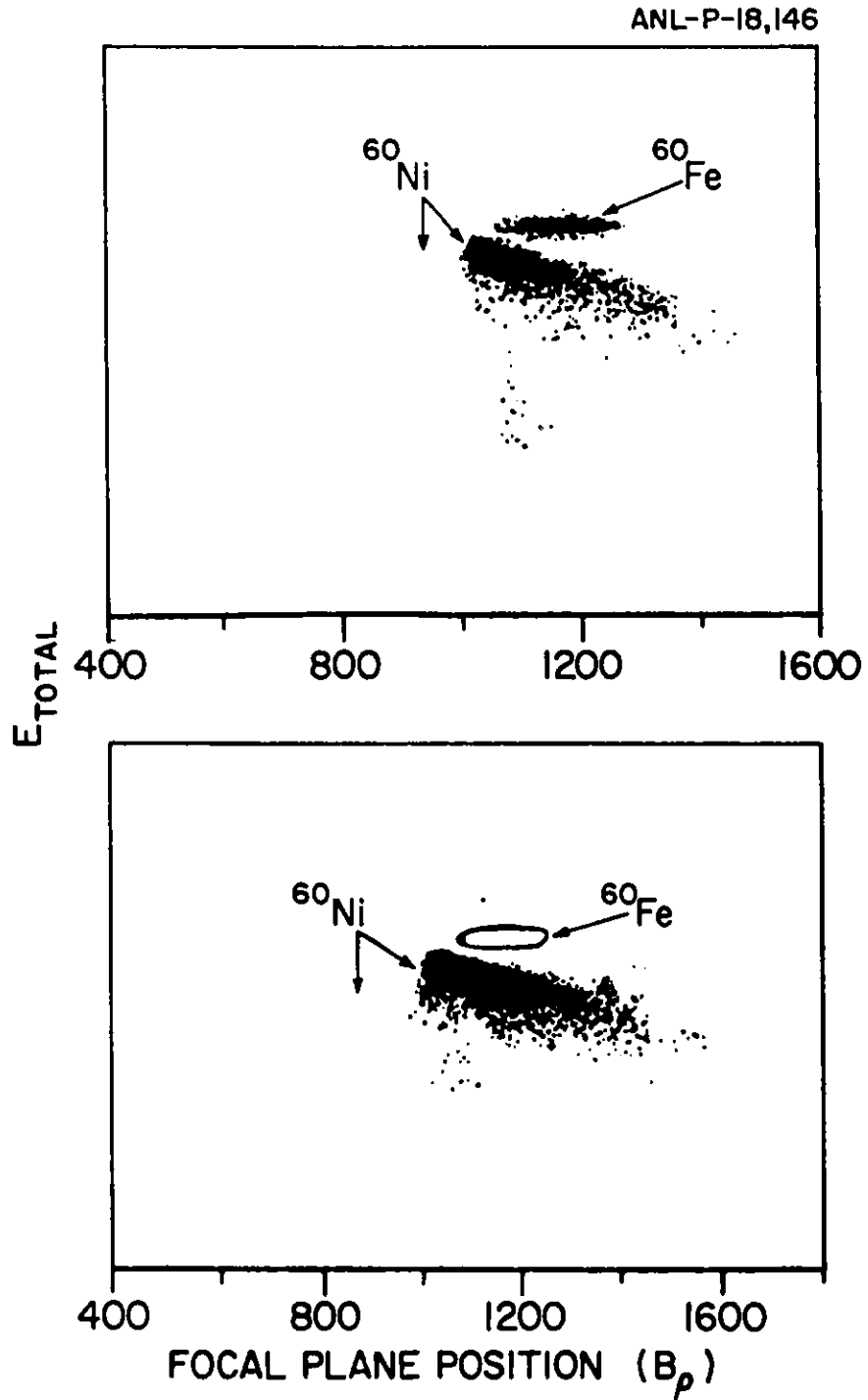


Figure II-25. Illustration of the separation of  $^{60}\text{Fe}$  ions from the  $^{60}\text{Ni}$  carrier beam.

- b. Accelerator Mass Spectrometry of  $^{205}\text{Pb}$  and Its Application to Solar Neutrino Detection (W. Henning, W. Kutschera, H. Ernst,\* G. Korschinek,\* P. W. Kubik,\* W. Mayer,\* H. Morinaga,\* E. Nolte,\* U. Ratzinger,\* M. Müller,† and D. Schüll†)

The radioisotope  $^{205}\text{Pb}$  was proposed for geological solar-neutrino detection eight years ago by M. Freedman and his collaborators at Argonne. Its attraction comes from an extremely low neutrino threshold ( $\approx 43$  keV) for the  $^{205}\text{Tl}(\nu, e^-)^{205}\text{Pb}$  reaction, and from the long half-life of the  $^{205}\text{Pb}$  radioisotope ( $T_{1/2} = 15$  million years). The low neutrino threshold provides the desired sensitivity to the low-energy part of the solar neutrino spectrum. The long half-life has two attractive consequences: i) collecting radioactive  $^{205}\text{Pb}$  nuclei over times comparable to their half-life allows accumulation of a large number of  $^{205}\text{Pb}$  atoms which can be more easily detected. ii) The long collection time averages over possible short-time fluctuations in the solar neutrino flux.

A year ago we had demonstrated that a high-energy heavy-ion accelerator (UNILAC at GSI) could be successfully used to determine low  $^{205}\text{Pb}$  concentrations via AMS. The experiments had also shown that present ion sources are not efficient enough for an experiment with only  $10^5$  atoms of the radioisotope. In addition, the nuclear charge resolution needs to be improved. These and other problems connected with a  $^{205}\text{Tl}$  solar neutrino experiment were discussed at a workshop in Munich last Fall. The general consensus was that there are still a large number of problems to be solved, but none of them seems insurmountable. We have decided to focus the present effort at Argonne on the aspect of isobar (nuclear charge) separation with our new technique of sending the ion through a gas-filled magnetic field. These studies are currently underway for medium-mass heavy ions and discussed in more detail in Sec. G.j. For the problem of interest here, i.e. the separation of  $^{205}\text{Pb}$  from  $^{205}\text{Tl}$ , it is interesting to note that the relative

---

\*Technische Universität, Munich, West Germany.

†GSI, Darmstadt, West Germany.

separation  $\Delta\bar{q}/\bar{q} = 2(\bar{q}_1 - \bar{q}_2)/(\bar{q}_1 + \bar{q}_2)$  varies surprisingly slowly over a large range of incident energy, extending to quite low energies. This is illustrated for  $^{205}\text{Pb} - ^{205}\text{Tl}$  in Table II-I. More experiments with the heaviest beams presently available at ATLAS are needed to establish to what level of relative concentration a reliable separation between these two heavy isobars can be expected to be possible.

Table II-I

<u><math>E_{\text{lab}}</math> (MeV)</u>	<u><math>\bar{q}(^{205}\text{Tl})</math></u>	<u><math>\bar{q}(^{205}\text{Pb})</math></u>	<u><math>\Delta\bar{q}/\bar{q}</math></u>
100	25.69	25.89	.0078
500	46.41	46.82	.0088
1000	56.69	57.22	.0093
2000	656.26	66.93	.0101
3000	70.98	71.74	.0107

c. <sup>41</sup>Ca-radioisotope Concentration in Natural Samples of Terrestrial Origin  
(W. Henning, W. A. Bell,\* P. J. Billquist, B. Glagola, W. Kutschera,  
Z. Liu, H. F. Lucas, M. Paul,† K. E. Rehm and J. L. Yntema)

We have measured the <sup>41</sup>Ca/Ca concentration in natural terrestrial samples in an accelerator mass spectrometry measurement with ATLAS. <sup>41</sup>Ca (half life  $t_{1/2} \approx 1.0 \times 10^5$  yr)<sup>1</sup> has been suggested as a tool for radiometric dating<sup>2</sup> and as a geological solar neutrino detector.<sup>3</sup> However, the natural <sup>41</sup>Ca/Ca concentration in terrestrial samples is expected to be very low, less than  $10^{-14}$ . The long half-life and electron capture decay with only the 3.3-keV X-rays as detectable radiation make decay counting not feasible. We have therefore used the highly-sensitive method of accelerator mass spectrometry to detect <sup>41</sup>Ca. Making use of pre-enrichment with an isotope separator, <sup>41</sup>Ca/Ca ratios in natural terrestrial samples have been measured for the first time.

Metallic calcium samples in an inverted negative-ion sputter source were sprayed with NH<sub>3</sub> to produce <sup>41</sup>CaH<sub>3</sub><sup>-</sup> ions for injection into the tandem. The choice of these ions is known to greatly reduced isobaric interference from <sup>41</sup>K. After single stripping and acceleration in the tandem, the linac accelerated <sup>41</sup>Ca<sup>10+</sup> ions to 200-MeV kinetic energy in the laboratory, sufficient for unambiguous particle identification. A very high suppression of neighboring stable Ca isotopes was achieved through the combined filtering action of the velocity-focussing linac and the magnetic beam-transport system. Particle identification was further enhanced through the use of a gas-filled magnetic spectrograph as isobar separator with a position-sensitive ionization chamber as focal-plane detector. Figure II-26 illustrates the performance of this detection system and shows examples of position spectra of <sup>41</sup>Ca and <sup>41</sup>K yields from various samples studied. For a blank sample, no <sup>41</sup>Ca counts were observed for a measuring time approximately three times longer than that for the cow-bone. The <sup>41</sup>Ca/Ca concentration at which actual <sup>41</sup>Ca yields can be unambiguously determined in the present system is  $> 6 \times 10^{-14}$ .  
Preenrichment with a Calutron isotope

---

<sup>1</sup>M. Mabuchi, H. Takahashi, Y. Nakamura, K. Notsu and H. Hamaguchi, J. Inorg. Nucl. Chem. 36, 1687 (1974)

<sup>2</sup>G. M. Raisbeck and F. Yiou, Nature 277, 42 (1979)

<sup>3</sup>W. C. Haxton and G. A. Gowan, Science 210, 897 (1980)

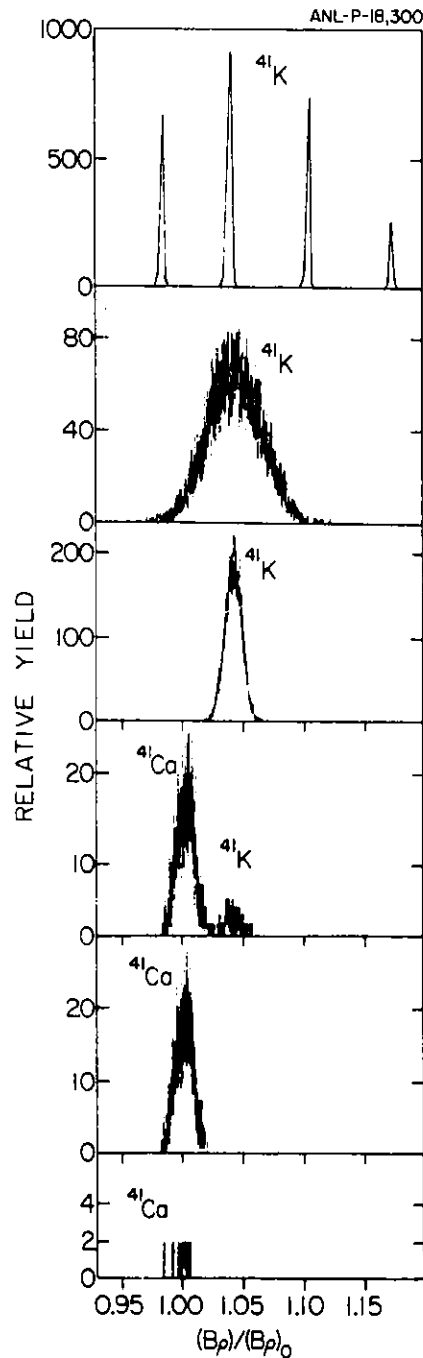


Figure II-26. Position spectra from the spectrograph focal-plane detector for  $^{41}\text{Ca}$  and  $^{41}\text{K}$  yields from various sample materials. a) - c) illustrate the collapse of the magnetically dispersed charge-state spectrum of  $^{41}\text{K}$  ions to a single line when nitrogen gas of 1.0 Torr (b) and 8.0 Torr (c) pressure is introduced into the magnetic-field region. e) - f) show yields for the gas-filled device at 8.0 Torr from (i) a calibration sample with known  $^{41}\text{Ca}$  concentration [d) and e)] and (ii) the contemporary bovine long (leg) bone (f). In e) and f) additional gating from the detector total-energy and energy-loss signals is applied.

separator intensifies sensitivity by about 2 orders of magnitude. Preenriched cow bone and limestone samples show a  $^{41}\text{Ca}/\text{Ca}$  ratio well above the limit observed with the blank sample. This excludes instrumental effects and cross contamination in the ion source from the calibration sample as the origin of the observed  $^{41}\text{Ca}$ . The deduced original  $^{41}\text{Ca}$  concentration for the cow bone is  $(2.1 \pm 0.4) \times 10^{-4}$ . This is close to the range estimated from thermal neutron fluxes at the earth's surface but comfortably at the upper limit which is encouraging for future applications. Third, the limestone samples show, within error, a factor three and six lower concentrations for the surface and deeper location, respectively.

A major interest in  $^{41}\text{Ca}$  stems from its potential as a practical method of dating calcium-containing materials up to possibly 1 million years of age. Particular interest arises in the feasibility of using  $^{41}\text{Ca}$  as a means of dating Middle and Late Pleistocene bone which contains significant amounts of calcium and is found at many sites of paleoanthropological interest.

While the relatively high  $^{41}\text{Ca}$  concentration that we have found in contemporary bone is quite encouraging, this by no means yet assures the utility of  $^{41}\text{Ca}$  as a dating tool.  $^{41}\text{Ca}$ , like  $^{14}\text{C}$ , is produced by cosmic-ray neutron secondaries. However, the bulk of the isotope is not made in the atmosphere, as is the case with  $^{14}\text{C}$ , but rather in the upper meter of the soil profile by neutron capture on  $^{40}\text{Ca}$ . Following production,  $^{41}\text{Ca}$  would be mixed with the other naturally-occurring calcium isotopes into the soil matrix through ground-water action. Calcium is taken up into the plant tissue in the form of  $\text{Ca}^{2+}$  through ion absorption into the root system. Radiocalcium, like all the other isotopes of calcium, would be incorporated into bone mineral through ingestion of plant materials and water. The fact that lithospheric rather than atmospheric production predominates raises the strong possibility that localized mixing and erosional effects may cause significant variations in initial  $^{41}\text{Ca}/^{40}\text{Ca}$  ratios in many environments. Obviously, careful systematic studies are necessary to obtain some answers to these questions.

## F. OTHER TOPICS

In addition to the programs described above, selected topics in nuclear physics have been studied, involving the linac and other facilities in the Physics Division. This includes measurements of the spontaneous emission of heavy clusters ( $^{14}\text{C}$ ,  $^{34}\text{Si}$ ....) from heavy nuclei; the measurement of the electron-capture decay branching ratio of  $^{81\text{m}}\text{Kr}$ , of interest for a  $^{81}\text{Br}$  solar-neutrino experiment; the measurement of E1 matrix elements in Ra nuclei, a test of the octupole deformation model; exploratory studies about the possibility of a condensed crystalline state in heavy-ion beams; and the search for positron resonances in the interaction of positrons with electrons.

a. Cluster Decay of  $^{241}\text{Am}$  (M. Paul\*, I. Ahmad, and W. Kutschera)

Recently it has been established that several Ra nuclei spontaneously decay by the emission of  $^{14}\text{C}$  nuclei. Calculations indicate many other cases where the emission of nuclei heavier than alpha particles is possible. It has been found that the half-life for the emission of cluster particles depends very strongly on the available decay energy, as might be expected. For  $^{241}\text{Am}$  the most favorable decay mode seems to be the emission of  $^{34}\text{Si}$  nuclei. We have used track recording foils in an attempt to measure the ratio between cluster decay and alpha decay. A 0.5-millicurie  $^{241}\text{Am}$  source was prepared on a platinum disk by electrodeposition. The source was  $2\text{ cm}^2$  in area and quite thin. The number of atoms in the source was determined both by low geometry alpha counting and also by counting the 59.5-keV gamma rays.

A polycarbonate foil was exposed to the  $^{241}\text{Am}$  source in vacuum for a period of 38 days. After the exposure, the foil was etched and the recorded tracks were counted under a microscope. These tracks were compared with tracks produced by 81-MeV  $^{28}\text{Si}$  ions from the Argonne Tandem accelerator and fission fragments from a  $^{248}\text{Cm}$  source (Fig. II-27). Thirty three fission fragments were identified which gave a fission/alpha ratio of  $(2.4 \pm 0.5) \times 10(-12)$ , in agreement with previous measurements. No Si tracks were observed; this gave an upper limit of  $1.4 \times 10(-13)$  for the  $^{34}\text{Si}/\text{alpha}$  ratio. This limit lies between the two theoretical calculations of  $1.1 \times 10(-15)$  and  $4.0 \times 10(-13)$ .

---

\*Permanent address: Hebrew University, Jerusalem, Israel.



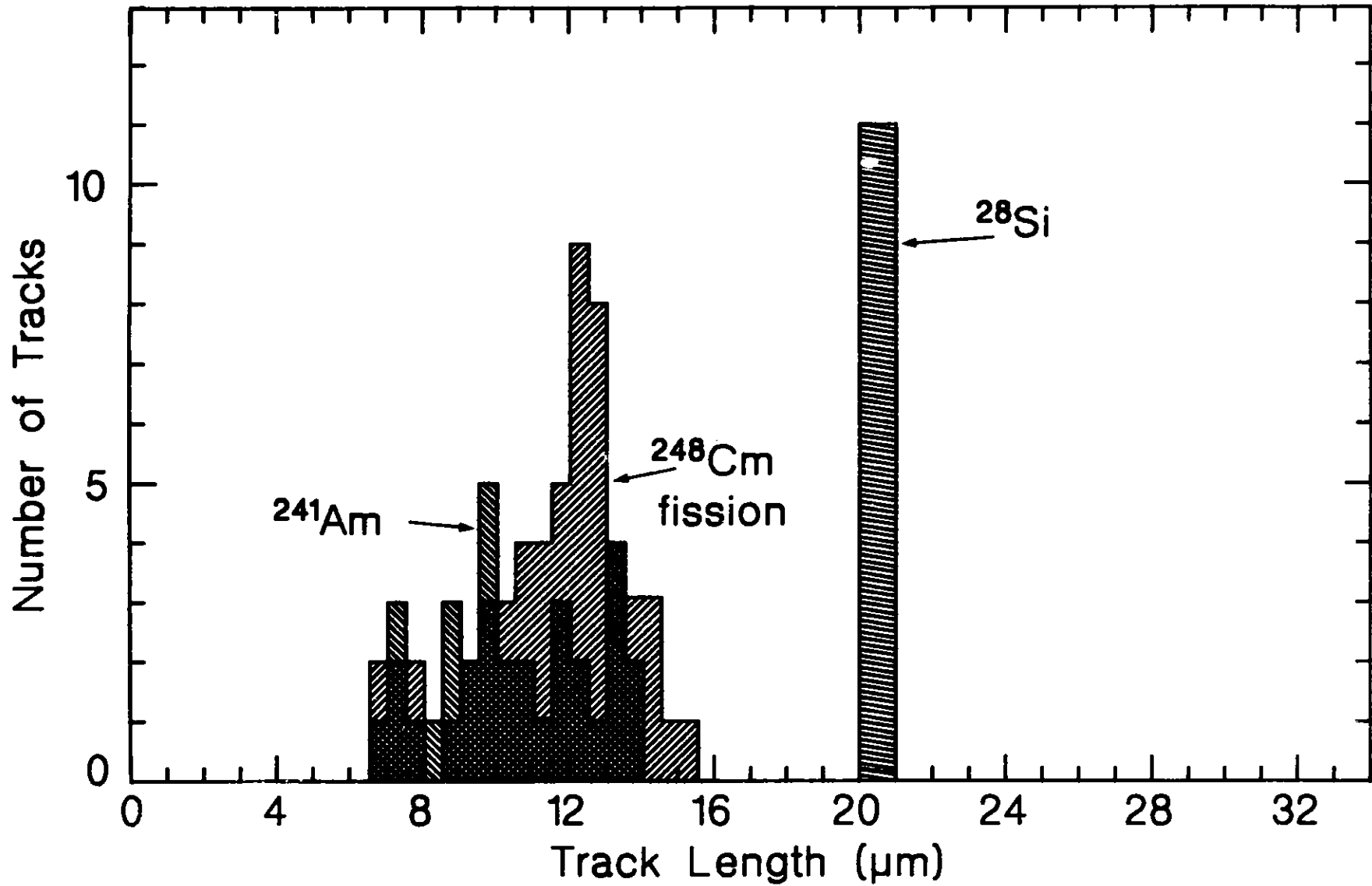


Figure II-27. Length spectrum of tracks produced by 81-MeV  $^{28}\text{Si}$  ions, spontaneous fission fragments from a  $^{248}\text{Cm}$  source and fragments emitted from the  $^{241}\text{Am}$  source. All tracks produced by the  $^{241}\text{Am}$  source are consistent with fission tracks. No tracks attributable to decay by  $^{34}\text{Si}$  emission were observed.

b. Electron-Capture Decay Branching Ratio of  $^{81m}\text{Kr}$  (C. Davids, I. Ahmad, R. V. F. Janssens, R. Holzmann, W. Kutschera, and A. Konstantaras)

A number of different solar neutrino detectors have been proposed to help shed light on the deficit of solar neutrinos observed by the  $^{37}\text{Cl}$  detector. One of these is  $^{81}\text{Br}$ , which is mainly sensitive to neutrinos coming from the decay of  $^7\text{Be}$  in the sun. In order to assess the feasibility of  $^{81}\text{Br}$  as a solar neutrino detector, it is necessary to know the neutrino capture rate leading to  $^{81}\text{Kr}$ . The matrix element for neutrino capture is the same, apart from spin factors, as the inverse process of electron capture.

The ground state of  $^{81}\text{Kr}$  ( $J^\pi = 7/2^+$ ) decays to the ground state of  $^{81}\text{Br}$  ( $J^\pi = 3/2^-$ ) by electron capture, with a first forbidden log ft of 11.2. The rate of neutrino capture for the inverse of this process is far too slow to make a practical solar-neutrino detector. However, there is an isomeric state in  $^{81}\text{Kr}$  at 190 keV with  $J^\pi = 1/2^-$ , and if this state were to decay to the  $^{81}\text{Br}$  ground state with an allowed electron capture, the associated inverse process of neutrino capture would most likely be fast enough to serve as a practical solar-neutrino detector. To obtain a quantitative answer to this question, it is necessary to determine the rate of electron capture decay of the  $^{81}\text{Kr}$  isomer.

With a half-life of 13s,  $^{81m}\text{Kr}$  decays predominantly by the emission of a highly-converted 190-keV E3 gamma ray, as well as a small electron capture branch. In this region of the nuclidic chart, electron capture decays occur between states of the requisite spins with log ft ranging from 4.9 to 6.2. If a log ft of 5.3 for the electron capture of  $^{81m}\text{Kr}$  is assumed, the branching ratio for this mode of decay is then  $1 \times 10^{-5}$ .

A group at Princeton University has measured the  $^{81m}\text{Kr}$  electron capture branching ratio, and their results imply a log ft of 4.6. This would be the fastest such rate in this region of the chart of the nuclides, so it is important to confirm these results.

We have assembled and are testing a detector system to measure the  $^{81m}\text{Kr}$  electron capture branching ratio. The signal that such a decay has taken place is the emission of an unaccompanied Br K X-ray. Thus the problem boils down to the observation of Br K X-rays in an intense background of Kr K X-rays. These Kr K X-rays are all accompanied by a conversion electron of energy  $>170$  keV, so if X-rays observed in coincidence with electrons can be

removed from the data, there is a good chance of seeing the unaccompanied Br K X-rays. Also required is an X-ray detector having excellent resolution, in order to resolve the Br X-rays from the Kr X-rays which will inevitably leak through the vetoing process.

Currently the system uses a small plastic scintillator coupled to a photomultiplier tube as a counting chamber to house the  $^{81\text{m}}\text{Kr}$  gas and to detect the conversion electrons with virtually 100% efficiency. The decays of the isomer are viewed by a Si(Li) X-ray detector through a thin window in this chamber. In addition, to further suppress background in the X-ray detector due to Compton-scattered 190-keV gamma rays, an array of four 2"  $\times$  2" NaI(Tl) detectors is suspended symmetrically behind the X-ray detector.

Tests are now being conducted using a long-lived source of  $^{83\text{m}}\text{Kr}$ , and data with  $^{81\text{m}}\text{Kr}$  sources will be taken in the near future.

c. El Matrix Elements and the Test of the Octupole Deformation Model in  $^{225}\text{Ra}$  (I. Ahmad, C. W. Reich\*, and G. A. Leandert†)

The signature of octupole deformation in odd-mass nuclei is the occurrence of parity doublets, which consist of two almost degenerate states with same spin but opposite parities. In the case of stable octupole deformation the members of the doublet derive from the same intrinsic state; that is the states will be identical except for their parities. Experimentally, the alpha decay rates, Coriolis matrix elements, and decoupling parameters for the two members of the doublet are found to be similar but not equal. Another approach to test the presence of stable octupole deformation is to determine the  $\Delta K=1$  El matrix element between the  $1/2^+$  and  $1/2^-$  members of the parity doublet. We have measured lifetimes of several levels in  $^{225}\text{Ra}$  to deduce El transition rates. From these rates we have determined the  $\Delta K=0$  and  $\Delta K=1$  El matrix elements. We find that the  $\Delta K=0$  matrix element (0.063 e.fm) is about an order of magnitude larger than the  $\Delta K=1$  matrix element (-0.0046 e.fm). For a stable octupole shape the  $\Delta K=1$  matrix element should vanish. Thus the nonzero value of the  $\Delta K=1$  matrix element indicates that although the  $^{225}\text{Ra}$  nucleus has large octupole-octupole correlations, it does not have a permanent octupole deformation. An alternate explanation would be that the nucleus has stable octupole shape but some additional effects cause a nonzero value for the  $\Delta K=1$  transition.

---

\*Idaho National Engineering, Idaho Falls, Idaho.

†UNISOR, Oak Ridge Associated Universities, Oak Ridge, Tennessee.

d. Measurement of Rates of Fast El Transitions in Ac-Ra Nuclei

(I. Ahmad, R. R. Chasman, A. M. Friedman\*, J. E. Gindler, T. Ishii† and S. B. Kaufman)

Recent calculations and experiments show that some Ac, Ra, and Pa nuclei have strong octupole-octupole correlations in their ground states giving rise to asymmetric shapes. Spectroscopic studies at high spin also indicate such asymmetric shapes for some Ra, Th and Ac nuclei. In the high spin studies it has been found that  $B(E1)$  values for transitions between the members of the  $K\pi=0^-$  and  $K\pi=0^+$  doublet bands are enhanced. The typical  $B(E1)$  value for  $\Delta K=0$  transitions in the mid-actinide region is  $10^{-4}$  Weisskopf units. The rates of El transitions at high spins in Ra-Th region range from  $10^{-3}$  to  $10^{-2}$  w.u. We have found a similar value for the El transition between the members of the ground state doublet in  $^{225}\text{Ac}$ . We have now measured the level lifetimes in  $^{225}\text{Ac}$ ,  $^{225}\text{Ra}$  and  $^{227}\text{Ac}$  by a delayed coincidence technique and derived the  $B(E1)$  values (Fig. II-28). The  $B(E1)$  values in  $^{225}\text{Ac}$  and  $^{227}\text{Ac}$  are  $3.5 \times 10^{-3}$  w.u. and  $8.2 \times 10^{-5}$  w.u. In both nuclei the El transitions occur between the  $3/2^-$  and  $3/2^+$  members of the parity doublet, and both nuclei possess strong octupole-octupole correlations. This result shows that although large enhancements in El transition rates occur in nuclei with octupole deformation, there is no one-to-one correspondence. Although plausible explanations have been suggested for the observed transition rates, as yet no quantitative calculations have been performed.

---

\*Deceased.

†Japan Atomic Energy Research Institute, Tokai, Ibaraki, Japan.

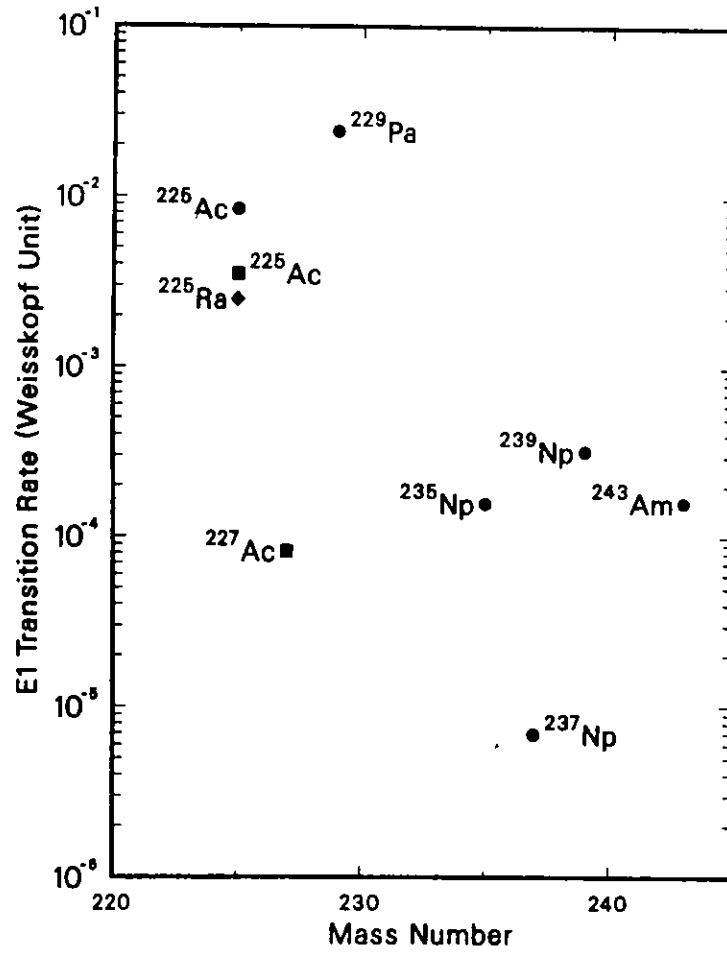


Figure II-28. Transition rates of the  $\Delta K = 0$  E1 transitions in odd-mass heavy nuclei.  $T_{\text{exp}}$  denotes the experimental  $\gamma$ -ray transition probability and  $T_{\text{w.u.}}$  refers to Weisskopf single-particle unit.

- e. Exploration of the Possibility of a Condensed Crystalline State in Heavy-Ion Beams (J. P. Schiffer, P. Kienle,\* O. Poulsen† and A. Rahman‡)

Present plans for storage rings for heavy ions include provisions for cooling these ions to very low internal temperatures. Calculations indicate<sup>1,2</sup> that at these temperatures the heavy ions within the beam will arrange themselves into an ordered array: a condensed crystalline state. The properties of such "Coulomb solids" have been the subject of theoretical investigations for many years. The recent plans at Aarhus to use laser cooling techniques on partially ionized beams seem particularly well suited for accomplishing such a state. The parameters of the storage ring may, however, be crucial and the possible advantages of weak focusing, as opposed to strong focusing planned for all presently envisioned storage rings, have been explored, and may be critical. It seems probable that the reported behavior of noise signals in the Novosibirsk proton storage ring may be related to one-dimensional order; it may take a weak focusing ring to achieve full three-dimensional order.

Recent molecular dynamics calculations shown in Fig. II-29 indicate that the particles actually would form cylindrical shells with triangular two-dimensional order within the shells and overall correlation that is approximately consistent with bcc order.

---

\*GSI, Darmstadt, W. Germany.

†University of Aarhus, Aarhus, Denmark.

‡University of Minnesota, Minneapolis, Minnesota.

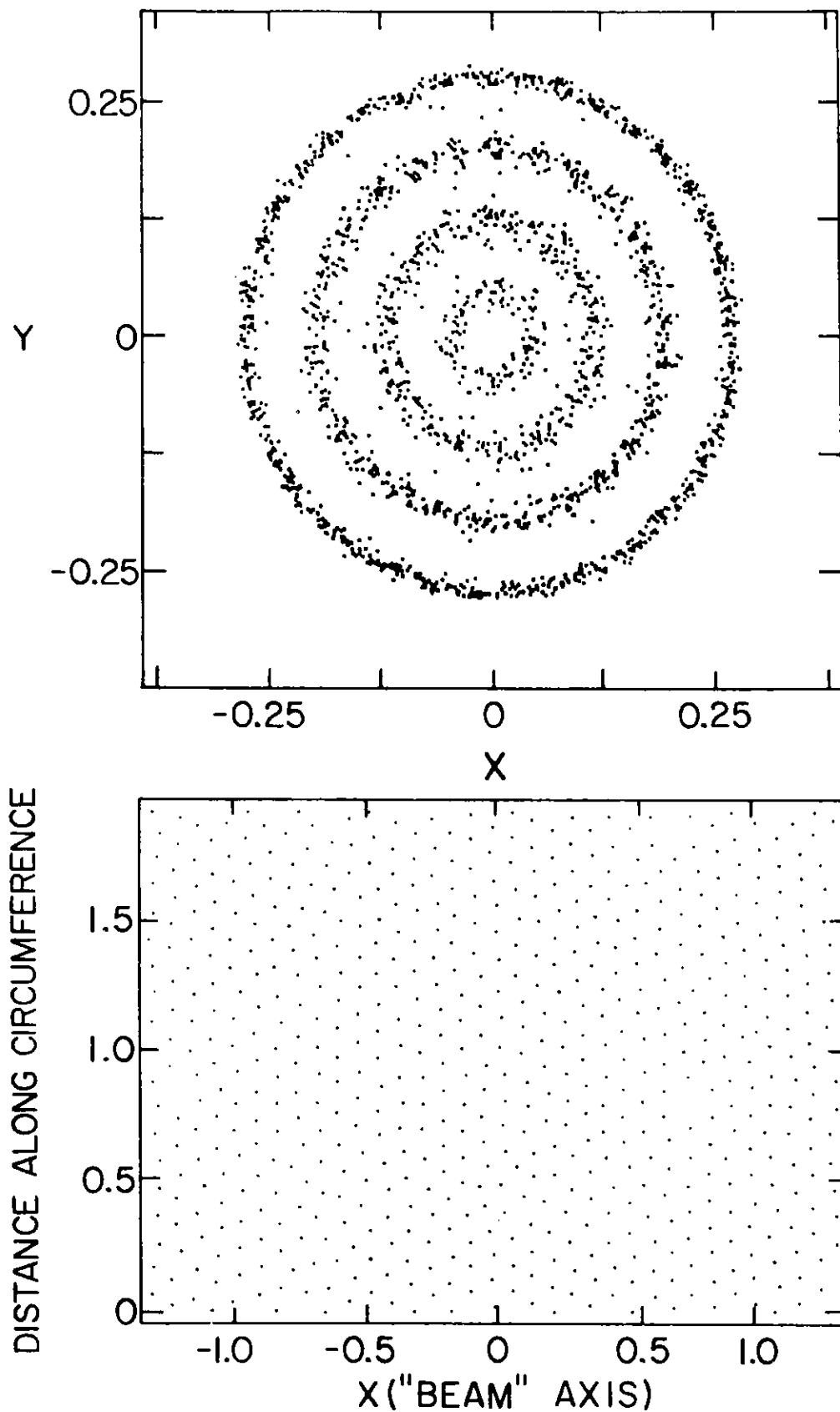


Figure II-29. Upper part: projection of 2000 particles in a molecular dynamics calculation onto the plane perpendicular to the beam ( $x$ -axis) for  $\Gamma = 180$ . Lower part: distribution of particles in the outer shell with the shell unfolded into a plane. All but the innermost shell show a similar pattern.



f. Search for Positron Resonances in the Interaction of Positrons with Electrons (W. Henning, J. P. Schiffer, S. Freedman, H. J. Lipkin, J. Napolitano, and Z. Vager)

There have been persistent reports from GSI of sharp positron lines associated with the collision of very heavy nuclei near the Coulomb barrier. Recently even lines seen in electron-positron coincidences have been reported. If these results are correct they would tend to lead one to a very important conclusion: the existence of a new light particle with a rest mass of about 1.7 MeV, that decays into an  $e^- e^+$  pair. It would follow that in the scattering of positrons from electrons at the appropriate energy one should see a corresponding resonance. We have explored the possible experiments which one could carry out in order to search for such a resonance. Using the short-lived positron emitter  $^{25}\text{Al}$ , scattered positrons were detected in coincidence with electrons at the appropriate angles. The range of possible widths for a new particle corresponding to the GSI positron line is from about  $10^{-6}$  eV to 50000 eV. Such scattering experiments could only see a resonance if its width were greater than 100 eV, possibly pushing the limit as low as 10 eV, with a great deal of effort. Theoretical arguments based on the anomalous magnetic moment of the electron suggest that the width of any such particle should be less than 1 eV. Therefore possible alternative experiments are also being explored, based on the possibility that such particles may be emitted in competition with photon emission in electromagnetic processes. Coincident events were recorded from two silicon surface-barrier detectors mounted behind a 3-mil thick Au foil which was bombarded by 1.2  $\mu\text{A}$  of 4-MeV protons. The sensitivity is presently limited by background from Compton scattering from one detector into the other. We are discussing ways to improve the experimental system to eliminate this background.

## G. EQUIPMENT DEVELOPMENT AT THE ATLAS FACILITY

The equipment development efforts are mainly concerned with two areas of activity. The major effort is directed at the new experimental equipment for research with ATLAS. In addition there is a general ongoing activity to improve existing equipment, and in particular developing better and more powerful detector systems. Equipment for ATLAS is well into the construction stage and several pieces of major apparatus are fully assembled and in use. Equipment for ATLAS is built in two phases. The first phase, which will be completed late this year, includes i) Several beam lines with beam diagnostics and beam-handling components to make optimal use of the good beam properties and beam-timing characteristics, ii) a large scattering facility, iii) phase I of a BGO sum-energy/multiplicity filter with a ring of Compton-suppressed Ge detectors, iv) the split-pole magnetic spectrograph which was moved from the tandem, v) and two general-purpose beam lines. In addition a new data-analysis system for on-line and off-line data handling was developed based on the architecture of a number of parallel processors. The second phase, where design and initial construction is starting in late 1986 includes i) phase II of the BGO ball with 50 BGO crystals and 12 Compton-suppressed Ge detectors, ii) a high-resolution broad-range mass spectrometer, iii) and two more general-purpose beam lines. During the first phase of equipment construction, highest priority was placed on this effort which restricted the research effort. During the second phase, priority will be shifted back to the research effort but a timely construction of the equipment will still be pursued.

a. Detector Development Laboratory (B. D. Wilkins and D. J. Henderson)

The detector development laboratory was started this past year with the goal of developing new and different types of detectors for use in heavy-ion physics research at ATLAS.

Thus far, two prototype detectors have been developed for use in a large-area time-of-flight system using the beam timing from ATLAS. The first of these, a large-area, fast two-stage, multiwire gas counter provides one with good time- and (X, Y) position-resolution. Considerable effort has been made to vary the detector parameters in order to optimize the time and position resolutions as well as provide a detector with thin entrance and exit windows ( $70 \mu\text{g}/\text{cm}^2$  polypropylene) and high efficiency for counting heavy-ion charged particles. At this stage time resolutions of near 300 pico-seconds and (X,Y) position resolution of  $\leq .7 \text{ mm}$  have been achieved. Further tests are proceeding to see if this performance can be improved.

The second detector, a large-area Bragg-Curve Spectrometer (described in detail in another section) has been constructed and tested on the ATLAS beam line. This detector provides one with good energy resolution and a high charge resolution. Results from the ATLAS beam test using 10 MeV/A  $^{58}\text{Ni}$  ions yielded an energy resolution of 0.8% and a  $Z/\Delta Z = 80$  for the elastically-scattered Ni ions. Further tests on this detector are underway to measure the charge and energy resolution obtained for charged particles with insufficient energy to achieve their Bragg peak. If the detector can be used effectively on particles in this category (i.e. fission fragments and fusion-evaporation residues) it will greatly enhance its versatility as a heavy-ion research detector.

Detector projects which are just beginning include the development of a small-area microchannel plate detector with good timing characteristics ( $\sim 100$  pico-second resolution) with X- and Y-position information. A second project, just starting, is the development of a plastic scintillator counter telescope using only one phototube. The  $\Delta E$  counter would be a thin, fast plastic and the E counter a thick slow plastic. Electronic means would be used to separate the light output from the two plastic detectors. This detector could be used on the long-range light particles which penetrate the Bragg-Curve Spectrometer or as an independent stand-alone detector.

b. Development of Large-Area Position-Sensitive Timing Detectors  
(F. L. H. Wolfs)

Two gas-filled position-sensitive Parallel-Gridded Avalanche Counters (PGAC) have been built. The counters have an active area of 20 cm × 20 cm and provide a timing signal and a two-dimensional position readout. Using the kinematic coincidence technique, the counters will initially be used to study fission reactions at bombarding energies around the Coulomb barrier.

The performance of this PGAC detector system was studied with a 250-MeV  $^{58}\text{Ni}$  beam on various targets. Measured position and timing resolution are 0.05 cm and 250 ps, respectively. A mass resolution of 2.5 amu was obtained using a 40-cm flight path.

c. Development Work on a Large Bragg-Curve Spectrometer (M. F. Vineyard, D. G. Kovar, B. Wilkins, D. Henderson, C. Beck, C. Davids and J. Kolata\*)

A large solid-angle Bragg-Curve Spectrometer (BCS) has been developed for use on the large scattering facility at ATLAS. The detector, which is of a cylindrical geometry, has an active area of approximately 300 cm<sup>2</sup> and an active depth which can be varied up to 36 cm. It was primarily designed to be used with a fast-timing position-sensitive Breskin detector which provides the fast trigger for a time-of-flight system where good mass-, charge- and energy-resolution and a large solid angle are necessary. The BCS has been successfully tested using Si, S and Ni beams, where it provided excellent Z-resolution on the order of  $\Delta Z/Z = 1.25\%$  and energy-resolution ( $\sim 0.5\%$ ) as good or better than obtained on the same particles using solid-state detectors (Fig.II-30). The range of particles which stop in the detector can also be measured quite accurately by recording the time difference between the first and last electrons of a given pulse which arrive at the anode of the detector. Such information may be useful in obtaining the mass of the stopped particle when the BCS is used in a stand-alone configuration.

Tests are currently underway to determine the resolution of the BCS on particles which have insufficient energy to reach their Bragg peak. Successful use of the BCS on this type of particle (e.g., fission fragments and low-energy evaporation residues) would enhance the value of this detector.

The performance of this prototype detector as discussed above demonstrated its suitability as a large-area stand-alone gas detector, as well as the back detector to a Breskin detector in the time-of-flight system. It is planned for the coming year to use this system to measure evaporation residues in studies of the systematics of heavy-ion induced fusion reactions.

---

\*Permanent address: University of Notre Dame, Notre Dame, Indiana.

ANL-P-18,334

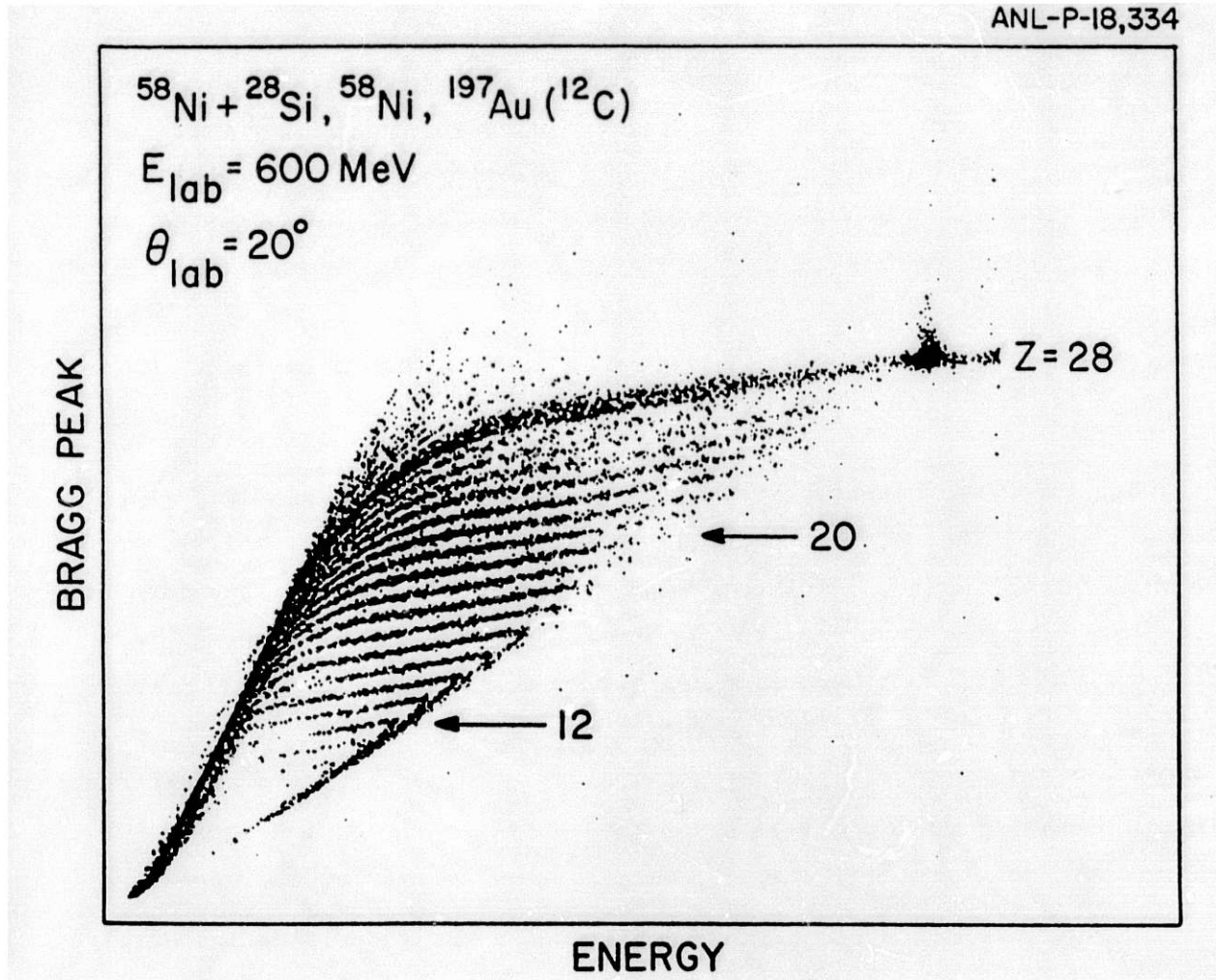


Figure II-30. Scatterplot of Bragg peak versus energy for 600-MeV  $^{58}\text{Ni}$  ions scattered at  $20^\circ$  from  $^{28}\text{Si}$ ,  $^{58}\text{Ni}$  and  $^{197}\text{Au}$  ( $^{12}\text{C}$ ) targets. In this case the detector subtended a solid angle of  $\sim 5.5$  msr.

d. Development of a Position Sensitive Timing Detector for the Split-Pole Magnetic Spectrograph (K. E. Rehm and F. L. H. Wolfs)

Based on the good experience with the parallel-plate avalanche timing detector which was used in several experiments at the LINAC spectrograph we have started to build an advanced position-sensitive timing detector. The position detector consists of  $10\mu$ -thick tungsten wires spaced 1 mm apart which are read out with integrated delay lines. Compared to the previous system the detector should have a cutoff at lower energies and should also handle higher count rates. The detector is just being assembled and first tests with heavy-ion beams are planned for spring of 1986.

e. Development of NaI(Tl) Charged Particle Detectors (C. Davids, D. Kovar, C. Beck, M. Vineyard, A. Konstantaras, C. Maguire,\* F. Prosser,† V. Reinert,‡ P. DeYoung,§ J. Kolata§)

In heavy-ion-induced reactions at laboratory energies greater than 10 MeV/nucleon, the velocity centroids of fusion residues are shifted below the value expected from complete fusion. This is interpreted as evidence for incomplete momentum transfer from projectile to composite system. This missing momentum is believed to be partly or completely removed by pre-equilibrium emission of light particles. As part of our study of the velocity spectra of fusion residues, we plan to measure the properties of light charged particles emitted during fusion events. Typically, protons up to 100 MeV and alpha particles of somewhat higher energies need to be detected.

Up to the present time the observation and identification of light charged particles has usually been done using silicon surface barrier detector telescopes. The disadvantages of such an array are small solid-angle, somewhat complex electronics requirements, and the imposition of a restricted dynamic range due to the need for a particle to penetrate through the first detector in order to be identified as a valid event. The costs and available thicknesses of detectors also limit the highest energy for protons to less than the range quoted above.

---

\*Vanderbilt University, Nashville, Tennessee.

†University of Kansas, Lawrence, Kansas.

‡Hope College, Holland, Michigan.

§University of Notre Dame, Notre Dame, Indiana.

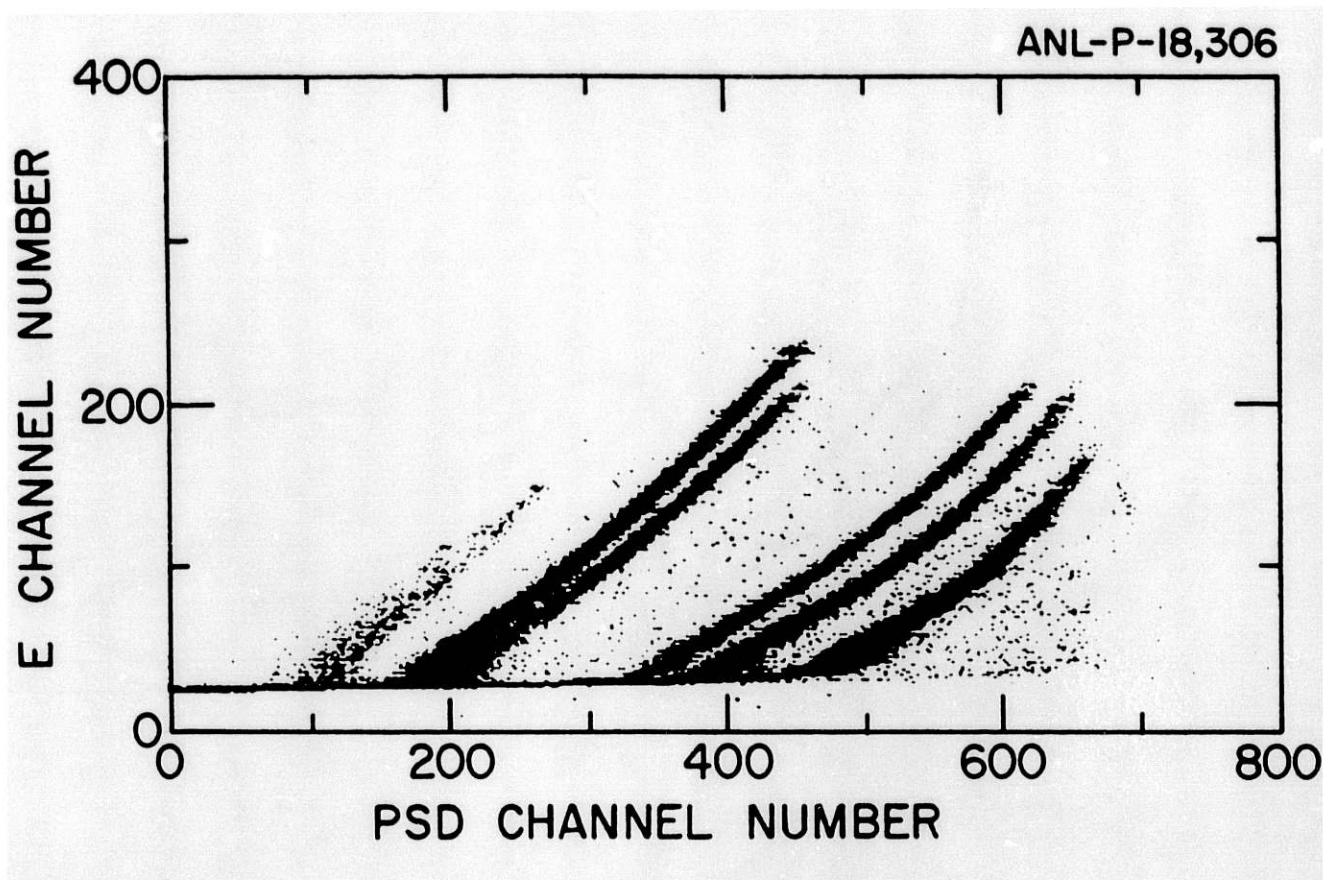


Figure II-31. Energy vs PSD for particles from 150-MeV  $\alpha$ 's in  $\text{CH}_2$ .



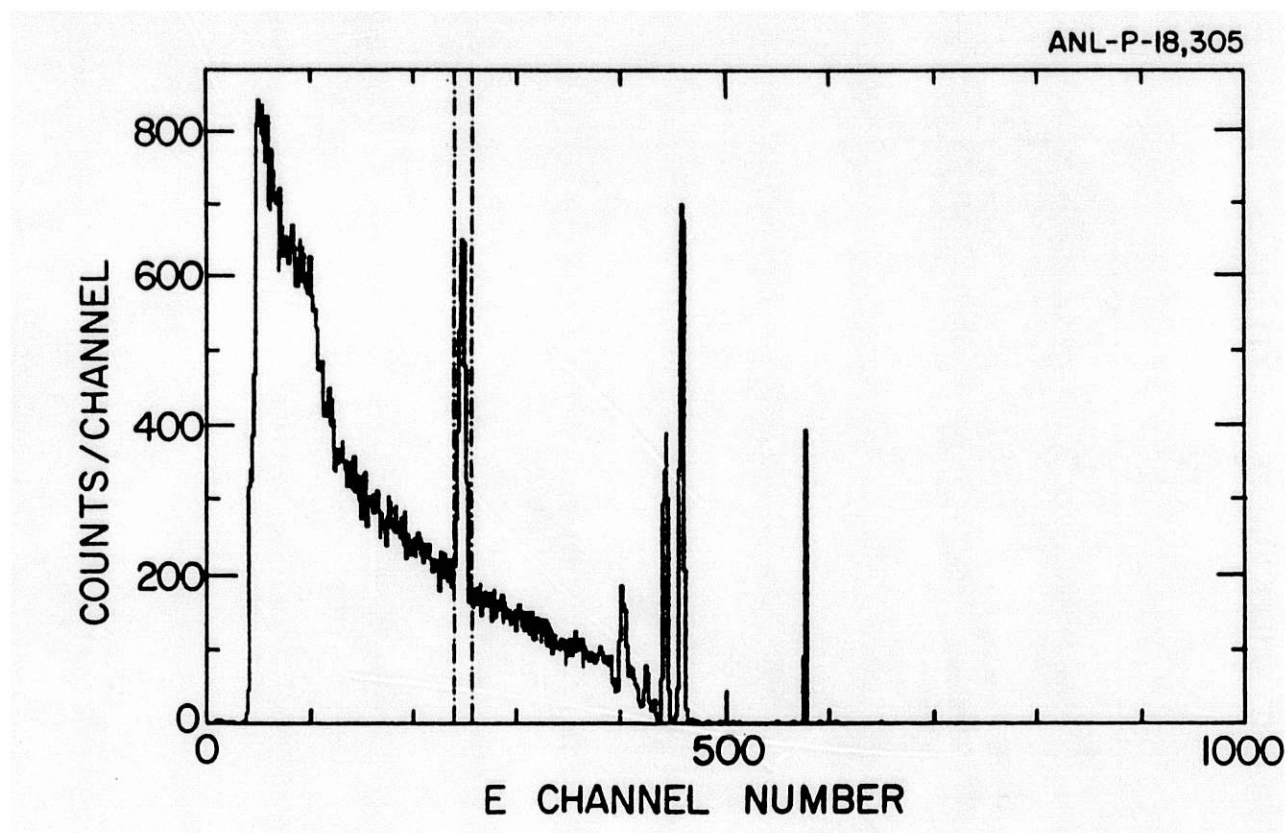


Figure II-32. Energy spectrum of particles from 150-MeV  $\alpha$ 's in  $\text{CH}_2$ .

Before the advent of silicon detectors, NaI(Tl) detectors were used for the detection of energetic charged particles. The energy resolution obtained using these detectors was typically a few percent, so when silicon detectors with vastly improved resolution capabilities became available in the early 1960's, virtually no further use was made of NaI(Tl). For the present work, however, NaI(Tl) has many advantages. The first is that detectors can be purchased with thicknesses more than sufficient to stop the most energetic protons expected. Secondly, the energy resolution is sufficient for our needs, since the experiments contemplated do not involve precise spectroscopy. Finally, a property of the NaI(Tl) scintillation mechanism allows one to identify light charged particles by means of pulse shape differences. This property had been known earlier, but modern electronic modules allow one to easily implement very clean separation of protons, deuterons, tritons, and alpha particles. Thus one detector can accomplish the aims formerly satisfied by up to three silicon detectors.

We have purchased five 3/4" dia x 1-1/2" deep detectors and have on order another five with dimensions 2" dia x 2" deep. They are designed to operate partially or totally in vacuum, and we have designed and built low-power bases utilizing FET transistors for these detectors. In trials at ATLAS, the Notre Dame tandem, and the Indiana Cyclotron, excellent particle separation was achieved down to ~1.5-MeV protons and 4-MeV alphas. Figure II-31 shows a 2-dimensional plot of energy vs pulse-shape discrimination (PSD) parameter for 150-MeV  $\alpha$  particles on a CH<sub>2</sub> target. The solid bands are, in order of decreasing PSD, protons, deuterons, tritons, <sup>3</sup>He, <sup>4</sup>He and Li particles. Figure II-32 shows the energy spectrum of all particles projected out from Fig. II-31. Besides the pulse peak at channel 580,  $\alpha$ -particle groups below channel 500 are seen from scattering on <sup>12</sup>C, and at channel 250 are the recoil protons from the H( $\alpha$ ,p)<sup>4</sup>He reaction. We are now in the midst of perfecting a way to calibrate the energy scale for the different types of particles.

The detectors also show sub-nanosecond time resolution, and, in conjunction with a Bragg-curve detector, we should be able to use a large array of NaI(Tl) detectors to study light particle-fusion residue correlations at ATLAS in the coming year.

f. Room Temperature Electron Detector (I. Ahmad)

Lithium-drifted silicon detectors are routinely used for measuring electron spectra. These detectors have to be cooled to liquid nitrogen temperature to minimize the thermal noise generated in the detector. Recently, passivated ion-implanted silicon detectors with very low leakage currents have become available. For example, 300-micrometer thick detectors of 20 mm<sup>2</sup> area have leakage currents of less than 5 nanoamperes. We have tested such detectors and found that they have resolutions (FWHM) of less than 3.5 keV at 100-keV electron energy (Fig. II-33). With alpha particles these detectors show an order of magnitude less tailing than surface barrier detectors of the same dimensions. The thickness of the detector used in the test can stop electrons up to 300-keV energy. These detectors look promising for in-beam electron spectroscopy. They could be profitably used with mini-orange magnets for on-line electron measurements. Because these detectors work at room temperature, they can be easily used in any experimental setup. The high resolution (FWHM=9.0 keV for 6 MeV alpha particles) and low tailing make these detectors suitable for conventional alpha particle spectrometry. We plan to test these detectors for the measurement of heavy-ion spectra. Because of thinner windows they might give better energy and time resolution.

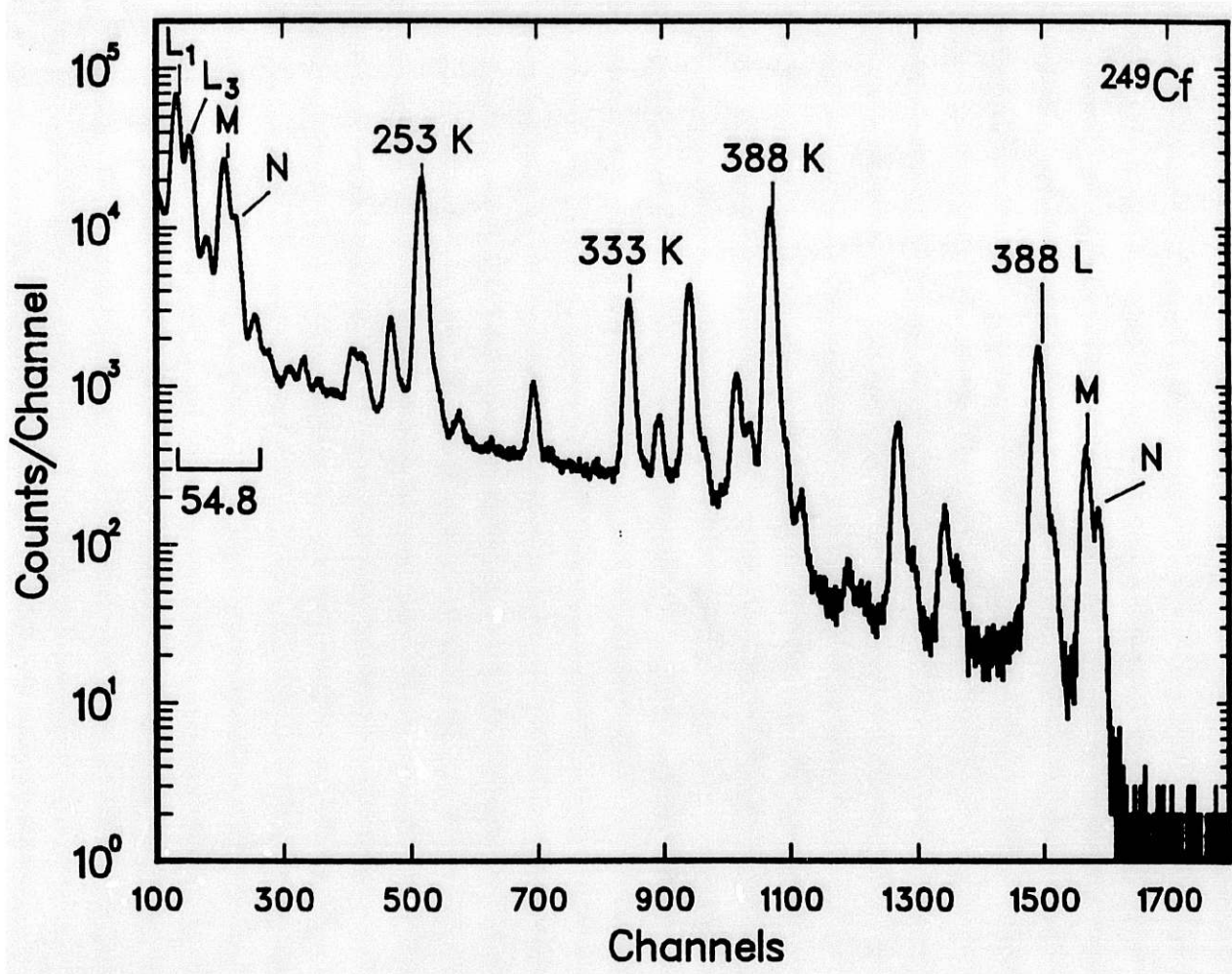


Figure II-33. Conversion electron spectrum of a  $^{249}\text{Cf}$  source measured with a passivated ion-implanted silicon detector. The peak resolution is 3.8 keV and the energy scale is 0.245 keV per channel.

- g. Superconducting Solenoid Lens Electron Spectrometer (P. J. Daly,\*  
Z. W. Grabowski,\* W. Trzaska,\* R. V. F. Janssens, and T. L. Khoo)

Work has continued on the construction of the Purdue superconducting electron spectrometer to be installed at ATLAS. Following the design studies of the spectrometer assembly, construction and final assembly has taken place at Purdue. Vacuum and detector testing have also been performed and minor problems have been corrected. The spectrometer is currently being installed at the 6-MV tandem facility of Purdue University for initial tests of all systems. Installation of the spectrometer in its final location at the linac is scheduled for the Fall of 1986.

---

\*Purdue University, W. Lafayette, Indiana.

- h. Development and Testing of an Air-Core Superconducting Solenoid for Measurements on the Linac (F. Becchetti,\* R. Stern,\* J. Janecke,\* P. Lister,\* D. G. Kovar, R. V. F. Janssens, M. F. Vineyard, W. Phillips, and J. J. Kolata†)

Two runs at ATLAS using a 20-cm dia. by 40-cm long 3.5 Tesla air-core superconducting solenoid<sup>1</sup> were completed. The runs used  $\approx 100$ -MeV  $^{16}\text{O}$  and  $^{18}\text{O}$  beams, respectively. The first run was a test and development run of the X-Y-dE-E-t focal-plane detection system, and the  $^{16}\text{O} + ^{12}\text{C}$  reaction products were observed. The second, recently completed run, was our first operational run looking for specific reaction products, from targets of  $^{18}\text{O}$  and  $^{26}\text{Mg}$ . The ultimate goal is to observe ( $^{18}\text{O}, ^{18}\text{Ne}$ ), ( $^{18}\text{O}, ^{17}\text{F}$ ), ( $^{18}\text{O}, ^{15}\text{O}$ ), ( $^{18}\text{O}, ^{14}\text{O}$ ), and other reactions leading to very neutron-rich nuclei. Although the spectrometer and detector system are far from optimized, the two (short) runs have produced very encouraging results. The measurements cover the range  $3^\circ$  to  $6^\circ$  with  $d\Omega = 30$  msr and a two-meter flight path, and used nearly full beam intensity ( $\approx 120$  nanoamperes). Well-focussed images of reaction products ranging from  $\alpha$  particles to fusion products were observed. Further improvement in timing resolutions (from the present  $\approx 600$  ps), e.g. by using better quality solid-state detectors, will greatly improve the mass resolution. Nonetheless, we have demonstrated that a large solid-angle air-core superconducting solenoid can be used to study heavy-ion and other nuclear reactions near zero degrees.<sup>2</sup> This opens up many applications which we wish to pursue in the next few years. The solenoid development is being done as part of a Ph.D. thesis (R. Stern).

---

\*University of Michigan, Ann Arbor, MI.

†University of Notre Dame, South Bend, IN.

<sup>1</sup>R. Stern et al., Proceedings of the Conference on Instrumentation for Heavy Ion Research, ORNL CONF-841005 (1984), p. 95.

<sup>2</sup>R. Stern et al., Bull. Am. Phys. Soc. 31, 819 (1986).

i. The Split-Pole Spectrograph in the New ATLAS Target Area (K. E. Rehm)

The installation of the Enge split-pole magnetic spectrograph in the ATLAS target area has been completed. Compared to the spectrograph in target area II the new system utilizes the largest bending radii in the magnet, an essential aspect for the higher energies from ATLAS. The magnet power supply and the NMR system are connected via CAMAC to the VAX 750 computer. The basic functions (status report, field setting, readout) have been tested. The software for a user friendly control of the magnet which includes also the readout of the angle and the screw settings is under development. The magnet was successfully used in several experiments using heavy-ion  $^{58}\text{Ni}$  beams from the ATLAS accelerator.

j. **Nuclear Charge and Isobar Separation in the Gas-Filled Enge Split-Pole Magnetic Spectrograph** (W. Henning, B. Glagola, M. Paul,\* J. G. Keller, W. Kutschera, Z. Liu, K.-E. Rehm, and R. H. Siemssen)

We have recently explored the possibilities of nuclear charge separation with a gas-filled magnet.

This technique, first proposed by Fulmer et al. is based on the fact that charge-changing processes of an ion in a gas, if they occur frequently enough in a magnetic field region, lead to trajectories determined by the average charge state of the ion in the gas. For isobars with different nuclear charge  $Z$ , the mean charge state  $\bar{q}$  will be different. The scatter in ion trajectories, which determines to what extent the two isobars can be separated is determined at low pressure by the statistics of the charge-changing processes and at higher gas densities by small-angle scattering and energy-loss straggling.

The use of a broad-range spectrograph like the Enge split-pole allows one to follow the evolution of this process as a function of pressure in great detail (see Fig. II-34). This was done for a 300-MeV  $^{58}\text{Ni}$  beam from ATLAS. Monte-Carlo simulations with the ion-optical code RAYTRACE, which was modified to include charge-changing processes statistically distributed along the ion trajectory show good agreement between data and calculations. We have used the technique to separate isobaric  $^{58}\text{Ni}$  and  $^{58}\text{Fe}$  ions and also in an Accelerator Mass Spectrometry measurement of  $^{60}\text{Fe}$ . While the present results are extremely encouraging, considerably more work is needed to optimize isobar separation as a function of ion species, energy, gas pressure and gas composition for energetic heavy ions.



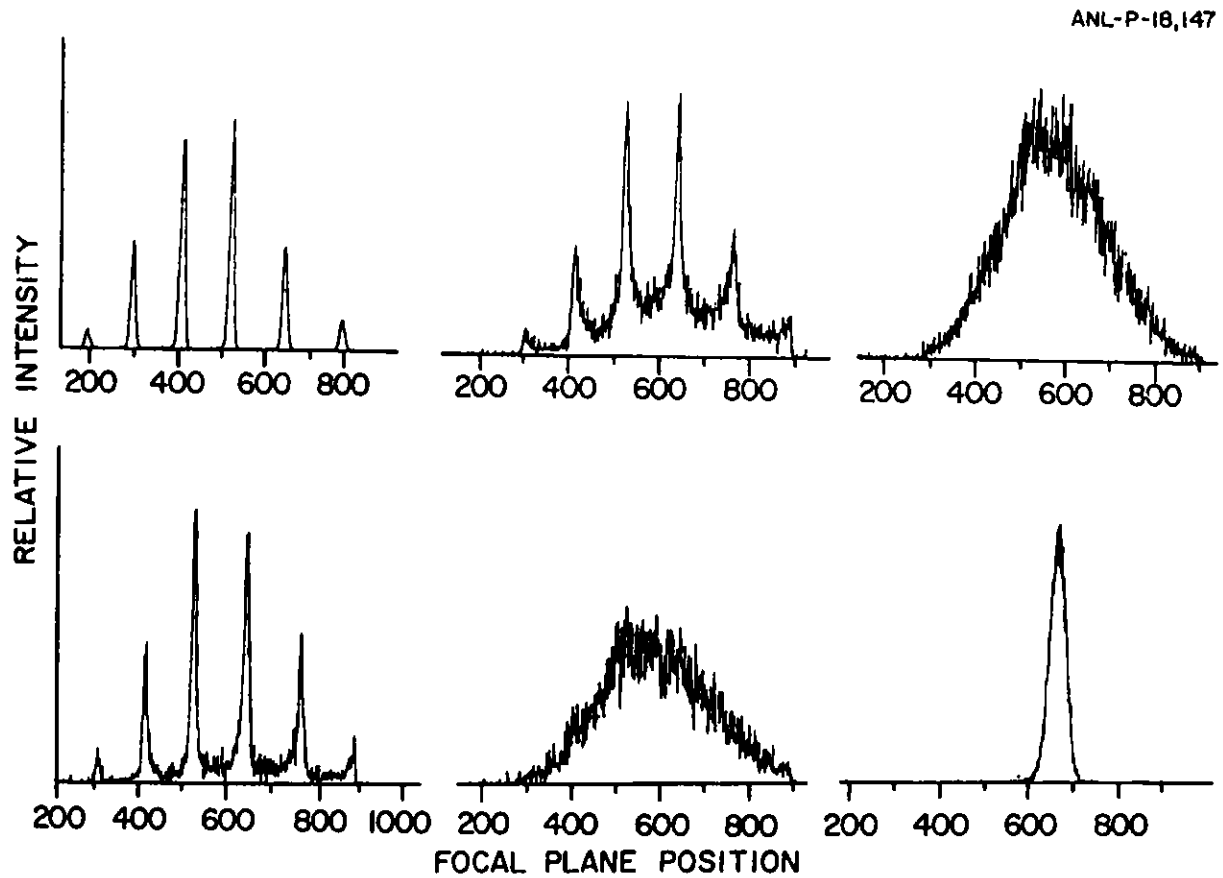


Figure II-34. Effect of the charge-state distribution of increasing the gas pressure.

- k. Construction of a Gamma-Ray Facility for ATLAS (R. V. F. Janssens, T. L. Khoo, R. Holzmann, W. Ray, U. Garg,† M. W. Drigert,† J. J. Kolata,† and P. Wilt†)

Phase I of the construction of the gamma-ray facility, which will ultimately consist of (a) a  $4\pi$  gamma-sum/multiplicity spectrometer with 50-56 hexagonal BGO elements and (b) 10-12 Compton-Suppressed Spectrometers (CSS) external to the hexagonal elements has been completed. Work on phase II has started and will hopefully be completed early in 1988, provided sufficient funding is available. The instrument is expected to have a powerful impact on a large class of experiments in heavy-ion research ranging from gamma-ray spectroscopy studies of great detail to the investigation of reaction mechanisms.

Work over the past year was concentrated on phase I of this project which consists of 14 elements of the inner array and 7 CSS's. The mechanical support structure is, however, constructed in such a way that it will accommodate the complete system without modifications. In the same spirit, the design of the electronics takes into account the need for expansion towards the full system. Phase I was completed, as expected, early in 1986 and work has started on phase II to bring the detector to the full specifications detailed in our initial proposal.

During the last year, much effort was devoted to the following activities:

- Extensive tests of the 14 CSS detectors for phase I were performed (see section F.j.) in order to ensure that all systems meet the specifications outlined after earlier tests on prototype detectors.
- Extensive test of all hexagonal BGO detectors were performed (see section F.k.) in order to ensure that all detectors meet the specifications outlined after earlier tests on prototype detectors.
- The fabrication of the mechanical support for the entire system was completed in the ANL and Notre Dame workshops.
- The assembly and alignment of the entire mechanical support was completed.
- Tests of the entire electronics necessary to handle the CSS's, were performed.

---

\*Hebrew University of Jerusalem, Israel.

†University of Notre Dame, South Bend, IN.

- Tests of the automatic liquid nitrogen filling system for the detectors were performed.
- Fabrication and test of the CAMAC-controlled constant-fraction discriminators were completed.
- Monte Carlo calculations performed to help finalize the design of the BGO modules placed in the outer ring of the array were completed and negotiations with potential vendors have been initiated.
- A first computer code was written which permits control, through CAMAC, of the electronics for the entire system. This code currently concentrates on the parameters of the array and facilitates greatly the set up of experiments (gain matching, threshold setting, fast timing, etc.)
- The design of several CAMAC units (time-to-charge converter, multiplicity logic unit, logic and analogic delay control . . .) is well under way.

As mentioned above, all detectors for phase I are now in place. Furthermore, the detector system was used for first tests with beam in November 1985 and a successful first experiment was completed in December 1985.

Work in phase II (i.e. the completion of the system) has started. Due to budgetary constraints, this construction is also expected to take two years. During the current fiscal year, the major emphasis will be placed on the completion of the array. The remaining hexagonal BGO detectors have already been ordered and, as stated above, the design of the detectors for the outer ring of the array has been completed and procurement will be initiated soon. The number of CSS detectors has already been increased to 7 and an 8th system is on order.

2. Results from the BGO Compton-Suppression Shields for the  $\gamma$ -ray Facility for ATLAS (R. Holzmann, R. V. F. Janssens, T. L. Khoo, I. Ahmad, U. Garg,\* M. W. Drigert,\* J. J. Kolata,\* and P. Wilt\*)

For the gamma-ray facility currently under construction for the ATLAS target area 5 BGO Compton-suppressions shields were purchased in addition to the 2 prototype shields obtained earlier. Together with these shields, 8 Ge detectors were also procured. The latter have a special cryostat (with a shape similar to a golf-club) in order to meet the requirements imposed by a tight geometry. Extensive tests on all of the systems have been performed with the following results.

All Ge detectors have efficiencies ranging from 23 to 26% and the energy resolution at 1.33 MeV is better than 2 keV FWHM. The timing resolution is better than 4.5 ns FWHM with respect to a plastic scintillator (with a  $^{60}\text{Co}$  source). When placed inside a Compton-suppression shield the peak/total ratios, for radiation from a  $^{60}\text{Co}$  source placed at the appropriate distance, were found to be typically 0.19 and 0.61 for the unsuppressed and suppressed spectra with variations between detector systems of 3.5% at most.

In the actual detector set up, all Compton-suppressed detectors were found to have peak/total ratios in excess of 0.58. In a gamma-gamma coincidence matrix >34% of the events are then in photo peak-photo peak coincidences to be compared with a typical value of <4% obtained with unsuppressed detectors.

- m. Tests of Prototype Hexagon BGO Detectors for the Inner Array of the  $\gamma$ -ray Facility for ATLAS (M. W. Drigert,\* U. Garg,\* J. J. Kolata,\* P. Wilt,\* R. V. F. Janssens, and T. L. Khoo)

Fourteen BGO detectors of hexagonal shape have been procured. They constitute the inner part of the BGO array for the  $\gamma$ -ray facility under construction at ATLAS. All detectors have been tested for energy and time resolution, homogeneity in light collection on all of the parts of the hexagons and accuracy in the mechanical construction.

All detectors were found to have energy resolution of the order of 15% (with the 662-keV  $\gamma$ -ray from a  $^{137}\text{Cs}$  source) and timing resolution better than 3.5 ns FWHM with respect to a plastic scintillator (with a  $^{60}\text{Cs}$  source). The detectors were also found to meet all other specifications except for the linearity in the gain of the R268 Hamamatsu photomultiplier tube. We plan to replace these tubes with the Hamamatsu R1398 tubes which have better properties for linearity while yielding results for the energy and time resolutions similar to those mentioned above.

In order to complete the array 12 more of the hexagonal detectors have been ordered and the design for the detectors of the outer ring has been finalized. We expect to complete the construction of the inner array this year.

---

\*University of Notre Dame, South Bend, IN.

n. Design and Construction of a Scattering Chamber Facility for ATLAS  
(D. G. Kovar, J. Falout, and B. Nardi)

During the last year the fabrication, installation, and testing of the ATLAS Scattering Chamber (ATSCAT) have been completed and the chamber has been used in several experiments with beams from ATLAS. The scattering chamber consists of a relatively small vacuum vessel (36-in dia.) whose upper half is rotatable by  $\pm 45^\circ$ , and whose lower half is fixed. The upper half has five (12"  $\times$  12") ports centered at beam height on which large-area gas detectors or vacuum extensions can be mounted, and a sliding vacuum seal for the entrance beam pipe to allow for upper chamber rotation under vacuum. The upper chamber is attached to a large rotatable platform which provides the torque for rotation and which serves as the platform for supporting the detector systems attached to the ports. The lower chamber houses three independently movable rings on which detectors can be mounted, the target assembly, and the various feed-throughs for cables and controls. The various motions (readouts) can be controlled (monitored) either locally or remotely using a dedicated PDP-11/23 computer. Provisions for controlling the voltages or gas pressures for the more complex multi-detector systems will be available.

The installation was finished, with first beam into the chamber, on May 1, 1985. Pumpdown times of the order of 1 hour are needed for  $10^{-5}$  Torr, and 2-3 hours for low  $10^{-6}$  Torr. The ANL design for the sliding seal has proven to be very successful, with only small fluctuations in pressure observed with rotation under vacuum. The design philosophy of machining most important alignments into the chamber itself has also proven to be very successful. Experiments have already made use of the flexibility of the chamber, utilizing the 12"  $\times$  12" ports for vacuum extensions (giving a 1.2 meter flight path), for mounting arrays of NaI detectors for charged-particle measurements, for mounting a large-area Bragg-curve Spectrometer, and after rotating the chamber by  $90^\circ$  mounting a target chamber for use in an atomic physics measurement.

Plans for this year involve the fabrication of the associated hardware for mounting experiments in the chamber (i.e., detector mounts, Faraday cups, beam collimators, provision for out-of-plane measurements, etc.) fabrication of the associated hardware for the external detectors (gas-

handling systems, electronics racks, detector supports, etc.), and the implementation of the computer control and monitoring of detector systems. Emphasis will be placed on the implementation of one or two detector systems which utilize the uniqueness of the ATLAS beams and the flexibility of the chamber design.

o. Process Control System for the Scattering Facility at ATLAS  
(S. J. Sanders, B. T. Miller\*, J. Kolenka\*)

The complexity of the experimental apparatus being developed for ATLAS has led to the need for improved methods of monitoring and controlling these instruments. To handle in a fairly general manner the necessary process-control functions, a computer program has been developed to run on a PDP 11/23 + computer system located in the ATLAS control room. Designed to be "user friendly", the program uses full-screen menus to lead the experimenter through possible control options. Communications with the experimental apparatus is by CAMAC modules using RS-232 crate controllers. Central to the program is a CAMAC command language (modeled after the MULTI command language) and supporting routines which enable the system to be easily tailored for specific user needs.

The program is initially being used to control the ring, upper chamber, and target motions for the 36" scattering chamber facility. The layout of the chamber, detectors mounted in the chamber, and target ladder can be displayed on a Tektronics 4107 color-graphics terminal. Requested ring motions are checked for possible overlap conflicts. The system also monitors the chamber pressure as well as the pressures and flow rates associated with gas handling systems being used at the chamber. Alarm functions can be set on any of the monitored quantities.

During the next year we plan to add the capability of plotting the time dependence of any of the monitored quantities and develop communications with the DAPHNE data-acquisition program. We are also developing documentation for the system.

---

\*Chemistry Division, ANL.

p. Nuclear Target Making and Development (G. W. Klimczak and G. E. Thomas)

The Physics Division operates a facility which produces and coordinates production of thin targets for charged-particle induced experiments, primarily at the ATLAS and Dynamitron accelerators. In addition, these thin films are occasionally prepared for other scientific purposes. The services of the nuclear target-making facility are available to the Physics Division, other Divisions of the Laboratory, and other scientific institutions. In addition to the typical production requirements, research work is performed in this facility to develop new techniques, as well as to implement and advance new state-of-the-art techniques developed at other institutions.

New facilities are being constructed to better utilize the production of thin film targets by the electron beam and saddle-field ion source techniques. Introduction of these facilities will make it more convenient to readily produce targets.

A new ultra-clean cryopump evaporator system has been designed and is currently being constructed. This system will permit the production of targets in a hydrocarbon-free environment. The existing evaporator systems have been reworked. New fixtures have been added to permit the production of larger quantities and improved uniformity of targets. A controlled atmosphere glove box that will permit the production of highly reactive materials is being designed and will be installed. Ultimately this system will be expanded to permit transfer of targets from the evaporator to the target storage chamber and to the experimental area under a controlled atmosphere.

A computerized inventory system has been established for monitoring all targets produced by the facility. Similar systems are operational for stable isotopes and chemicals. The construction of the computerized turbo-pump target storage system has been completed, except for the computer software which is currently under development. Feasibility studies are in progress to determine the possibility of construction of a laser evaporation system and a controlled atmosphere rolling mill. Future plans also include completion of the ultra-clean evaporator system as well as the upgrading of an existing evaporator system, further computerizing our target record systems, completion of the target storage system, further development of the sputter system, and possible cooperative target research with other laboratories.



q. Physics Division Computer Facilities (L. C. Welch, D. Cyborski,  
T. Moog, T. Coleman and S. Monhardt)

The VAX 780 (DecNet node PHYA) continues to serve as the major facility within the Division for replay and analysis of experimental data (see Fig. II-35). The performance has been enhanced during the past year by increasing the physical memory from 4MB to 16MB by a backplane swap and the addition of 4 4MB boards. The additional memory plus system software which adjusts priorities of interactive jobs using relative CPU time consumption has greatly improved responsiveness even though the "mean" number of users has increased by about a third. Unintentional downtime has been less than 100 hours during the past year. Presently VMS 4.4 has been installed. Disk space is a continuing problem even with the addition of the RUA81 last year and the initial steps are under way to obtain another RA81. In order to accommodate the replaying of data tapes about a fourth of the present RA81 has been declared a temporary storage and all files older than a day are erased from it each day. Plans are also underway to decommission the dual 28MB RK07 disk drives because of high maintenance costs and low useage. Two QMS 800 laser printers have been installed. One proved defective and has been returned for warranty repairs. The other has been working satisfactorily.

An Equinox DSS-5 Data PBX has been ordered, received and is in the process of being installed at this time. To make use of the data PBX, the portion of Building 203 that the Physics Division occupies had to have extensive wiring installed. As of this moment all of the wiring has been done and one wing of the building has been connected to the PBX with satisfactory results. The PBX and associated wiring has been given the acronym PHYLIS (PHYSics LIne System).

The three VAX 750's have all functioned well in the past year in a role which combined acquisition and replay of data. All three have 8MB physical memory, floating-point accelerators, and at least one TU78 attached. One of the 750's was taken to SLAC where it served as a data-acquisition computer. It currently has returned and is being used to replay

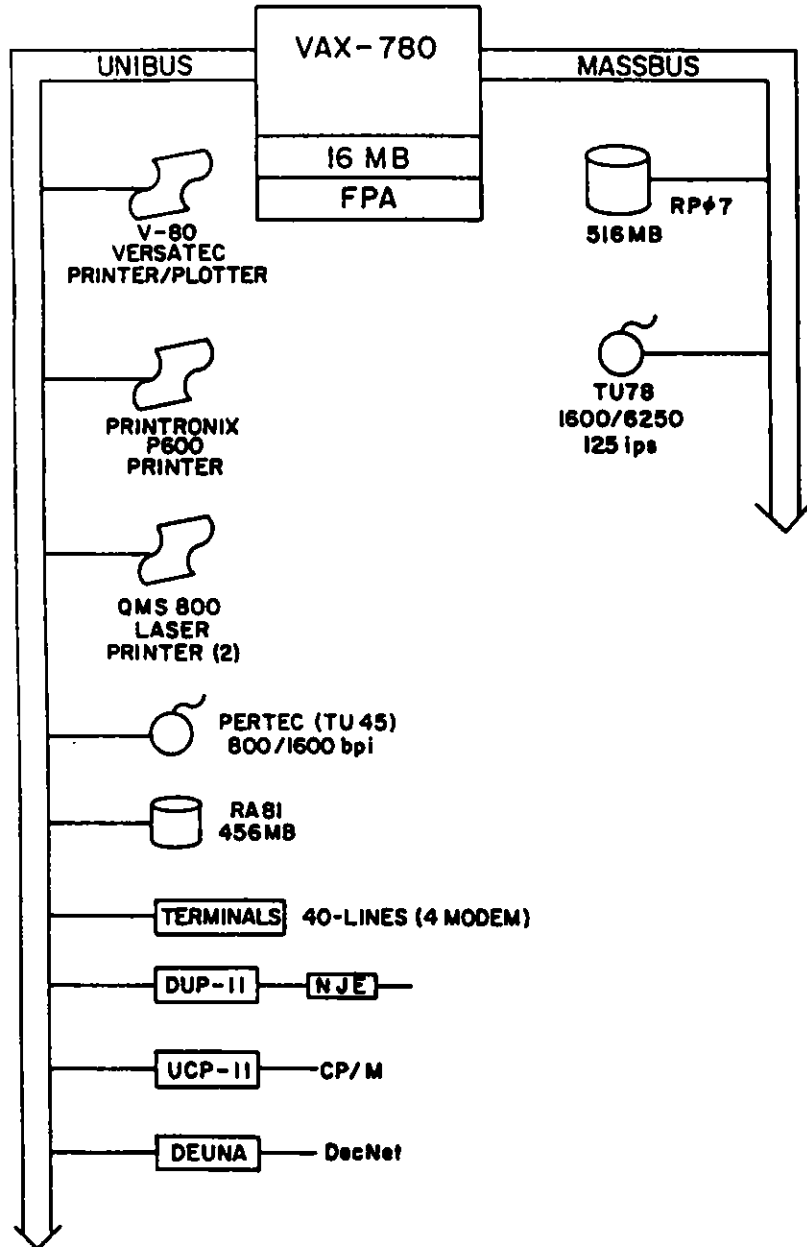


Figure II-35. The Physics Division's VAX configuration.

data. The proprietary software program SPEAKEASY has been added to the TRLA VAX 750. Each VAX 750 has a "SAM" module to monitor the environment and provide an automatic shutdown in case of problems.

The intermittent problems with the V-80 on ATLA are still present and due to the high cost of Versatec on-site maintenance service a laser printer as a substitute will be considered.

r. The Data-Acquisition System DAPHNE (L. C. Welch, T. Moog, Y. Y. Zhou, T. Coleman and S. Monhardt)

DAPHNE, the new data-acquisition system developed for ATLAS, has been successfully used at this point in many experiments on both ATLA and DYNA. The system, while it meets most of the needs of the experimental program, is not yet considered as complete. The major enhancement needed is linearizations. Simultaneous use of DAPHNE by two experiments has been tested and used successfully.

Major features implemented are windows (both 1-D and 2-D), an elaborate set of conditions for histogramming data, event-mode tape recording, SAVE and RESTORE of histogram data, hardcopy output, parameter viewing, user specified transformations, CAMAC scaler readout, multiple-event types, projections, and a preliminary version of variable-length events.

Investigations have proven the ability of a microVAX II to serve as a DAPHNE host and initial plans are proceeding to purchase a microVAX II to serve as a replacement for the 11/45 system in the area-2 data room. The 11/45 in the Dynamitron data room has been decommissioned.

### III. THEORETICAL NUCLEAR PHYSICS

#### Introduction

The principal areas of research in the nuclear theory program are:

1. Nuclear forces and sub-nucleon degrees of freedom.
2. Intermediate energy physics with pions, electrons and nucleons.
3. Heavy-ion interactions.
4. Variational calculations of finite many-body systems.
5. Nuclear structure studies in deformed and transitional nuclides.
6. Binding of hypernuclei from  $\Lambda N$  and  $\Lambda NN$  forces.
7. Other Theoretical Physics

In these areas we stress reliable calculations of proposed models or theories and comparison with data, much of which is obtained by the experimental program of the Division.

In 1985 we used our model of  $\pi$ -N- $\Delta$  dynamics to make a unified study of reactions such as  $\pi d$  elastic scattering,  $pp \rightarrow pn\pi$ , and  $\pi$ -absorption in nuclei. In general the experimental data are well reproduced. A surface-response model has been successfully applied to a large body of proton-nucleus scattering data. Our study of the EMC effect and related data via a conventional nuclear-physics model of the nucleus as a system of nucleons and pions has been further pursued. All aspects of the data are reproduced within the quoted errors.

In heavy-ion calculations we are continuing to study the influence of coupled-transfer channels on fusion cross sections. We are also investigating the form factors for inelastic scattering.

Our wave functions for few-nucleon systems have been used to make a good prediction of the proton momentum density observed in  ${}^3\text{He}(g, e'p)$  reactions. We have finished computing ground states of liquid  ${}^3\text{He}$  drops; this is part of our preparation for computing nuclear ground states.

## A. NUCLEAR FORCES AND SUBNUCLEON DEGREES OF FREEDOM

(F. Coester, T.-S. H. Lee, R. B. Wiringa,  
and collaborators from other Argonne Divisions and other institutions)

Much of our work is motivated by three central questions. (1) What should be the active degrees of freedom in a microscopic description of nuclei? (2) What is the Hamiltonian that governs the nuclear many-body dynamics? (3) What can electromagnetic probes reveal about short-distance nuclear structure?

For conventional nuclear theory, which assumes that nucleons are the only active degrees of freedom, it is not required that two-body forces alone are sufficient, but it is essential that the same Hamiltonian account for both light and heavy nuclei and that the importance of the  $n$ -body forces decrease rapidly with increasing  $n$ . We have previously established that two-body forces alone cannot account for the properties of nuclear matter. For three-body forces as well as two-body forces, the long-range part is governed by the pion exchange mechanism while acceptable short-range features must first be determined phenomenologically. We have constructed a reasonably good three-body force, but further improvements are needed. High accuracy in the calculation of the wave functions is absolutely essential and we continue to make necessary improvements in this area.

Requirements of relativistic invariance can be satisfied by unitary representations of the Poincaré transformations (Lorentz transformations and translations) on the same Hilbert space. We have found only small quantitative effects of the relativistic invariance in ground-state properties. Recently "relativistic" formalisms based on Dirac-spinor wave functions have received much publicity. These formalisms are not Poincaré invariant, but they introduce new active degrees of freedom which are the source of their empirical success. Our studies indicate that if this dynamics is translated into a nonrelativistic three-body potential, the saturation properties of nuclear matter are improved, but those of light nuclei are made worse. So far there is no mutually consistent few-body and many-body dynamics on Hilbert spaces of Dirac-spinor wave functions even in the absence of any requirements of relativistic invariance. Our efforts to solve this problem have had only peripheral success.

The extension of conventional nuclear theory to energies above the pion production threshold requires the inclusion of pions and isobars among the active degrees of freedom. Applications of such models are described in Sec. B. We have demonstrated in the past that models of this type can be realized in a Poincaré invariant manner. However, the invariance requirements introduce considerable computational complexity and the quantitative importance of the invariance remains to be explored.

Evidence for subnucleon degrees of freedom from spectroscopic and elastic scattering data is always indirect. In contrast, inclusive deep inelastic scattering reveals directly the charge and momentum carrying constituents. Deep inelastic electron scattering provided the definitive evidence for the existence of quarks and gluons. Recent data on nuclear effects in deep inelastic lepton scattering are thus of prime importance. We have shown that the dynamics of nucleons and pions with unaltered quark

structure can account for the existing data within the experimental uncertainties. The crucial physical parameter in this picture is the radius of the nucleon-pion vertex, which in our calculations was fixed at the outset by the properties of the nucleon-nucleon potential. The sensitivity of the results to this parameter should be investigated further. Significant theoretical progress requires the construction of dynamical quark models of hadrons, which are capable of predicting nucleon and pion structure functions in agreement with experiment.

There is little doubt that a full understanding of the nuclear force must be based on the underlying quark dynamics. In practical terms this involves the study of constituent quark models, which should be based on the essential physical features of quantum chromodynamics and be subject to the requirements of relativistic invariance. We are engaged in the study of such models.

Much of the quantitative information that will determine the success or failure of competing models will come from electromagnetic probes. Observed quantities are directly related to matrix elements of the electric charge and current densities. A valid interpretation requires mutually consistent representations of the current operators and the target wave functions. Work in progress on the form factors of the deuteron should provide a continuous transition between the regime of low momentum transfer and the asymptotic regime governed by perturbative QCD.

a. Nuclear Effects in Deep-Inelastic Lepton Scattering  
(F. Coester and E. L. Berger\*)

We have carried out a detailed study of a conventional nuclear model in which the observed differences between the deep inelastic structure functions of nuclei and of free nucleons are due to scattering from the pions present in the nuclei. These "exchange" pions are associated with the mechanism responsible for nuclear binding. We have shown that the deep inelastic structure functions of a nucleus may be expressed directly in terms of the empirical structure functions of the constituent nucleons and mesons and the wave function of the nuclear bound state. All but one feature of deep inelastic neutrino and charged-lepton data are reproduced by our model. The exception is the magnitude of the excess above unity of the ratio  $F_2^A(x)/F_2^D(x)$  for  $x < 0.2$ , observed only by the European Muon Collaboration (EMC) experiment. If these EMC data are reduced by 5%, consistent with experimental uncertainties, then all the features of the data are reproduced. A paper describing this work has been published. Invited talks on this work were presented at the "International Conference on Hadronic Probes and Nuclear Interactions" in Tempe, AZ, March 1985 and at the Workshop on Nuclear Chromodynamics, in Santa Barbara, CA, August 1985.

---

\*High Energy Physics Division, ANL

b. Variational Monte Carlo Calculations of Few-Body Nuclei  
 (R. B. Wiringa, R. Schiavilla\* and V. R. Pandharipande\*)

Variational Monte Carlo studies have been extended beyond the calculation of ground-state binding energy and density reported two years ago to the nucleon momentum distribution and two-cluster breakup momentum distribution in  ${}^3\text{H}$ ,  ${}^3\text{He}$  and  ${}^4\text{He}$ . These calculations required the development of a new Monte Carlo sampling technique, since the initial and final states of the system differ. For ground-state expectation values, such as  $\langle \psi | H | \psi \rangle$ , Monte Carlo samples are drawn from the positive-definite probability distribution  $\langle \psi | \psi \rangle$ . In the case of the proton momentum distribution in  ${}^3\text{He}$ , the integrand is  $\langle \psi(r_1, r_2, r_3) | \exp(ik \cdot (r_1, -r_1)) | \psi(r_1, r_2, r_3) \rangle$ , and  $\langle \psi(r_1, r_2, r_3) | \psi(r_1, r_2, r_3) \rangle$  cannot be used as a probability distribution because it is not positive definite. Instead, a product of central correlations,  $f^c(r_{1,2})f^c(r_{1,2})f^c(r_{1,3})f^c(r_{1,3})[f^c(r_{2,3})]^2$  (where  $f^c$  is from the construction of the variational wave function and is positive definite) is used as the weight function. Both the numerator and denominator of the variational expectation value must be calculated separately.

Results have been obtained for the proton and neutron momentum distributions,  $N_p(k)$  and  $N_n(k)$  in the  $A=3$  and  $4$  nuclei, the  $d+p$  amplitudes in  ${}^3\text{He}$ , and the  $t+p$  and  $d+d$  amplitudes in  ${}^4\text{He}$ . These results are obtained for the Urbana and Argonne NN potentials with and without the Urbana three-nucleon potential. The Hamiltonians including the three-nucleon potential give reasonable binding energies and density distributions in both the light nuclei and nuclear matter. The corresponding momentum distributions and two-body amplitudes agree well with recent  $(e, e'p)$  data from Saclay. An example is shown in Fig. III-1. This work has been published in Nucl. Phys. A499, 219 (1986).

The calculations use both improved variational wave functions and a 5-channel Faddeev wave function for the trinucleon system. The binding energies and momentum distributions for these two kinds of wave functions are very similar. The improvements made in the variational ansatz were facilitated by a careful analysis of the 5-channel Faddeev wave function. Recently an improved 34-channel Faddeev wave function has been made available to us by the Los Alamos-Iowa group and this gives significantly larger binding energies.

---

\*University of Illinois, Urbana, Illinois.



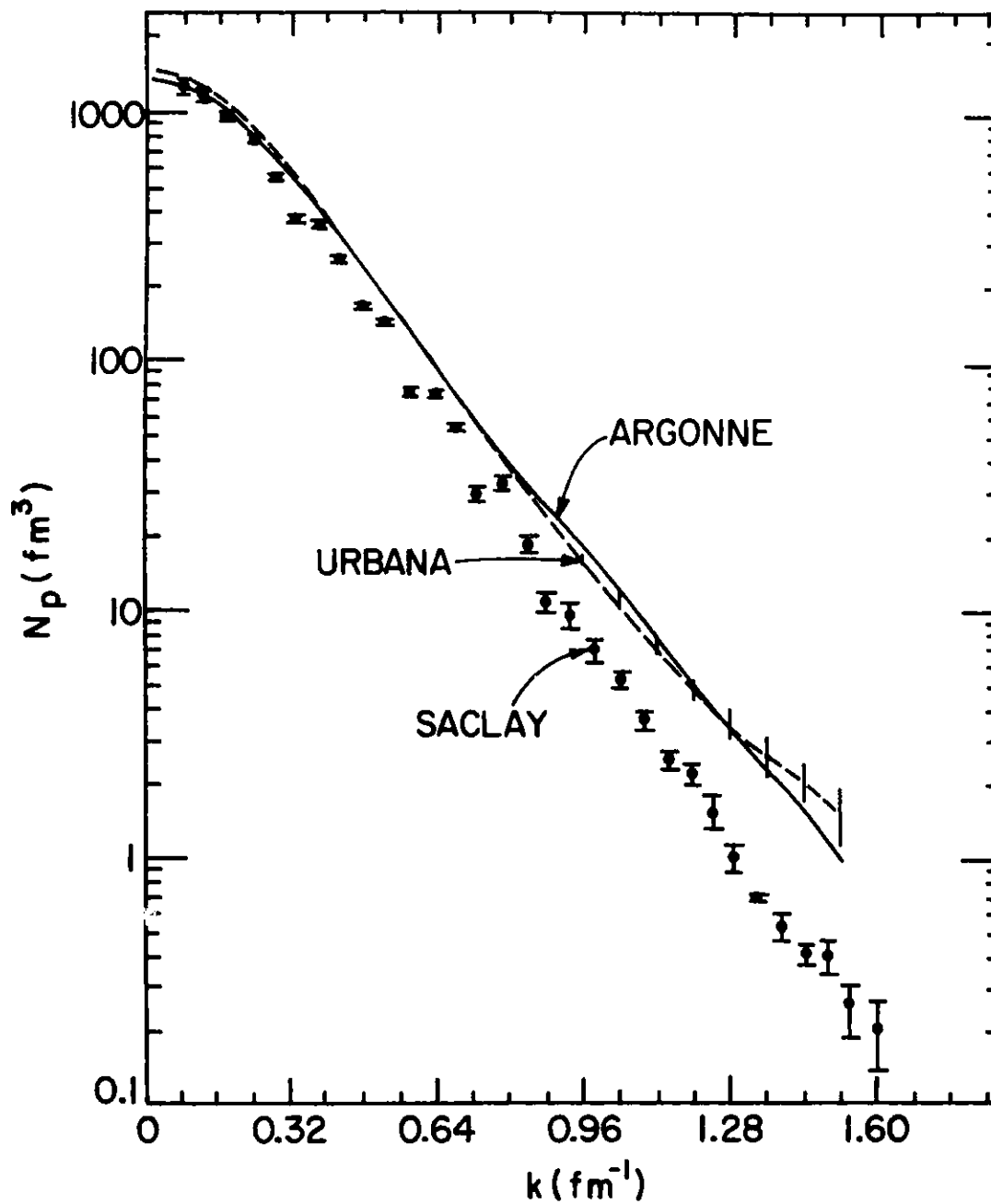


Figure III-1. The calculated  $N_p(k)$  in  ${}^3\text{He}$  with the Urbana + model VII and Argonne + model VII interactions is compared with the results of PWIA analysis of the Saclay electron-scattering data.

We intend to repeat our momentum distribution calculations with this better wave function, and to continue trying to improve the ansatz for the variational wave function so it can be applied to the alpha particle.

c. Coupled Cluster and Variational Calculations of Nuclear Matter  
(R. B. Wiringa and B. D. Day\*)

Coupled-cluster and variational calculations of nuclear matter have been performed for the Argonne  $v_{14}$  potential. This potential can be written as the sum of central, isospin, spin, tensor,  $L \cdot S$ ,  $L^2$ , and  $(L \cdot S)^2$  operators, and gives a good fit to NN scattering data. The most realistic potential for which both methods had previously been used is the  $L$ -independent  $v_6$  model of the Reid soft-core potential. The solution of the coupled-cluster equations, including both two- and three-body correlations, requires as input the matrix elements of the two-body potential in momentum space. Until now, this has restricted use of the method to potentials that can be analytically transformed to momentum space. We have now developed a satisfactorily fast and accurate numerical method for transforming coordinate-space potentials, such as Argonne  $v_{14}$ , to momentum space. This enlarges the class of NN potentials for which the coupled-cluster equations can be solved.

The variational method has been developed only for configuration-space potentials that can be expressed in operator form like Argonne  $v_{14}$ . The method uses  $L$ -independent correlations in constructing a cluster expansion of the variational energy, while treating the  $L$ -dependent terms at a lower level. This calculation has been improved by calculating the Jackson-Feenberg form of the kinetic energy, in addition to the Pandharipande-Bethe form, and by including all three-body separable diagrams for the  $L$ -dependent terms of the potential. The adequacy of the treatment of  $L$ -dependent terms is probably best tested by the direct comparison with the coupled-cluster results.

Comparison of the results for Argonne  $v_{14}$  shows a great similarity with those obtained for the semi-realistic Reid  $v_6$  potential. The variational nuclear matter energy lies above the coupled-cluster energy for densities up to  $1.8 \text{ fm}^{-1}$ . The variational method predicts a saturation point for Argonne  $v_{14}$  of  $-16.6 \text{ MeV}$  at  $1.7 \text{ fm}^{-1}$ , compared to  $-17.8 \text{ MeV}$  at  $1.6 \text{ fm}^{-1}$  for the coupled-cluster method. This is quite good agreement, considering that the uncertainty in the energy is  $\sim 2 \text{ MeV}$  at these densities. The comparison indicates that the variational treatment for the  $L$ -dependent terms in the potential, which are necessary for obtaining good fits to NN scattering data, is probably adequate.

---

\*AT&T Bell Laboratories, Naperville, IL

Coupled cluster calculations for the Bonn and Paris potentials and variational calculations for the Urbana  $v_{14}$  potential were also done. All the potentials give very similar binding energy curves and all saturate matter at too high a density. A paper reporting these results has been published in Phys. Rev. C 32, 1057 (1985).

d. Electromagnetic Form Factors of the Deuteron

(F. Coester, P.-L. Chung\*, B. D. Keister,† and W. N. Polyzou\*)

Measurements of the deuteron form factors over a wide range of momentum transfer can provide important clues to the role of subnucleon degrees of freedom in nuclear dynamics. For a meaningful calculation of the form factors it is essential that the current-density operators and the deuteron wave function transform under Lorentz transformations in a mutually consistent manner. Conventional "nonrelativistic" deuteron wave functions can be interpreted as relativistic wave functions of a deuteron at rest. The general Lorentz transformations to other frames depend on the dynamics. Depending on the choice of a form of dynamics, a subgroup of the Lorentz transformations is kinematic, that is these transformations are independent of the interactions. In the "light-front-form" dynamics any rotation that changes the orientation of the light front is a dynamic transformation. The invariance under the dynamic transformations always requires the presence of two-body current operators. The advantage of the "light-front form" of dynamics stems from the following features: (1) The initial and final states of the deuteron are related to each other and to the deuteron's rest frame by kinematic transformations. (2) All matrix elements of the single-nucleon current required for the calculation of form factors are related to each other by kinematic Lorentz transformations. (3) It is very easy to add simple ad hoc two-body currents designed to restore invariance under the dynamic rotations. It is therefore possible to calculate the contributions of one-body operators to the deuteron form factors for arbitrary momentum transfer in a consistent fashion. These calculations of the contribution of the one-body currents to the form factors are complete. Calculations of exchange-current effects are in progress.

---

\*University of Iowa, Iowa City, Iowa

†Carnegie Mellon University, Pittsburgh, PA

e. Relativistic Effects in Three-Body Nuclei  
(F. Coester, W. Glockle\* and T.-S. H. Lee)

It is well known that realistic two-body forces alone cannot account quantitatively for the observed binding energy of the triton. A suitable three-body force is the main candidate to remove this discrepancy. Requirements of a Lorentz invariant dynamics may also have a significant influence. Rough approximations by Coester and Wiringa indicated that relativistic effects in the binding energy of few-body nuclei are comparable in size to the effect of the three-body forces. However, both positive and negative contributions occur in the relativistic corrections to the binding energies and the accuracy of the approximations is suspect. More than a decade ago Coester, Pieper and Serduke found high-order cancellations in the relativistic corrections to the binding energy of homogeneous nuclear matter. We have therefore investigated a simple three-body model amenable to exact numerical solution of both the relativistic and the nonrelativistic Faddeev equations. We have obtained momentum distributions and expectation values of both kinetic and potential energies. We have also evaluated the expectation values of various approximate relativistic corrections. We find that the net relativistic effect on the binding energy is a small decrease of about 3%. In general we can expect that the magnitude of both the kinetic and potential energy will be smaller in the relativistic case. The net effect on the binding energy depends sensitively on the amount of cancellation of the two effects and the sign could easily be different for different models. We found that the expectation values of the relativistic kinetic and potential energy operators are fair approximations to the exact values. On the other hand approximate kinetic and potential energy operators obtained with expansions in powers of the momenta overestimate the relativistic effects by substantial factors. The errors preclude a reliable estimate of the relativistic effects in the binding energy by expansion in powers of the momenta. We have two main conclusions: (1) The quantitative effects of the Lorentz invariance of the dynamics are small. (2) Easy approximations of relativistic effects can be quite misleading. A paper on this work has been prepared.

---

\*Ruhr Universität Bochum, Bochum, West Germany

f. Relativistic Effects in Nuclear Many-Body Systems (F. Coester)

Different approaches to the formulation of relativistic many-body dynamics yield different perspectives of the nature and the magnitude of "relativistic effects". Requirements of relativistic invariance leave a very large amount of freedom in the formulation of dynamical nuclear models: The conventional nonrelativistic nuclear many-body dynamics can be generalized to satisfy the requirements of Poincaré invariance without altering the space of functions which represent the states. On the other hand quantum field theory suggests models in which the metric of the Hilbert space is determined by the dynamics. This approach naturally accommodates Dirac-spinor wave functions. Large relativistic effects appear as a manifestation of subnucleon degrees of freedom and Lorentz invariance seems unimportant. (Indeed, none of the popular "relativistic" models are Lorentz invariant.) In a perturbative quantum field theory of nucleons and mesons the "small components" of the Dirac-spinor wave functions are directly associated with probability densities of antinucleons. This interpretation is implausible if the fundamental fields are quark and glue fields, and it is not required by the success of Dirac phenomenology. Invited papers on these topics were presented at the "International Symposium on Medium Energy Nucleon and Antinucleon Scattering" at Bad Honnef, Federal Republic of Germany, June 1985, the "Bates Users Theory Group Work Shop" at MIT August 1985, and the "Fourth International Conference on Recent Progress in Many-Body Theories", San Francisco, CA, August 1985.

g. Implications of Dirac Nucleon Dynamics for the Binding of Light Nuclei. (R. B. Wiringa and B. D. Keister\*)

Four-component Dirac nucleon dynamics has been used in recent years to describe medium-energy polarized proton-nucleus scattering and nuclear matter saturation properties, with better apparent agreement with experiment than given by conventional NN potentials and the Schrödinger equation. While the differences between the Dirac and Schrödinger approaches are commonly referred to as "relativistic effects", they are not a necessary consequence of Lorentz invariance, but arise as a dynamical consequence of treating the nucleon as a four-component Dirac particle. The additional dynamics of the Dirac approach corresponds to the presence of many-body forces in the Schrödinger approach.

To study the implications of the Dirac approach for light nuclei, we have constructed a three-body potential from time-ordered diagrams containing one antinucleon line, excited and deexcited by scalar and/or vector mesons. Such diagrams should represent the presence of lower components which are the primary feature of recent Dirac calculations. The contribution of this three-body potential is calculated perturbatively with the Schrödinger equation by taking its expectation value in correlated variational wave functions obtained for realistic NN potentials. The potential is repulsive and gives a significant saturating effect in nuclear matter, consistent with Dirac calculations, that reduces the overbinding found with NN potentials alone.

In light ( $A=3$  and  $4$ ) nuclei, the potential is also repulsive, giving about a 3 MeV reduction in binding for the alpha particle. However, this is a definite worsening of agreement with experiment, since NN potentials alone underbind the light nuclei to begin with. This would seem to be a significant drawback to the Dirac nucleon approach. A letter reporting these results is scheduled to appear in Physics Letters B.

---

\*Carnegie Mellon University, Pittsburgh, Pa.



h. Quark Models of Hadron Interactions (F. Coester and W. N. Polyzou\*)

Quark models of single hadrons have been successful in accounting for hadron spectroscopy. They are not automatically applicable to multi-hadron dynamics. We are investigating quark models of multi-hadron dynamics which emphasize the following features: (1) spatial confinement of quarks is tied to color confinement (gauge invariance), (2) absence of long-range Van der Waals forces, (3) Poincaré invariance. Starting from ideas due to Greenberg and Hietarinta we realize these requirements in zeroth order by models which feature quarks confined to noninteracting hadrons, each of which has infinitely-many stable excited states. The manifest defects of these zero-order models are removed by the interactions: (1) String breaking interactions remove the stability of the unphysical excited states in a manner that guarantees the existence of scattering states with the right asymptotic properties. (2) String-rearranging interactions establish the short-distance exchange symmetry between quarks in different hadrons. We have developed a pilot model of a quark-antiquark system coupled to two-quark-two-antiquark states with a string breaking interaction.

---

\*University of Iowa, Iowa City, IA

## B. INTERMEDIATE ENERGY PHYSICS

(H. Esbensen, J. Johnstone, T.-S. H. Lee and  
collaborators from other institutions)

Our research in the area of intermediate energy physics consists of three parts. The first part is the development of a theory which can describe the extensive data available for  $\pi N$ ,  $NN$  and  $\pi d$  reactions up to the intermediate energy region where non-nucleonic degrees of freedom, such as the  $\Delta$  and the possible (one-body) six-quark states are excited. This year we have extended our  $NN$  study of the past couple of years to construct a unitary  $\pi NN$  theory, taking into account both the conventional meson-exchange mechanism and short-range quark dynamics. The theory has been applied to study  $NN$  scattering up to 1 GeV and  $\pi d$  scattering up to 300 MeV. The main focus of our extensive Faddeev-type coupled-channel calculations is to explore rigorously the kinematic regions in which the limitations of the conventional meson-exchange model can be clearly identified. This study is the basis of our subsequent investigations of the  $N\Delta$  interaction at short distances and the  $\pi N$  interaction above the pion production threshold from the point of view of quark dynamics. The constructed  $\pi NN$  model has also been applied to study electromagnetic interactions with the deuteron in the GeV energy region.

The second part of our investigation is the application of the constructed  $\pi NN$  theory to the study of nuclear dynamics in the region where the pion and  $\Delta$  degrees of freedom play important roles. This year, our focus was on the problem of pion absorption by nuclei. A study of the  $\Delta$  effect in determining the Gamow-Teller transition strengths has also been carried out within the framework of the Landau-Migdal theory.

The third part is a study of inclusive nuclear scattering induced by intermediate energy hadronic probes. This study is based on the surface response model, which has been developed previously. The basic interaction of the projectile and the nucleons in the target, which generates the nuclear excitations, is represented by the free  $t$ -matrix constructed from the well-determined  $NN$  phase shifts. The eikonal approximation is used to describe the attenuation of the projectile wave function inside the target nucleus. The nuclear response in the different spin-isospin channels is calculated from the surface response of semi-infinite nuclear matter. The effect of residual interactions on the response has been treated in the random phase approximation (RPA). With essentially the same physical input, our calculation is very efficient compared with the usual Distorted Wave Impulse Approximation approach. Extensive calculations of proton-nucleus scattering at 300-800 MeV have been carried out. The  $\Delta$  excitation in  $({}^3\text{He}, t)$  charge exchange reactions has also been investigated, using the information extracted from our earlier studies of intermediate energy  $NN$  and pion-nucleus scattering. We will continue attempting to improve the short-range features of our model by studying the ramifications of six-quark dynamics.

a. Theory of Mesonic and Dibaryonic Excitations in the  $\pi NN$  System  
(T.-S. H. Lee and A. Matsuyama\*)

The NN studies of the least few years have led us to develop a  $\pi NN$  theory which incorporates mesonic and dibaryonic excitation mechanisms in a unified description of NN and  $\pi d$  reactions. The mesonic mechanism is built into the theory by extending the conventional meson theory of nuclear forces to include the isobar  $\Delta$  excitation. The dibaryonic excitation at short distance is introduced according to current understanding of six quark dynamics. The theory is free of the nucleon mass renormalization problem and is therefore tractable in practice. The model Hamiltonian consists of: (a)  $V_{BB}$  for two-baryon interactions between NN,  $N\Delta$  and  $\Delta\Delta$  states, (b)  $h_{\pi N \rightarrow \Delta}$  for  $\Delta$  excitation, (c)  $v_{\pi N}$  for  $\pi N$  two-body interactions in nonresonant channels, (d)  $F_{\pi NN \rightarrow NN}$  for nonresonant pion production, and (e)  $H_{D \rightarrow BB}$  for the formation of a dibaryon state D. Dynamical equations for the NN and  $\pi d$  processes can be described in a subspace spanned by NN,  $N\Delta$ ,  $\Delta\Delta$ ,  $\pi NN$  and the dibaryon state D. The resulting scattering theory satisfies the essential two-body (NN) and three-body ( $\pi NN$ ) unitarity relations. The projection technique is applied to cast the theory into a form such that all NN and  $\pi d$  reaction transition matrix elements can be calculated by solving, separately, a two-body integral equation and a Faddeev-type three-body equation. Both can be solved by well-established numerical methods. This makes calculations based on the most sophisticated meson theory of nuclear force possible. Explicit formalisms have also been developed for exploring the question of the excitation of a dibaryon resonance during NN and  $\pi d$  scattering from the point of view of six quark dynamics. A paper describing the theory has been published. The numerical results obtained from the theory are presented in the following sections.

---

\*TRIUMF, Vancouver, BC, Canada

b. Unitary Study of NN and  $\pi$ d Scattering Based on Meson-Exchange Model  
 (T.-S. H. Lee and A. Matsuyama\*)

Our coupled-channel NN calculations with  $\Delta$ -excitations in the past few years have indicated some difficulties of the conventional meson theory of nuclear forces in describing NN scattering up to about 2 GeV. Within the unitary  $\pi$ NN theory described in Sec. B.a these calculations, however, are not conclusive since the coupling to the  $\pi$ d channel and the effects due to nonresonant pion production are neglected. In order to implement the quark dynamics into the theory, it is necessary to examine these two long-range pionic effects so that the limitations of the meson-exchange model can be more accurately determined. In addition, we need to know the corresponding  $\pi$ d predictions by the same theory. These two studies have been accomplished in FY86. The calculations involve solving a two-body Lippman-Schwinger equation and a three-body Faddeev equation. The method of contour rotation is used to treat the  $\pi$ NN branch cut in scattering amplitudes. To examine the model dependence, we have considered four different meson-exchange models, which are constructed by extending the Paris, Bonn, Argonne- $V_{14}$  and Reid potentials to include the  $\Delta$ -excitation and nonresonant pion production interaction. Our main conclusions are: (a) The main effect due to the coupling to the  $\pi$ d channel in NN scattering is to change the  $^1D_2$  phase shifts by less than 5%. Its effect in other partial waves is negligible. The coupled-channel method, which has been widely employed to study the  $\Delta$ -excitation in intermediate energy NN scattering, is a valid approximation. (b) The only noticeable effect due to nonresonant pion production is to increase the inelasticity of the  $^1S_0$  channel to a value close to the data. Its effect in other partial waves is small compared with the  $\Delta$ -excitation, and cannot resolve the difficulty of meson-exchange models in describing the strong energy dependences of polarization cross sections near 800 MeV. (c) The  $\pi$ d elastic scattering can also be described by our meson-exchange models to a very large extent (see Fig. III-2). The quality of our fits to the data is comparable to the existing  $\pi$ d calculations. The main new result from our study is to show that in a unitary  $\pi$ NN theory the effect of pion absorption in  $\pi$ d scattering is severely constrained by the fit to the NN data. The usual

---

\*TRIUMF, Vancouver, BC, Canada

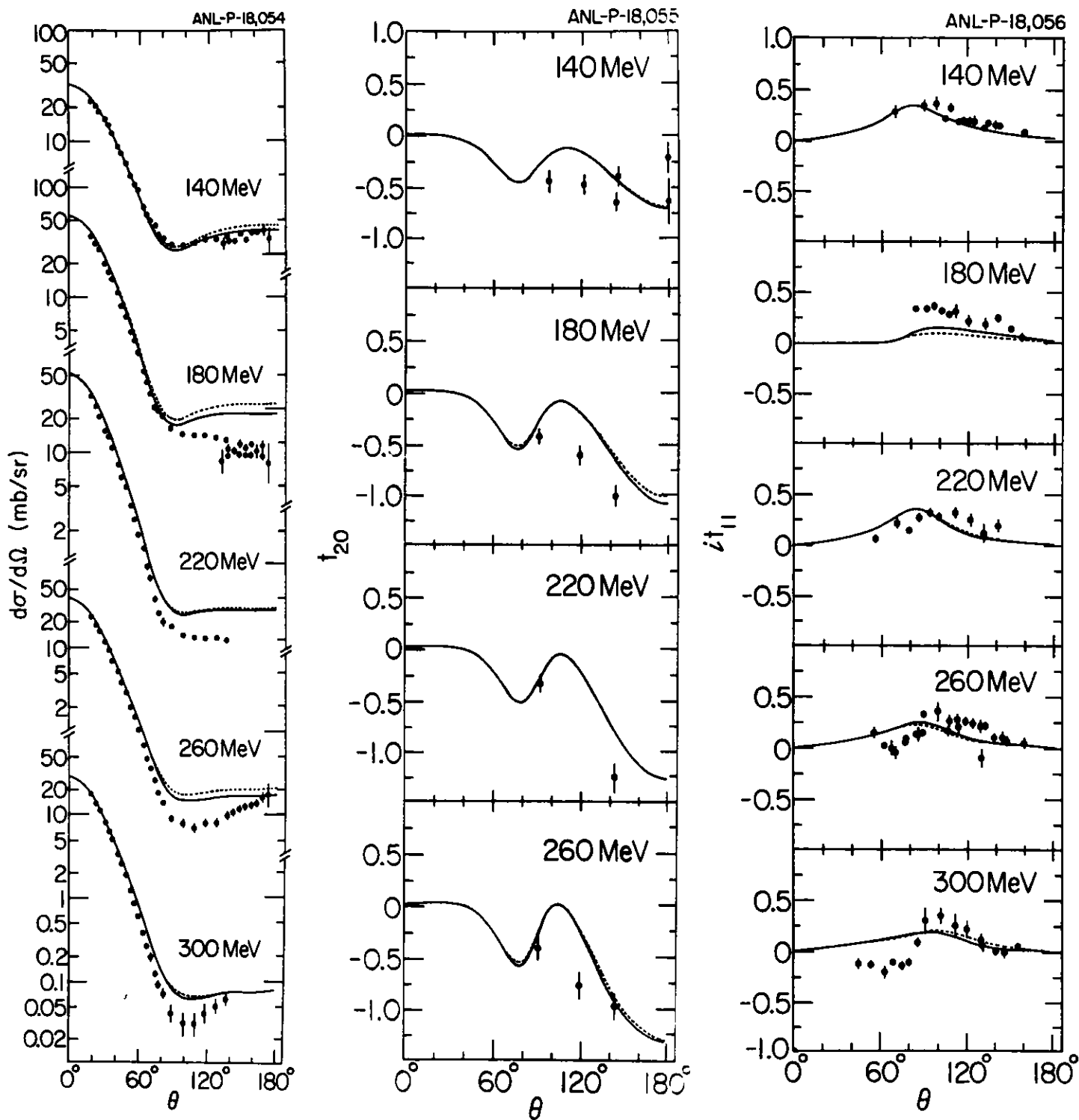


Figure III-2. Comparisons of unitary meson-exchange calculation of  $\pi d$  elastic-scattering with the data. The solid curves are obtained by neglecting the pion absorption effect.

procedure of splitting the  $\pi N P_{11}$  amplitude into a nucleon pole term and a background term is highly model dependent and cannot be justified unless the same procedure also yields a good description of NN scattering. (d) Within the freedoms allowed by the considered four meson-exchange Hamiltonian, there is no possibility to describe all NN and  $\pi d$  data, especially the strong energy dependences of NN polarization cross sections. It is necessary to implement quark dynamics into the theory. The result (a) has been published. A detailed paper describing our numerical methods and the results is being prepared for publication.

c. Unitary calculation of  $NN \rightarrow NN\pi$  (T.-S. H. Lee and A. Matsuyama\*)

Extensive data for pion production from nucleon-nucleon collisions have been obtained in the last few years. The study of these data is an important step in testing theories for the coupled  $NN \rightarrow NN\pi$  theory. To further explore the dynamical content of our  $\pi NN$  theory described above, we have carried out calculations for the  $pp \rightarrow pn\pi^+$  reaction. Within our unitary formulation of the problem, the calculation involves solving a Faddeev scattering equation for the final  $\pi NN$  state and a  $NN \rightarrow N\Delta$  coupled-channel Lippman-Schwinger equation for the initial  $NN$  state. The major numerical difficulty of the calculation is the treatment of the  $\pi NN$  branch cut in the final state interaction. This has been overcome by using the spline function method previously developed in a study of  $\pi d$  breakup reactions. The main difference between our approach and the only other existing unitary approach (by Deubach, Kloet, Cass and Silbar) is that we go beyond the one-pion-exchange mechanism by using our meson-exchange model based on the Paris potential. In addition, the  $NN$  interaction in the final  $\pi NN$  state is also included rigorously without using the usual on-shell prescription based on the  $NN$  phase shifts. Calculations have been carried out at 800 MeV. It is found that our meson-exchange model can describe, to a very large extent, both the shapes and magnitudes of the coincidence differential cross sections of  $pp \rightarrow pn\pi^+$  at several coincidence angles (see Fig. III-3). The theory, however, only gives a very qualitative description of the analyzing power  $A_y$ . These results further indicate the need for an improvement of  $\pi NN$  theory in the direction of considering quark dynamics in describing the  $NN \rightarrow N\Delta$  transition which is directly tested in the  $NN \rightarrow N\Delta \rightarrow NN\pi$  production calculation. A paper describing these results has been submitted for publication.

---

\*TRIUMF, Vancouver, BC, Canada

ANL-P-18,145

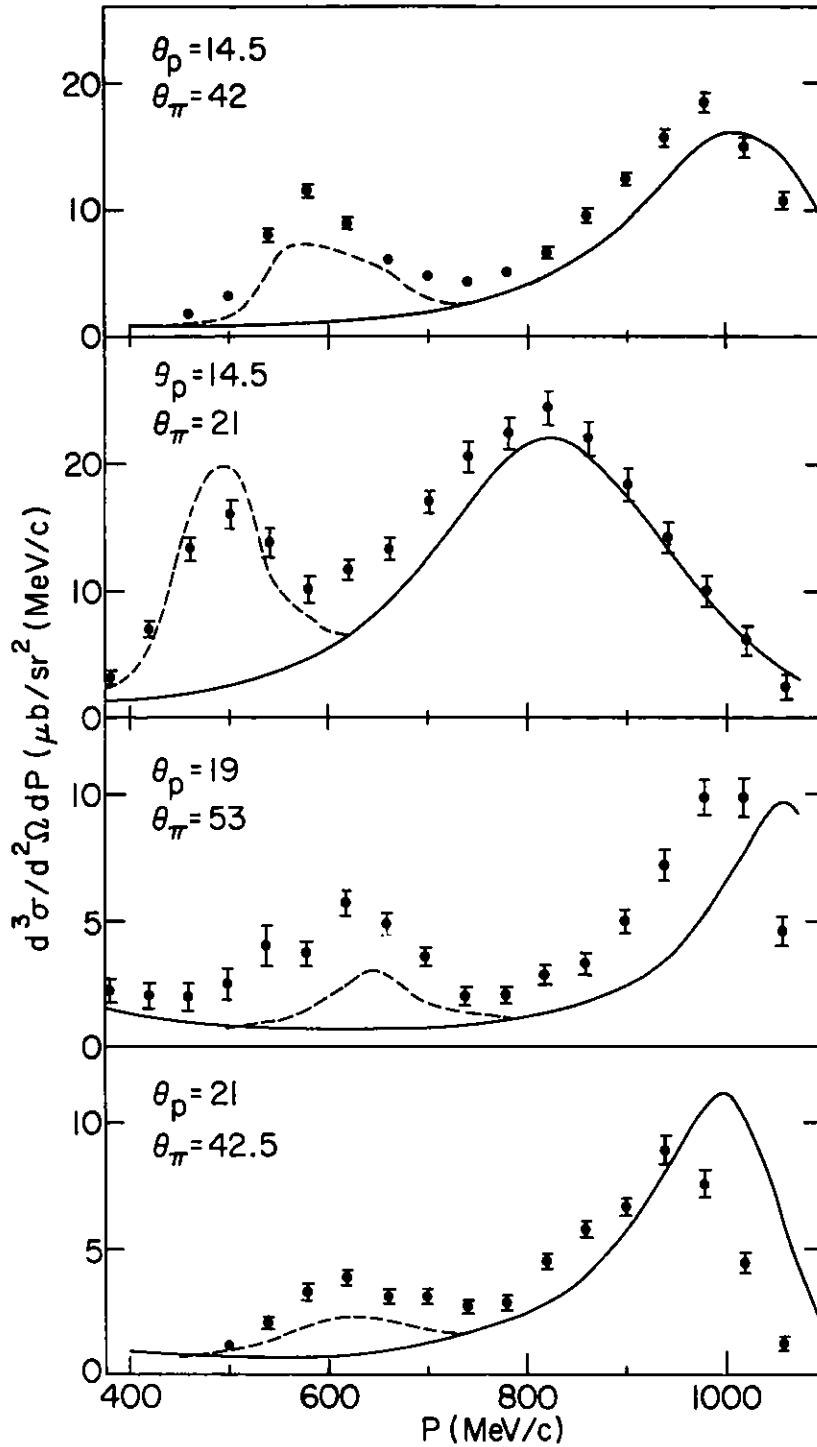


Figure III-3. Comparison of unitary meson-exchange calculation of  $pp \rightarrow pn\pi^+$  with the data at 800 MeV. The solid curves are the results calculated from keeping only the direct  $\Delta$ -production mechanism. The dashed curves include final-state interactions.



d. Study of Quark Dynamics in NN $\rightarrow$ N $\Delta$  Transition  
 (T.-S. H. Lee and A. Matsuyama\*)

Our extensive NN and  $\pi$ d calculations described above have suggested that the one-pion-exchange model of the NN $\rightarrow$ N $\Delta$  transition is not sufficient to describe the NN data at intermediate energies. Adding the conventional  $\rho$ -exchange to the model does not lead to an improvement. We therefore turned to exploring methods for including quark dynamics in describing the NN $\rightarrow$ N $\Delta$  transition at short distances which can be sensitively tested in our unitary calculation at intermediate energies. Our first attempt was to apply our unitary formulation described in Sec. B.a to investigate the excitation of a dibaryonic state D in each of the  $^5S_2$ ,  $^3P_0$ ,  $^3P_1$ , and  $^3P_2$  N $\Delta$  channels, where D is a six-quark state predicted by the MIT bag model. Extensive NN calculations have been carried out by including in each partial wave the effect due to a vertex interaction  $H_{N\Delta\rightarrow D}$ . Our objective is to search for the strengths of these vertex interactions so that the discrepancies between the meson-exchange predictions and the Arndt's phase shifts can be removed. It is found that improvements in fitting the NN phase shifts can be made only when significant background interactions, parameterized as separable forms, are also added in the fit.

These results are presented in the same paper describing our unitary NN and  $\pi$ d calculations of Sec. B.b. Our next research aim is to understand the extracted background NN $\rightarrow$ N $\Delta$  transition from the point of view of direct reactions between two composite hadrons. We are carrying out analyses based on the quark-exchange mechanism within the nonrelativistic quark model.

---

\*TRIUMF, Vancouver, BC, Canada

e. Electromagnetic Interaction with the Deuteron Above the Pion Production Threshold (T.-S. H. Lee and C. Fasano\*)

The main feature of intermediate energy electromagnetic interactions with the deuteron is the excitation of the  $\Delta$  and its associated pion production. Our unitary  $\pi NN$  model described above is most suitable for this study. To carry out the study, we have extended our theory to include one-body transition currents  $\gamma N \rightarrow N$  and  $\gamma N \rightarrow \Delta$ , taking into account relativistic kinematics. The transition amplitudes for  $\gamma d \rightarrow n p$  and  $d(e, e' \pi)$  are then determined by the  $N \Delta \rightarrow NN$  and  $N \Delta \rightarrow NN \pi$  amplitudes generated from our unitary  $\pi NN$  theory. An important dynamical feature of GeV electromagnetic interactions is that the momentum transfer to the deuteron can be very high and hence the reaction will be more sensitive to the short-range part of the  $N \Delta$  interaction. It allows us to have a more direct test of the quark mechanisms revealed in our studies of  $NN$  and  $\pi d$  scattering described above. Calculation of  $\gamma d \rightarrow n p$  has been carried out. Our results show a striking difference between the meson-exchange model and the QCD-prediction by Brodsky. A paper describing this result is being prepared. We are now carrying out a calculation including the dibaryonic excitation and quark-exchange mechanisms as described in Sec. B.c. Our work will be used to analyze two Argonne experiments being carried out at SLAC and Saclay.

---

\*Thesis Student, University of Chicago, Chicago, Illinois.

f. Effects of  $\pi\pi$  Correlations in  $\pi N$  Scattering  
(John A. Johnstone and T.-S. Harry Lee)

The primary intent of this work is to gauge the significance of  $\pi\pi$  correlations in  $\pi N$  interactions. The  $P_{11}$   $\pi N$  channel is particularly appropriate for studying second-order effects since the low-energy phase shifts result from delicate cancellation of repulsive and attractive mechanisms. The standard cloudy-bag model description of  $\pi N$  scattering is extended to include contributions at the two-pion level. The fundamental  $\pi\pi$  interactions are constructed in a phenomenological separable form consistent with the known  $\pi\pi$  s- and p-wave phase shifts. This interaction is then embedded in the  $\pi N$  problem to account for scattering of the incident pion from the nucleon's virtual pion cloud. A self-consistent analysis of the coupled  $\pi N$ ,  $\pi\Delta$ , and  $\pi N^*(1470)$  systems results in excellent reproduction of both the phase shifts and inelasticity in the  $\pi N P_{33}$  channel up to 2 GeV. In the  $P_{11}$  channel, without two-pion intermediate states, no acceptable fit to the data is possible for any values of the bag parameters. The additional attraction provided by the incident  $\pi$  scattering from the virtual pion cloud is essential for reproducing the low-energy phase shifts and fixing their sign change at the correct energy (see Fig. III-4). This work has been accepted for publication in Phys. Rev. C.

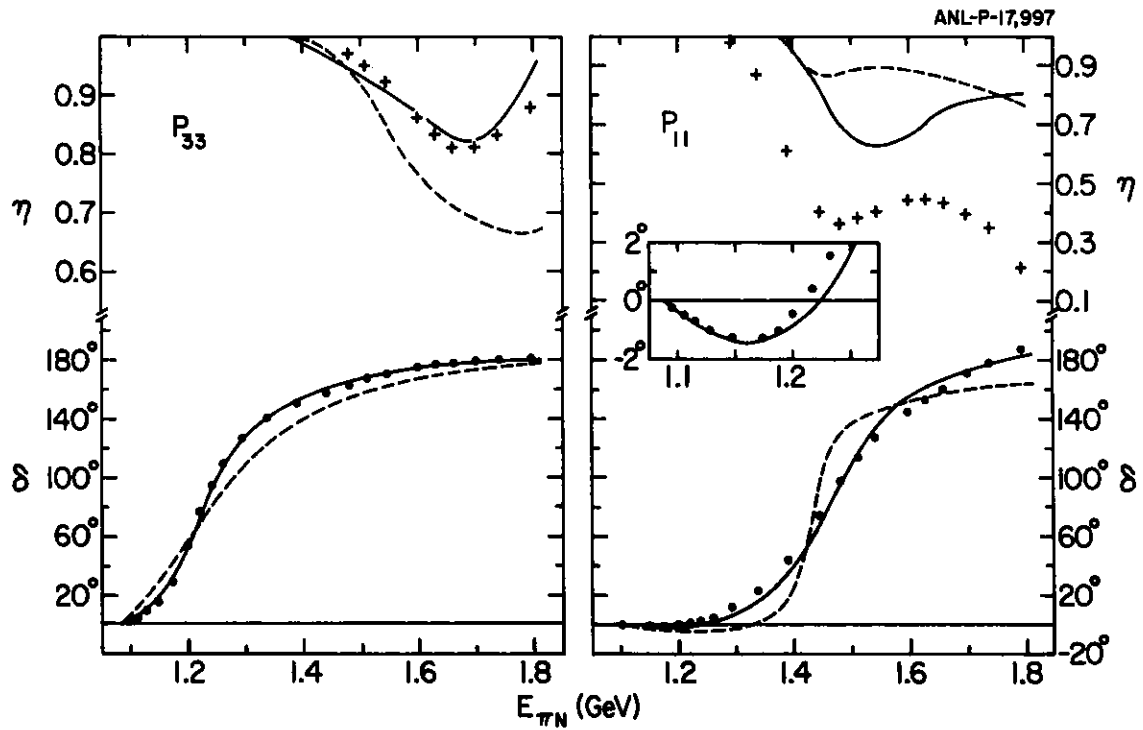


Figure III-4. Results of the fit to the  $P_{33}$  and  $P_{11}$  phase shifts. The dashed curves are the standard cloudy-bag model fit. The solid curves include the attractive effect due to pion scattering from the virtual pion cloud around the nucleon.

g. The Strange Quark Mass in a Chiral SU(3) Bag Model  
(John A. Johnstone)

The cloudy bag model of baryon structure is extended to include the coupling of quarks to kaons, according to  $SU(3)_L \otimes SU(3)_R$  symmetry. Assuming that a single set of bag parameters apply to both the octet and decuplet, the self-energy corrections of the baryons are calculated to the order of two-pion and one-kaon intermediate states. An excellent reproduction of the mass splittings between isomultiplets is obtained and it is concluded that these splittings are entirely due to mesonic effects (see Fig. III-5). The strange quark mass in this treatment is degenerate with the up and down quarks, and consistent with zero. This is radically different from conventional approaches which assign the strange quark a mass some 200 MeV or more greater than that of the up and down. This work has been accepted for publication.

ANL-P-18,212

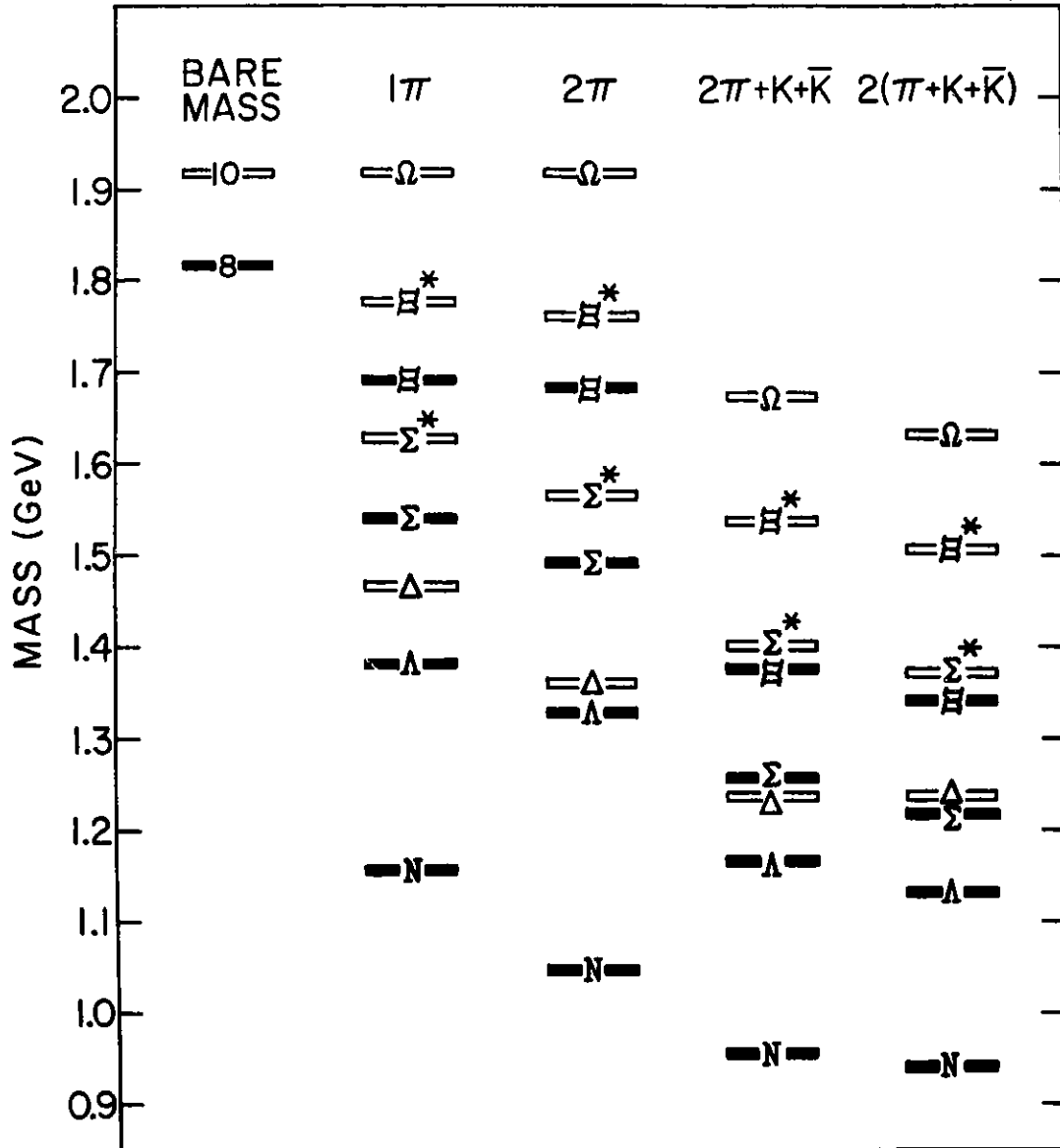


Figure III-5. Self-energy contributions to baryon masses generated by the coupling of the baryons' (massless) u, d, and s quarks to the pseudoscalar mesons. The right-hand spectrum shows convergence at the experimental masses by including virtual states up to the 2-meson level.

h. Study of the Two-Nucleon Mechanism of Pion Absorption in Nuclei  
(T.-S. H. Lee, K. Ohta,\* and M. Thies,\*)

The two-nucleon mechanism of pion absorption by nuclei is investigated in the energy region of the  $\pi N P_{33}$   $\Delta$ -resonance. The basic absorption process is governed by a  $\pi NN \rightarrow N\Delta \rightarrow NN$  transition matrix, derived from the phenomenological Hamiltonian of Betz and Lee, which was constructed to describe NN scattering phase-shifts up to 1 GeV. The model allows a realistic description of pion absorption on a pair of bound nucleons with quantum numbers and relative radial wave functions different from those of the physical deuteron. The deuteron-like  ${}^3S_1(T=0)$  pairs are shown to play a privileged role, in accordance with the assumption underlying the conventional quasi-deuteron model. We then embed the two-nucleon mechanism into complex nuclei, using the impulse approximation. The many-body effects on the two-body absorption mechanism are analyzed in detail by using the Faddeev wave function for  ${}^3\text{He}$  and harmonic oscillator shell-model wave function for  $1p$ -shell target nuclei in our calculations. All nonlocal effects owing to nucleon Fermi motion and  $N\Delta$  off-shell propagation are treated rigorously. The main features of  $(\pi^+, p)$  reactions on  ${}^3\text{He}$ ,  ${}^4\text{He}$ , and  ${}^{12}\text{C}$  are predicted correctly, when large pion distortion effects are taken into account by using the isobar-hole model with all of the parameters predetermined from earlier studies of pion nucleus scattering. By combining our results and calculations by Matsutani and Yazaki, it is concluded that a large part of the total absorption cross section could originate from the inelastic absorption process:  $(\pi, \pi, N)$  nucleon knockout followed by pion absorption. We are, however, unable to calculate microscopically this inelastic absorption cross section unambiguously, and hence the existence of other absorption mechanisms and possible contributions to proton spectra from target fragmentation cannot be excluded from our analysis. These possibilities are further suggested by the fact that the weaker  $(\pi^-, p)$  cross section is very much underestimated in this theory. The origin of this problem is identified to be the suppression, by nuclear geometry and isospin selection rules, of the two-body process  $\pi NN \rightarrow N\Delta \rightarrow NN$  initiated by  $\pi^-$ . A paper describing this work has been published.

---

\*Natuurkundig Laboratorium der Vrije Universiteit, Amsterdam,  
The Netherlands

i. Mechanism of  ${}^3\text{He}(\pi^-, pn)$  Reaction (T.-S. H. Lee)

The above study of pion absorption indicates the need for considering mechanisms other than the  $\Delta$  excitation. We have therefore investigated  $\pi^-$  absorption by  ${}^3\text{He}$  in a model study based on the nucleon pole mechanism  $\pi NN \rightarrow NN \rightarrow NN$ . The main effort is devoted to calculating the influence due to the final three-nucleon scattering. We find that the amplitude of the three-body rescattering mechanism can have a strong interference effect with the amplitude of the direct two-body absorption process even in the region where the two-body process dominates. The main experimental signature of this important coherent effect is a sharp peak near the high energy end of the proton spectrum measured in a coincident experiment. Our results suggest that in order to extract the isospin dependence of pion absorption by a pair of nucleons from the recent  ${}^3\text{He}(\pi^\pm, NN)$  data, the three-nucleon rescattering amplitude must be calculated accurately and included coherently in the analysis. A paper describing this result has been published.



j. Calculation of Landau Parameters for the  $\Delta$ -hole Interaction  
 (T.-S. H. Lee, K. Ohta,\* and H. Sagawa†)

The Landau-Migdal theory has been used successfully to describe energies and transition strengths of nuclear excited states. Moreover, the theory predicts various exotic phenomena, ranging from the precursor effect of pion condensation to the quenching of spin-isospin transition strength due to the  $\Delta$ -hole coupling. The crucial quantities determining all of these interesting phenomena are the so-called Landau parameters which characterize the short-range NN interaction at the nuclear Fermi surface. A theoretical calculation of the Landau parameters is therefore very important for the application of the Landau-Migdal theory of nuclei. By applying our meson-exchange Hamiltonian for  $\pi$ , N, and  $\Delta$  (Sec. B.a), we have carried out a Bruckner G-matrix calculation for the coupled NN and NA interaction in nuclear matter. The calculated G-matrix for NN  $\leftrightarrow$  NA transitions is used to calculate the effect of  $\Delta$ -hole coupling on the Landau parameters. Our results show that the NA interaction in p-waves plays the most important role; this clearly shows the importance of the use of a model Hamiltonian which can describe the NN  $\leftrightarrow$  NA transition in each partial wave. Our approach is therefore more realistic than previous works because our model Hamiltonian can describe the NN phase shifts in the regions where the inelastic process NN  $\rightarrow$  NA  $\rightarrow$  NN $\pi$  takes place. A paper describing our results has been published.

---

\*University of Tokyo, Japan.

†Michigan State University, E. Lansing, Michigan.

k. Nuclear Structure in the  $(p, \pi^+)$  Reaction (D. Kurath)

There is a considerable amount of data on excitation of individual states in the  $1p$ -shell by means of the  $(p, \pi^+)$  reaction with protons of about 200 MeV. The data indicate clearly that a two-body mechanism is active, so the interpretation of results is quite complicated. It is known that in the proton-proton case the  $(p+p \rightarrow d\pi^+)$  channel is dominant at low energy. An attempt is being made to embed this channel in the proton-nucleus reaction and to see if there is a doorway in the two-particle one-hole operator which will permit a relatively simple interpretation of the observed spectra. Preliminary results are encouraging and this study will be pursued in the coming months.

2. Quasielastic Proton-Nucleus Scattering at 300-800 MeV  
(H. Esbensen and G. F. Bertsch\*)

Inclusive spectra for quasielastic proton scattering on heavy nuclei are now available over a wide range of energies. Recent data obtained by R. Segel et al. cover the range of 300-500 MeV. The (p,p') spectra are compared to calculations using the surface response model, and the dependences of the quasielastic peak on the momentum transfer, the beam energy and the mass of the target nucleus are studied.

The surface response model describes quasielastic nucleon-nucleus scattering in terms of free nucleon-nucleon scattering, Glauber theory for single scattering, and the surface response of heavy nuclei, which we represent by the surface response of semi-infinite nuclear matter. The effects of residual interactions are treated in the random-phase approximation.

The comparison to measured spectra shows that Glauber theory for single scattering accounts quite well for the target dependence of the quasielastic peak. Moreover, the surface responses of nuclei ranging from carbon to lead are very similar and reasonably well represented by the surface response of semi-infinite nuclear matter. Major discrepancies occur at higher excitation energies, and they become more significant at large momentum transfers (see Fig. III-6) and lower beam energies. These discrepancies are estimated and ascribed to multistep processes.

At small momentum transfers the main discrepancy is due to the shell structure of finite nuclei, which is not included in the model. The results of the comparison have been written up for publication. The total effect of residual interactions on the surface response in the different spin-isospin channels is not very important for the height of the quasielastic peak, at least not at those momentum transfers considered in the comparisons. The residual interaction is important in some specific channels, and it becomes more important at lower momentum transfers. This has been studied in previous publications.

---

\*Michigan State University, East Lansing, MI

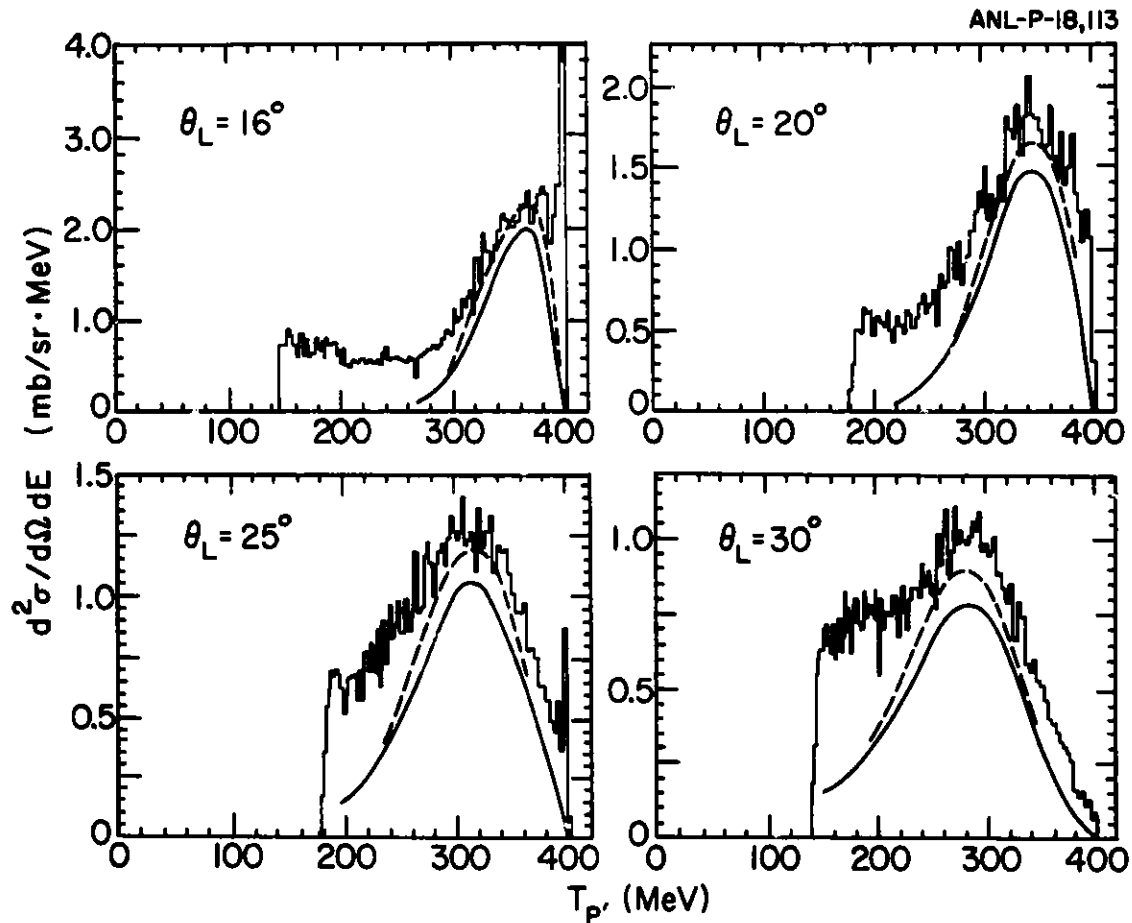


Figure III-6. Energy spectra for 400-MeV  $(p,p')$  reactions on  $^{58}\text{Ni}$  at four different laboratory scattering angles. The measured spectra (histograms) are from R. Segel et al. The calculated results in the surface response model are based on the total nucleon-nucleon cross sections for free scattering (fully drawn curves) and the effective value obtained from a local Fermi gas approximation (dashed curves).

m. Delta Excitations in Heavy Nuclei Induced by Charge Exchange Reactions (H. Esbensen and T.-S. H. Lee)

We have studied delta excitations induced in heavy nuclei by ( $^3\text{He},t$ ) and (p,n) reactions. The surface response model is used to calculate the inclusive cross section. The elementary delta production mechanism in free nucleon-nucleon collisions is described by the meson-exchange Hamiltonian theory. The self-energy of the delta (both the real and the imaginary part) is modified in a nuclear medium, and we use the empirical values extracted from pion-nucleus scattering. The effects of Fermi motion of target nucleons, as well as the residual pion-exchange interaction in the nucleus, are also included in the calculation of the cross section for reactions on heavy nuclei. We use a local Fermi gas model to determine the RPA response. The response is generated by a field that is consistent with Glauber theory for single scattering.

Our calculations reproduce the main features of measured zero-degree cross sections for ( $^3\text{He},t$ ) reactions on heavy nuclei.<sup>1</sup> The magnitude of the calculated cross section is reasonable. It is partly determined by Glauber theory for single scattering, and it originates from the surface region of the target nucleus. The most striking feature compared to reactions on protons is the shift of the delta peak by some 60 MeV to lower excitation energies. In our calculations this shift is mainly due to the modification of the delta self-energy in a nuclear medium, whereas the residual pion exchange interaction is less important (see Fig. III-7). The observed shift is independent of the mass of the (heavy) target nucleus. This feature is also consistent with our model of a surface reaction.

The calculations for (p,n) reactions in the delta region do not reproduce the measured cross sections, in particular at the higher excitation energies. This discrepancy is ascribed to the neutron decay of the delta, which has not been included in the calculation. The ( $^3\text{He},t$ ) reaction is more favorable in this respect, since the contribution from a delta excitation in the  $^3\text{He}$  projectile and a subsequent decay into a triton must be strongly suppressed. The results of our study have been published.<sup>2</sup>

---

<sup>1</sup>D. Contardo et al., Phys. Lett. 168B, 331 (1986).

<sup>2</sup>H. Esbensen and T.-S. H. Lee, Phys. Rev. C 32, 1966 (1985)

ANL-P-17,921

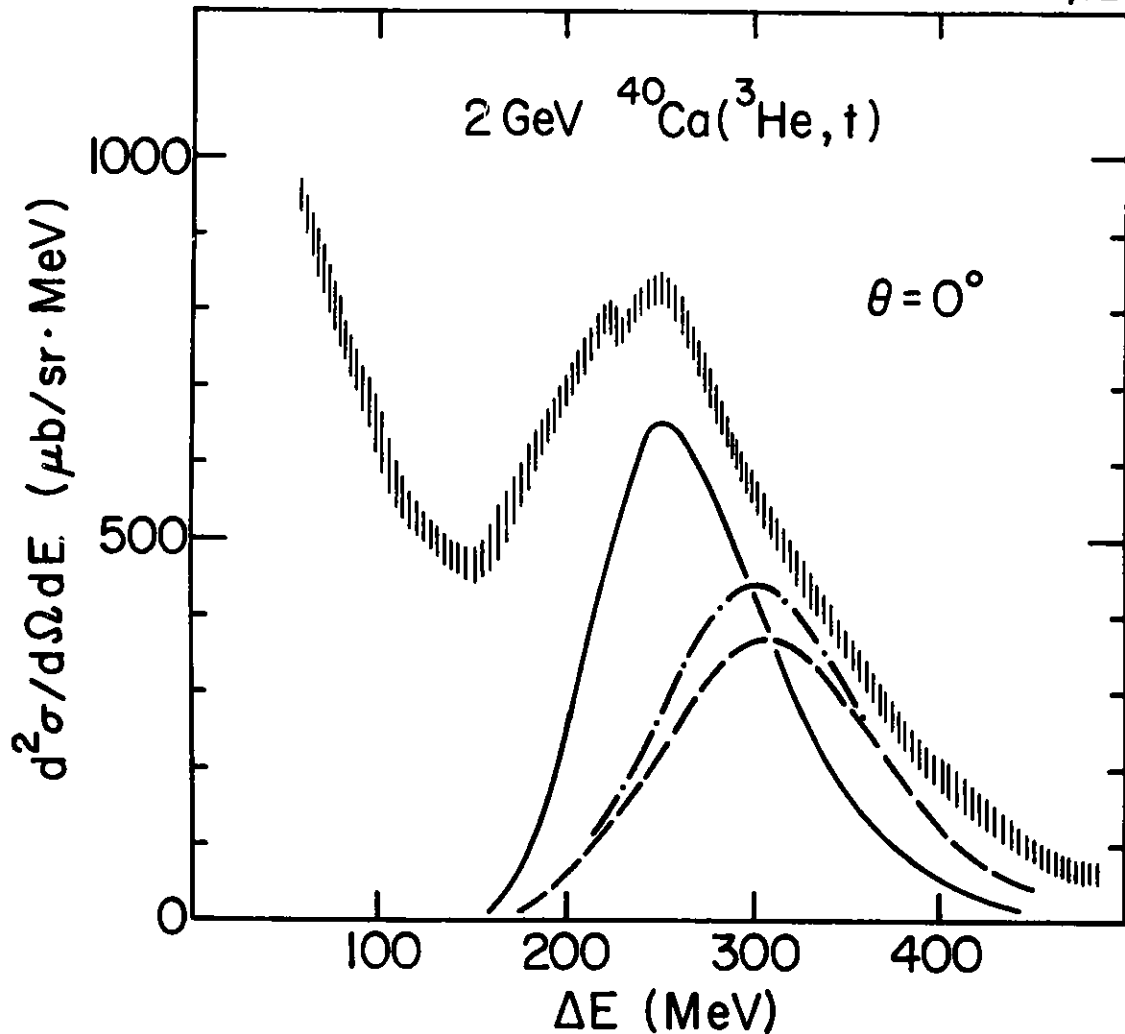


Figure III-7. Differential cross sections for 2-GeV ( ${}^3\text{He}, t$ ) reactions on  ${}^{40}\text{Ca}$  at  $\theta = 0^\circ$ , as functions of the energy loss and scattering angle of the detected triton. The experimental results (hatched curve) are from Ref. 1. The calculated curves are based on response functions of semi-infinite nuclear matter. The dashed curve was obtained from the free response; the residual pion-exchange interaction is included in the dashed-dotted curve; the full-drawn curve includes both pion-exchange and delta self-energy in the nuclear medium.

n. Continuum Polarization Transfer in Proton-Nucleus Scattering

(H. Esbensen, L. B. Rees,\* J. M. Moss,\* T. A. Carey,\* K. W. Jones,\* J. B. McClelland,\* N. Tanaka,\* and A. D. Bachert†)

A complete set of polarization transfer observables<sup>1</sup> have been measured for 500-MeV quasielastic proton scattering on deuterium, calcium and lead targets, and spin-flip probabilities have been extracted for the longitudinal and the transverse directions (with respect to the momentum transfer). The data are analyzed and interpreted in the surface response model for single scattering,<sup>2</sup> and provide important information about the isovector longitudinal-spin response of heavy nuclei. The results are related to the pion-excess interpretation of the European Muon Collaboration (EMC) effect.

The residual interactions in the isovector spin channels are governed by meson exchange and a short-range repulsive interaction. The longitudinal-spin excitation is associated with pion exchange, and the total residual interaction in this channel is believed to be attractive at large momentum transfers. The associated response is expected to be enhanced compared to the free (non-interacting) response, and this enhancement has been related by some authors to a pion excess in heavy nuclei.

An important aspect of our analysis is that it accounts for the difference between the two types of experiments discussed above. The EMC effect is based on muon scattering. The absorption of muons is weak and they probe the entire nucleus. The proton data arise from scattering at the surface of the target nucleus due to a strong absorption. In the latter case only the surface response is probed, and the effect of the residual interaction on the response is much less at the surface than in the interior of a nucleus. We have accounted for this difference between the two experiments by using the surface response model to analyze the proton scattering experiment, since this model has been very useful in describing many aspects of quasielastic nucleon-nucleus scattering.

---

\*Los Alamos National Laboratory, Los Alamos, New Mexico.

†Indiana University Cyclotron Facility, Bloomington, Indiana.

<sup>1</sup>T. A. Carey et al., Phys. Rev. Lett. 53, 144 (1984).

<sup>2</sup>H. Esbensen et al., Phys. Rev. C 31, 1816 (1985).

The proton scattering data were taken at a fairly large scattering angle, and our analysis does not show any evidence of an enhancement of the longitudinal response. A numerical calculation of this response in the surface response model, using the same interaction that was used to explain the EMC effect, shows a significant enhancement, in particular at the lower excitation energies. Conversely, if we adjust the short-range part of the residual interaction in order to get agreement with the proton scattering data, the associated pion excess is much too small to explain the EMC effect. Unfortunately, the short-range part of the residual interaction is not accurately known at the large momentum transfers that are important for the pionic interpretation of the EMC effect and the present proton scattering experiment. Our analysis has been written up for publication.



o. The (p,n) Reaction and the Nucleon-Nucleon Force  
(H. Esbensen and G. F. Bertsch\*)

We have been working on a review article for Reports on Progress in Physics, on "The (p,n) Reaction and the Nucleon-Nucleon Force". At present, we are completing a detailed discussion of the nucleon-nucleon interaction in free space and the effective interaction in a nuclear medium, with special emphasis on the interactions in channels associated with isovector excitations of the target. We have discussed the Distorted Wave Impulse Approximation, and also further approximations, in connection with the (p,n) reaction as a spectroscopic tool to study the strength of Gamow-Teller resonances.

---

\*Michigan State University, East Lansing, MI

p. The Classical Limit of the Surface Response in Fermi Liquids  
(H. Esbensen and G. F. Bertsch\*)

We have studied the connection between the surface response of Fermi liquids and classical concepts and models of the properties of heavy nuclei. Such a connection can be established in the low-frequency, long-wavelength limit of the isoscalar surface response. The RPA response diverges in this limit and its analytic behavior has been investigated for semi-infinite nuclear matter. We show that the divergence is equivalent to a diffusion equation for the displacement of the surface from its equilibrium position. The diffusion coefficient is determined by fundamental physical quantities, viz. the surface tension and a friction force. The surface tension is decomposed into a kinetic and a potential energy contribution. The latter depends critically upon the range of the particle-particle interaction that is responsible for the isoscalar residual interaction. Using a reasonable range of one fermi, the response theory yields a value that is close to the empirical surface tension of nuclear matter. The value of the friction force is consistent with the classical piston model, expressed in the wall formula of Blocki et al. The response theory also predicts a small inertial term in the dynamical equation for the surface position. We are not aware of any model that predicts an empirical value for the inertia. The results of this work have been published in Phys. Lett. 161B, 248 (1985).

---

\*Michigan State University, East Lansing, MI

## C. HEAVY-ION INTERACTIONS

(H. Esbensen, S. Landowne, S. C. Pieper and Others)

We have continued to investigate coupled-channels effects in heavy-ion reactions near the Coulomb barrier, concentrating on the impact of transfer channels on the fusion cross sections. We will continue to apply this approach to systems studied experimentally at Argonne and elsewhere. We also will be improving our treatment of transfer in the coupled-channels formalism.

a. A Coupled-Channels Analysis of Silicon-Nickel Fusion Reactions  
(S. Landowne, S. C. Pieper and F. Videbaek)

The series of  $^{28,30}\text{Si} + ^{58,62,64}\text{Ni}$  fusion reactions show interesting variations at subbarrier energies. We are making systematic calculations for this series within the coupled-channels framework, taking into account the different (prolate, oblate) deformations of the projectiles, the low-lying collective excitations of the targets as well as the one-particle and two-neutron transfer reaction channels. Figure III-8 shows results for the  $^{28}\text{Si} + ^{58,64}\text{Ni}$  cases. The long dashed curves are obtained without coupling, while the short dashed curves are obtained with only inelastic excitations. This is sufficient to explain the  $^{28}\text{Si} + ^{58}\text{Ni}$  case. The full curves are obtained with both inelastic and transfer reactions, which are clearly required in the  $^{28}\text{Si} + ^{64}\text{Ni}$  system. Also shown in the figure are the estimated transfer reaction cross sections.

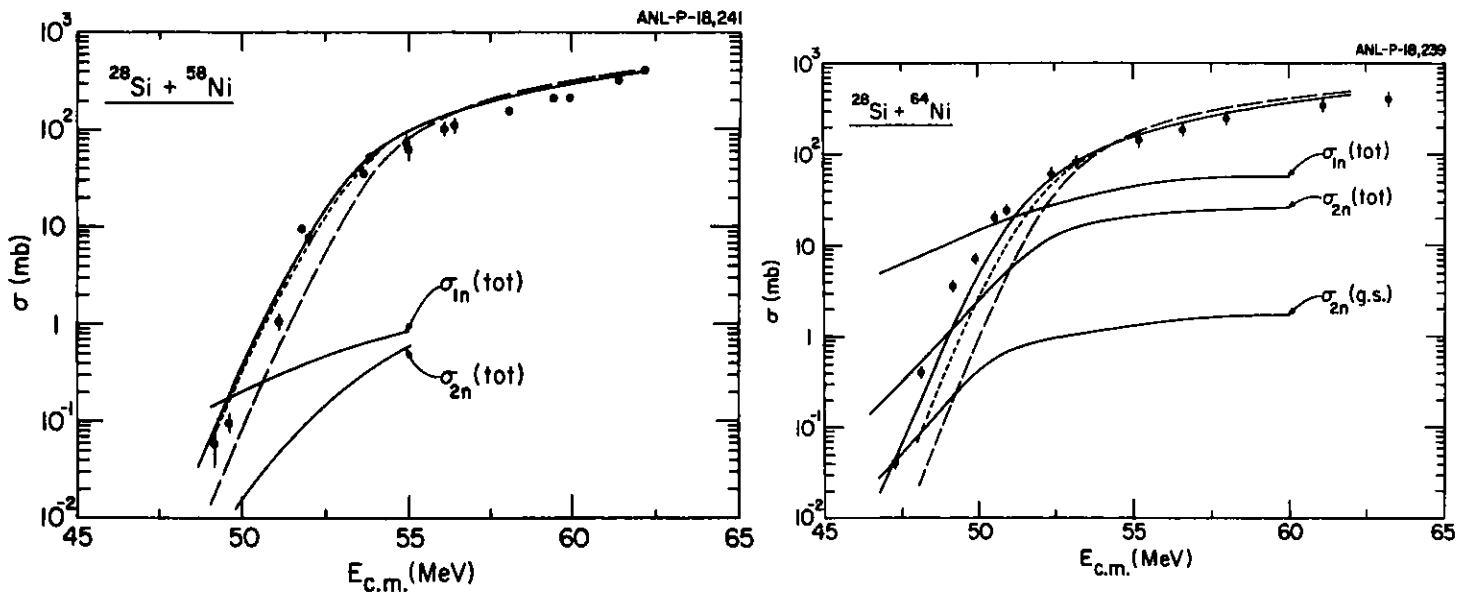


Figure III-8. Calculated fusion and transfer reaction cross sections for  $^{28}\text{Si} + ^{58,64}\text{Ni}$ .

b. On the Nuclear Polarization Potential for Heavy-Ion Scattering  
(S. Landowne, C. H. Dasso,\* G. Pollarolo,† and A. Winther\*)

A microscopic semiclassical formalism is used to study the real part of the polarization potential due to transfer reactions in heavy-ion collisions. Second-order perturbation theory and a localization approximation leads to a transparent expression for the polarization potential in terms of the squares of the basic coupling form factors weighted by a kinematical factor. This factor is determined by the collision time and the energy distribution (Q-values) of the intermediate transfer channels.

Estimates and detailed calculations show that the real polarization potential is typically of the same order of magnitude as the corresponding absorptive potential. An example is shown in Fig. III-9. For a heavy system about 20% of the total potential could be due to dynamical effects. The balance between polarization and absorption depends on the bombarding energy and the Q-value distribution. Typically the polarization effect dominates at low energies. Calculations of the energy dependence show structures similar to the effects deduced from recent data analyses.

---

\*The Niels Bohr Institute, Copenhagen, Denmark

†University of Torino, Torino, Italy

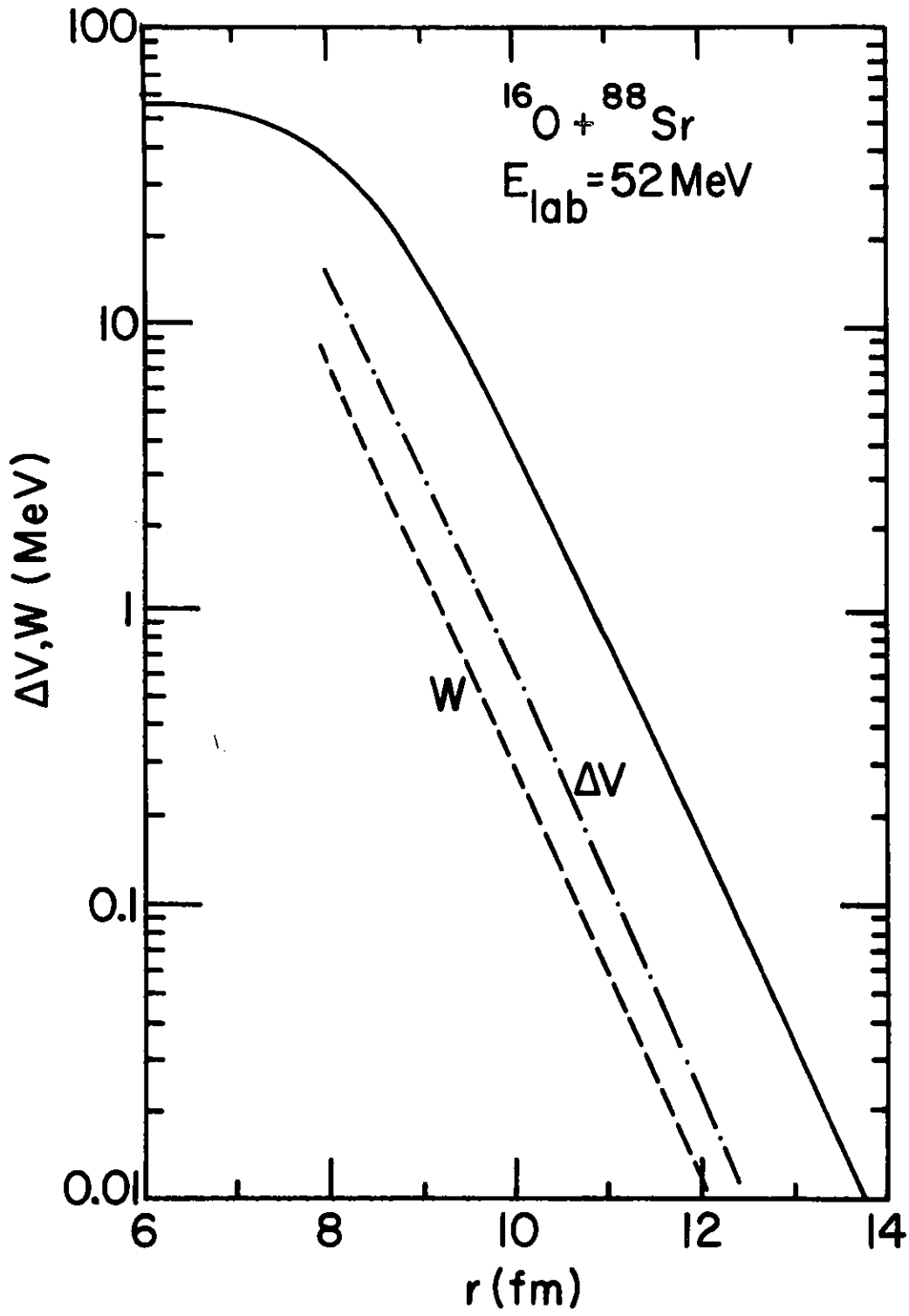


Figure III-9. Calculated absorptive ( $W$ ) and polarization ( $\Delta V$ ) potentials for  $^{16}\text{O} + ^{88}\text{Sr}$ .

c. Coupled Channel Approach to Heavy-ion Reactions Near the Coulomb Barrier (H. Esbensen)

A previously developed coupled-channels code has been used to study systematic trends of fusion and to test various approximations used in heavy-ion reaction models. It is found that the coupling to one-particle transfer channels can affect the spin distribution for fusion at the highest partial waves, whereas the effect on the total fusion cross section is less dramatic. General features of the effect on fusion due to the coupling to low-lying quadrupole modes have also been studied.

Different ion-ion potentials have been used to calculate the Coulomb barrier in order to see which of them is most consistent with subbarrier fusion data. The necessity of more reliable ion-ion potentials and form factors than those commonly used has motivated an investigation based on double folding. A simple dependence on nuclear radii and on the multipolarity of form factors for inelastic excitations has been found. The strength of these form factors at higher multiplicities becomes weaker than predicted by the commonly used model based on the derivative of the ion-ion potential.

d. Conversion of Ptolemy to the ER Cray (S. C. Pieper)

The coupled-channels part of Ptolemy was successfully converted to run on a single processor of the ER Cray at the MFE computing center. All of the required changes were made in the master source in such a way that the same source deck is used for the IBM, Cray, CDC and VAX versions. Typical coupled-channels calculations run some 20 times faster on the Cray than on Argonne's IBM 3033 computers.

## D. QUANTUM-MECHANICAL VARIATIONAL CALCULATIONS OF FINITE MANY-BODY SYSTEMS

(S. C. Pieper, R. B. Wiringa, and V. R. Pandharipande\*)

In the last few years we have been developing techniques and programs for quantum-mechanical variational Monte Carlo (VMC) calculations of the ground states of finite many-body systems. Our long-term goal is to be able to calculate the ground states of nuclei. We started with calculations of drops of  ${}^4\text{He}$  atoms for which there are two substantial simplifications over nuclei: 1) the particles are bosons and 2) the interparticle potential is very simple. We are now completing our ground-state calculations of drops of  ${}^3\text{He}$  atoms which require Fermi statistics but still have a simple potential.

The "warm-up" calculations of  ${}^4\text{He}$  drops have had several interesting spin-offs. We know the parameters of accurate variational wave functions for these drops. These wave functions have been used to make detailed studies of properties of the pair-correlation function in the drops and to compute the energies of excited states of the drops. We have used our pair-correlation function results to develop an energy density functional (EDF) for liquid  ${}^4\text{He}$  and by comparison with the Monte Carlo calculations we have shown its strengths and weaknesses. The excitation energy studies show that the frequently used hydrodynamical approximations for excitation energies are not accurate for small to medium-size drops. We are beginning to study the momentum distributions of atoms in the  ${}^4\text{He}$  drops.

We are now ready to consider methods for dealing with the complicated correlations required by nucleon-nucleon potentials. We will also repeat many of our subsidiary studies of the  ${}^4\text{He}$  drops with the  ${}^3\text{He}$  drops to see if the conclusions are modified by Fermi statistics.

---

\*University of Illinois, Urbana, IL.



a. Elementary Excitations of Liquid  $^4\text{He}$  Drops  
 (R. B. Wiringa, S. C. Pieper and V. R. Pandharipande\*)

We have made microscopic variational calculations of low-energy elementary excitations of liquid  $^4\text{He}$  drops containing  $N$  atoms. The calculations have been done for  $20 \leq N \leq 240$  with the VMC method, and for  $20 \leq N \leq 10,000$  using a local density approximation (LDA) for the pair distribution function. The excitations studied include the  $J=0$  breathing mode and the  $J=2,3$ , and  $4$  surface excitations, as well as the ripplon spectrum of the plane surface.

The excited-state wave function is taken as a sum of single-particle excitation operators acting on the variational ground state. The operators include two or three variational parameters and are constructed with the appropriate angular momentum and parity of the excitation. The excited state energy is computed in the Feynman-Cohen approximation, which would be exact if we had the exact ground state. Although our variationally-determined ground state is not the true ground state, the Feynman-Cohen approximation is believed to give a good measure of the energy required for one quantum of excitation.

The results of these calculations are shown in Table III-I. They provide an interesting contrast with the classical sharp-surface liquid drop (SSLD) model commonly used in nuclear physics for studying nuclear vibrations. The SSLD model predicts the  $J=0$  breathing mode energy to be  $\sim 26N^{-1/3}$  K (degrees Kelvin) based on the measured incompressibility of the liquid. Both the VMC and LDA calculations give a significant deviation from this prediction for  $N \leq 240$ . The VMC energies are almost constant at 2.5-3.0 K, while the LDA energies are well fit by  $(25N^{-1/3} - 48N^{-2/3})K$ , lying slightly above the VMC energies, but significantly below the SSLD prediction. Nevertheless the liquid incompressibility can be extracted from the drop calculations.

---

\*University of Illinois, Urbana, Illinois.

TABLE III-I. Excitation energies (in K) obtained with the VMC and LDA methods. The LDA(L) and LDA(D) use liquid and droplet pair distribution functions, respectively.

N	VMC	LDA(D)	LDA(L)	VMC	LDA(D)	LDA(L)
	BM	BM	BM	J=2	J=2	J=2
20	2.24(3)	2.24	2.33	1.65(1)	1.78	1.91
40	2.94(3)	2.64	2.83	1.79(1)	1.78	1.99
70	2.29(3)	2.05	2.24	1.34(1)	1.37	1.60
112	2.14(4)	1.88	2.10	1.24(2)	1.21	1.47
240	2.24(5)	1.68	1.99	1.01(2)	0.97	1.26
	J=3	J=3	J=3	J=4	J=4	J=4
20	2.35(3)	2.44	2.49	-	-	-
40	2.44(2)	2.48	2.61	3.12(2)	3.12	3.17
70	1.88(2)	1.90	2.07	2.33(3)	2.39	2.49
112	1.62(3)	1.68	1.89	2.05(4)	2.11	2.25
240	1.33(3)	1.37	1.65	1.64(3)	1.75	1.97

The surface excitation calculations are not so satisfactory. The SSLD model states that the surface excitation is equal to the energy of a ripplon for the plane surface of wave number  $k(J,N)=[(J-1)J(J+2)]^{1/3}/r_0N^{1/3}$ , where the ripplon energy  $\propto t^{1/2}k^{3/2}$  and  $t$  is the liquid surface tension. The LDA calculation for the ripplon spectrum fails to give the correct small- $k$  dependence, and consequently the surface excitations deviate from the SSLD model for large  $N$ . This failure is probably a consequence of the form chosen for the variational ground-state wave function. However the spectrum is not unreasonable for  $0.3 \ll k(\text{\AA}^{-1}) \ll 0.6$  so the LDA and VMC excitation energies, which are in close agreement, may be fairly good for the corresponding regions of  $J$  and  $N$ . A paper on this work has been submitted for publication.

b. Variational Monte Carlo Calculations of  $^3\text{He}$  Drops  
(S. C. Pieper, R. B. Wiringa and V. R. Pandharipande\*)

The ground-state energy and density distributions for drops of  $^3\text{He}$  atoms with  $N=40,70,112,168$ , and 240 have been calculated with the VMC method starting from the Aziz interatomic potential. The variational wave functions include a Slater determinant of single-particle correlations to confine the drop and ensure antisymmetry, two- and three-body correlations, and Feynman-Cohen backflow. The MC random walk is controlled by the full wave function and the kinetic energy is evaluated in the Pandharipande-Bethe form. The resulting calculation is far more computer intensive than that for the boson  $^4\text{He}$  drops, but various attempts to simplify the random walk always led to unacceptably large MC variances. The calculations were made feasible by access to the Energy Research Cray-XMP computer, which ran at speeds up to 40 times faster (for the largest drops) than the Argonne IBM 3033 computers.

The  $^3\text{He}$  drops are much more weakly bound than the  $^4\text{He}$  drops, due to the Fermi statistics and the larger zero-point motion. Our calculations suggest that the minimum number of atoms required to form a bound drop is just under 40. Fitting the calculated energies to a semi-empirical mass formula gives a volume energy of  $-2.1\text{K}$  that agrees well with independent VMC calculations of the liquid energy, but is above the experimental value of  $-2.47\text{K}$ . The surface term gives a surface tension that is  $0.13 \text{K}\text{\AA}^{-2}$ , about 20% high compared to experiment. The unit radii of the drops can also be fit (although with less precision) to infer a liquid density of  $0.016\text{\AA}^{-3}$  that is 5% below the experimental value.

The density profiles of the drops are fairly smooth, with some interior wiggles that are the remnants of the single-particle shell structure which is largely washed out by the strong two-body correlations. The central density of the largest drops is  $\sim 10\%$  below the liquid density, and the surface thickness is  $\sim 8\text{\AA}$ . The density profiles are shown in Fig. III-10.

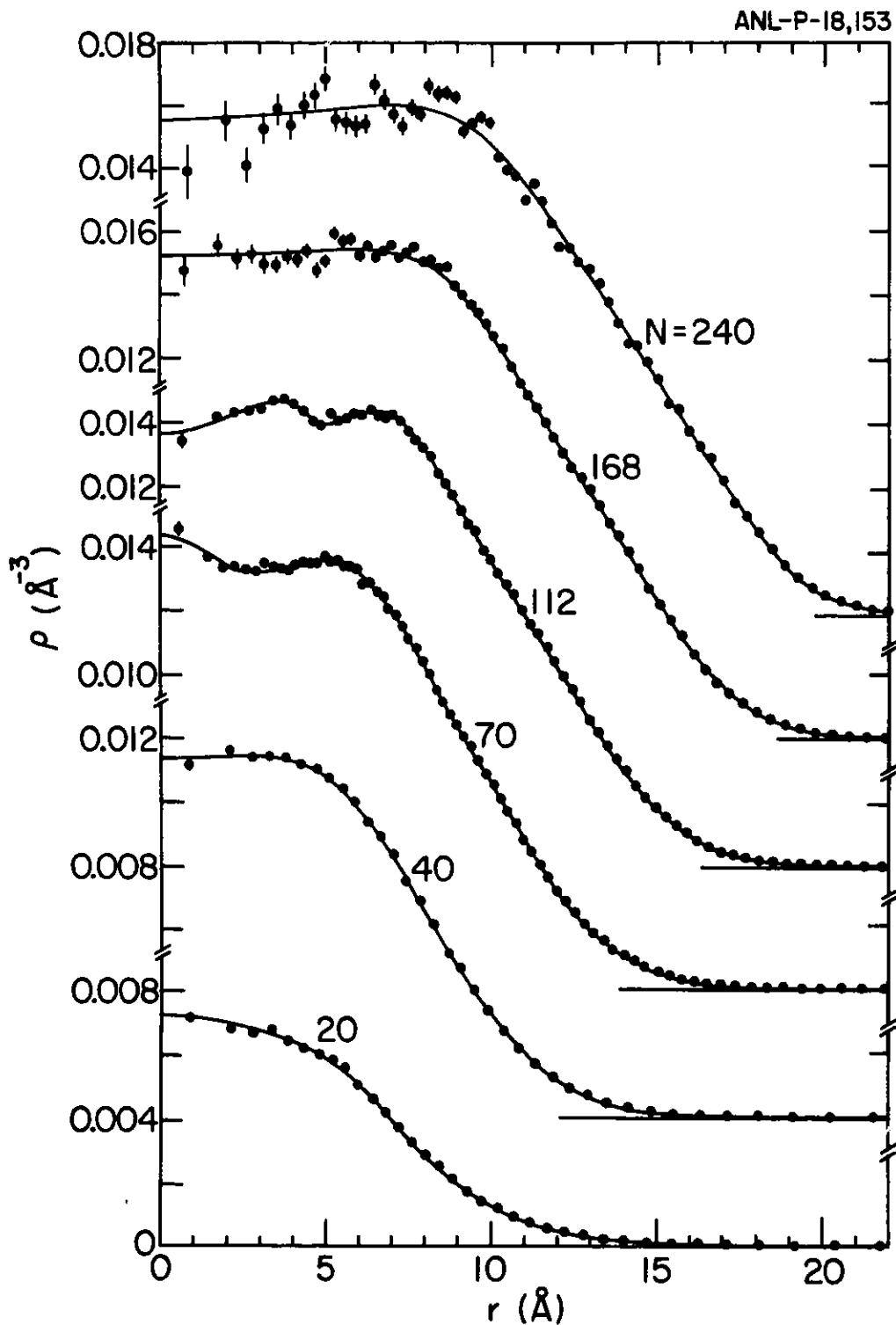


Figure III-10. Density profiles for the  $^3\text{He}$  drops. The error bars show the Monte Carlo binning of the densities; the curves are drawn to guide the eye. The curves are labeled with the number of atoms in the drops.

We have also calculated the energy and density distribution for a 68-atom drop, where the wave function is that of the 70-atom drop with the least bound single-particle orbital, a 3s state, unfilled. The difference between the 70- and 68-atom density distributions has a clear 3s shape, but its peak is reduced by a factor of five compared to the square of the missing single-particle wave function, and its nodes have been pushed out. This study is a simple theoretical analog to the experimental observation of single-particle orbitals in electron scattering from  $^{206}\text{Pb}$  and  $^{205}\text{Tl}$  nuclei. A paper reporting this work has been submitted for publication.

## E. NUCLEAR STRUCTURE STUDIES IN DEFORMED AND TRANSITIONAL NUCLIDES

(R. R. Chasman)

The goal of this program is to understand the effective two-body interactions that give rise to strong correlations in nuclei. These correlations are most clearly manifested in deformed nuclei and can be most precisely studied in mass regions where there is a transition from undeformed to deformed shapes, or under conditions that induce changes in nuclear collective properties such as the strong Coulomb fields in fission or the deposition of large amounts of angular momentum in heavy-ion reactions. Our major interests are: (1) nuclear octupole deformation, discovered in this program, which depends rather sensitively on the details of the valence orbitals occupied by unpaired nucleons; (2) the transition from spherical to oblate nuclear shapes with increasing angular momentum that is seen in nuclides near  $^{146}\text{Gd}$  and  $^{208}\text{Pb}$ ; (3) the  $2^6$ -pole deformation that we find accounts for several features in the spectra of nuclides in the mass region  $220 < A < 230$ ; (4) the superdeformed prolate nuclear deformations that play an important role in fission and possibly in the yrast spectra of nuclides near  $A=154$ ; (5) the competition between octupole correlation effects and  $\gamma$ -deformation, at both low and high spins, in the mass region  $220 < A < 230$ . Our studies of all of these problems involves a collaboration with the experimental nuclear structure programs at Argonne.

We have been converting our programs to the ER Cray and tuning them for that machine. We will investigate the effects of  $\gamma$ -deformation combined with angular momentum on single-particle levels.

a.  **$\gamma$ -Deformation in a Reflection Asymmetric Single-Particle Potential**  
(R. R. Chasman)

When a single-particle potential is reflection asymmetric, the calculation of eigenstates involves the diagonalization of a set of basis states with both positive and negative parity. However, the projection of angular momentum on the nuclear symmetry axis,  $j_z$ , is still a good quantum number and can be used to reduce the size of the arrays that must be diagonalized. In studies of the heavy elements, these arrays are  $\sim 120 \times 120$ . When  $\gamma$ -deformation is introduced into the potential,  $j_z$  is no longer a good quantum number and the eigenstates are calculated by diagonalizing matrices that are  $\sim 600 \times 600$ . A further complication introduced by  $\gamma$ -deformation is that the evaluation of matrix elements involves triple integrals rather than double integrals. We are developing a computer code to obtain the single-particle eigenstates of a reflection asymmetric potential with  $\gamma$ -deformation.

b. **Many-Body Treatment of Quadrupole and Octupole Correlations in Nuclei** (R. R. Chasman)

A deformed one-body potential model is not adequate for handling the residual interaction correlations in nuclear states, when the effects are only moderately strong. We have developed a many-body calculation method that gives a good description of such nuclear states, as well as states in which the correlation effects are strong; i.e. both vibrational and deformed states. In our approach, the pairing force and cylindrically symmetric particle-hole interactions are treated on an equal footing. In the past year, we have developed a number of programs to calculate one-body matrix elements using these many-body wave functions. We have obtained some results for magnetic moments, decoupling constants, coriolis interaction matrix elements and M1 transition probabilities. Our results show deviations from a simple picture of octupole deformation in the mass region  $220 < A < 230$ . In this picture, one expects an equality of matrix elements between appropriate members of parity doublet rotational bands, independent of the parity of the specific states. In contrast, using the many-body wave functions, we find substantial deviations from this deformed model prediction of equality of matrix elements.



c. Incipient Octupole and  $2^6$ -Pole Deformation in the Mass Region  $220 < A < 230$  (R. R. Chasman)

Octupole correlations play an important role in determining the nature of the states of nuclides in the mass region  $220 < A < 230$ . Calculations using the Strutinsky procedure suggested that the octupole correlation effects should be markedly stronger for the nuclides near  $A=220$  as compared to those near  $A=230$ . However, experimental studies of the nuclides in this region do not show any great increase of octupole correlation effects. One of the elements missing in the calculations using the Strutinsky procedure was a consideration of the effects of  $2^6$ -pole deformation. Motivated by the discrepancies between experiment and the theoretical description of levels in  $^{225}\text{Ra}$ , we have introduced  $2^6$ -pole deformation into the single-particle description of the nuclides in this mass region. We find that it plays an important role, quite comparable in magnitude to the octupole deformation mode. It increases the calculated binding energies of nuclides in this mass region by  $\sim 1$  MeV. The inclusion of this mode also improves the agreement between the theoretical description of  $^{225}\text{Ra}$  and the experimental observations, although there are some remaining discrepancies.

d. Octupole Correlations in  $^{227}\text{Ac}$  (R. R. Chasman, H. Martz,\*  
R. Sheline,\* R. Naumann,† D. Burke,‡ G. L. Struble,§ and D. Decman§)

$^{227}\text{Ac}$  is one of the few accessible odd-proton nuclides in which octupole correlations are important. One-particle transfer reactions, with a  $^{226}\text{Ra}$  target, have been used to populate states in  $^{227}\text{Ac}$ . We have carried out an angular-momentum decomposition of single-particle states in a potential with octupole deformation in order to analyze the proton transfer data. This analysis suggests that the octupole deformation of the ground state  $3/2^{\pm}$  bands is best characterized with  $\epsilon_3 \approx 0.03$ . Larger octupole deformations predict a population of the  $13/2^{+}$  state that is substantially smaller than is experimentally observed. The study of the  $1/2^{\pm}$  excited bands in  $^{227}\text{Ac}$  shows that they are not deformed in an octupole sense. This difference in the  $3/2$  and  $1/2$  bands was predicted in our calculations with many-body wave functions.

---

\*Florida State University, Tallahassee, FL

†Princeton University, Princeton, NJ

‡McMaster University, Hamilton, ON Canada

§Lawrence Livermore Laboratory, Livermore, CA

e. Spectroscopic Studies of  $^{225}\text{Ra}$  (R. R. Chasman and I. Ahmad)

$^{225}\text{Ra}$  is one of the few accessible odd-neutron nuclides in which octupole correlation effects are important. We have included both octupole correlations and  $2^6$ -pole correlations, in addition to the usual quadrupole and hexadecapole deformation modes, to get a description of  $^{225}\text{Ra}$  that agrees fairly well with experiment. However there remain some large discrepancies between the theoretical picture and the experimental data on the low-lying  $1/2^{+}$  and  $1/2^{-}$  bands. One cause of these discrepancies may be the neglect of  $\gamma$ -deformation in the theoretical description.

F. BINDING ENERGIES OF HYPERNUCLEI AND  $\Lambda$ -NUCLEAR INTERACTIONS

(A. R. Bodmer and Q. N. Usmani\*)

Studies of the interaction of a  $\Lambda$  with nucleons in nuclei have been continued. In particular, strongly repulsive  $\Lambda NN$  three-body forces are found to be required for an adequate description of hypernuclear binding energies. The role of more complicated NN potentials, such as tensor potentials, will be investigated.

---

\*Physics Department, Aligarh Muslim University, Aligarh, India

a. Binding Energies of Hypernuclei and 3-body ANN Forces (A. R. Bodmer and Q. N. Usmani\*)

We have continued our variational calculations of the  $\Lambda$ -separation energies of the s-shell hypernuclei ( ${}^3_{\Lambda}\text{H}$ ,  ${}^4_{\Lambda}\text{He}$ ,  ${}^5_{\Lambda}\text{He}$ ) using Monte Carlo techniques, and also for a  $\Lambda$  in nuclear matter (well depth D) using the Fermi hypernetted chain method. These calculations which are mostly with central two-body  $\Lambda\text{N}$  and three-body  $\Lambda\text{NN}$  forces are now complete and a detailed paper is being prepared for publication. A less detailed account has been presented in an invited paper (for the International Symposium on Hypernuclear and Kaon Physics, Brookhaven National Laboratory, September 1985, which will be published in a general issue of Nuclear Physics.)

In summary, we have found that  $\Lambda\text{p}$  scattering, the s-shell binding energies, the well depth, and probably also  ${}^9_{\Lambda}\text{Be}$  (representative of intermediate mass hypernuclei), can all be fitted with  $\Lambda\text{N}$  plus  $\Lambda\text{NN}$  forces consistent with meson-exchange models. Both two-pion-exchange  $\Lambda\text{NN}$  forces consistent with theoretical expectations and strongly repulsive dispersive  $\Lambda\text{NN}$  forces are required. For the latter we have used both a spin-independent form as well as a novel spin-dependent form. The two forms are equivalent for nuclei with spin-zero cores, i.e. for  ${}^5_{\Lambda}\text{He}$  and D. The  $\Lambda\text{p}$  scattering and  ${}^5_{\Lambda}\text{He}$  require strongly repulsive dispersive  $\Lambda\text{NN}$  forces, a result already obtained earlier. It is significant that this conclusion is also required by a comparative analysis of  ${}^5_{\Lambda}\text{He}$  and D which is largely independent of the scattering data. The spin-dependent dispersive  $\Lambda\text{NN}$  force is strongly preferred over the spin-independent one by the well-depth results when use is made of the limits of the p-state  $\Lambda\text{N}$  potential obtained from scattering. The  $\Lambda\text{NN}$  spin dependence reduces the spin dependence of the two-body  $\Lambda\text{N}$  force by  $\approx 1/3$ , and correspondingly contributes  $\approx 1/3$  to the  $0^+-1^+$  splitting of the  $A=4$  hypernuclei. However even this reduced  $\Lambda\text{N}$  spin dependence is quite appreciable and significantly larger than the most commonly accepted values.

On the more technical side, a significant feature is the important  $\Lambda\text{NN}$  three-body correlations required by the two-pion-exchange  $\Lambda\text{NN}$  force in the s-shell hypernuclei.

---

\*Physics Dept., Aligarh Muslim University, Aligarh, India.

b. Coulomb Effects and Charge Symmetry Breaking for the A=4 Hypernuclei (A. R. Bodmer and Q. N. Usmani\*)

The effect  $\Delta B_c$  of the Coulomb interaction on the  $\Lambda$  separation energy  $B_\Lambda$  of  ${}^4_\Lambda\text{He}$  was obtained by variational calculations made for  ${}^4_\Lambda\text{He}$  and  ${}^3\text{He}$ . These calculations were made for several values of  $q^2$  in the range  $0 < q^2 < 9$  where  $qe$  is the proton charge, i.e., the Coulomb repulsion was artificially boosted. For  $q^2 < 3$ , the dependence on  $q^2$  is linear, and interpolation to  $q^2=1$  gives the physical values with improved accuracy:  $-\Delta B_c = 0.05 \pm 0.02$  and  $0.025 \pm 0.015$  MeV for the ground and excited state. This procedure also gives more accurate values for the differences between the proton and neutron radii of  ${}^3\text{He}$ . The corresponding differences of  $B_\Lambda$  between  ${}^4_\Lambda\text{He}$  and  ${}^4_\Lambda\text{H}$ , to be attributed to charge symmetry breaking (CSB) effects, are then  $0.40 \pm 0.06$  and  $0.27 \pm 0.06$  MeV. From these values we obtain a phenomenological CSB potential which is effectively spin independent. This is consistent with meson-exchange CSB models for the triplet but not for the singlet case indicating that there may be important quark structure contributions for the latter. This work has been published.

c. Alpha-Cluster Calculations of  ${}^9_\Lambda\text{Be}$  (A. R. Bodmer and Q. N. Usmani\*)

Variational calculations are being continued for  ${}^9_\Lambda\text{Be}$ , using a  $2\alpha + \Lambda$  model. The best available local but  $l$ -dependent  $\alpha\alpha$  potentials (fitted to  $\alpha\alpha$  phase shifts) are used. The  $\alpha\Lambda$  potential is obtained from effective interaction calculations by folding effective  $\Lambda N$  and  $\Lambda NN$  potentials into the  $\alpha$ -particle density to reproduce  $B_\Lambda({}^5_\Lambda\text{He})$ . Repulsive dispersive  $\Lambda NN$  forces also imply a repulsive  $\alpha\alpha\Lambda$  potential. We have allowed for a  $p$ -state  $\Lambda N$  interaction which is different from the  $s$ -state one, and have obtained a reduction of 0.3 MeV in the ground-state energy (close to our earlier crude estimate of 0.4 MeV) using a  $p$ -state  $\Lambda N$  potential of half the strength of the  $s$ -state potential. We are also allowing for the  $l$ -dependence of the  $\alpha\alpha$  potential. In addition to the ground-state calculation for  ${}^9_\Lambda\text{Be}$ , we are also calculating the energy of the lowest excited (doublet) state built on the first  $J=2^+$  state of  ${}^8\text{Be}$ . Preliminary calculations indicate an excitation energy of  $\approx 3$  MeV, consistent with experiment, implying that the state is particle stable (with respect to breakup into  ${}^5_\Lambda\text{He} + \alpha$  at a threshold 3.5 MeV above the ground state) and that it should decay by  $\gamma$  transitions to the ground state.

---

\*Physics Dept., Aligarh Muslim University, Aligarh, India.

## G. OTHER THEORETICAL PHYSICS

a. Magnetic Monopoles and Dipoles in Quantum Mechanics  
(H. J. Lipkin\* and M. Peshkin)

It has been understood since Dirac's 1931 work on the subject that conventional quantum mechanics is incapable of dealing with mixed electric (e) and magnetic (g) charges, even in the static limit, unless the charges obey  $eg/c = n\hbar/2$  with integer n. The difficulty comes about formally because it is impossible to represent the magnetic field as the curl of a vector potential unless the magnetic field is free of divergence. Physically, this effect is fundamentally related to the quantization of the angular momentum (eg/c) in the crossed electric and magnetic fields. We have considered the Hamiltonian description of systems wherein magnetic monopoles or dipoles made of monopoles ("di-monopoles" in the limit) move in the magnetic field of an electric current. We find that in the limit where the magnetic field is stationary, no Hamiltonian exists for the motion of a magnetic monopole or di-monopole. The magnetic object exchanges energy with the source of the magnetic field and no Hamiltonian works correctly unless it contains the dynamical variables of that current source. That exchange of energy comes about in the case of the monopole because the stationary field can do nonvanishing work on the monopole which is carried around a closed orbit. Work can also be done in a  $2\pi$  rotation of a di-monopole located at a point where a stationary external electric current does not vanish. This approach does not rely upon any assumption about the existence of a vector potential, singular or nonsingular, and it has two interesting features: it illuminates the magnetic monopole problem by a physical consideration which is different from and in some ways more general than the usual one, and it shows that the same consideration applies to the magnetic di-monopole.

Part of this work has been reported as an invited paper (M. Peshkin) at the conference "New Techniques and Ideas in Quantum Measurement Theory" in New York, January 21-24, 1986. A complete report is being prepared for publication.

b. The Spins of Cyons and Dyons (H. J. Lipkin\* and M. Peshkin)

A dyon is an "atom" formed by binding an electron (e) to a magnetic monopole (g) by a scalar force. For present purposes both the electron and the monopole can be spinless. Such dyons in their ground states are known to have spin  $1/2$  if the charges obey Dirac's quantization condition  $eg/c = n\hbar/2$  with  $n=1$ , and they are fermions in the sense that tritons are fermions. A cyon is formed by confining the spinless electron to the interior of a torus surrounding a line of magnetic flux. In the interesting case, the flux line is infinite in both directions, and any return flux is infinitely far away. It has been observed that because of the multiple connectivity of the electron's domain, it is possible to associate a gauge transformation with rotations about the flux line (the z axis) in such a way that the angular momentum component  $J_z$  has eigenvalues  $J_z = (j - e\Phi/2\pi c)\hbar$ ,  $\Phi$  being the flux and  $j$  the integers. Cyons can then have any spin and there have been many interesting speculations about their possibly unusual statistics. Specific dynamical models based on Lagrangian field theories in which the flux line is a dynamical quantity have been shown to generate spin one-half cyons, but not arbitrary spins.

We have analyzed the spins of cyons and dyons in terms of the angular momentum in the electromagnetic field and found that all the general results can be obtained purely in terms of the quantization of the total angular momentum in the system, independently of all considerations of quantum field theory and gauge fields. We first consider the angular momentum in a finite system. In the cyon case the flux line is replaced by a long thin solenoid with return flux outside the domain of the electron. For the dyon, Dirac's flux string leading into the monopole is replaced by an infinitesimally thin solenoid of finite length; in other words, the monopole is replaced by a monopole-antimonopole pair. For those finite systems, the canonical angular momentum in the gauge where  $\nabla \cdot \mathbf{A}$  vanishes obeys  $\mathbf{J} = \mathbf{r} \times \mathbf{mv} + \int \mathbf{r}' \times \mathbf{P}(\mathbf{r}') d^3r'$ , where  $\mathbf{P}$  is the Poynting vector in the crossed electric and magnetic fields. (Using another gauge introduces nothing useful and leads to the same physics slightly less simply.) The second term is the angular

---

\*1985-86 Argonne Fellow, on leave from the Weizmann Institute of Science, Rehovot, Israel.

momentum in the crossed fields, so that  $J$  is the classical total angular momentum; it is also the generator of rotations in quantum theory and its eigenvalues are the integers. We then go to the appropriate limit which represents the single monopole or the cyon. We find that the unusual spins are obtained by discarding the angular momentum in return fields at infinity. The remaining angular momentum in the dyon case agrees with the usual,  $J_d = r \times mv + (eg/c)\hat{r}$ , the unique generator of the rotations when the only dynamical variables are those of  $e$  and  $g$ . The discarded angular momentum at infinity equals  $\hbar/2$  when the Dirac charge quantization condition is obeyed and  $J_d$  is then half-integral.

For the cyon, the same general remarks apply except that the flux in the solenoid is not quantized and the angular momentum  $e\phi/2\pi c$  in the return flux need not be integer or half-integer valued. Then going to the limit and discarding the angular momentum at infinity can give any spin for the cyon. However, the symmetry in the cyon case is only that of rotations in two dimensions and  $J_z$ , the only angular momentum generator, is not observable in principle unless the dynamical system is expanded to include the sources of the magnetic field. The eigenvalues of  $J_z$  in the 2-dimensional case have the form  $(\gamma+j)\hbar$ , where  $j$  are integers and  $\gamma$  is an arbitrary number in  $0 \leq \gamma < 1$ . There is no general constraint on  $\gamma$ . Absent a dynamical model, the cyon does not have to contain a magnetic field. The electron must only be excluded from the  $z$  axis. Specific dynamical models add constraints, and if the magnetic flux in the solenoid varies, then  $\gamma$  changes in such a way that  $\delta\gamma = (eg/\hbar)\delta\phi$ .

Although  $\gamma$  is arbitrary in general, it can be restricted to 0 or 1/2 by introducing either time-reversal symmetry or invariance under proper Lorentz transformations in  $(x,y,t)$  space. Either of those symmetries makes  $J_z$  observable in principle. The eigenvalue restriction can be obtained directly from the commutation relations  $TJ_z = -J_z T$  or  $[K_x, K_y] = -i\hbar J_z$ . In that sense, the emergence of half-integer cyons from field-theoretic models arises from symmetry rather than from the dynamics of the model.

Parts of this work have been reported as invited papers (M. Peshkin) at the NATO Workshop "Fundamental Questions in Quantum Theory" in Como, Italy, September 2-7, 1985, and at the conference "Symmetries in Nature II" in Carbondale, Illinois, March 24-26, 1986. A complete report is being prepared for publication.



c. Saddle-Point Variational Method for the Dirac Equation  
(M. Peshkin and B. D. Keister\*)

We have briefly examined a recent proposal of Franklin and Intemann which appears to obtain useful variation solutions of the Dirac equation with forces that may be realistic for few-quark systems. They solve two-body problems with attractive Coulomb and linear potentials, both Lorentz scalar and fourth component of a four-vector. Using simple two-parameter trial functions, they obtain ground-state binding energies that are typically within a few percent of the exact values, and no worse than 20%, even for strongly relativistic binding. Their variational wave functions also give remarkably accurate expectation values for the operators  $\langle 1/r \rangle$  and  $\langle r \times r' \rangle$ , with typical errors comparable to those of the binding energy. These results are surprising because the Dirac Hamiltonian is unbounded below, and all its eigenfunctions should be expected to defy easy variational approximation, as do the non-lowest eigenvalues of nonrelativistic Hamiltonians. No theoretical basis for the reported success with QCD-like interactions has been given, except for the intuitive suggestion that a good trial function should give minimum energy with respect to variation of some parameter that appears to measure positive energy contributions to the wave function and maximum with respect to a negative-energy measuring parameter.

We have investigated some additional properties of the variational wave functions in an attempt to find out to what extent they include the right physics. We have been unable to provide any general theoretical explanation of their successes in determining  $\langle H \rangle$ . Instead, we have found that these two-parameter trial functions give very poor estimates of  $\langle H^* H \rangle$  (a positive-definite quantity) which become worse in cases of strong relativistic binding. These trial functions apparently contain substantial admixtures of negative-energy states and get their encouraging result for  $\langle H \rangle$  by cancellation of large positive and negative contributions. The successes in approximating  $\langle 1/r \rangle$  and  $\langle r \times r' \rangle$  appear to be related to virial-like theorems, peculiar to the potentials chosen, which relate these matrix elements to  $\langle H \rangle$ , and therefore do not signal any additional merit of the variational wave functions. The variational principle as applied does not appear to be part of a systematic approximation scheme. The authors note that trial functions with

---

\*Carnegie-Mellon University, Pittsburgh, PA

additional parameters may fail to yield a variational saddle point. We find that one such class of trial functions is actually closer to the correct physical wave function than their "successful" saddle-point trial functions, which again raises doubts about the physical content of this variational method.

d. High-Spin States in  ${}_{45}^{97}\text{Rh}$  (A. Amusa\*)

Data on decay modes of high-spin states in the neutron-deficient isotope  ${}^{97}\text{Rh}$  have been published recently. A shell-model study of this nucleus was carried out in the space  $(1g_{9/2})^5$  for protons and  $(1g_{7/2}, 2d_{5/2}, 2d_{3/2}, 3s_{1/2})^2$  for neutrons. The energy spectrum and E2 and M1 transitions were calculated. An approximation was also carried out limiting the protons to a maximum seniority of 3. The two spectra were quite similar, but the gamma-transition probabilities differ considerably, reflecting the effect of seniority selection rules for a half-full shell. A report of the calculation is in preparation.

---

\*University of Ife, Ile-Ife, Nigeria

#### IV. SUPERCONDUCTING LINAC DEVELOPMENT

R. Benaroya, J. M. Bogaty, L. M. Bollinger, P. Markovich, R. C. Pardo,  
K. W. Shepard, G. P. Zinkann, J. Aron, \* B. E. Clifft, \*\* J. M. Nixon,  
and M. F. Waterson

##### INTRODUCTION

The superconducting linac project at Argonne consists of a broad range of activities including (1) completion of the ATLAS project, (2) continuing refinements of the technology associated with ATLAS, and (3) development of the new technology required for the planned positive-ion injector for ATLAS. All of this work involves developmental activities that are of rather general interest.

Until October 1985, this program was carried out jointly by the Chemistry and Physics Divisions. Since then, the program has been directed entirely by the Physics Division, but several members of the Chemistry Division continue to be involved in the work.

##### A. THE ATLAS PROJECT

###### 1. Completion of ATLAS

The Argonne Tandem-Linac Accelerator System (ATLAS) was completed on schedule and within budget in September 1985. Since then, the accelerator has been operated routinely and effectively for research.

The main features of the ATLAS technology have been discussed in earlier reports and the tasks that were completed during the past year are listed in Sec. V of this report. Also, the operation of ATLAS is discussed in Sec. V.

###### 2. Refinement of ATLAS Technology

Although the ATLAS linac has been completed, a continuing effort is being devoted to the refinement of some aspects of the technology with the objectives of increasing operational reliability and of increasing the on-line accelerating fields of resonators to the high levels that are routinely achieved off line. Two such topics that are of general interest are (1) an effort to increase the on-line Q's of the resonators and (2) an effort to increase the reliability and tuning capacity of the fast tuner.

---

\*Retired.

\*\*Chemistry Division, ANL.

No doubt several factors contribute to the fact that the on-line performance of the superconducting resonators is poorer than is routinely demonstrated in off-line tests. Such factors might be contamination by pump oil and dust, inadequate cooling, mechanical defects, and loading by any one of the three probes used to drive and control the resonator. During the past year, a diagnostic technique for investigating some of these possible problems has been developed. This technique involves a determination of the power dissipation in the housing by measuring the very small temperature drop caused by the flow of heat from the housing to the helium-cooled base of the resonator. Power losses of 0.1 W can be measured with ease. By now, all 42 of the ATLAS resonators have been studied on line, and the Q's of some of them were found to be surprisingly low. Two sources of this difficulty have been identified: (a) weld failures apparently caused by thermal stresses during many years of operation and (b) power dissipation in the RF power input probe. These problems are being corrected (i) by rewelding the defective parts and (ii) by developing a better power probe. This latter work is still in progress.

Another developmental effort still in progress is an effort to increase the lifetime and perhaps the tuning capacity of the fast tuner. This fast tuner is a voltage-controlled reactance (VCX) that has 10 PIN diodes operating in parallel. After about half of the diodes have failed, the VCX is no longer able to operate at full power. The mean lifetime of one of these tuners is rather long (many years), but nevertheless the failure rate for the whole linac is several tuners per year, a significant maintenance problem because the tuners are inside the cryostats. This problem is being attacked by designing a tuner in which the cooling of the PIN diodes is improved by using bare diode chips that are immersed in liquid nitrogen.

Almost every major subsystem of ATLAS is being refined in some way, but most of these tasks make use of conventional technology and hence are not discussed in this section. One task of more general interest is the control of the liquid-helium system, which consists of two refrigerators and distribution lines operating in parallel with several cross connections. This rather complex system has evolved over the years to satisfy changing needs, and there was some worry that the parallel feeding of different parts of the linac with changing heat loads might be very difficult to control. This

potential problem has been solved, however, with a rather simple control system that automatically shares the heat load and helium mass flow between the two refrigerators, regulates the liquid-helium flow between the two parts of the linac, and controls the liquid-helium level in two large storage dewars. The system does not show any sign of instability or unexpected heat loss.

In view of our good experience with the operation of two refrigerators in parallel, a third refrigerator required for the operation of the planned positive-ion injector will also be tightly coupled to the present cryogenic system.

## B. THE POSITIVE-ION INJECTOR

Plans for the positive-ion injector for ATLAS have taken definite form during the past year. The objective is to replace the present ATLAS injector, a tandem electrostatic accelerator and its negative-ion source, with a positive-ion source and a new form of superconducting injector linac. This new approach is expected to increase the beam intensity by two orders of magnitude and to lead to a system that will enable ATLAS to accelerate uranium beams of good quality and intensity. The planned layout of the new injector system is shown in Fig. IV-1.

The positive-ion source for the new system will be an electron cyclotron resonance (ECR) source on a 350-kV voltage platform. Both mass analysis and a first stage of bunching will be carried out on the voltage platform. A second-stage buncher will be added in front of the linac, at ground potential. The ECR source provides ions with very high charge states, and thus the injector linac can be rather small.

### 1. Description of the Positive-Ion Injector

The technology of the ECR source is well developed and our design is being strongly influenced by the work of others. Major design features are that both the first-stage and second-stage plasma are driven by a single 10-GHz transmitter, and the second-stage chamber is about 10 cm in diameter. Since the source must be mounted on a high-voltage platform, effort is being devoted to the reduction of power requirements. Also, since our unit must be

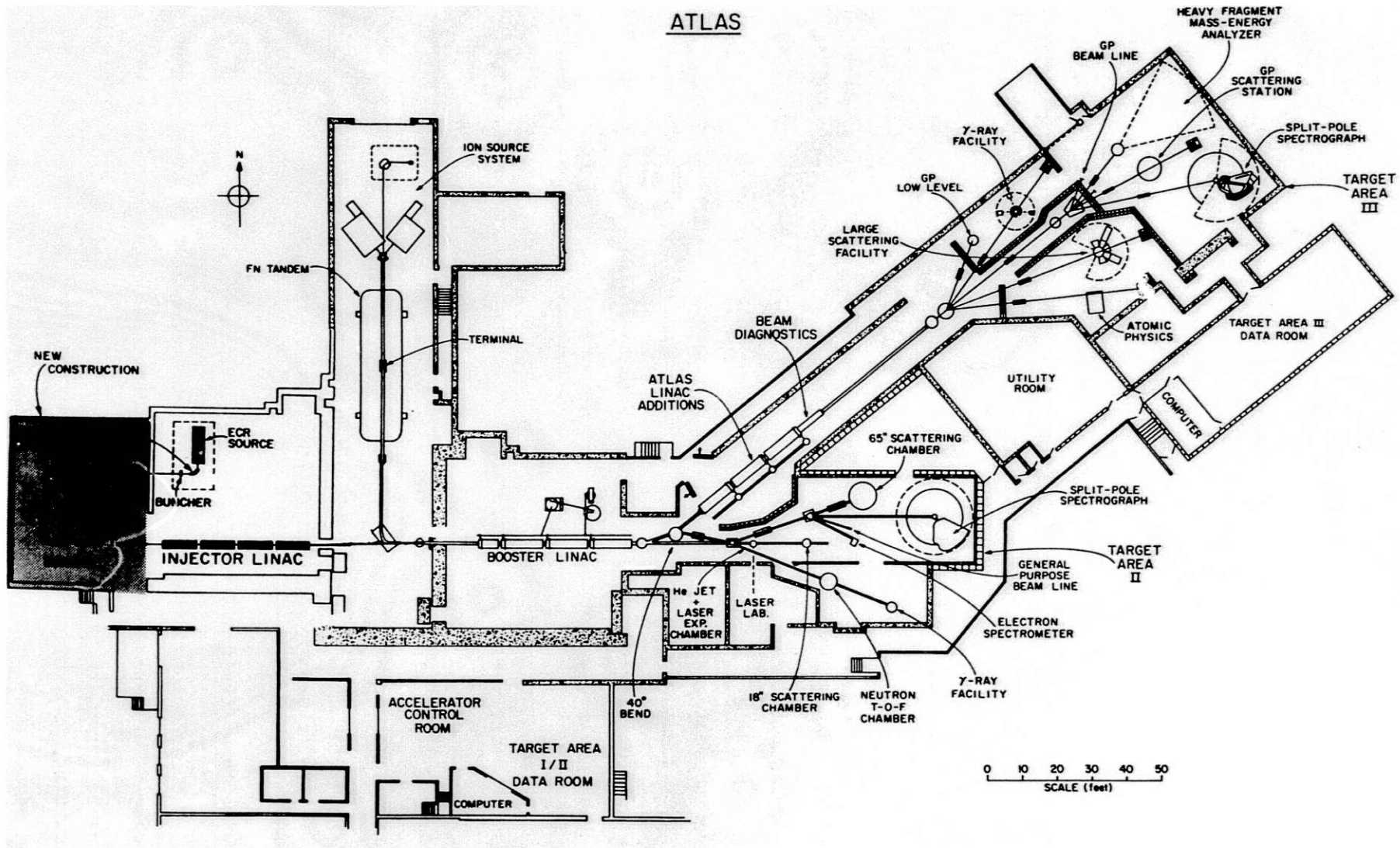


Figure IV-1. Layout of ATLAS and (on the left) the planned layout of the positive-ion injector.

able to produce ions from all kinds of solid materials, convenient access to the interior of the plasma chamber is being emphasized.

The injector linac used to accelerate the low-velocity ions from the source will consist of an array of four different kinds of independently-phased superconducting accelerating structures, all operating at the low frequency of 48.5 MHz. The three types of resonators in the low-energy part of the linac will all be 4-gap interdigital structures formed by 3 drift tubes. Starting at the input of the linac, the active lengths of these units will be 10 cm, 16 cm, and 24 cm. For the fourth type of resonator, in the high-energy part of the machine, there are several satisfactory options, but we tentatively plan to use a half-wave (3-gap) structure with an active length of 24 cm.

The construction of the positive-ion injector will be carried out in three phases. In Phase I, the goal is to build a small but useful prototype system consisting of a 3-MV linac and an ECR source on its voltage platform. The linac will have a total of 5 or 6 resonators. Even this small system will be superior to the existing tandem as an injector for all ions with  $A > 40$  and will be vastly superior for two classes of ions: (a) those that are difficult to make with a negative-ion source and (b) those with  $A > 80$ . Our goal is to have the Phase I positive-ion injector be operational by early 1989.

The planned Phase II will enlarge the injector linac to 8 MV, which will allow ATLAS to accelerate ions up to the rare earth region. And finally, in Phase III the injector linac will be further enlarged to 12 MV, enough to allow ATLAS to accelerate uranium ions well above the Coulomb barrier. If funding is available as planned, the Phase III system will be in operation by early 1991.

Work is proceeding actively on both the ECR source and on the injector linac. Major parts of the source have been ordered and it is expected that the source will be assembled and ready for testing by mid-1987.

Most of the effort on the injector linac is being devoted to the development of the four new types of resonators required to accelerate low-velocity ions. The prototype of the first of the interdigital resonators was completed and tested in 1985. This  $\beta = 0.008$  unit operated stably at accelerating fields far beyond our original design goal of 3 MV/m. (See Sec. B.2.)

The prototype for the second type of interdigital structure is under construction and is expected to be completed in September 1986. Construction of the final two units will begin immediately thereafter.

## 2. Tests of the 4-gap 10-cm Accelerating Structure

A uranium ion from the planned ECR source is expected to arrive at the injector linac with a relative velocity  $\beta = 0.008$ . The superconducting resonator suitable for the acceleration of such a slow-moving ion is a 4-gap structure formed by three drift tubes and the end plates. The outer pair of drift tubes are driven by a tapered coaxial quarter-wave line, and the inner drift tube is grounded to the housing. The outer housing consists of a composite material formed by explosively bonding niobium to copper. The active length of the structure is about 10 cm along the beam path, and each gap between drift tubes is about 1 cm. The outside appearance of the resonator is pictured in Fig. IV-2.

The prototype 10-cm resonator has been thoroughly tested and found to have excellent performance characteristics. It has been operated stably at an accelerating field of 10 MV/m, and it operates at 7 MV/m with a power dissipation of only 4 watts. Thus, although it is too early to know what the maximum accelerating field will be in long-term on-line operation, it is almost certain to be substantially greater than the 3 MV/m that was originally assumed. Our guess at this time is that 5 MV/m will prove to be a practical on-line operating field for the 10-cm unit, implying that it will provide about 500 kV of acceleration.

Originally, a major question about the new resonator was whether the RF frequency variations induced by mechanical vibrations of the long 48.5-MHz quarter-wave line would be small enough to be controllable. Our tests show that such frequency variations are only about  $\pm 75$  Hz and, because of the small stored energy of the device, a fast tuner similar to the one used on ATLAS should be able to control the phase with ease.

The excellent performance of the first of the interdigital accelerating structures is very encouraging for the future success of our whole positive-ion injector program. Also, this exceptional performance suggests that the technology being developed will have cost-effective applications that extend well beyond the one of immediate interest to us.





Figure IV-2. Ken Shepard with the first prototype of his superconducting interdigital accelerating structures. The split-ring resonators used in ATLAS are on the left.

### 3. Estimates of Performance

The performance of the injector linac depends sensitively, of course, on the performance of the ECR source. In order to estimate beam intensities and charge states for the many source materials that have not been studied yet, we make use of Fig. IV-3, which summarizes most of the data available in 1985. These data are consistent with the hypothesis that the behavior of all isotopes available in pure form fall on curves such as are drawn through the data. The few cases (such as gold) that fall well below the curve can be explained by the fact that the technique used to vaporize these substances was inadequate. This is thought to be a practical problem that can be solved, and the design of our source is proceeding with this in mind.

The calculated performances of ATLAS for three different sizes of injector linacs are plotted in Fig. IV-4 in comparison with the present performance. In these calculations, the accelerating fields of all of the present resonators in ATLAS are assumed to be 3.0 MV/m, a much smaller value than is routinely obtained in off-line tests and about equal to the average value achieved on line when well-understood problems are removed. For the injector, the accelerating field is also assumed to be 3.0 MV/m except for the first ( $\beta = 0.009$ ) resonator, for which we assume 4.5 MV/m. Foil stripping is assumed to be available and used, if desirable, at three locations along the ATLAS linac.

In Fig. IV-4, the maximum energy achievable for light ions is seen to be roughly the same for all of the injectors because the velocity of ions incident on ATLAS is high enough for its resonators to accelerate effectively. However, for the heavier ions there is a dramatic difference because the acceleration efficiency of the ATLAS linac depends sensitively on the incident velocity when the velocity is low.

In addition to the source and accelerator characteristics, for the tandem we take into account a requirement that the lifetime of the terminal stripping foil must be at least two hours. This condition is the main limitation on beam current, and hence on beam energy, for ions with mass greater than about 60.

In addition to beam energy and intensity, users of ATLAS are greatly concerned with beam quality and with energy variability. Since the energy of

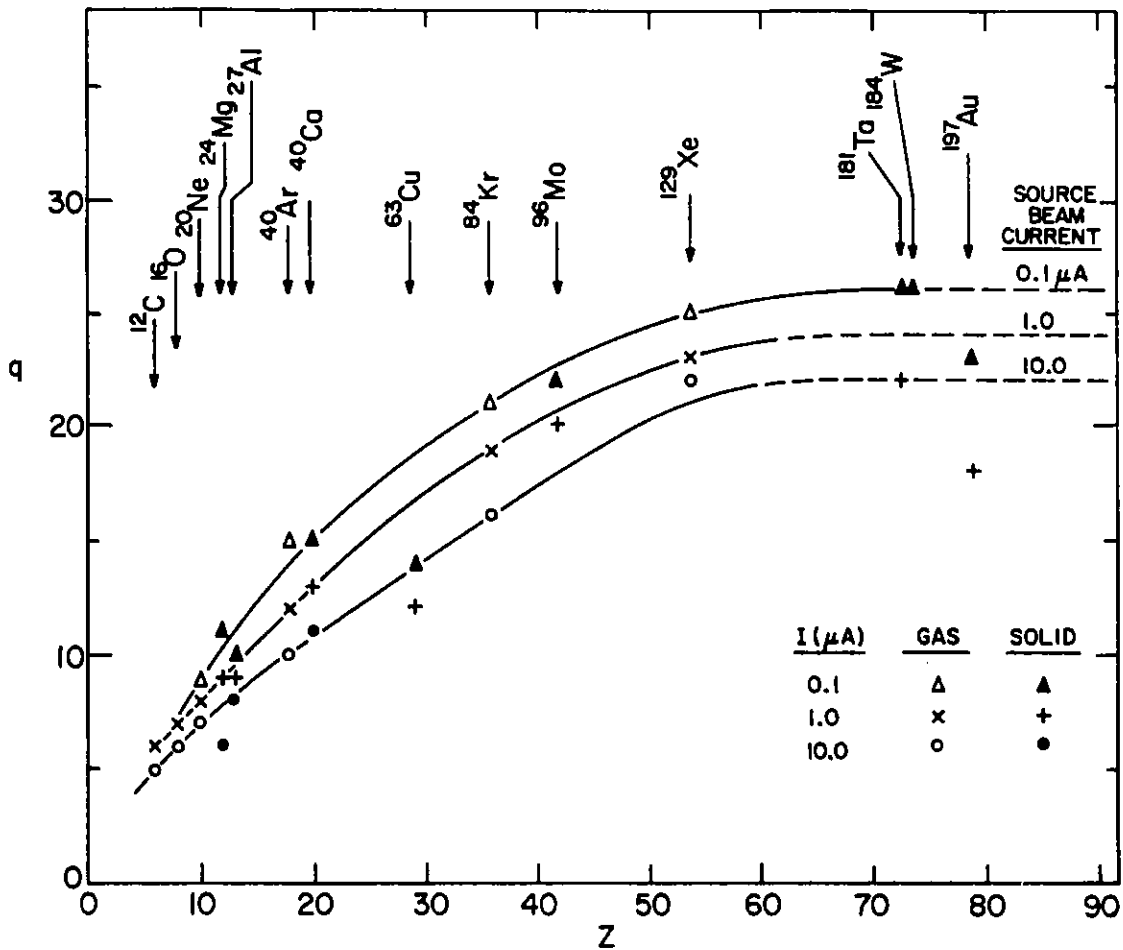


Figure IV-3. Performance of the ECR source. The plotted points were obtained by interpolation from the best results reported before October 1985.

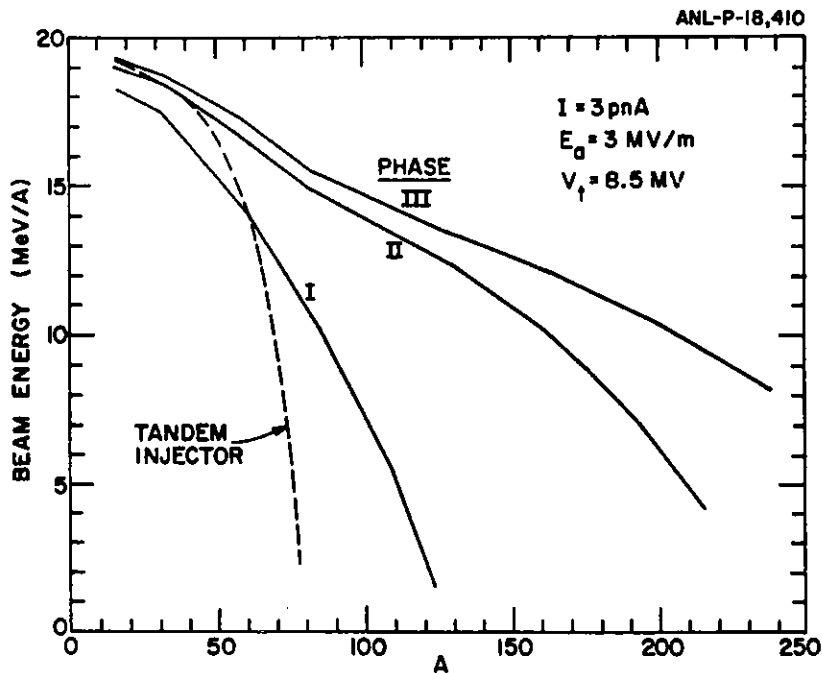


Figure IV-4. Comparison of the performance of ATLAS for different injectors: the present tandem with 8.5 MV on the terminal and the three phases of injector linac. The beam current is assumed to be 3 pA throughout.

the system is varied by changing the operating parameters of resonators at the end of the linac, the positive-ion injector will not change the easy energy variability of the present machine.

The beam quality of ATLAS now depends primarily on the bunching and stripping processes that take place before the beam enters the linac. The situation is expected to be similar for the positive-ion injector. For it, the transverse emittance is expected to be dominated by the ion source, for which the normalized emittance is thought to be less than  $20 \pi \text{ mm-mrad MeV}^{-1/2}$ . Note that this value is similar to that of the beam out of the tandem.

The longitudinal emittance ( $\Delta E \Delta t$ ) of the beam from the positive-ion injector is also expected to be as good or better than the tandem provides. This perhaps surprising result comes about mainly because the positive-ion injector does not require a stripping foil; that is, all strippers are further down stream, where the beam pulse is very narrow and the beam-energy spread is already large enough that energy straggling in the foil does not have much impact. Consequently, it is expected that  $\Delta E \Delta t$  will depend mainly on two factors: nonlinear effects in the acceleration process and voltage variations in power supplies. Calculations that take into account all effects except space charge show that the nonlinear effects can in principle be made very small if the bunching system is as good as we expect it to be. Also, the stability of the voltage platform and other elements can, with sufficient effort, be made very good indeed. Overall, then, there seems to be no reason in principle why the beam quality should not be better than that of the tandem.

Our design goals are  $\Delta E \Delta t < 40 \text{ keV-nsec}$  for the lighter ions and  $\Delta E \Delta t < 200 \text{ keV-nsec}$  for uranium beams out of ATLAS, where  $\Delta E$  and  $\Delta t$  are both FWHM. When debunching is used, these values of emittance imply energy spreads in the range 40 to 800 keV, depending on the beam energy and the ion species; the relative energy spread  $\Delta E/E$  is expected to be  $< 10^{-3}$  for all beams. When rebunching is used, we expect  $\Delta t < 100 \text{ ps}$  for ions such as oxygen and  $< 200 \text{ ps}$  for uranium.

Finally, and very important for most experiments, the beam out of ATLAS will have a 100% duty cycle -- i.e. no pulsed macrostructure.

## C. SUPERCONDUCTING MAGNETS

### 1. Dual-beam Capability

The plan to form two independent heavy-ion beams at the 40° bend of ATLAS was described in last year's report. During the past year, a detailed design has been developed for the magnetic system required to perform the beam splitting. The implementation of this design, which involves the use of a superconducting magnetic shield (a super tube), is expected to start during the coming year. One of the two beams will be accelerated further and the other will be used in the linac tunnel for detector development and other parasitic measurements.

### 2. Superconducting Switch Magnet

The superconducting beam-switching magnet described in last year's report has been used regularly since May 1985, and no difficulties have been encountered.

## V. ACCELERATOR OPERATIONS

### Introduction

This section is concerned with the operation of both ATLAS and the Dynamitron, two accelerators that are used for entirely different research. Developmental activities associated with the tandem injector of ATLAS and with the Dynamitron are also treated here, but developmental activities associated with the superconducting linac of the ATLAS system are covered separately in Sec. IV, because this work is a program of technology development in its own right.

## A. OPERATION OF ATLAS

The Argonne Tandem-Linac Accelerator System (ATLAS) is operated as a source of energetic heavy-ion projectiles for use in nuclear-physics research and occasionally in other areas of science. The accelerator now consists of a 9-MV tandem electrostatic accelerator followed by a 40-MV superconducting linac. As shown by Fig. V-1, the linac has two major parts, the original prototype "booster" that has been in operation since 1978 and the ATLAS addition completed in September 1985. Beams can be directed either to the experimental apparatus in Area II or, with greater energy, to the newly installed apparatus in Area III. This arrangement contributes considerably to operational flexibility and efficiency.

Some aspects of the technology of the ATLAS linac are discussed in Sec. IV.

### 1. Summary of Operations

(P. K. DenHartog, S. L. Craig, R. Harden, G. P. Zinkann)

Accelerator operating statistics are summarized in Table V-I. As may be seen from the Table, during fiscal year 1985 the operation of the accelerator was seriously impacted by activities required for the installation and commissioning of the full ATLAS system. These activities were successfully completed by the end of September 1985, and routine operation of the accelerator was started immediately.

Because of the fragmented operating schedule during 1985, the allocation of beam time was badly distorted in favor of in-house users, who had the principal responsibility for testing and debugging the experimental systems and who tended to be available on short notice. In 1986, beam-time allocation is expected to return to a more normal pattern in which running time is divided almost equally between in-house and outside users.

The present regular operating schedule of ATLAS is 5 1/2 days per week. In addition to this running time, the operation is extended through the weekend to the extent needed to make up for unscheduled down time during the week. This mode of operation has proved to be quite effective in allowing users to complete experiments without delaying the operating schedule as a whole. The regular operating schedule will be extended to a 6-day week later in 1986, after an additional operator has been hired and partially trained.

In addition to extending the operating schedule, every effort is being made to improve the quality of the operation. This involves three

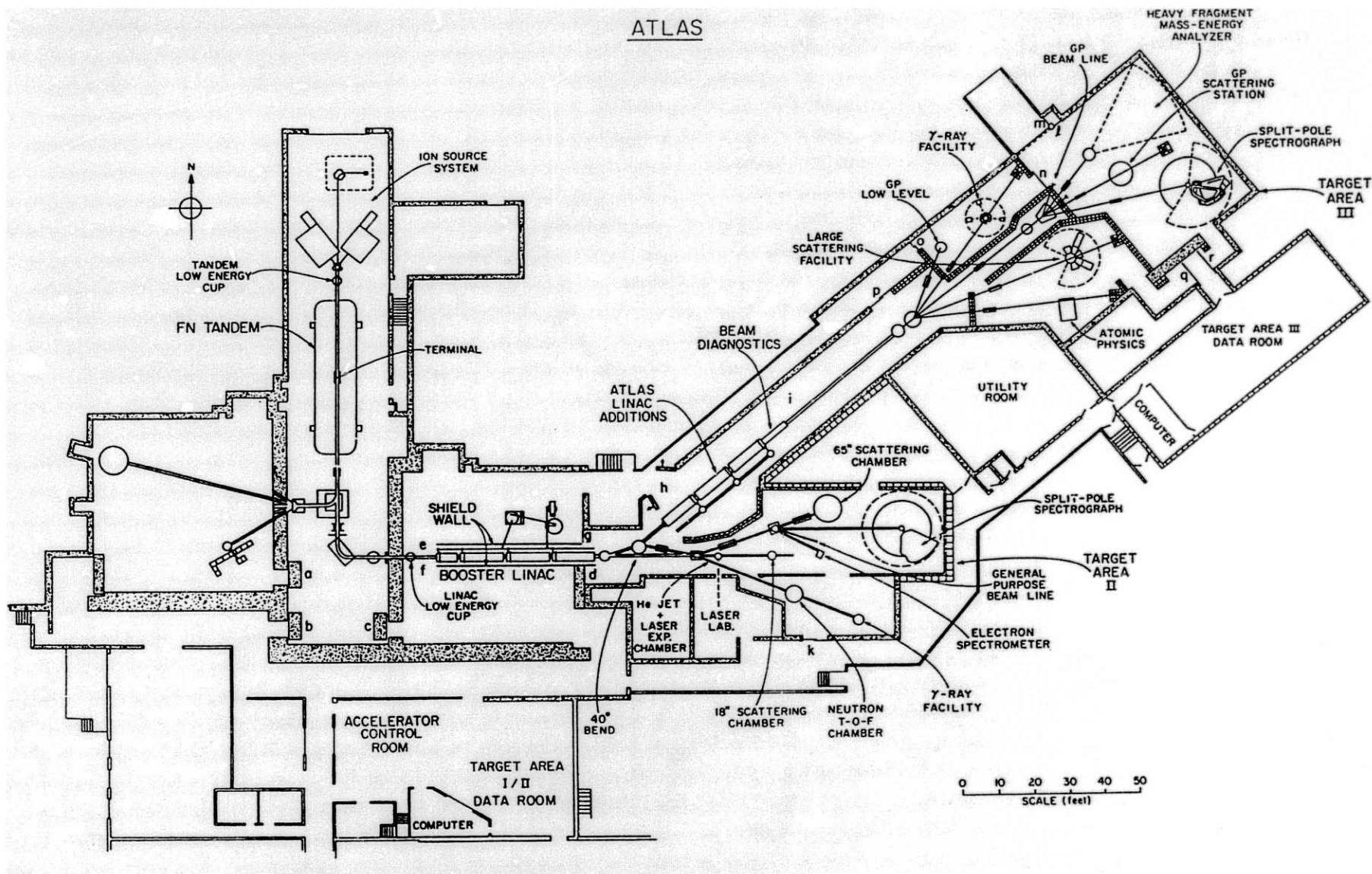


Figure V-1. The ATLAS heavy-ion accelerator facility.



Table V-I. Operating Statistics for ATLAS.

	Fiscal Year	
	<u>1985</u>	<u>1986*</u>
<u>Distribution of Machine Time (hr)</u>		
Research	1576	4000
Tuning	300	800
Machine studies	171	800
Unscheduled maintenance	222	600
Scheduled shutdown	<u>6491</u>	<u>2560</u>
Total (1 yr)	8760	8760
<u>Distribution of Research Time (%)</u>		
ANL Staff	55	45
Universities (U.S.A.)	36	45
DOE National Laboratories	5	3
Other Institutions	<u>4</u>	<u>7</u>
Total	100	100
<u>Outside Institutions Represented</u>		
Universities (U.S.A.)	8	18
DOE National Laboratories	1	2
Other	2	6

\*Projections based on experience through March 31, 1986.

factors: (a) modification in the priorities of the program in favor of operation for research rather than the development of the technology, (b) systematic training of both staff-level and technician operators, and (c) the systematic development of specialized technical skills. In connection with the realignment of priorities, the program of ion-source development has been reduced to the lowest level that is consistent with the beam-users' needs in order to free skilled manpower for the management and improvement of the on-line ion-source system.

## 2. Completion of the ATLAS Project

The ATLAS project was completed at the end of September 1985, on schedule and within budget. A large number of persons from several Argonne Divisions contributed to this success.

The final year of the project was one of intensive work in many areas. This work included completion of the following tasks.

- (a) The last of three beam-line cryostats was fabricated and assembled.
- (b) The 18 resonators required for the linac addition were fabricated, tested, and mounted in their cryostats.
- (c) The three loaded cryostats were then installed on line.
- (d) A new 200-W helium refrigerator and all the plumbing associated with it were installed and put into operation.
- (e) The helium-distribution system for the ATLAS linac addition was installed, tested, and put into service.
- (f) The liquid-nitrogen distribution system was extended to the new linac.
- (g) The RF system and the associated cabling system were installed and debugged.
- (h) The computer control system was expanded so as to control the new linac and also most of the beam lines.
- (i) A new high-resolution 300-kV injector for the tandem was installed and put into operation.
- (j) The high-energy beam line of the tandem was modified and improved.
- (k) The beam line (including two bending magnets) connecting the two parts of the linac was installed.

- (l) The beam line from the ATLAS linac into the target area was installed and tested.
- (m) Two new rebunchers were installed and tested.
- (n) A large superconducting beam-switch magnet was installed on the output beam line.
- (o) Each of these many sub-systems was tested, debugged, and then the whole system was put into service.

Most of the ATLAS system had been assembled by March 1985, and testing of the system began immediately. In the first such test, a beam from the prototype linac was transmitted through the new part of the accelerator without acceleration. This important test was carried out with surprising ease.

After several preliminary tests in which several of the new resonators were used to accelerate a beam, the key milestone of the project was passed on April 26, 1985 when 15 of the 18 new resonators were used to accelerate a beam of  $^{32}\text{S}$  to an energy of 325 MeV. Again, this test was carried out with relative ease, considering how much new equipment was being used as a system for the first time.

Following this and other successful tests of the accelerator itself, the beam from ATLAS was transmitted through the three new beam lines in the experimental area to the three new experimental systems. Having passed these final tests, ATLAS was ready for use.

The completed ATLAS system was formally dedicated as a national heavy-ion facility on June 3, 1985.

The final installation tasks required for the completion of the ATLAS project were carried out during the summer of 1985.

### 3. Status of ATLAS

ATLAS is a working accelerator that to date has operated with remarkable reliability for a new machine. All sub-systems operate as planned, and only a moderate level of equipment failure has been experienced.

All 42 accelerating structures of ATLAS are functional. The average accelerating field of this whole set of units is about 3.0 MV/m, which provides a total accelerating voltage of almost 40 MV (the sum of maximum

voltages for individual resonators). Examples of beam energies obtainable at this level of performance are 20 MeV/A for  $^{16}\text{O}$  and 13 MeV/A for  $^{58}\text{Ni}$ . This level of performance is approximately what was expected for the initial year of operation.

The primary weakness of the ATLAS system at this time is that the refrigeration capacity is about 30% less than is required to achieve the maximum accelerating voltages that the resonators could reliably support. If the needed capacity were available, it is probable that the beam energies could be increased by about 10% relative to values stated above.

The deficit in refrigeration capacity will be greatly relieved in 1987 when a third refrigerator is added to the system. It is not clear at this writing (April 1986) what refrigerator will be installed. We have on hand an old 100-W unit that was replaced by a 200-W unit as part of the ATLAS project. However, we are making an effort to acquire a 300-W unit as surplus from another ANL program. This larger refrigerator would provide the capacity needed both for ATLAS and the planned superconducting positive-ion injector.

The quality of operation of the accelerator system has been improved in numerous ways by the changes made during the past year. Starting at the front end, the high resolution of the new injector allows the tandem to be injected with a much cleaner beam, and its higher voltage has increased the tandem transmission somewhat.

A significant operational limitation in the past has resulted from the difficulty that the tandem-beam analyzer has in selecting a single ion species from the complex mass-energy spectrum of a heavy-ion beam subjected to two strippings. This problem has now been mitigated to a large extent by moving the beam chopper to a location where it can serve as a velocity selector for beams from the tandem; thus, in most cases only one ion species arrives at the second stripper and the resulting doubly-stripped spectrum is relatively simple.

Proceeding down the accelerator, the installation of the new linac and its cryogenic system is considerably improved, relative to the prototype linac, and this has already resulted in increased reliability. The cabling and cryogenics associated with the prototype linac will be gradually brought up to this new standard as time and funds permit.

Similarly, the software associated with the linac control system is being steadily expanded and refined. The new capability of controlling and monitoring beam-line components with the computer is proving to be quite valuable.

A unique characteristic of the tandem-linac system is its ability to produce exceptionally narrow beam pulses, a valuable tool for various fast-timing measurements. In the past, we have not been able to deliver to the experimenter the narrow pulses from the linac because of the cramped conditions in the original Target Area II, which required the beam rebuncher to be located too close to the linac. This geometrical problem has been largely removed in the new ATLAS area, and as a result it has been demonstrated that beam pulses that are only 150 psec wide can be delivered on target for ions as heavy as  $^{58}\text{Ni}$ .

The beam pulses from ATLAS are also being made more useful for some research needs by adding a fast-acting beam sweeper that can eliminate unwanted pulses with an exceptional degree of flexibility. Heretofore, the beam-bunching system has provided pulses with repetition rates of either 48.5 MHz or 12.125 MHz. The new beam sweeper, installed in March 1986, can eliminate any individual pulse from the 12.125 MHz sequence, thus forming a sequence that is any sub-harmonic of 12.125 MHz or any other pattern that might be needed.

Finally, the new experimental Area III is proving to be quite satisfactory. In particular, the radiation shielding is entirely adequate and yet the open geometry allows the crane to be used to good advantage.

#### 4. Plans for 1987

During 1987 the focus will continue to be on the effective operation of ATLAS for research. The only foreseen down period of any length is the three-week period required for the installation of the third refrigerator discussed in the preceding section.

If the level of funding in the President's budget is appropriated, it will be possible in 1987 to enlarge the operating staff by two persons, the number required to permit the operating schedule to be expanded to 7 days per week. Perhaps more important than the expanded schedule is that we expect the

quality of the operation to be improved by having qualified staff-level operators present on most shifts.

Until now, a primary limitation on the performance of our on-line resonators has been that it has not been feasible to maintain them in peak operating condition without causing an unacceptable interruption of the operating schedule. This problem will be largely eliminated in 1987 when the extra accelerating section now under construction is completed and put into service. The plan is to perfect the operation of this section while off line and then, when convenient, to interchange it with an on-line section that needs maintenance. This interchange can be done rapidly while both cryostats are cold. By repeating this interchange systematically, the performance of all units will gradually be maximized.

In addition to the increase in refrigeration capacity, several significant technical improvements are planned for 1987. One of these is the implementation of the plan to separate the beam into two independent beams by means of a magnetic separator at the 40° bend after the prototype linac. An investigation of the supertube technology to be used in this beam separator has been under way for several years, and an engineering design of the planned system has been largely completed. Fabrication of the system will be started in late 1986, and the system will be finished and installed in 1987. One of the two beams formed by this system will be accelerated further by the ATLAS linac whereas the other will be directed, by means of a minimal beam-transport system, to a test facility in the linac tunnel. This secondary beam is expected to be useful for detector development and possibly for a few specialized research measurements.

An effort to improve the fast tuners used for phase control of resonators has started. This will involve a modification of the present design and the use of a new and hopefully better type of PIN diode. The objective is to increase the RF power limit and the reliability of the fast-tune system. If this developmental effort is successful, the improved type of fast tuner will be installed on some of the ATLAS resonators during 1987.

The long-term effort to upgrade the beam-line performance of the ATLAS resonators will continue through 1987. One important task is to do a thorough off-line investigation of a good resonator that is loaded with all of its normal on-line auxiliary components - power input, field pick up, fast

tuner, and slow tuner. This has never been done because of the pressure of schedule and the lack of an extra resonator. However, the test should be done because it might reveal that the auxiliary components limit the accelerating field in some unexpected way.

#### 5. Plans for 1988

During most of 1988 ATLAS will continue to be operated continuously for research, with no significant interruptions now foreseen.

By 1988, we will begin to have operating experience in the use of the dual-beam capability that will be installed in 1987. This attempt to use two beams simultaneously will be a valuable learning experience that may have a significant impact on future developments. The future positive-ion injector will provide enough beam for several simultaneous users, but it is not yet clear to what extent this would be useful.

The first planned major interruption of the operating schedule will come in late 1988 or early 1989, when the planned 3-MV prototype positive-ion injector is ready to be linked to ATLAS and tested. If this new injector is successful, as expected, it will immediately be used as the injector for at least part of the research program. Regular operating experience of this kind is believed to be the best way to obtain realistic information about imperfections in the new injector technology.

## 6. Assistance to Outside Users of ATLAS

During the past year, substantial progress has been made in providing organized assistance to outside users of ATLAS. The continuing strong interest in ATLAS (outside users were involved in 2/3 of all experiments performed in 1985) makes it clear that the user-assistance program fills an essential function.

A user-liaison physicist continues to play a key role in channelling assistance to outside users. The major components of his responsibility are: (1) to provide the needed information and organizational assistance to committees, workshops, and other meetings involving outside users; (2) to provide instruction in the use of and technical information about ATLAS and its experimental systems to users; (3) to assist outside users in all aspects of initiating and planning an experiment; (4) to the extent appropriate and feasible, to assist users in the actual performance of experiments; (5) to provide instruction and help with the use of computer hardware and software; (6) to instruct the users in the safety procedures to be followed when using the ATLAS facility; (7) to assist in the operation of the technical support group; and (8) to provide an interface between the technical support group and the user.

The Program Advisory Committee (PAC) for ATLAS (having four members from other institutions and two from Argonne) continues to meet regularly about three times a year. In 1985 PAC meetings were held on 2 February and 30 August to recommend experiments for running time at ATLAS. In accordance with PAC policy, two members have been rotated off the committee. David Balamuth (Univ. Pa.) and Birger Back (ANL) have replaced Eric Cosman (MIT) and Russell Betts (ANL) on the PAC. The continuing members are: Walter Benenson (MSU), Richard Diamond (LBL), John Fox (FSU) and Walter Henning (ANL).

The Executive Committee of the Organization of ATLAS Users held a workshop as part of a two-day event celebrating the completion of ATLAS on June 4, 1985. The workshop was used to present the latest plans and to report progress on the construction of ATLAS and the associated experimental facilities. It was attended by approximately 90 scientists. The next major activity for the group will be a users' meeting to be held during the APS meeting in Washington, D.C., in late April 1986.



During the last year, one issue of the report entitled "ATLAS Report to Users" was distributed, providing up-to-date information about the operation of the accelerator and the experiments that have been performed.

In the last year the amount of time available for experiments was limited by the necessity of completing the construction of ATLAS. Though only about six months were available for experiments, the magnitude of the outside use of the accelerator during the past year has been substantial, as may be judged from the following two lists giving (1) the experiments performed by outside users and (2) the institutions represented. As may be seen from the names associated with each experiment, university groups are playing a major role in an important fraction of the experiments and a dominant role in some.

a. Experiments Involving Outside Users

All experiments in which outside users participated during calender year 1985 are listed below. The spokesperson for each experiment is given in square brackets after the title. The names in parentheses are Argonne collaborators.

- (1) Spectroscopy of Proton Rich  $N = 81, 82$  Nuclei [Daly]  
P. J. Daly, M. Quader, W. H. Trzaska, J. McNeill, Z. W. Grabowski, H. O. Helppi, Purdue University; (R. V. F. Janssens, T. -L. Khoo, R. Holzmann)
- (2) Radiation Chemistry Studies with Heavy Ions [LaVerne]  
J. A. LaVerne, R. H. Schuler, University of Notre Dame;  
(B. G. Glagola)
- (3) Test of New Method of Light Particle Identification in Fusion Reactions at 20 MeV/u [Maguire]  
C. F. Maguire, W. Ma, Vanderbilt University; F. W. Prosser, University of Kansas; (D. G. Kovar, C. N. Davids, M. F. Vineyard, B. Wilkins, D. Henderson)
- (4) Beam Line Test for Bragg Curve Spectrometer [Vineyard]  
C. F. Maguire, Vanderbilt University; F. W. Prosser, University of Kansas; (M. F. Vineyard, B. Wilkins, D. Henderson, D. Kovar, B. Back, S. Sanders, S. Kaufman, A. Worsham, B. G. Glagola)
- (5) Properties of gamma-ray spectra in  $^{153}\text{Ho}$  Measured with Compton-Suppressed Spectrometers [Holzmann]  
M. Driggert, U. Garg, Notre Dame University; P. J. Daly, Z. Grabowski, M. Quader, W. Trazaska, H. O. Helppi Purdue University; (R. Holzmann, T. -L. Khoo, R. V. F. Janssens)

- (6) Incomplete Fusion at 10 MeV/u in Heavy Asymmetric Systems:  
( $^{12}\text{C} + \text{A}=100-200$ ) [Tserruya]  
I. Tserruya, Weizmann Institute; (W. Henning, D. Kovar,  
M. Vineyard, B. Glagola)
- (7) Very-High-Energy Nucleon Production in H.I. Collisions [Becchetti]  
F. Becchetti, J. Janecke, P. Lister, R. Stern, P. Schulman,  
University of Michigan; C. Maguire, Vanderbilt University;  
F. Prosser, University of Kansas; (D. Kovar, M. Vineyard)
- (8) Calibration of NaI(Tl) Charged Particle Detector Performance and  
Investigation of Possible Super-Heavy Nucleus Production Mechanism  
[Maguire]  
C. F. Maguire, A. V. Ramayya, Vanderbilt University; F. W. Prosser,  
University of Kansas; (D. G. Kovar, C. N. Davids, M. F. Vineyard,  
C. Beck)
- (9) Very-High-Energy Light-Particle Production in H.I. Collisions Near  
Zero Degrees [Becchetti]  
F. Becchetti, R. Stern, J. Janecke, University of Michigan;  
J. Kolata, University of Notre Dame; C. F. Maguire, Vanderbilt  
University; (D. G. Kovar, C. N. Davids, M. F. Vineyard, C. Beck)
- (10) Masses and Levels of Very Neutron-Rich Nuclei [Stern]  
R. Stern, F. Becchetti, J. Janecke, University of Michigan;  
(W. Phillips, D. Kovar, M. Vineyard, C. Beck)
- (11) Test of the Gamma-Ray Beam Line at ATLAS [Janssens]  
U. Garg, M. Drigert, E. Funk, J. Kolata, J. Mihelich, University  
of Notre Dame; (R. V. F. Janssens, T. -L. Khoo, R. Holzmann)
- (12) High-Spin States in  $^{154}\text{Dy}$  With Compton-Suppressed Spectrometers [Emling]  
P. J. Daly, Z. Grabowski, M. Quader, M. Piiparinen, W. Trzaska, Purdue  
University; M. W. Driggert, U. Garg, University of Notre Dame;  
(H. Emling, I. Ahmad, R. Holzmann, R. V. F. Janssens, T. -L. Khoo)
- (13) Pre-Equilibrium Light Particle - Light Particle Coincidence  
Measurements at  $E > 10 \text{ MeV/A}$  [McGrath]  
R. McGrath, M. Gordon, J. Gilfoyle, J. Alexander, SUNY Stonybrook;  
P. DeYoung, K. Kossen, M. Hammond, Hope College; (D. Kovar,  
M. Vineyard, C. Beck)
- (14) Light Particle - Light Particle Coincidence Measurements at  $E > 10 \text{ MeV/A}$   
[DeYoung]  
P. DeYoung, K. Kossen, M. Hammond, Hope College; J. Alexander,  
R. McGrath, M. Gordon, J. Gilfoyle, SUNY Stonybrook; (D. Kovar,  
M. Vineyard, C. Beck)
- (15) Radiation Chemistry Studies with Heavy Ions, II [LaVerne]  
J. A. LaVerne, R. H. Schuler, R. T. Steinback, University of Notre  
Dame

- (16) Doppler-Free Auger Electron Spectroscopy from Ne-like High-Z Atoms [Schneider]  
D. Schneider, L. Curtis, R. Schectman, University of Toledo;  
(E. Kanter)
- (17) Resonant Transfer and Excitation for Highly Charged Nickel Ions [Tanis]  
J. A. Tanis, E. M. Bernstein, M. W. Clark, W. Graham, Western Michigan University; K. Berkner, Lawrence Berkeley Laboratory  
(E. Kanter)
- (18) Study of Quasielastic Processes for the System Ni + Sn Close to the Coulomb Barrier [Rehm]  
W. Freeman, Fermi National Laboratory; L. Lee, SUNY - Stony Brook;  
(E. Rehm, A. van den Berg, W. Henning, K. Lesko, J. Schiffer, and G. Stephens)

b. Outside Users of ATLAS and of ATLAS Technology During the Period January 1985 - January 1986

- (1) Hope College  
P. DeYoung  
M. Hammond  
K. Kossen
- (2) Purdue University  
P. J. Daly  
Z. W. Grabowski  
H. O. Helppi  
J. McNeill  
M. Piiparinen  
M. Quader  
W. H. Trzaska
- (3) SUNY-Stonybrook  
J. Alexander  
J. Gilfoyle  
M. Gordon  
L. Lee  
R. McGrath
- (4) University of Kansas  
F. W. Prosser
- (5) University of Michigan  
F. Becchetti  
J. Janecke  
P. Lister  
R. Stern  
P. Schulman

- (6) University of Notre Dame
  - U. Garg
  - M. Driggert
  - E. Funk
  - J. Kolata
  - J. A. LaVerne
  - R. H. Schuler
  - R. T. Steinback
  
- (7) University of Toledo
  - L. Curtis
  - R. Schectman
  - D. Schneider
  
- (8) Vanderbilt University
  - C. F. Maguire
  - W. Ma
  - A. V. Ramayya
  
- (9) Weizmann Institute
  - I. Tserruya
  
- (10) Western Michigan University
  - E. M. Bernstein
  - M. W. Clark
  - W. Graham
  - J. A. Tanis
  
- (11) Fermi National Accelerator Laboratory
  - W. Freeman
  
- (12) Florida State University
  - J. Fox
  - A. Frawley
  
- (13) Kansas State University
  - T. Gray
  - K. Karnes
  - V. Needham
  
- (14) Lawrence Berkeley Laboratory
  - K. Berkner

c. Summaries of the USER Programs, January 1985 to January 1986

c.i. The University of Notre Dame

1. Nuclear Physics (U. Garg, M. Drigert, E. Funk, J. Kolata, and J. Mihelich)

A group from the University of Notre Dame is playing an important role in developing the research program at ATLAS. One of their main interests is the study, in collaboration with ANL staff members, of the behavior of nuclei at high spin in the Pt-Os-Ir region, with emphasis on the origins of the backbending phenomenon in these nuclei, and measurements of the lifetimes of high-spin yrast states. Another project concerns the study of incomplete fusion, quasielastic reactions and the emission of light fast particles.

A major activity of this past year was the completion of the Phase I construction of a gamma-ray facility consisting of a BGO sum-multiplicity array of 14 elements combined with 7 Compton-suppressed germanium detectors. In this project, the Notre Dame group has been responsible for assembling and testing the BGO detectors and for developing the electronic read-out system. This detector system was used in several experiments late in the year.

2. Nuclear Chemistry (R. Schuler, J. LaVerne and R. Steinback)

In the last year, a Nuclear Chemistry group has undertaken studies of the process of track formation, local density of radicals and other reactive intermediates formed in a heavy-ion track in water. The understanding of these processes is important because of increased usage of heavy ions in radiation biology and medical therapy. This program is an extension to higher energies of work begun at Notre Dame. In the last year, experiments were performed using  $^{11}\text{B}$ ,  $^{12}\text{C}$  and  $^{16}\text{O}$  projectiles at booster linac energies. In the next year, these experiments will be extended to the full ATLAS energy and to higher Z-projectiles.

- c.(ii.) Purdue University (P. Daly, Z. Grabowski, J. McNeill,  
M. Piiparinen, M. Quader, and W. Trzaska)

The Purdue University group is working on high-spin nuclear states at ATLAS, with several thesis students. They use in-beam gamma-ray techniques directed at several aspects of nuclear structure at high spin, testing the validity of the  $Z=64$  sub-shell closure through spectroscopic studies of  $N=82$  nuclei close to the proton drip line. They have extended these studies in the last year by making use of the Compton-suppressed germanium detectors of the BGO facility.

The group is also building a superconducting solenoid lens to be used as a conversion-electron spectrometer. The solenoid is being constructed at Purdue and, after testing there, will be installed at Argonne on a beam line in Target Area II of ATLAS. Arrival at Argonne is expected after May 1986.

- c.(iii.) University of Kansas and Vanderbilt University Collaboration  
(C. F. Maguire, W. Ma, A. V. Ramayya, and F. W. Prosser)

A program was pursued at ATLAS to study the energy and projectile dependence of fusion and incomplete fusion processes for light- and medium-weight heavy-ion systems. Experiments at ATLAS are planned to perform a coincidence measurement of the evaporation residue (mass and velocity) in conjunction with emitted light (proton or alpha) particles. During the last year, tests of a prototype light-particle detector were performed. The detector consists of single-element NaI(Tl) scintillators whose light output is proportional to the energy deposition. The identification of the mass and charge is obtained using pulse shape discrimination and time-of-flight. The tests of this system were performed successfully in the new ATLAS 36" scattering chamber. Maguire and Prosser have also participated in tests of the Bragg Curve Spectrometer that was constructed at Argonne.

- c.(iv.) University of Michigan (F. Becchetti, J. Janecke, P. Lister,  
R. Stern, P. Schulman)

A program is being pursued on ATLAS for the development and use of a large-aperture superconducting-solenoid particle spectrometer. An experiment was run in the last year to detect and measure the mass and low-lying energy

levels of very neutron-rich nuclei using an  $^{18}\text{O}$  beam from ATLAS. The measurements resulted in the observation of well-focused reaction products ranging from alpha-particles to fusion products. Improvements in time resolution are planned for the future, but it was demonstrated that the superconducting solenoid can be used to study heavy-ion and other nuclear reactions near zero degrees. This was the first experiment to use DAPHNE for both data acquisition and analysis. This experiment is part of a thesis project at the University of Michigan (R. Stern).

The group is also testing a detector system consisting of a thin plastic scintillator and a BGO crystal. This detector has been used to measure and identify light particles at zero degrees in a search for particles emitted at energies approximately equal to the beam energy. This study will continue with the addition of several 5x5 inch NaI crystals.

c.(v.) SUNY, Stony Brook and Hope College Collaboration (R. McGrath, J. Alexander, J. Gilfoyle, M. Gordon, P. DeYoung, M. Hammond, and K. Kossen)

This collaboration has undertaken measurements to understand the mechanisms of light-particle production in heavy-ion collisions. Experiments to measure inclusive spectra and coincidences between light particles were carried out in the new ATLAS 36" scattering chamber in the last year. The particles were detected using a seven NaI(Tl) detector array (developed at Stony Brook) and two back angle dE-E Si telescopes. The system allows the measurement of energy, charge and mass of the detected particle. The inclusive measurements covered an angular range of  $\theta_{\text{LAB}}=6^{\circ}-170^{\circ}$ . The coincidence measurement was carried out to study the relative momentum of particles emitted at small relative angles. This series of measurements is to be continued at ATLAS to study the role of the entrance channel, and the dependence on the bombarding energy.

c.(vi.) University of Toledo (D. Schneider, L. Curtis, and R. Schectman)

This group, in collaboration with scientists at ANL, has performed an experiment to study the level structures of highly-stripped high-Z ions. In particular, a beam of Ne-like  $\text{Ni}^{18+}$  ions was used to study LMM Auger emission. In the experiment, the Auger electrons ejected from the excited

projectile ions were analyzed by an electron spectrometer at zero degrees with sufficient resolution to resolve individual Auger lines. The experiment is a test of fundamental atomic structure theory and of models regarding the dynamic excitation processes in highly-ionized multi-electron systems.

c.(vii.) Western Michigan University and Lawrence Berkeley Laboratory Collaboration (J. Tanis, M. Clark, W. Graham, E. Bernstein, and K. Berkner)

This group has begun a series of atomic-physics studies at ATLAS to measure coincidences between x-rays and the outgoing projectile charge states in ion-atom collisions. The goal of this work is to probe fundamental atomic interactions in ion-atom collisions by correlating projectile charge-state changing events with x-ray emission. In the experiment, a range of energies was used to span the region of resonant transfer and excitation for high-energy Li-like nickel ions. This process is a close analog of dielectronic recombination which is of fundamental interest in plasma physics. The experiments carried out at ATLAS with fast Ni beams represent the heaviest system studied to date. This work is planned to be continued in the future.

c.(viii.) Weizmann Institute of Science, Rehovot (I. Tserruya)

This collaboration carried out an experiment to measure the cross sections for complete fusion and incomplete fusion for the reactions  $^{12}\text{C} + ^{90}\text{Zr}$ ,  $^{120}\text{Sn}$ ,  $^{160}\text{Gd}$ , and  $^{197}\text{Au}$ . The main purpose was to determine the onset of the incomplete fusion process and to study its target-mass dependence. The experiment was carried out by measuring the velocity spectrum of the reaction products with a single large-area Breskin counter at zero degrees. This detector measures in a single run 80% of the total yield of evaporation residues and uses time of flight to discriminate between complete and incomplete fusion. It is planned to continue this work in the next year.

d. ATLAS - Technology Transfer

In addition to providing assistance to outside users of the ATLAS beam, we are also providing assistance in the use of the ATLAS technology.



d.(i.) Florida State University (J. Fox and A. Frawley)

Argonne is fabricating the niobium resonators and some auxiliary devices required for the superconducting-linac energy booster being built at Florida State University. Under this arrangement, personnel from FSU come to ANL to assemble and test the resonators. The resonator-fabrication work for FSU will be completed during 1986.

d.(ii.) Kansas State University (T. Gray, K. Karnes, and V. Needham)

Argonne is fabricating the niobium resonators and other linac components required for the superconducting decelerating linac being built at Kansas State University. Several staff members from KSU spent a substantial period of time at ANL during 1985 in order to learn the technology, and they will return to assemble and test the resonators now being built. This relationship will continue during 1986 and 1987.

## B. OPERATION OF THE DYNAMITRON FACILITY

The Physics Division operates a high-current 4.5-MV Dynamitron accelerator which has unique capability as a source of ionized beams of most atoms and many molecules. A layout of the facility is shown in Fig. V-2. Among the unusual facilities associated with the Dynamitron are (1) a beam line capable of providing "supercollimated" ion beams permitting angular measurements to accuracies of 0.005 degree, (2) a beam-foil measurement system capable of measuring lifetimes down to a few tenths of a nanosecond, (3) a set-up for testing a polarized deuterium target for use in high-energy storage rings, (4) a variety of experimental apparatuses for weak-interaction studies, (5) a laser/ion-beam interaction beam line where laser beams from an argon pump and a dye laser are available coaxially and simultaneously with the Dynamitron ion beam, (6) a post-acceleration chopper system giving beam pulses of variable width from about one nanosecond to the millisecond range at repetition rates variable up to 8 MHz, (7) a scattering chamber for electron spectroscopy with electrostatic parallel-plate electron spectrometers with variable energy resolution (0.1% to 5%) and the capability to measure electron energies up to a few keV as a function of observation angle, and (8) two general-purpose beam lines used for a variety of short-term experiments. PDP-11/45 and VAX-11/750 computer systems are available for on-line data analysis and for the control of experiments.

Among the experimental developments during 1985 was the development of a highly-polarized deuterium gas target for use as an internal target in the PEP storage ring at SLAC. In preliminary tests at the Dynamitron, 80 mW of laser power was absorbed by flowing potassium vapor and contributed to the spin-exchange process with deuterium. This corresponds to a flux of  $2 \times 10^{16}$ /sec of polarized deuterium nuclei, the approximate yield available from the most intense conventional atomic beam sources.

Another major breakthrough was the successful use of the MUPPATS detector system to study the structures of the  $\text{OH}_2^+$  and, for the first time, the  $\text{CH}_2^+$  molecular ions. These experiments have demonstrated that because of the high efficiency of this system, it is possible to carry out such experiments with very weak sources of selectively-excited molecules, as are being currently developed for that program.

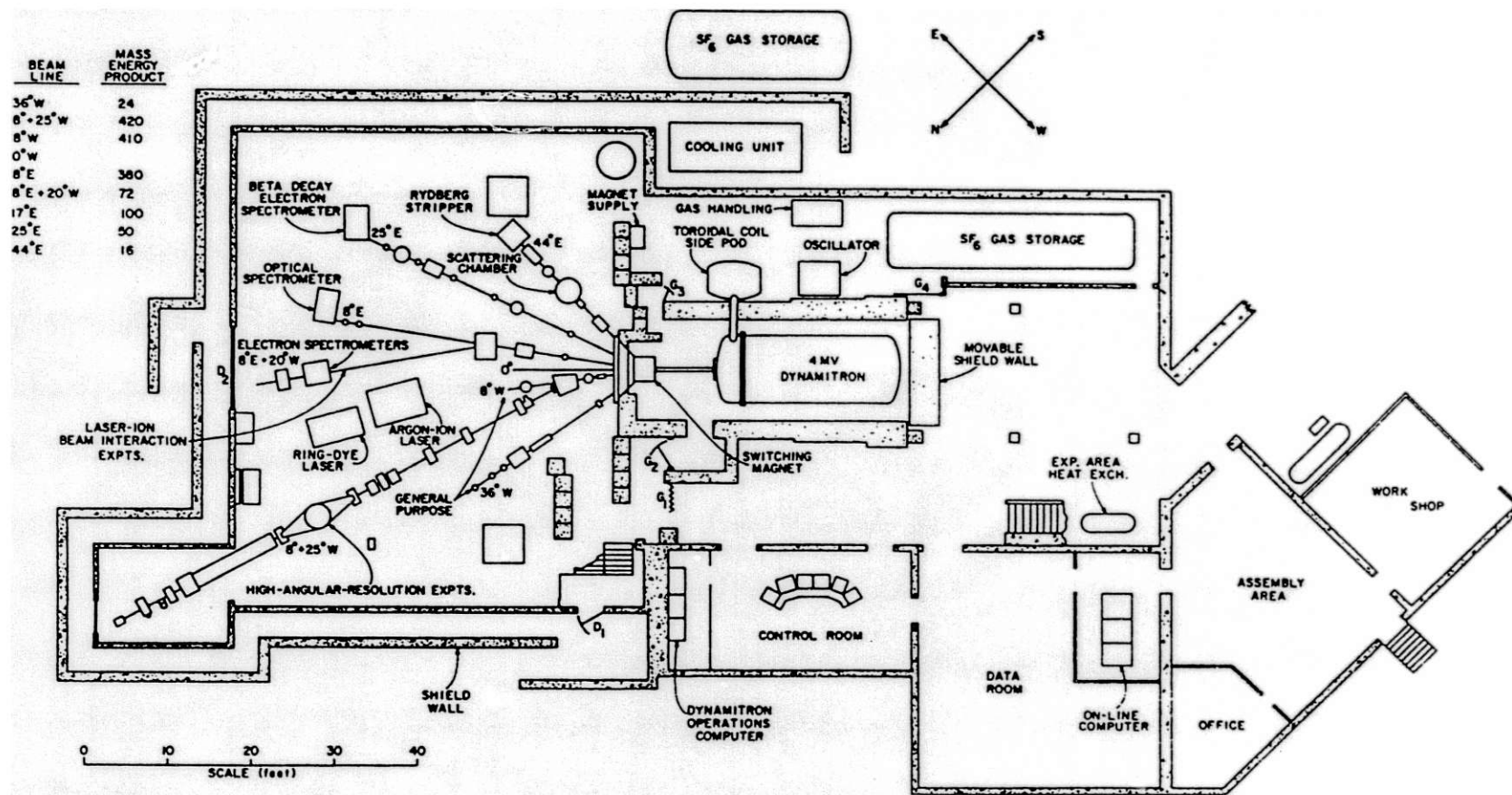


Figure V-2. Layout of the Dynamitron Accelerator Facility.

## 1. Future Developments at the Dynamitron

(H. G. Berry)

The Dynamitron will be used primarily by two of the atomic physics programs of the Physics Division. These include the work on molecular-ion dissociation and structure measurements, and the atomic structure laser/beam-foil program. Hence, most developments are aimed to benefit these two programs.

As the final part of the accelerator upgrade program, we have ordered a Physicon universal ion source. This source is expected to be able to provide some multicharged ion beams and possibly beams with high metastable-state populations. The coupling of this source and others to the accelerator tube will be investigated to optimize beam currents and beam-velocity profiles.

Other ion-source development projects include new sources of molecular ions with low internal energy. These would be appropriate for higher precision Coulomb-explosion studies of molecular-ion structures. These sources may necessitate new control coupling systems within the Dynamitron high pressure tank, plus source pumping to reduce the gas load on the accelerator tube.

The program of stabilization of the terminal voltage is continuing. The principal source of instability is mechanical and of low frequencies (less than 1 kHz). Most of these sources have now been reduced to the  $\pm 50$ -volt level (at 1-MV terminal voltage). High-frequency ripple has been measured to be less than these values. Further work is continuing on both measuring reliability and in reducing the remaining sources of voltage ripple. This work should make feasible several collinear laser/fast-beam experiments.

A longer-range goal is to study the feasibility of installing a low-power ECR source in the Dynamitron terminal. The objective will be to allow production of ion charge states in the range of  $\alpha = +3$  to  $+10$ , and consequent beam energies of up to 50 MeV for heavy atomic ions.

## 2. Operational Experience of the Dynamitron

(B. J. Zabransky, R. L. Amrein, and A. E. Ruthenberg)

Overall, the Dynamitron continued to perform well during the past year. The number of technical staff has been reduced by 50% during the last year (from 4 to 2 full time staff). Also the Dynamitron was shut down for a three-month period while the technical staff assisted in the construction of the ATLAS accelerator. The Dynamitron is now usually staffed 8 hours a day, but can also be operated by experienced scientific personnel. This system has proved to be effective. If the experiment requires it, the Dynamitron can continue to run through the night, manned only by the experimenters, or upon request, the Dynamitron can be staffed for two shifts a day. This is normally done with outside users or others not familiar with the operation of the accelerator.

During the year the accelerator was operated a total of 2414 hours. Of this time 1898 hours (79%) were scheduled for experimental research during which a beam was provided to the experimenters 85% of the time. Machine preparation time used up 13% of the scheduled research time and machine malfunctions 2%. Scheduled accelerator improvements (including the upgrading program) and modifications used a total of 516 hours or 21% of the total available time.

The great versatility of the Dynamitron continued to be exploited by the research staff. Ion currents on target varied from less than a nanoampere to 210 microamperes with ion energies ranging from 0.6 to 4.7 MeV. A wide range of both atomic and molecular ions was delivered on target. They include:  $^1\text{H}^+$ ,  $^1\text{H}_2^+$ ,  $^2\text{H}^+$ ,  $^1\text{H}_3^+$ ,  $^3\text{He}^+$ ,  $^4\text{He}^+$ ,  $^4\text{He}^{++}$ ,  $^7\text{Li}^+$ ,  $^7\text{Li}^{++}$ ,  $^7\text{Li}^{+++}$ ,  $^{12}\text{C}^+$ ,  $^{12}\text{CH}^+$ ,  $^{12}\text{CH}_2^+$ ,  $^{12}\text{CH}_3^+$ ,  $^{16}\text{OH}_2^+$ ,  $^{20}\text{Ne}^+$ ,  $^{24}\text{Mg}^+$ ,  $^{24}\text{Mg}^{++}$ ,  $^{12}\text{C}_2^+$ ,  $^{14}\text{N}_2^+$ ,  $^{12}\text{C}^{16}\text{O}^+$ ,  $^{40}\text{Ar}^+$ ,  $^{40}\text{Ar}^{++}$ ,  $^{84}\text{Kr}^+$ , and  $^{132}\text{Xe}^+$ .

A total of 32 investigators used the Dynamitron during 1985 in some phase of their experimental research. Of these, 16 were from the Physics Division, 8 were outside users from other research facilities, 2 were members of the Resident Graduate Student Program. In addition, 5 graduate students and one undergraduate student participated in research at the Dynamitron. Of the scheduled time, 92% went to experiments involving members of the Physics Division and 8% was exclusively assigned to outside users. However, outside

users collaborated in experiments that used 19% of the total available time. Graduate students, undergraduate students, and participants in the Resident Graduate Student Program worked on experiments that used 63% of the time.

During the year there were a few relatively minor accelerator problems. In one case a surge protection resistor broke (probably due to a spark) and caused arcing on the surface of the Lucite column structure. The sparking created carbon tracks in the Lucite which were removed with a hand grinder. All of the surge protection resistors were later removed and replaced with a simple copper bar. These resistors are not needed when using the new rectifiers. The Accelerator Improvement Project allowed us to purchase the remaining new rectifiers needed to complete the replacement of the old rectifiers. The surge protection resistors were removed when the new rectifiers were installed. We have not had any failures of the rectifiers or further damage to the column since that time.

On one occasion the Dynamitron could not exceed 0.9 MV without sparking. This was caused by a broken divider resistor string on the accelerating tube. The failure was caused by a bad solder joint when the resistor string was constructed. There have been no further problems after the string was replaced.

On a routine tank opening one of the two Delrin tension rods was found to be broken. The rods are used to keep the accelerating tube under compressive forces. The failure was probably due to a defect in the Delrin rod. Both tension rods were replaced and have not failed again.

The new accelerating tube installed last year has been performing flawlessly. We were concerned when we found a white coating on the titanium aperture and first dynode at the entrance to the accelerating tube. This was found after a week-long run of  $Mg^{++}$ . The white coating was probably  $MgO$ . The  $Mg$  metal from the source oxidized when exposed to air. Not much seemed to have been deposited further down the accelerating tube. We have not yet observed any detrimental effects of this coating.

The largest project this year was the installation of a new sulfur hexafluoride ( $SF_6$ ) gas-handling system. The old system had been purchased with the Dynamitron in the late 1960's and was inadequate for the higher pressures needed for operation above 4.0 MV. It used a 150 cfm vacuum pump

and two compressors with a total capacity of 70 cfm. Its maximum operating pressure was 90 psi. Pumping times lengthened significantly near 90 psi. The heat generated by the compressors at these pressures was enough to cause some of the solder joints to fail.

The new system uses a 300-cfm vacuum pump and three compressors with a total capacity of 180 cfm. This new system was installed in the same limited space as the old one. Aftercoolers and high-temperature solder prevent the joints from failing at high pressures. The new system is capable of pumping to 150 psi although in practice we will probably not exceed 120 psi. This is more than adequate for operation at 5 MV.

The new piping was arranged so that the compressors can be run in series, parallel, or a combination of both. The placement of the valves required by the limited space resulted in some of them being almost inaccessible. Automatic valve actuators were added to the new pumping system. They are controlled from a valve control panel. All the valves, including old existing hand valves, now have position sensors installed on them with readouts on the SF<sub>6</sub> valve control panel.

The performance of the new SF<sub>6</sub> gas-handling system is outstanding. When pumping to pressures normally used with the old system, gas transfer times are cut in half. We can now pressurize to 120 psi with no increase in pumping time. This enhanced speed has been crucial to our ability to operate with limited technical support.

The accelerator improvements made during the past two years have measurably increased the Dynamitron performance. We can now quickly go to 4.0 MV and we routinely run for long periods of time at 4.5 MV. Before these improvements, we were not able to operate above 4.0 MV. Although we have accelerated beam at 4.7 MV, the capabilities of the Dynamitron at voltages above 4.5 MV has not yet been fully explored.

The Dynamitron console computer has been running very reliably for the past year. It monitors the control console and takes logs of various parameters. This is especially needed now since the machine is not always operated by Dynamitron personnel. It is also used to calculate magnet settings for the various beams of ions accelerated by the Dynamitron.

A VAX-11/750 computer system has been purchased and installed for data acquisition and analysis. Although the intelligent front end of the new DAPHNE software system is just nearing completion, the computer has already been used extensively in experiments with the MUPPATS detector. An interim data-acquisition system of software (MUPDAS) has been developed for this purpose. MUPDAS is an extremely flexible system capable of accepting data from a variety of hardware sources including CAMAC (parallel and serial), FASTBUS, and tape replay. The software has been exported to SLAC by the Division's medium-energy physics program. It is anticipated that when the DAPHNE system is completed during 1986, the older PDP-11/45 system will be removed.

### 3. University Use of the Dynamitron

(B. J. Zabransky)

The Argonne Dynamitron continues to be a valuable research facility for scientists from outside institutions. It is not only the accelerator itself that attracts outside investigators but also the unique associated experimental equipment as well as the on-going research programs being conducted at the Dynamitron.

Most visiting scientists chose to collaborate with local investigators on problems of common interest. A few, however, worked as independent groups. Some came for a one-time-only experiment, but most are participants in research programs that have spanned a period of several years.

During the year eight scientists came from seven outside institutions to use the Dynamitron. They came from five states and one foreign country. They participated in experiments that used 19% of the time scheduled for research. A list of those institutions from which users of the Dynamitron came during FY 1985 is given below. The list includes the name of the institution, the title of the research project, and the name of the principal investigators at each institution. The names of their Argonne collaborators (if any) are enclosed in parentheses.

- (1) Fermi National Accelerator Laboratory, Batavia, Illinois  
Nonresonant Capture of Protons by  $^{27}\text{Al}$   
A. Elwyn, G. Hardie,\* R. E. Segel†
- (2) Marquette University, Milwaukee, Wisconsin  
Radiation Damage of Covalent Crystal Structures  
L. Cartz, F. G. Karioris, A. R. Reheem, M. Wong

---

\*Western Michigan University, Kalamazoo, Michigan.

†Northwestern University, Evanston, Illinois.



- (3) Millersville University, Millersville, Pennsylvania  
 Charge-State Distributions of Coulomb Explosion Fragments  
 P. J. Cooney, (A. Faibis, E. P. Kanter, W. Koenig, D. Maor,\*  
 Y. Yamazaki,† and B. J. Zabransky)
- (4) Northwestern University, Evanston, Illinois  
 Nonresonant Capture of Protons by  $^{27}\text{Al}$   
 R. E. Segel, G. Hardie,\* A. J. Elwyn‡
- (5) Tokyo Institute of Technology, Tokyo, Japan  
 Electron Emission from Foil Excited Molecular Ions  
 Y. Yamazaki, (P. J. Cooney,§ A. Faibis, E. P. Kanter, W. Koenig,  
 and B. J. Zabransky)
- (6) University of Toledo, Toledo, Ohio  
 Lifetime Measurements in Be-like Mg  
 L. Curtis, (H. G. Berry and L. Engstrom)
- (7) Western Michigan University, Kalamazoo, Michigan  
 Nonresonant Capture of Protons by  $^{27}\text{Al}$   
 G. Hardie, R. E. Segel,¶ A. J. Elwyn‡

---

\*The Technion, Haifa, Israel.

†University of Tsukuba, Ibaraki, Japan.

‡Fermi National Accelerator Laboratory, Batavia, Illinois.

§Millersville University, Millersville, Pennsylvania.

¶Northwestern University, Evanston, Illinois

The Resident Graduate Student Program is open to students who have finished their course work and passed their prelims. They come to Argonne and perform their Ph.D. thesis research here. Two members of this program worked at the Dynamitron during 1985. Altogether they participated in experiments that used 41% of the time allotted to research. Those who used the accelerator are listed below, together with their home university and their local thesis advisor.

- (1) P. W. Arcuni, University of Chicago  
 H. G. Berry, advisor
- (2) J. Camp, University of Chicago  
 G. T. Garvey, advisor

In addition, the following graduate students and undergraduate students have participated in research based at the Dynamitron.

Graduate Students

- (1) M. Kroupa, University of Chicago  
G. T. Garvey, advisor
- (2) A. R. Raheem, Marquette University  
L. Cartz, advisor
- (3) N. Reistad, University of Lund  
H. G. Berry, advisor
- (4) D. Wark, California Institute of Technology  
G. T. Garvey, advisor
- (5) M. Wong, Marquette University  
L. Cartz, advisor

Undergraduate Students

- (1) M. O'Keefe, Lewis University  
B. J. Zabransky, advisor

## ATOMIC AND MOLECULAR PHYSICS RESEARCH

## Introduction

The Atomic Physics research in the Physics Division currently consists of the following programs:

- (1) Photoionization-photoelectron research (J. Berkowitz et al.)
- (2) High-resolution laser-rf spectroscopy with atomic and molecular beams (W. J. Childs, et al.)
- (3) Photon interactions with fast ions and beam-foil spectroscopy (H. G. Berry, L. Young et al.)
- (4) Interactions of fast atomic and molecular ions with solid and gaseous targets (E. P. Kanter, Z. Vager et al.)
- (5) Theoretical atomic physics (currently staffed by Visiting Scientists)
- (6) Atomic physics at ATLAS (to be headed by R. W. Dunford who will join the Staff in September 1986)

Following the commissioning of ATLAS in the first part of 1985 and the completion of an atomic physics beam line, the potential of this facility for atomic physics research is now beginning to be realized through the implementation of experimental programs, both from Argonne scientists and from the outside user community. Argonne's in-house program of accelerator-based atomic physics research will be significantly strengthened in the Fall of 1986 with the addition to the staff of Dr. Robert W. Dunford (Princeton University). He will head up a program of atomic physics research at ATLAS.

Reestablishment of a resident atomic theory program has a high priority and we are actively seeking a suitable candidate. In the meantime we have been fortunate in being able to have a series of distinguished visiting scientists join our program. Dr. Charlotte Froese-Fischer of Vanderbilt University visited the Physics Division for six months beginning in January 1986. In September 1986 Dr. Chris Bottcher (ORNL) will begin a one-year stay and Dr. Chii-Dong Lin (Kansas State University) will commence a 4-month visit.

Early in 1986 the multiparticle position-and-time-sensitive detector (MUPPATS) was brought into operation and was already showing its powerful capabilities in conjunction with our program on molecular-ion stereochemical structure measurements.

During the past year we have also brought into operation the "BLASE" accelerator. This is a low-energy (150-kV) facility that will provide very high-quality beams of a variety of atomic and molecular ions. This will now enable us to embark on a wide range of studies involving colinear laser-ion spectroscopy.

## VI. PHOTOIONIZATION-PHOTOELECTRON RESEARCH

### Introduction

Our photoionization research program is aimed at understanding the basic processes of interaction of light with molecules, the electronic structures of molecules and molecular ions, and the reactions of molecular ions, both unimolecular and bimolecular. The processes and species we study are implicated in a wide range of chemical reactions, and are of special importance in outer planetary atmospheres and in interstellar clouds. Our work also provides fruitful tests for theories of electronic structure, which help in the evaluation of widely applicable models for multi-electron systems. Most of this work is of a fundamental nature, but we also use the precise methods developed here to determine thermochemical quantities (heats of formation and ionization potentials) directly relevant in, e.g., reactions with ozone in the stratosphere, possible side reactions in a magnetohydrodynamic generator and reactions in interstellar clouds. Our experimental studies utilize five pieces of apparatus - two photoionization mass spectrometers and three photoelectron energy analyzers - each with special features.

(1) A three-meter normal-incidence vacuum-ultraviolet monochromator combined with a quadrupole mass spectrometer. This apparatus is capable of the highest resolution currently achieved in photoionization studies. It is also convenient for investigations of wavelength-dependent photoelectron spectra.

(2) A one-meter normal-incidence VUV monochromator mated with a magnetic-sector mass spectrometer. This apparatus has higher mass resolution, is less discriminatory in relative ion-yield measurements, and can be used to study metastable ions. Higher intensity for weak signals can also be achieved.

(3) Two cylindrical-mirror photoelectron-energy analyzers, which accept a large solid angle of photoelectrons, close to the "magic angle" of  $54^{\circ}44'$ . One has been extensively used for the determination of the photoelectron spectra of high-temperature species in molecular beams, and the other has on occasion been mated with the three-meter monochromator for studies of photoelectron spectra as a function of wavelength.

(4) A hemispherical electron-energy analyzer incorporated in a chamber which permits one to rotate the analyzer over a substantial fraction of  $4\pi$ . This device is intended for angular-distribution measurements, and also enables us to study very-high-temperature species.

The experiment involving UV laser photodissociation of molecular ions has progressed to the point where photofragment signals can be readily detected, without long searches. The magnetic mass spectrometer is now being dedicated to this work.

A modified mixing chamber was constructed, for generating transient species by reacting atoms with selected molecules. By use of selected wall coatings, and defining potentials, it was possible to measure the products of consecutive chemical reactions.

Progress on individual experiments is detailed as follows.

a. Photoionization of the  $\text{NH}_2$  Radical (S. T. Gibson, J. P. Greene and J. Berkowitz)

After trying a variety of microwave discharge sources for generating  $\text{NH}_2$  (and also the reaction of F atoms with  $\text{NH}_3$ ), all unsuccessful, we found that the reaction of H atoms with  $\text{N}_2\text{H}_4$  under controlled flow conditions produced a sufficient concentration of  $\text{NH}_2$  for detailed photoionization studies. The cross section for forming  $\text{NH}_2^+$  at threshold ( $v' = 0$ ) is weak but measureable by our method (see Fig. VI-1), whereas it was hidden in a recent photoelectron spectroscopic study. Our adiabatic I.P. ( $\text{NH}_2$ ) is  $11.14 \pm 0.01$  eV, 0.32 eV lower than that reported by PES. A prominent autoionizing Rydberg series is observed, converging to the excited  $\tilde{\text{A}}^1\text{A}_1$  state at  $12.445 \pm 0.002$  eV. By extrapolation,  $\text{NH}_2$  should absorb strongly at  $\sim 1150$  Å. From the threshold for formation of  $\text{NH}^+$  ( $\text{NH}_2$ ), we obtain  $\Delta H_{\text{fo}}^{\circ}(\text{NH}^+) = 396.3 \pm 0.3$  kcal/mol. With auxiliary data, we compute  $\Delta H_{\text{fo}}^{\circ}(\text{NH}) = \pm 0.4$  kcal/mol,  $\Delta H_{\text{fo}}^{\circ}(\text{NH}_2) = 45.8 \pm 0.3$  kcal/mol,  $D_0(\text{H}_2\text{N-H}) = 106.7 \pm 0.3$ ,  $D_0(\text{HN-H}) = 91. \pm 0.5$ , and  $D_0(\text{N-H}) = 79.0 \pm 0.4$  kcal/mol. Additional photoionization measurements on  $\text{N}_2\text{H}_4$  and  $\text{N}_2\text{H}_3$  were also performed. This work has been published in J. Chem. Phys. 83, 4319 (1985).

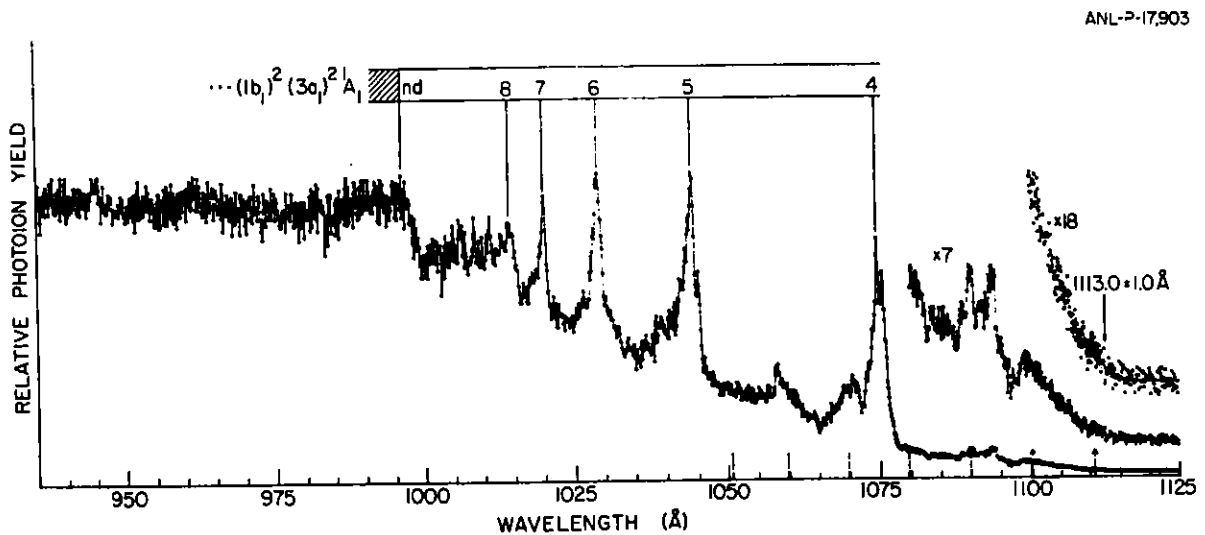


Figure VI-1. Photoion yield curve of  $\text{NH}_2^+(\text{NH}_2)$  from threshold to 935 Å. Wavelength resolution = 0.83 Å (FWHM), threshold to 1080 Å; 0.28 Å for  $\lambda < 1080$  Å. Contributions from  $\text{NH}_2^+(\text{N}_2\text{H}_4)$  and  $\text{NH}_2^+(\text{NH}_3)$  are also noted. The threshold region is shown in expanded form and fitted to a model function. Dashed vertical lines between ~1050–1080 Å denote the energies of the lowest four vibrational peaks from PES. Dashed vertical lines with arrows denote the approximate energies of the next three lower levels, inferred from the present experiment.

- b. Photoionization Mass Spectrometric Study and ab initio Calculations of Ionization and Bonding in P-H Compounds; Heats of Formation, Bond Energies, and the  $^3B_1$ - $^1A_1$  Separation in  $PH_2^+$  (J. Berkowitz, L. A. Curtiss,\* S. T. Gibson, J. P. Greene, G. L. Hillhouse† and J. A. Pople‡)

The ion yield curves of  $PH_3^+$ ,  $PH_2^+$ , and  $PH^+$  from photoionization of  $PH_3$  have been measured. The free radical  $PH_2$  has been generated by pyrolysis, and the ion yield curve of  $PH_2^+$  ( $PH_2$ ) determined. These measurements yield directly I.P. ( $PH_3$ ) =  $9.870 \pm 0.002$  eV, and I.P. ( $PH_2$ ) =  $9.824 \pm 0.002$  eV. In addition, we deduce  $D_0$  ( $H_2P-H$ ) =  $82.46 \pm 0.46$  kcal/mol,  $D_0$  ( $HP-H$ ) =  $74.2 \pm$  kcal/mol,  $D_0$  ( $P-H$ ) =  $70.5 \pm 2$  kcal/mol, I. P. ( $PH$ ) =  $10.18 \pm 0.1$  eV, and other thermochemically related quantities. The ionization energies of  $PH$ ,  $PH_2$ , and  $PH_3$ , are computed by ab initio molecular orbital methods to fourth order in Møller-Plesset theory, and are found to be in good agreement with experiment. The ground state of  $PH_2^+$  is inferred to be  $^1A_1$ , with the  $^3B_1$  state higher by  $> 0.71$  eV. This ordering is the reverse of that in  $CH_2$  and  $NH_2^+$ . This work has been published in J. Chem Phys. 84, 375 (1986).

\*Chemistry Division, ANL

†Dept. of Chemistry, University of Chicago, Chicago, IL

‡Dept. of Chemistry, Carnegie-Mellon University, Pittsburgh, PA

- c. **Bond Energies of Nitrogen and Phosphorus Hydrides and Fluorides**  
(J. Berkowitz, S. T. Gibson, J. P. Greene, O. M. Nesković\* and  
B. Rusčić†)

Recent measurements of bond energies in the  $N-H_n$  and  $P-H_n$  systems by photoionization mass spectrometry are compared with modern ab initio calculations and a semi-empirical theory. Good agreement is noted, providing confirmation for the level of accuracy of the ab initio parametrization. However, the  $N-F_n$  and  $P-F_n$  systems, also measured, are currently beyond the capabilities of such high quality ab initio calculations, and the trends observed in the bond energies indicate that other parametrizations are necessary in the semi-empirical approach.

---

\*Boris Kidric Institute of Nuclear Sciences, Vinca, Beograd, Yugoslavia  
†Rugjer Bosković Institute, Zagreb, Yugoslavia



d. Autoionization in Molecules - a Path Toward Better Understanding  
(J. Berkowitz, B. Kusić\*, S. T. Gibson and J. P. Greene)

The understanding of autoionization in molecules is even more limited than in atoms. One approach which we have been pursuing is to examine the behavior of isoelectronic sequences involving an atom, diatomic monohydride and triatomic dihydride. The correlation involving the change in symmetry ( $R_3$ ,  $C_{\infty v}$ ,  $C_{2v}$ ) of the respective ion cores, and also the corresponding Rydberg states is shown. Recognizing that molecules have additional channels for decay (vibrational and rotational autoionization, predissociation into neutrals) we nevertheless hope that this approach will ultimately reveal some inherent similarity in autoionization propensity between atoms and related molecules. One intriguing example, which we have studied, is the autoionization resonance behavior in the sequence F - OH - NH<sub>2</sub>. The descent in symmetry of the ionic state ( $^1D + ^1\Delta + ^1A_1$ ) can be traced in the autoionizing Rydberg series converging to the corresponding limits. Other examples are also being examined.

---

\*Rugjer Bosković Institute, Zagreb, Yugoslavia

e. Photoionization of Atomic Sulfur (S. T. Gibson, J. P. Greene, B. Rusčić\* and J. Berkowitz)

We had recently (1983-4) succeeded in obtaining the photoionization spectra of the transient atomic halogen species, F, Cl and Br which, together with earlier work on the noble gases, began to reveal some systematic trends in autoionization resonances. We sought to extend these studies to the atomic chalcogen series (S, Se) but we were pessimistic because of the well-known tendency of these elements to form clusters. In a parallel investigation of transient molecular species formed by chemical reaction, we found that the reaction  $H + H_2S$  not only generated the radical SH, but also atomic sulfur, depending upon the relative flow rate of reactants. We thereupon shifted our attention, and obtained the photoionization spectrum of atomic sulfur, from ionization threshold to 925 Å. The portion to 1000 Å is shown in Fig. VI-2. We found that autoionization peaks assigned to quasi-discrete levels ...  $(^2D^\circ)nd\ 3S^\circ, 3P^\circ$  are sharp, whereas those designated ...  $(^2D^\circ)nd\ 3D^\circ$  are broad. This latter feature parallels the discontinuity observed between first row and heavier elements in the noble gases and halogens. There is evidence for severe perturbation in the ...  $(^2D^\circ)nd\ 3P^\circ$  series, which could conceivably be attributed to a proximate  $3s3p^5\ 3P^\circ$  state.

---

\*Rugjer Bosković Institute, Zagreb, Yugoslavia

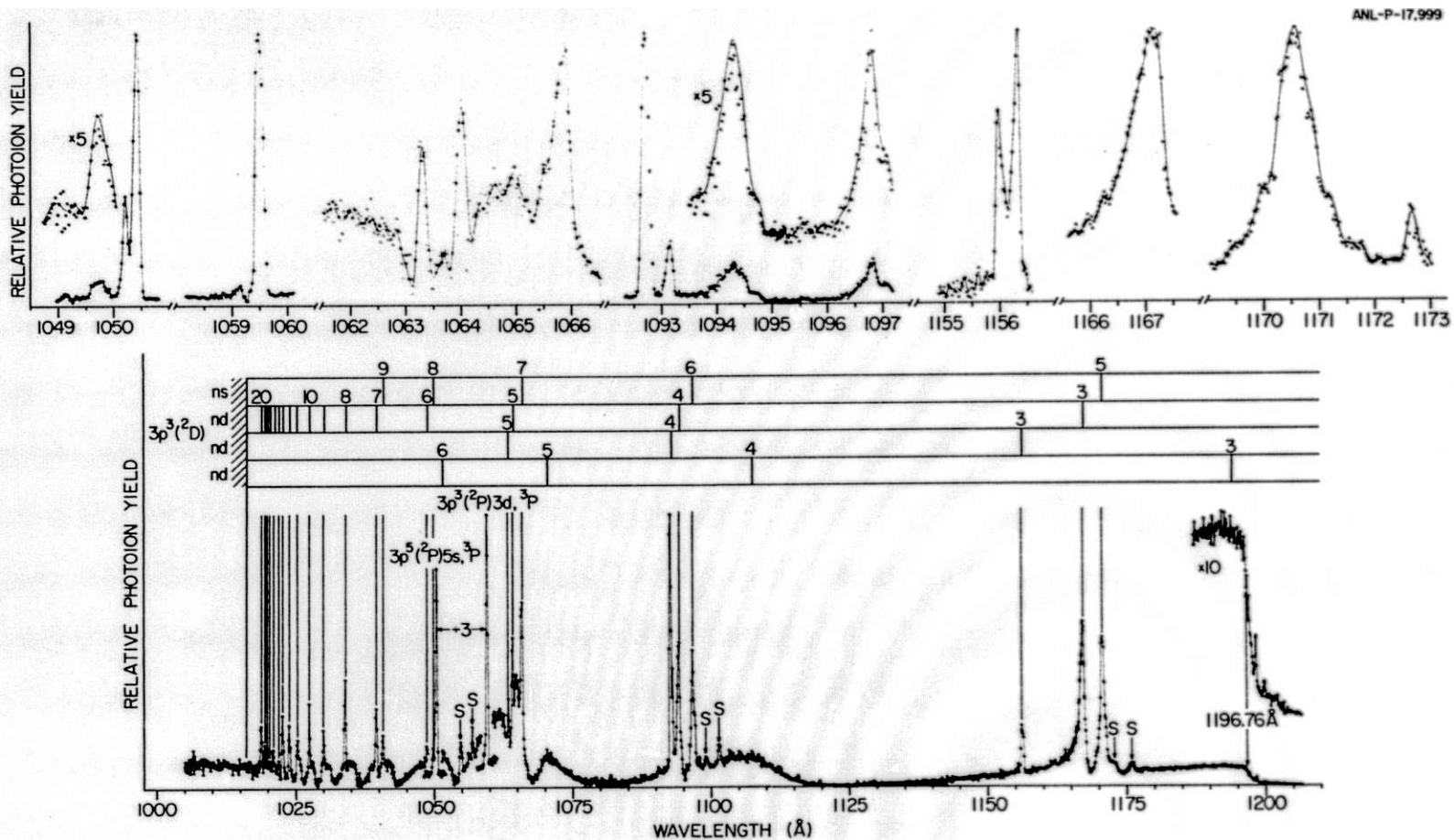


Figure VI-2. Lower panel: Photoion yield curve of atomic sulfur from threshold to 1005 Å with a wavelength resolution of 0.28 Å. Satellite absorptions are denoted by S. Upper panel: Selected portions re-examined with 0.14 Å resolution (FWHM). The solid lines in the upper panel were obtained by applying a smoothing program to the data, using a fast Fourier transform method.

f. Photoionization of Atomic Selenium (S. T. Gibson, J. P. Greene, B. Ruscic\* and J. Berkowitz)

After our good fortune in generating atomic sulfur, we attempted the preparation of atomic selenium by an analogous method - the reaction  $H + H_2Se$ . The difficulty of this experiment is exacerbated by the isotopic distribution of selenium, a situation not encountered with sulfur. It becomes necessary to distinguish  $H_2 \text{ } ^m\text{Se}^+$ ,  $H \text{ } ^{(m+1)}\text{Se}^+$   $^{(m+2)}\text{Se}^+$ , all of which appear at the same  $m/e$  ratio ( $m$  = the atomic mass of a particular selenium isotope). Also, the distribution of isotopic abundances means that only a fraction of the total  $Se^+$  ( $Se$ ) occurs at a particular mass which thereby incurs a loss of signal. Nevertheless, it was possible to obtain a good photoionization spectrum of atomic selenium, partly because the conversion efficiency turned out to be high. The spectrum was rather analogous to that of atomic sulfur, as previously we had found bromine to closely parallel chlorine. In selenium, we were able to extend our study to 600 Å, because of the high conversion efficiency, and thereby to observe 3 members of a window resonance series assigned to  $\dots 4s^2 4p^4 + hv \rightarrow 4s 4p^4 np$ , whose convergence limit is  $4s4p^4 ({}^4P_{5/2})$ . Two prominent peaks (rather than windows) are assigned to the first members of the series,  $4s4p^5 {}^3P_{2,1}$ . This observation and interpretation is similar to earlier work from our laboratory on atomic tellurium, and implies that the  $sp^5$  level in Se and Te is above the ionization potential, as it is known to be in atomic oxygen. This interpretation appears to put us into conflict with some ab initio atomic theorists, who base their conclusions partly on older data.

---

\*Rugjer Bosković Institute, Zagreb, Yugoslavia

g. UV Laser Photodissociation of Molecular Ions (K. Lee, J. P. Greene and J. Berkowitz)

The apparatus, dormant for over a year, is now functioning again. Photodissociation of  $O_2^+$  reveals two distinct regions in the  $O^+$  velocity spectrum, which are assigned to photodissociation of two  $O_2^+$  states in the target ion beam,  $X^2\Pi$  and  $a^4\Pi$ .

## VII. HIGH-RESOLUTION LASER-rf SPECTROSCOPY WITH ATOMIC AND MOLECULAR BEAMS

This program is directed toward increasing our understanding of atomic and molecular structure through high-resolution laser and radiofrequency studies of certain key atoms and small molecules. The emphasis throughout is on making the studies both systematic and of high precision. Work has continued in both of these areas during the past year. We have just completed measurements of the electric-dipole moments and the spin-rotation and hyperfine (hfs) interaction strengths for the calcium monohalide radicals CaF, CaCl, CaBr, and CaI in the electronic  $X\ 2\Sigma^+$  state. The work has been extended to the excited B-state where possible, and has stimulated a number of theoretical papers aimed at understanding the whole body of results in a systematic way. This year we have extended our studies to LaO, which is isoelectronic to the previously studied BaF, and comparison of the results is of great interest. This has led us to a preliminary study of PrO, in which the open 4f-shell leads to a very large number of low-lying electronic states. The initial results are unexpected and very puzzling. Our high-precision measurements of the hfs of neutral rare-earth atoms has stimulated the first ab initio multiconfiguration Dirac-Fock (MCDP) calculation for the hfs of such heavy atoms. Comparison of our data with the new calculations shows areas of discrepancy, especially in excited levels of  $^{167}\text{Er}$ , and these are being investigated further both experimentally and theoretically. A newly-operating apparatus will allow extension of our studies to beams of atomic and molecular ions using a collinear laser-ion geometry.

Our high-precision systematic study of the properties of the calcium monohalide radicals was completed during the last year with measurement of the electric-dipole moment of CaI. The value of the moment is now known (for the  $X\ 2\Sigma^+$  electronic ground state) for CaF, CaCl, CaBr, and CaI and the data have stimulated a number of theoretical studies. Detailed study of the spin-rotation and hfs interactions have just been completed for the related molecule LaO. The results show that the excited B-state and ground X-states are very different. Comparison is made with the isoelectronic system BaF. The techniques are now being extended to PrO with its open 4f-electron shell. The line-widths seen in the rf spectra of PrO are extremely wide and not at all understood as yet.

In our atomic studies we have extended our earlier measurements<sup>1</sup> of the hfs of excited  $4f^{12}6s^2$  levels in  $^{167}\text{Er}$  to  $4f^{11}5d6s^2$  levels in an effort to understand why the ab initio, zero-parameter MCDP theory fails to account for the observed quadrupole hfs. The atom  $^{139}\text{La}$  will also be studied to determine how well the theory works for the 5d-shell just before the onset of the filling of the 4f-shell.

---

<sup>1</sup>K. T. Cheng and W. J. Childs, Phys. Rev. A 31, 2775 (1985).

- a. Electric-dipole Moments in CaI and CaF by Molecular-beam Laser-rf Double-Resonance Study of Stark Splittings (W. J. Childs, G. L. Goodman, and L. S. Goodman)

In analogy with our earlier work on CaF, we have measured<sup>1</sup> the electric-dipole moment in the  $X^2\Sigma^+$  ground electronic state of CaI for both  $v = 0$  and 1. The moments are now known for the four calcium monohalides CaF, CaCl, CaBr, and CaI, and the measurements have led directly to several theoretical efforts to account for the results. The moments agree somewhat better with the predictions of a Ligand-field type model of Rice et al. than with those of a modified Rittner model by Törring et al. A paper on this work has been accepted for publication in the Journal of Molecular Spectroscopy.

---

<sup>1</sup>W. J. Childs, G. L. Goodman and L. S. Goodman, J. Mol. Spectrosc. 115, 215 (1985).

- b. Hyperfine Structure of Excited  $4f^{11}5d6s^2$  Levels in  $^{167}\text{Er I}$ : Measurements and MCDF Calculations (W. J. Childs, L. S. Goodman, and K. T. Cheng\*)

In our report last year we discussed serious discrepancies between experimental and new ab initio MCDF calculations of quadrupole hyperfine structure in excited  $4f^{12}6s^2$  levels of  $^{167}\text{Er I}$ . To examine this question more closely we have now made analogous measurements<sup>1</sup> for 11 excited  $4f^{11}5d6s^2$  levels in the same atom. The theory accounts for the dipole hfs rather well (just as for the  $4f^{12}6s^2$  levels), but is again less successful in accounting for the quadrupole interaction. This is most pronounced for those levels for which there is substantial cancellation between the contributions of the 4f and 5d electrons. A paper on this work has been accepted for publication.

---

\*Lawrence Livermore National Laboratory, Livermore, CA

<sup>1</sup>W. J. Childs, L. S. Goodman and K. T. Cheng, Phys. Rev. A 33, 1469 (1986).

c. High-precision Laser and rf Spectroscopy of the Spin-rotation and hfs Interactions in the X  $^2\Sigma^+$  and B  $^2\Sigma$  States of LaO

(W. J. Childs, G. L. Goodman, L. S. Goodman, and L. Young)

The spin-rotation and hyperfine interactions in the X  $^2\Sigma^+$  and B  $^2\Sigma$  electronic states of  $^{139}\text{La}^{16}\text{O}$  have been studied<sup>1</sup> in detail using Doppler-free laser-induced fluorescence and molecular-beam, laser-rf, double resonance. Measurements were carried out over a wide range of vibrational and rotational states so that the principal interaction strengths, together with their  $v$ - and  $N$ -dependences, could be evaluated for both the X- and B-states. The two states are very different, as evidenced by the observed ratios of the interaction strengths in the B-state to those in the X-state. These ratios are: for the spin-rotation interactions, -114.75; for the contact hfs, 0.1616; for the dipole-dipole hfs, 2.11; and for the quadrupole hfs, 2.29. In addition, the  $v$ -dependence for all of the strengths is small and positive in the X-state but very large and negative for the B-state. The results for  $^{139}\text{La}^{16}\text{O}$  are compared with earlier results for the isoelectronic system  $^{137}\text{Ba}^{19}\text{F}$ . After making allowance for specifically nuclear effects, the electronic parts of the dipole-dipole and quadrupole hfs interactions are found to be the same for the X  $^2\Sigma^+$  electronic ground states of the two molecules to within experimental error. The contact dipole interaction is about 25% larger in the LaO while the spin-rotation interaction is about 18% smaller. Because of the striking differences between the X- and B-states in LaO it is of the greatest interest to determine whether the differences are paralleled in the isoelectronic radical BaF. Figure VII-1 shows a small section of a Doppler-free laser scan through the  $v = 1 \rightarrow 0$  band of the B-X transition in LaO. For the transition marked R<sub>24</sub>, the upper and lower state hyperfine splittings add, causing very broad hfs patterns. The reverse is true for the R<sub>23</sub> transitions. Figure VII-2 shows a typical laser-rf double-resonance observation in LaO. The fluorescence increases nearly 50% when the rf is swept through resonance. Such observations give extremely precise values for the molecular hfs interactions.

---

<sup>1</sup>W. J. Childs, G. L. Goodman, L. S. Goodman, and L. Young, accepted for publication in J. Mol. Spectrosc., 1986.

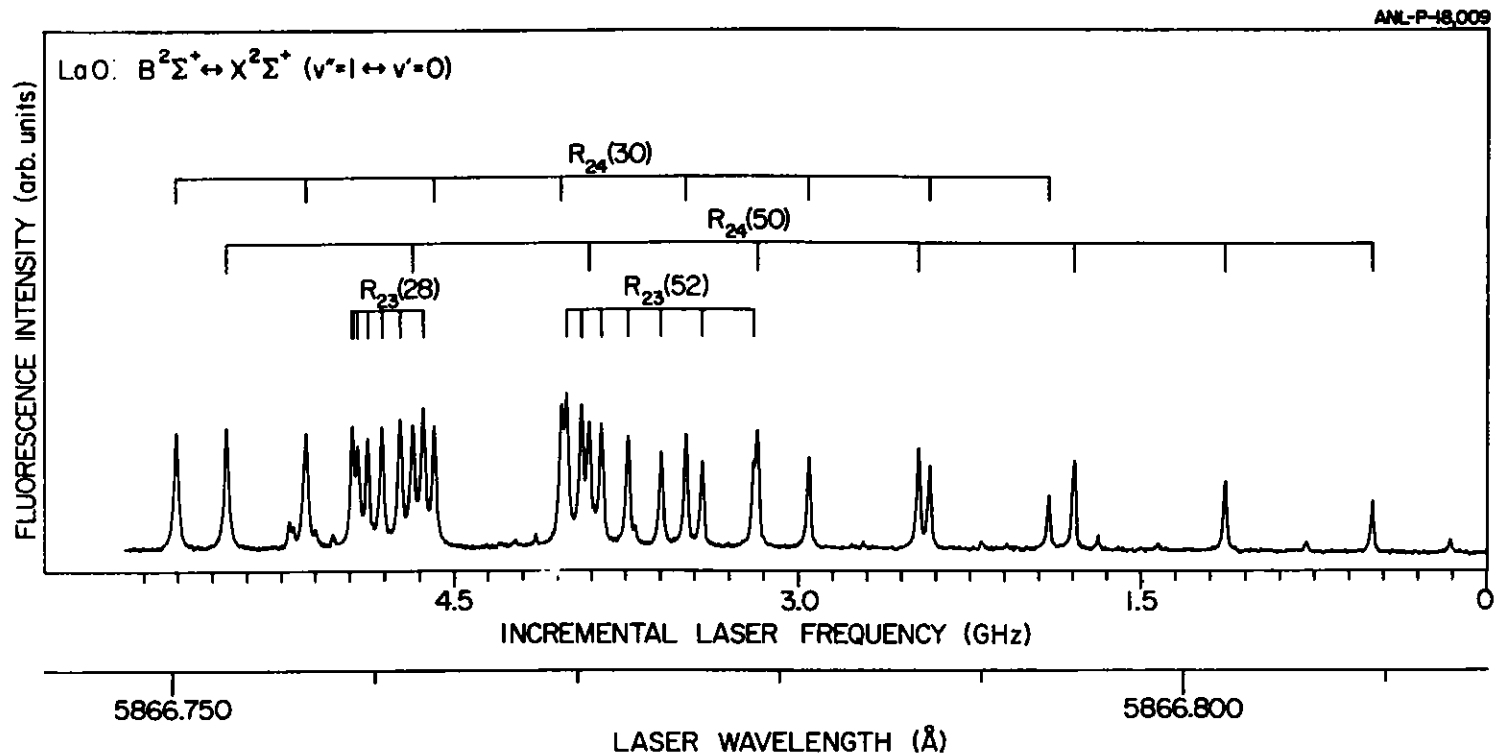


Figure VII-1. A small section of a Doppler-free laser scan through the  $v = 1 \leftrightarrow 0$  band of the B-X transition in LaO. For the transition marked  $R_{24}$ , the upper and lower state hyperfine splittings add, causing very broad hfs patterns. The reverse is true for the  $R_{23}$  transitions.



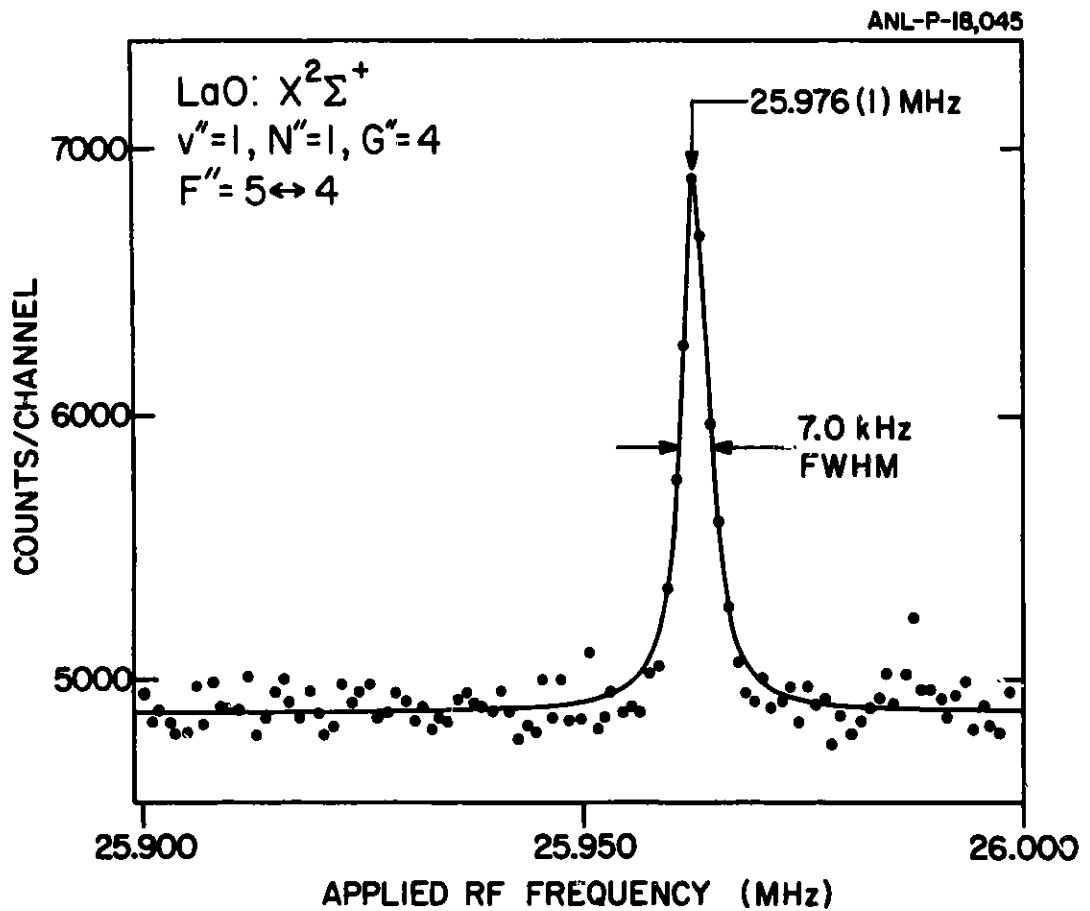


Figure VII-2. A typical laser-rf double-resonance observation in LaO. The fluorescence increases nearly 50% when the rf is swept through resonance. Such observations give extremely precise values for the molecular hfs interactions.

d. Extension of Molecular-beam hfs Studies into Rare-earth Monohalides: Hfs of PrO (W. J. Childs and L. S. Goodman)

Our detailed study of the hfs of LaO suggests an extension into the rare-earth monoxides, a rapidly intensifying area of research within the last few years. Our successful production of a molecular beam of PrO has allowed the first Doppler-free spectroscopy in this group of compounds. The resulting narrowing of the linewidths by a factor of a hundred results in (1) observation of previously unresolvable structure within known lines, and (2) observation of many new lines between those previously observed in a vapor. Application of the molecular-beam, laser-rf, double-resonance method reveals the expected resonances, but the observed linewidths are 50-100 times greater than those observed in other atoms or molecules. The effect is so far very surprising and not understood. It does not appear to arise from short lifetimes, but may be due to many extremely closely-spaced resonances. It is of great interest to determine the cause of this completely new and unexpected result.

e. Hfs of Even-parity Levels in  $^{139}\text{La}$ : Theory and Experiment  
(W. J. Childs, L. S. Goodman and U. Nielsen\*)

The low-lying (below  $15,000\text{ cm}^{-1}$ ) levels of  $^{139}\text{La}$  arise from the  $(5d + 6s)^3$  electron configurations. The observed hyperfine structure has been the subject of a number of theoretical papers over the years. The effective-operator theory previously used enjoyed limited success despite the large number of adjustable parameters employed. The zero-parameter, ab initio MCDF theory is now being applied to the problem, and new hfs measurements are being made for the higher-lying (previously unreachable)  $(5d + 6s)^3$  metastable states to complete the systematic study.

---

\*University of Aarhus, Aarhus, Denmark

f. Apparatus for Collinear Laser Spectroscopy of Slow Atomic and Molecular Ions (L. S. Goodman, A. Sen, C. Kurtz, U. Nielsen,\* and W. J. Childs)

Work on the apparatus for collinear laser spectroscopy of slow atomic and molecular-ion beams has just resumed with the arrival this Fall of A. Sen from the University of Western Ontario. The magnet installed last year, together with the two new sets of electrostatic quadrupole pairs, provides good mass resolution. Strong fluorescence is observed from ion beams of Ba and Eu.

---

\*University of Aarhus, Aarhus, Denmark

VIII. BEAM-FOIL RESEARCH, ION-BEAM/LASER RESEARCH,  
AND COLLISION DYNAMICS OF HEAVY IONS

Introduction

Our program consists of investigations of the structure and dynamics of atomic ions principally using photon detection techniques. The experiments involve fast ion beams produced at either ATLAS (50-500-MeV ion energy) or the Argonne Dynamitron accelerator (0.5--4.5-MeV ion energy) or a low energy "BLASE" (Beam-laser) facility (0.02--0.12-MeV ion energy). Laser excitation of the fast beams is being applied to study atomic structure and hyperfine structures principally of low ionization stages.

In 1985, ATLAS was used to study (foil-excited) spectra of highly ionized titanium to obtain a precision wavelength measurement of a transition in its two-electron spectrum.

Experiments at the "BLASE" facilities continued our studies of the foil interaction process. The polarization of light emitted from highly excited Rydberg states in hydrogen was measured to investigate the shapes of wave functions produced on leaving the foil. Beam-foil spectroscopy of sodium- and magnesium-like argon is continuing.

Our fast-beam/laser interaction studies have continued with studies of the laser-induced fluorescence from barium, neon and sodium. This program has principally used the BLASE facility, and has involved extensive re-building of the accelerator system. Similar work is continuing to reduce the ripple voltage of the Dynamitron high voltage supply.

a. Fast Ion-Beam Laser Interactions (H. G. Berry, L. Young, L. Engström and C. Kurtz)

We have been making a comprehensive upgrade of the BLASE (20 keV - 120 keV) facility in order to attack the proposed atomic structure problems. The upgrade consists of improvements in two areas: 1) ion-beam quality and 2) detection efficiency.

In the first area, an active feedback system has been designed which should reduce energy fluctuations from the current 2 parts in  $10^4$  to 4 parts in  $10^6$ . In addition, a new high-voltage platform containing stabilized power supplies for the ion source and extraction system is in the design stage. A new high-resolution analyzing magnet is due to arrive in March 1986 and will be incorporated into the beam-line. With optimized beam optics and the aforementioned improvements, the limiting resolution in these experiments should be the natural linewidth.

The beam quality has also been improved by a significant upgrade of the vacuum system. The vacuum has been improved by approximately 1 order of magnitude and is now close to the  $10^{-8}$  torr range in all parts of the system. This necessitated significant rebuilding of most of the beam-line and interaction chambers.

In the second area, the collection efficiency for fluorescence has been enhanced by a factor of 100. This has been tested using the Ba II  $5d - 2^2D_{5/2} - 6p^2P_{3/2}$  transition. Without the additional improvement in the energy stability, we were able to observe, without interference from neighboring isotopes, the  $^{137}\text{Ba}$  hyperfine structure with a resolution that was three times the natural linewidth.

We have made two attempts to observe hyperfine structure in Na II  $2p^53s \rightarrow 2p^5 3p$  transitions. From the failed attempts to observe the resonances we concluded that less than  $10^{-6}$  of the beam was in the desired metastable state. Attempts to produce the desired state by non-resonant gas-collisional excitation served to broaden the velocity distribution of the beam, as monitored by the Na I resonance line. Further attempts will be made after 1) reducing excess photon noise due to collisional excitation of radiating states in the detection region or 2) incorporation of phase-sensitive detection.

b. Alignment and Orientation Production in Hydrogenic States (H. G. Berry, J. C. DeHaes,\* D. Neek,† and P. Somerville)

We have made further measurements to investigate the final surface interaction of a thin foil on a fast ion beam. The excitation distribution and wavefunction shapes depend on the bulk of the foil and, more critically, on the final surface interaction. Previous measurements have already allowed some preliminary analysis of the observed total charge-state distributions (see for example, Argonne reports by Berry and Brooks and also by Gemmell et al.). Our present objective is a more detailed microscopic understanding of the important final surface processes. Our observations show clearly the effects of surface electric fields, both those induced by the moving ion (image fields etc.), and those produced by the secondary electron flux.

Polarization measurements of Balmer emission following the population of states with  $n=5$  to 15, show an apparent strong increase in the alignment of high- $n$  Rydberg states. These correspond closely to maximum orientation of the states around  $n=9$ . However, these high  $n$ -states are very sensitive to small electric fields. Thus, by measuring the "zero-field" quantum beats, we are able to obtain quantitative measurements of the surface field. We find that surface fields of up to 15 volts/cm exist out to a few mm from the foil surface. The true zero-field quantum beats start only after this field is small enough to minimize the mixing within the  $n$ -manifold being measured.

We have developed a model of the surface electric field which explains many features of our data, but is so far only in qualitative agreement for the magnitude of the polarizations observed. The model assumes a finite electrical conductivity of the thin foils. New measurements during a summer visit by Dr. DeHaes with thin gold foils and some non-conducting foils gave quite different, but still inconclusive results. Our results indicated that carbon-build-up on the surfaces changed the data, and suggest that the experiments should be repeated in improved vacuum.

---

\*University of Brussels, Belgium.

†University of Illinois, Chicago, IL.

c. Precision Measurements of the  $1s2s\ ^3S - 1s2p\ ^3P$  Transitions in Li II (H. G. Berry, L. Young, L. Engström, E. Riis,\* O. Poulsen,\* and S. A. Lee,†)

We have completed the wavelength calibration of the collinear laser fluorescence spectrum of  $^7\text{Li II}$ , with a measurement of the saturated absorption spectrum of iodine reference lines at Colorado State University (by S. A. Lee and E. Riis). The final results give wavenumbers precise to 1 in  $10^8$ , corresponding to 90 ppm of the QED corrections.

Initial attempts have been made to produce the same lithium transition in a cooled discharge. We hope to obtain a Doppler-free saturated absorption spectrum directly in this way and further improve our precision about a factor of two. This work is continuing at Argonne.

---

\*University of Aarhus, Aarhus, Denmark

†Colorado State University, Fort Collins, CO

d. Autoionization of Helium Following Excitation by Fast, Multiply-Charged Ions (P. Arcuni,\* and H. G. Berry)

We have completed measurements of the autoionization spectra of doubly-excited helium, following excitation by lithium ions produced by the Dynamitron. In particular, we studied the effect of projectile nuclear charge on the helium autoionization profiles and the continuum in which they are embedded. Experimental data for the  $2s2p\ ^1P$  and  $2p^2\ ^1D$  resonances were analyzed in detail: these excitation amplitudes, and the "Fano" interference between them, yields measurements of the excitation function in this velocity range. The results were fitted to a model of a new type of post-collision interaction between the emitted electron and the fast ion. The interaction between the outgoing fast ion and the autoionization electron leads to a distorted-velocity distribution of the electrons. The observed distortions of the emission profiles are dependent on the angle of electron emission. Further studies may include autoionization of atomic systems which are produced in the laser fast-ion-beam interactions.

---

\*Graduate Student from the University of Chicago, Chicago, IL.

e. Accurate Transition Probabilities for the Resonance Transitions in Na- and Mg-like Ar (L. Engström, H. G. Berry and N. Reistad\*)

The decay of the  $3p\ ^2P_{1/2,3/2}$  and the  $3d\ ^2D_{3/2,5/2}$  levels in Ar VIII, and the  $3s3p\ ^1P$ ,  $3s3d\ ^1D$ ,  $3p^2\ ^1S$  and  $^1D$  levels in Ar VII has been studied by the beam-foil technique, using the 4.5-MV Dynamitron accelerator (see Fig. VIII-1).

Previous experimental measurements of the lifetime of the  $3p\ ^2P$  and the  $3s3p\ ^1P$  levels have shown considerable deviations from the values predicted by various modern theoretical calculations. In our study, we show that this discrepancy is due to the inability of the standard technique (curve-fitting) to extract the correct lifetime from the measured decay curves when these are severely perturbed by cascades. However, by measuring also the decay of the most prominent directly cascading levels,  $3d\ ^2D$  in Ar VIII and  $3s3d\ ^1D$ ,  $3p^2\ ^1S$  and  $^1D$  in Ar VIII, and explicitly including this information in the analysis (using the ANDC technique) accurate lifetimes are obtained.

The final  $3p\ ^2P$  and  $3s3p\ ^1P$  lifetimes are found to be in excellent agreement with the majority of the theoretical results. Results of this study have been submitted for publication.

---

\*University of Lund, Lund, Sweden



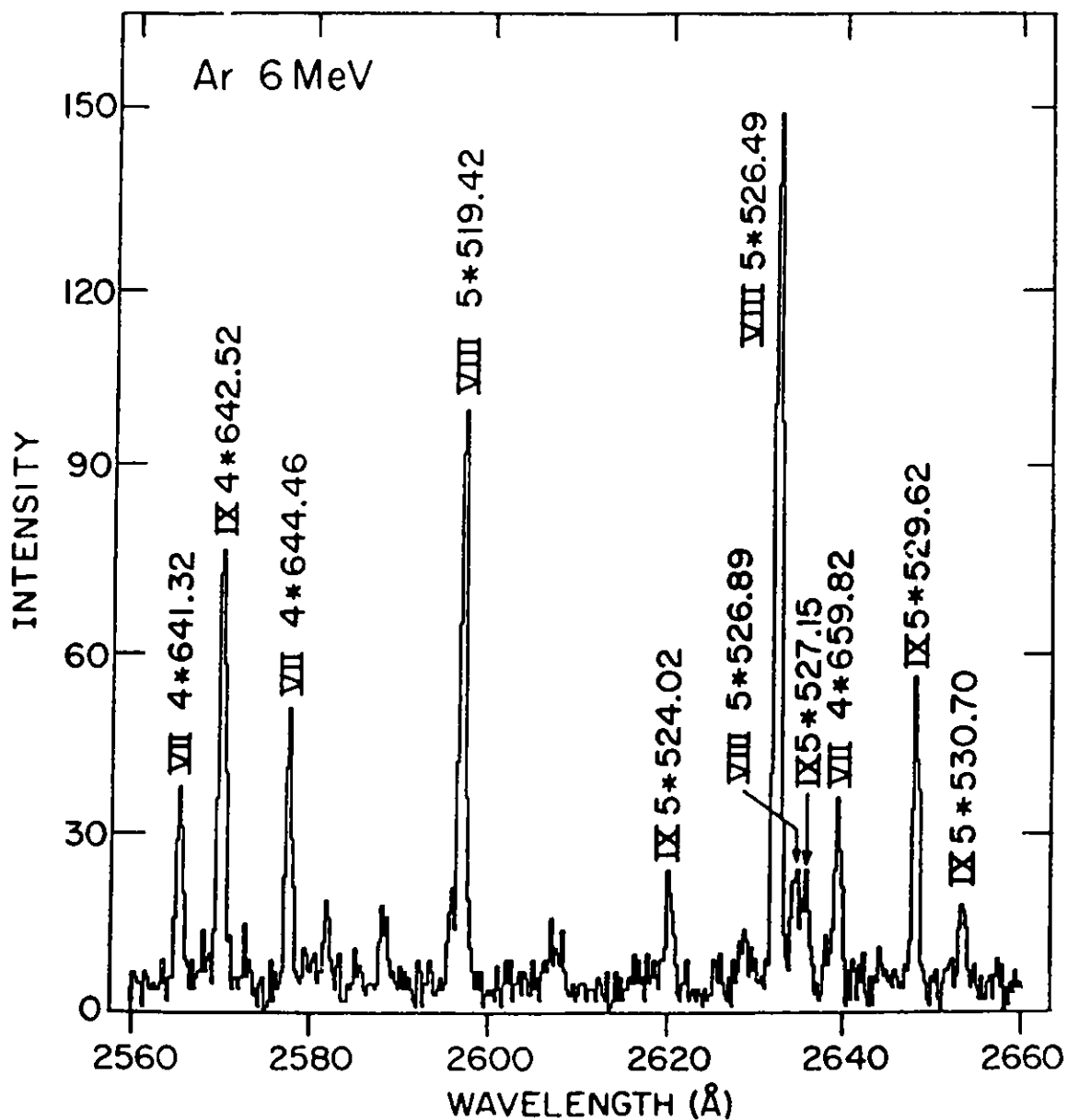


Figure VIII-1. Partial spectrum of foil-excited argon recorded in high spectral orders at an energy of 6 MeV.

f. Extended Analysis of the  $2p^53s$ ,  $3p$  and  $3d$  Configurations in Ne-like Argon (Ar IX) (L. Engström and H. G. Berry)

Considerable interest has recently been focussed on the  $3p^53s$ ,  $3p$  and  $3d$  levels along the Ne I isoelectronic sequence. For example, a promising scheme to achieve a XUV laser involves the  $2p^53s - 2p^53p$  transitions in Ne-like ions. Furthermore, based on isoelectronic extrapolations of differences between experimental and theoretical wave numbers, twenty four lines in the solar-flare spectra have been identified as transitions between these configurations in Fe XVII and Ni XIX.

In our work, high-quality Ar-spectra have been obtained with the beam-foil technique utilizing  $Ar^+$  and  $Ar^{2+}$  beams accelerated to energies between 3 and 8.4 MeV at the Dynamitron. Comparisons of the relative intensities of the observed Ar lines at the different energies allow accurate charge-state assignments of the spectral lines. So far, 33 lines (with a wavelength uncertainty of less than 0.05 Å) have been identified as transitions between the  $3s,3p$  and  $3d$  configurations in Ar IX, leading to the establishment of 24 out of the possible 26 energy levels. In addition, transitions between the core-excited  $2s2p^63s,3p$  and  $3d$  configurations in Ar IX as well as the  $2p^43s$ ,  $3p$  and  $3d$  configurations in F-like Ar (Ar X) are also prominent in our spectra. The Ar IX study is soon to be published, and work is in progress on the analyses of the Ar VII and Ar X spectra (see Fig. VIII-2).

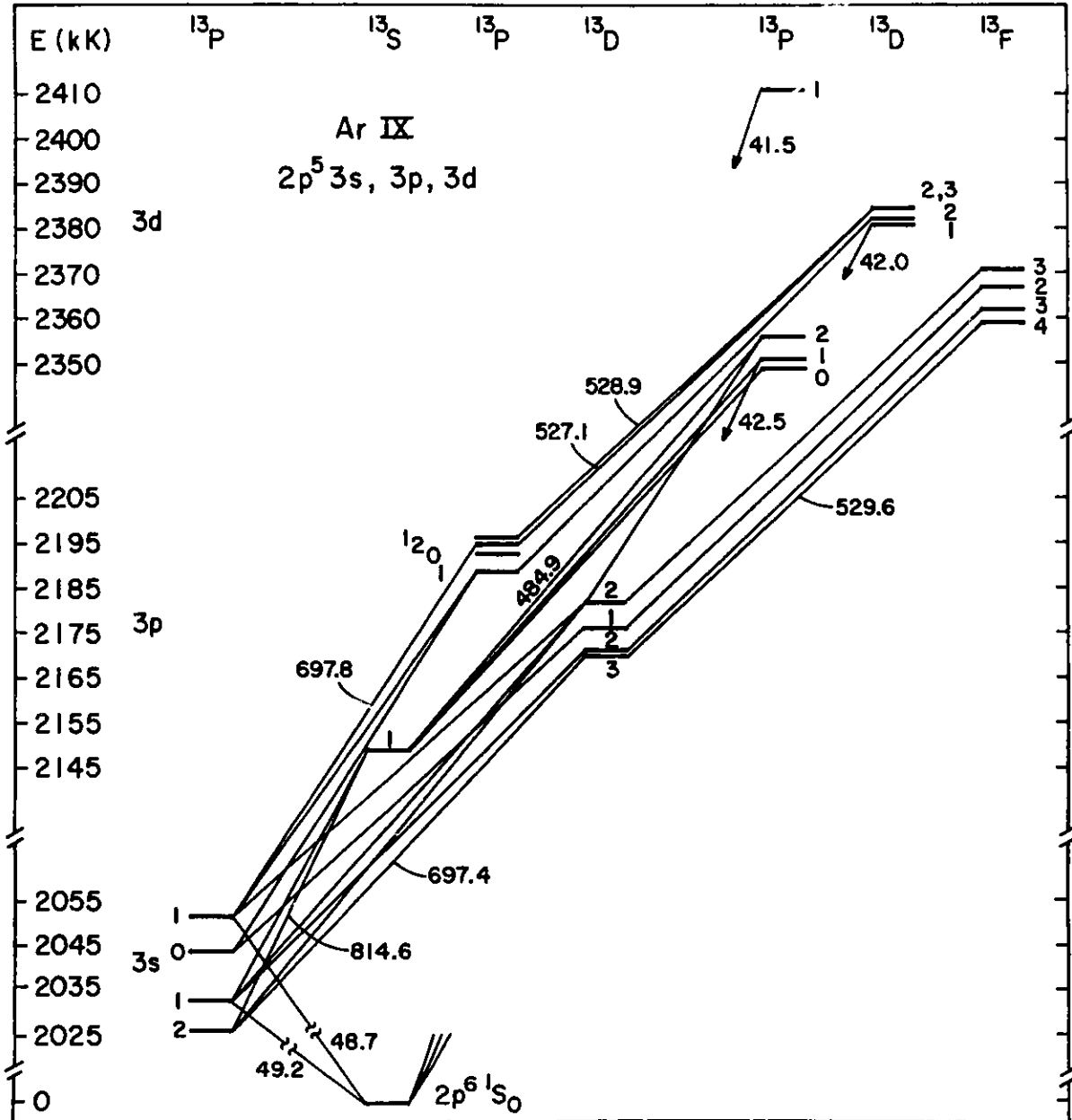


Figure VIII-2. The level structure of the  $2p^5 3s, 3p$  and  $3d$  configurations in Ar IX. Only a few of the observed transitions are drawn, and the  $3p 1S_0$  level (which is not observed in this work) is omitted from the figure.

g. Lamb Shifts and Fine Structures of  $n = 2$  in Helium-like Ions

(H. G. Berry, L. Engström, J. E. Hardis,\* A. E. Livingston,† D. Zei'‡  
P. Somerville, L. Young, and C. Kurtz)

(i) Further measurements have been made on foil-excited titanium and nickel beams at the Tandem-Linac. The titanium results from several runs at the Argonne Linac have yielded a measurement of the  $2s-2p(J=2)$  transition which is in excellent agreement with the latest calculations. Nickel spectra obtained with 365-MeV nickel beams showed many new yrast transitions in three- and more electron nickel ions, and the new ATLAS energy will be sufficient to measure the  $2s - 2p$  transitions in helium-like nickel. (submitted for publication).

(ii) Measurements on the same transitions ( $J=0,1,2$ ) in neon have been completed and accepted for publication. These results provide a valuable check of the theory in the low/intermediate range, and provide a connection with the laser/fast beam measurements at low nuclear charge ( $Z=2-5$ ).

---

\*University of Chicago, Chicago, IL.

†University of Notre Dame, Notre Dame, IN.

‡Ripon College, WI.

**IX. INTERACTIONS OF FAST-ATOMIC AND MOLECULAR IONS  
WITH SOLID AND GASEOUS TARGETS**

The bulk of our effort during 1985 was directed toward the continuing development and refinement of a new type of large-area multiparticle imaging detector system. This new technology shows great promise of overcoming many of the difficulties which had prevented the use of Coulomb-explosion techniques to determine directly the geometrical structures of molecular ions for all but the most simple molecules. In the course of developing techniques for determining the stereochemical structures of molecular projectiles by coincident detection of dissociation fragments, preliminary data have shown us the important problems which need to be addressed in order to obtain precise structural information. Most prominently, these problems include the need for a more detailed understanding of the physical processes involved in the interactions of these fast molecular ions with solid targets and in the formation of final electronic states. From our studies of charge-changing processes acting on fast ions as they exit from solid targets, together with new experiments studying cluster effects in the charge-state distributions of heavy ions exiting foils, we have developed a quantitative model that successfully describes these effects in terms of enhanced electron capture cross sections which can be simply approximated. These data have helped shed new light on the processes which lead to the final charge-state distributions observed when fast ions emerge from solid targets. We have also exploited the use of the MUPPATS detector to study a variety of different atomic collision phenomena with selectively-oriented projectile molecules. In particular, this technique has allowed us to study the electron density fluctuations induced in solids by the passage of swift ions. Some of the highlights in 1985 included:

a. Development of a Multiparticle Imaging Detector

(A. Faibis, E. P. Kanter, W. Koenig, Z. Vager and B. J. Zabransky)

It has long been recognized that Coulomb-explosion techniques offer a potentially very powerful means of determining directly the geometries of individual molecules contained in a beam. Unfortunately, there have been considerable technical difficulties in performing such measurements in all but a few very selective cases. Recently, due to advances in detector technology by nuclear and particle physicists, a new generation of low-pressure multiwire avalanche counters has been developed capable of overcoming these difficulties. Specifically, these counters can now image multiparticle events in three dimensions so that it is possible to determine uniquely the final trajectories for all fragments from a Coulomb-exploding cluster.

The detector which we have developed consists of five planes of wires (see Fig. IX-1). An anode, at a positive potential ( $\sim 350\text{V}$ ) is sandwiched between two cathodes (with 5 mm separating each plane) which are at negative potential ( $\sim -350\text{V}$ ). The final two planes are "pick-up" cathodes, at ground potential, which are interspersed between each of the cathodes and the anode at a distance of 2 mm from the anode. The wire spacing is 1 mm for the anode and 0.5 mm for the cathodes. All  $\sim 3000$  wires are gold-plated rhenium-doped tungsten, 20 microns in diameter. The active area of the wire planes forms a symmetric hexagon with a diagonal length of 34 cm. The active volume of the detector is filled with isobutane at  $\sim 3$  Torr pressure which is contained by a thin foil window (of stretched polypropylene  $\sim 60 \mu\text{g}/\text{cm}^2$ ).

The MUPPATS detector has now been extensively tested with a variety of diatomic and triatomic molecular-ion beams. We have also studied the 4-atom  $\text{CH}_3^+$  molecule. In tests with 2-MeV carbon ions, we have determined the position and time resolutions to be 260 microns (FWHM) and 1.0 ns, respectively, when averaged over all three readout planes. Our most extensive measurements have been with the  $\text{CH}_2^+$  and  $\text{OH}_2^+$  ions (see Fig. IX-2). For these ions, we find mean structures which are in good agreement with theory. Specifically, we find HXH angles of 147 and 106 degrees for  $\text{CH}_2^+$  and  $\text{OH}_2^+$  respectively. The distribution widths however (100 and 60 degrees, respectively) are exceedingly large, characterizing a vibrationally hot incident beam. We have also been able to further excite this incident beam, by passage through a 10-cm-long gas cell prior to dissociation. This leads to further broadening of these bond-angle distributions. Studies of  $\text{CH}_4^+$ ,  $\text{C}_2\text{H}_3^+$ , and  $\text{N}_2^{++}$  are planned for 1986.

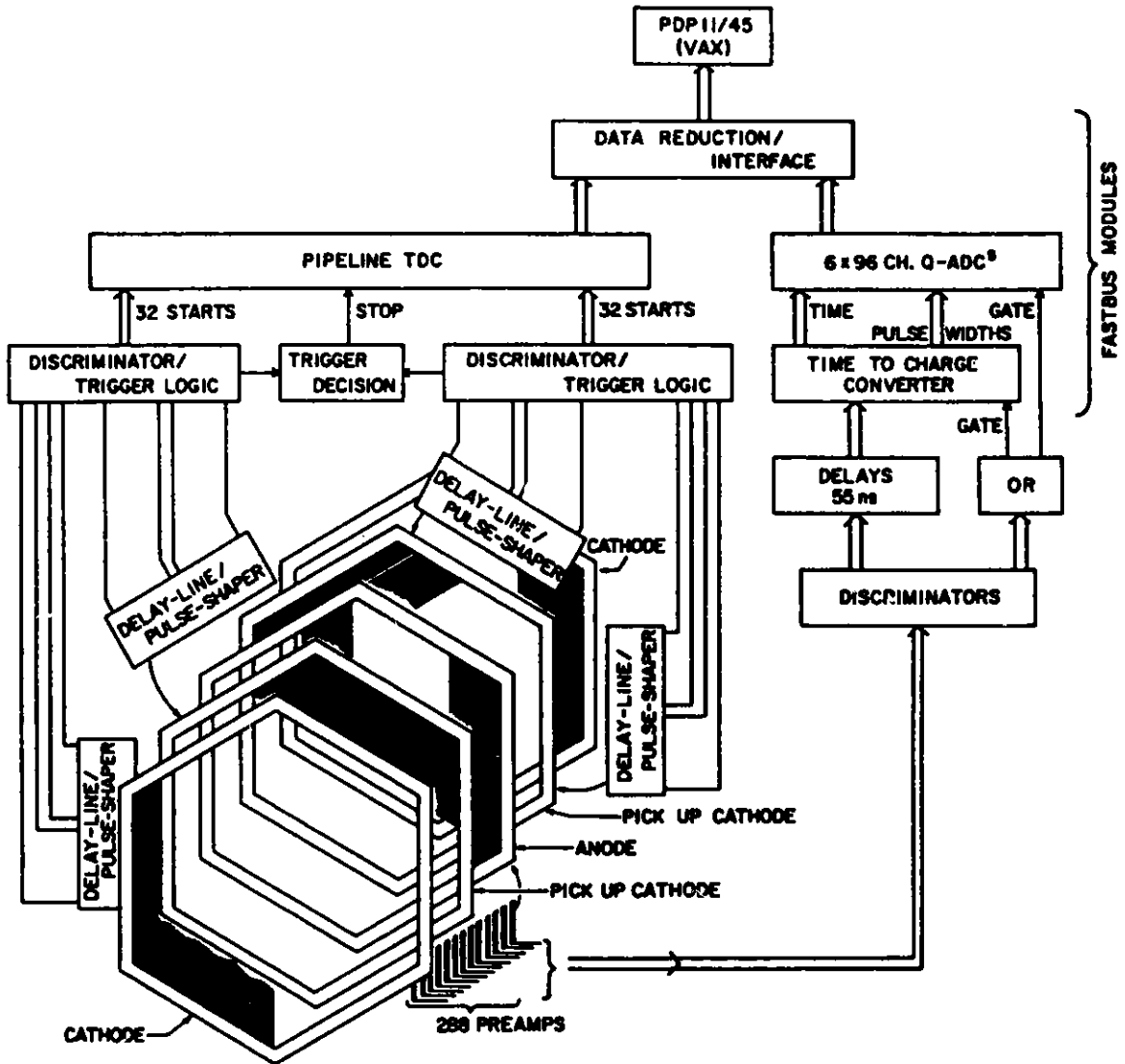


Figure IX-1. Schematic drawing of the electrode arrangement and signal readout in the MultiParticle Position And Time Sensitive detector.

b. Enhanced Electron Capture by Fast Heavy Di-clusters Exiting Solids  
 (P. J. Cooney,\* A. Faibis, E. P. Kanter, W. Koenig, D. Maor,† and  
 B. J. Zabransky)

We have studied the dependence of the charge-state distributions of heavy-ion fragments resulting from the foil-induced dissociation of 4.2-MeV  $N_2^+$  ions on the thickness of the carbon target foil. The results were compared to those distributions measured for impact of 2.1-MeV  $N^+$  projectiles. Whereas the charge-state distributions for atomic-ion impact are already equilibrated in the thinnest targets used ( $2 \mu\text{g}/\text{cm}^2$ ), those measured for molecular-ion impact are strongly dependent on the target thickness, even for the thickest targets ( $100 \mu\text{g}/\text{cm}^2$ ). The distributions for molecular-ion impact show a marked shift towards lower charge states (see Fig. IX-3), evidencing an enhanced electron capture probability over the case of monatomic-ion impact. A quantitative model was developed to explain this phenomenon by reducing the two-center potential of the cluster fragments to a separation-dependent one-center effective potential. With this simple model, it is now possible to calculate the charge-state distributions for heavy ions resulting from the foil-induced dissociation of molecular ions and thus reliably predict the most probable charge states.

Using the MUPPATS detector, we have extended these measurements to include the simultaneous measurement of the charge of each atomic ion resulting from the foil-induced dissociation of 4.5-MeV  $N_2^+$  and  $O_2^+$ . These data reveal that the enhancement of electron capture decreases exponentially with increasing total charge on the dicluster exiting the foil, but is relatively insensitive to the difference between the charge on each of the two exiting ions (see Fig. IX-4). These results have provided additional insights into the process of electron capture by the quasimolecular cluster exiting the foil.

---

\*Millersville University, Millersville, Pa.

†The Technion, Israel.



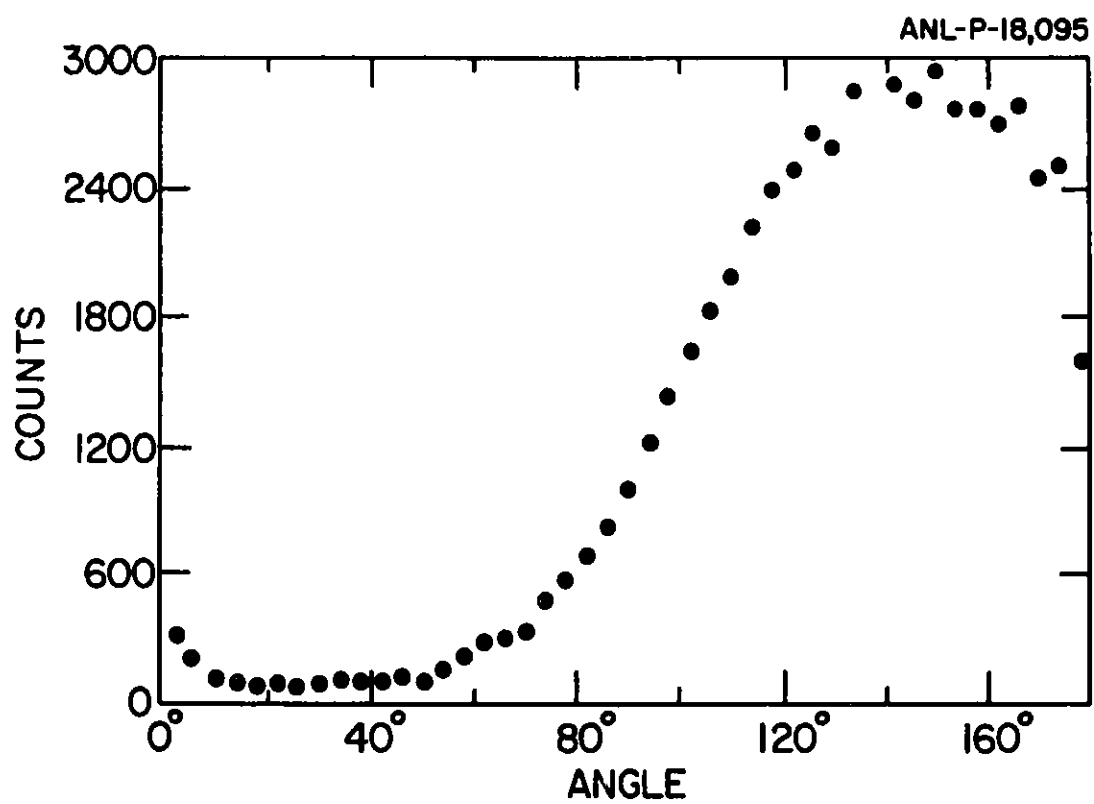


Figure IX-2. Observed distribution of bond angles for 4.0-MeV  $\text{CH}_2^+$  on a  $2\text{-}\mu\text{g}/\text{cm}^2$  carbon foil.

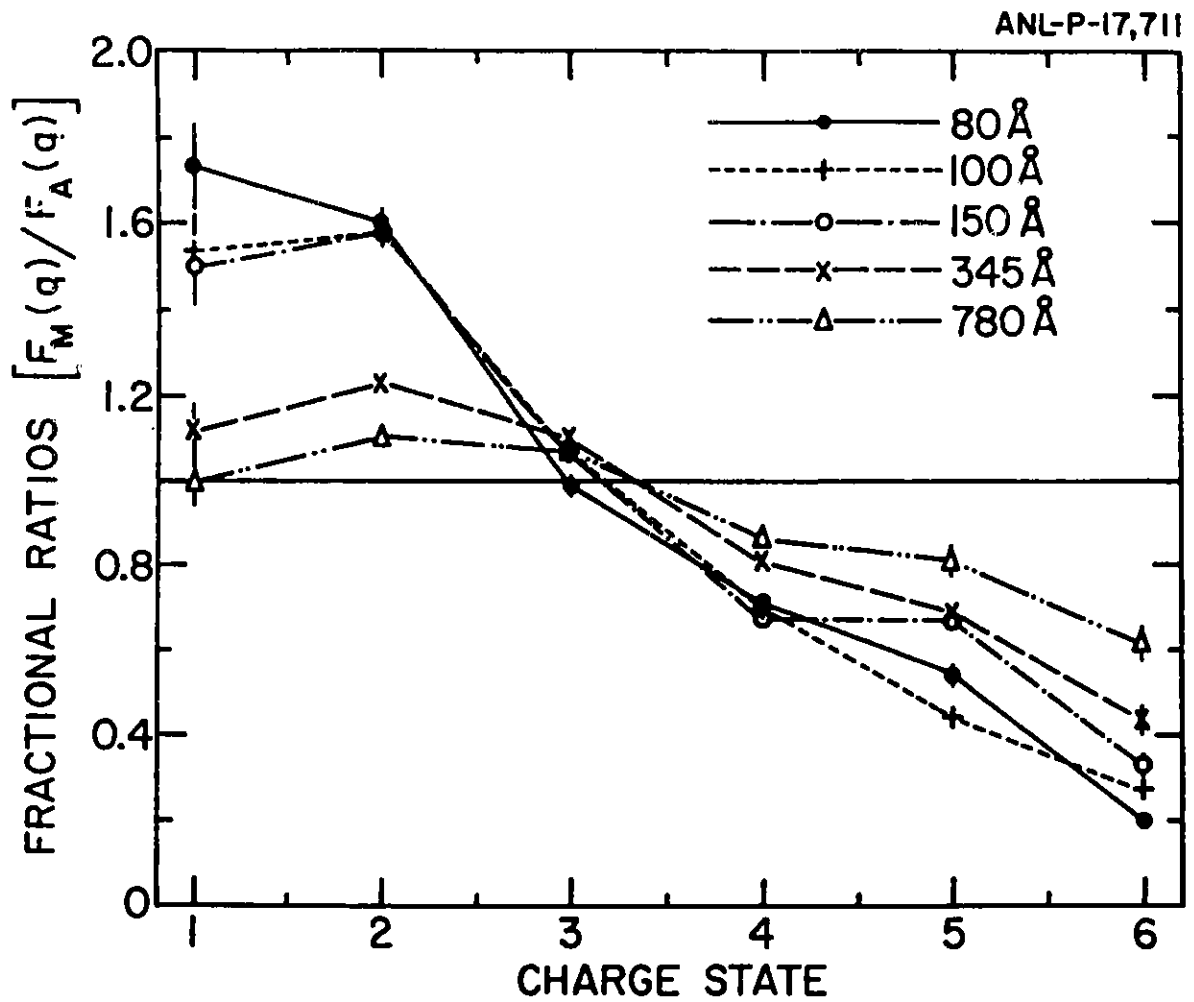


Figure IX-3. Ratios of the charge-state fractions for molecular- and atomic-ion impact as a function of the final exit-ion charge state for varying target thicknesses as shown.

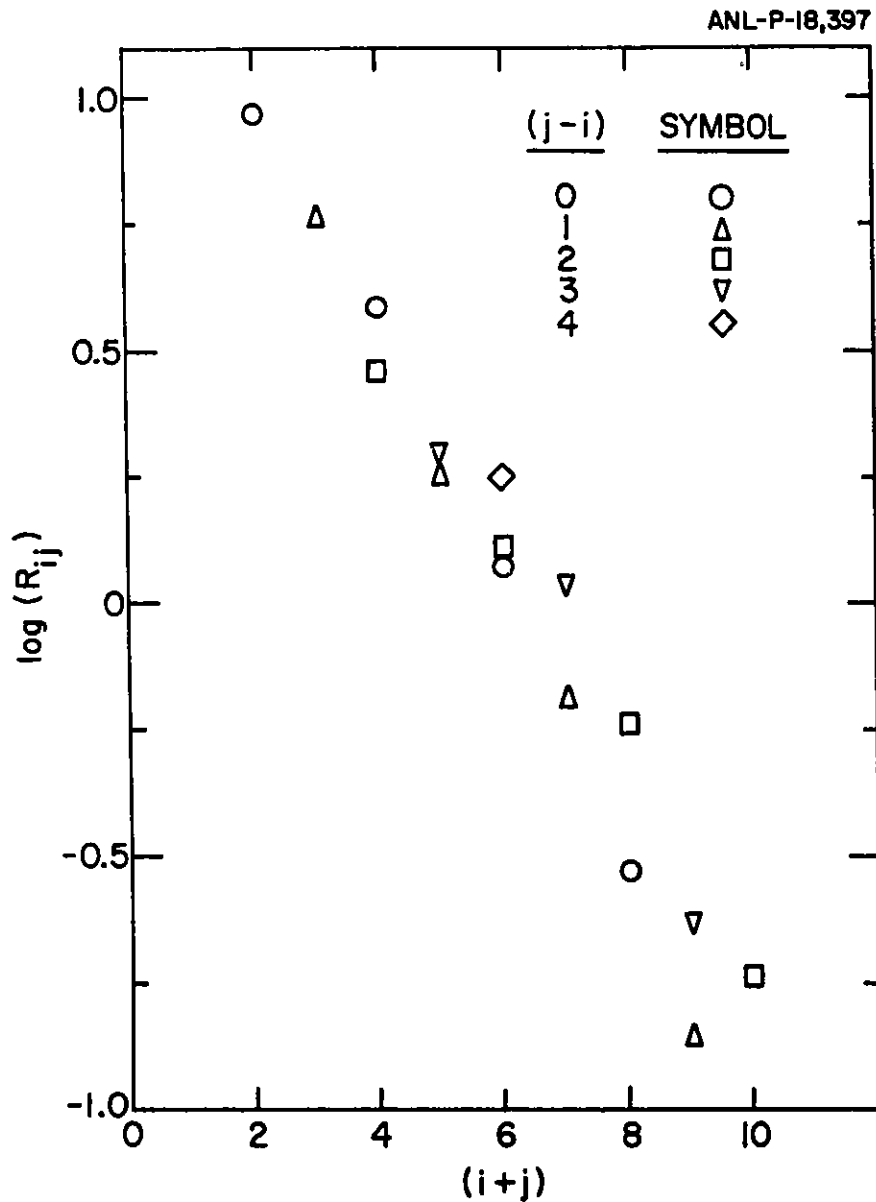


Figure IX-4. Ratios,  $R_{ij}$ , of the correlated charge-state fractions for 4.5-MeV  $N_2^+$  incident on a  $2\text{-}\mu\text{g}/\text{cm}^2$  carbon foil, relative to the result expected from the measured charge-state fractions for  $N^+$  incident at the same velocity if there were no correlation between the final charge of the outgoing ions  $N^{i+}$  and  $N^{j+}$ . This ratio is plotted as a function of the net charge,  $i + j$ , on the outgoing dicluster.

c. Charge-state-distributions of Foil-excited Heavy Rydberg Atoms  
(A. Faibis, E. P. Kanter, W. Koenig, and B. J. Zabransky)

Studies of foil-excited fast (MeV/amu) heavy ions have demonstrated large yields of high Rydberg atoms formed in such beams. Further experiments have suggested a strong target-thickness dependence of the yields of such atoms. These results have been puzzling in view of the supposed short mean-free paths of such atoms in solids. In an effort to better understand these results, we have previously measured the yields of Rydberg atoms ( $n \sim 100-200$ ) in foil excited  $^{32}\text{S}$  ions at an incident energy of 125 MeV. The Rydberg atoms were field-ionized in a longitudinal electric field ( $\sim 5$  kV/cm) and the detached electrons were detected in coincidence with the remaining charge-state-analyzed ionic cores. We studied the dependences of the yields on both the mean charge of the ions in the solid and on the final core-charge states. The experiments show that while the yields of foil-excited Rydberg atoms depend strongly on the incident ionic charge state and the target thickness, they are relatively insensitive to the final charge states. These results show the importance of bulk processes over surface effects in the formation of foil-excited Rydberg atoms. Additionally, these experiments also found some unexpected anomalies in the final-charge-state dependence of the yields which suggested possible shell effects.

We have now repeated these measurements with beams of sulphur and silicon ions in various incident charge states (and specific energies from 2-4 MeV/amu) and find that these anomalies persist. Specifically, we find a decreased yield of Rydberg ions with 3-electron cores for thin targets. For thick targets, we find a strongly enhanced yield of Rydberg ions with 2-electron cores. There is no dependence on final charge state for the other core charges. Furthermore, by reversing the "cleaning" and "ionizing" field strengths, we have found that the enhanced 2-electron yield appears to arise from a delayed rearrangement process downstream of the exciting foil. This latter question is still not understood and is being pursued further.

d. Observation of Electron Density Fluctuations Induced in Solids

(P. J. Cooney,\* A. Faibis, E. P. Kanter, W. Koenig, Y. Yamazaki,† and B. J. Zabransky)

The knock-on collision electrons ( $v_e \sim 2v_i$ ) emitted in the forward direction were measured when 4.5-MeV  $N_2^+$  ions bombarded thin carbon foils. By detecting the Coulomb-explosion fragment ions (with the MUPPATS detector) in coincidence with the secondary electrons, we were able to study the dependence of the electron emission process on the orientation of the internuclear axis of the molecular projectile ions. These experiments have revealed several characteristic features of the electron density fluctuations induced in solids by fast ions. We have found that the overall behavior of the yield is well reproduced by a classical Monte-Carlo simulation incorporating a realistic velocity distribution of the valence electrons [see Fig. 5(a)]. The marked decrease in the knock-on electron yield at an  $N_2^+$  orientation angle of  $\sim 25^\circ$  is due to the enhanced density of electrons expected in the conical region of half angle  $23^\circ$  behind the leading nitrogen ion. This conical region is defined by the Mach cone resulting from the incident ions traversing the carbon foil at about twice the Fermi velocity of the target electrons. For orientation angles which place the trailing ion outside this Mach cone, the observed yield of knock-on electrons is consistent with the Coulomb scattering of free electrons from a point charge of 3.5 [see Fig. 5(b)].

---

\*Millersville University, Millersville, Pa.

†Tokyo Institute of Technology, Tokyo, Japan

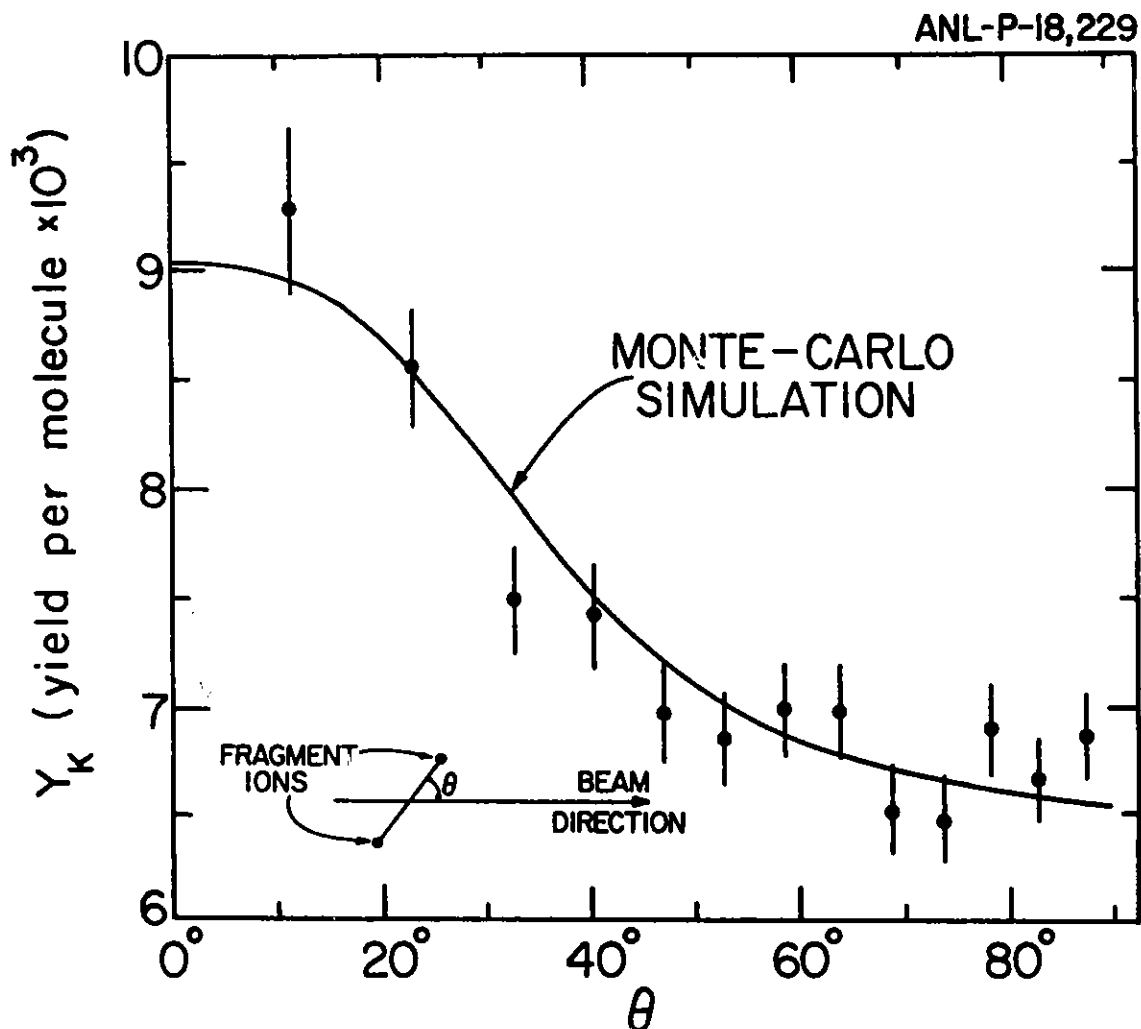


Figure IX-5. (a) The knock-on electron yield as a function of the orientation of the exiting dicluster for 4.5-MeV  $N_2^+$  incident on a  $2\text{-}\mu\text{g}/\text{cm}^2$  carbon foil. The solid line shows the results of a Monte Carlo simulation, taking into account the initial-electron-velocity distribution. The calculation is arbitrarily normalized to the experimental data. (b) The density distribution of electrons scattered by a pure Coulomb potential produced by a point charge of 3.5 plotted as a function of polar angle  $\theta$  at a distance of 2.2 a.u. This distance corresponds to exiting the separation of the fragment ion  $2\text{-}\mu\text{g}/\text{cm}^2$  foil.

## X. THEORETICAL ATOMIC PHYSICS

The Atomic-Physics effort in the Physics Division has normally included a theoretical component which is independent of the experimental programs. Some degree of commonality of interests with one or more of the atomic/molecular experimental groups is clearly a "plus", however. In the recent past this program included K. T. Cheng (ab initio atomic structure theory) and G. L. Goodman (various molecular and atomic problems, on a consulting, part-time basis). Both Cheng and Goodman left the Physics Division early last year and their absence is acutely felt.

Substantial efforts have been made over the past year or so to locate a suitable, strong candidate. In response to letters sent out we have discussed the position with a number of interested theorists, and the process is continuing. Charlotte Froese-Fischer of Vanderbilt University spent the period from January 1 through June 30 of 1986 with us (together with one of her theoretical students), and efforts to attract another outstanding atomic/molecular theorist for a sabbatical stay in the coming year have resulted in arrangements whereby Dr. Chris Bottcher (ORNL) will join us for 12 months beginning in September, 1986 and Dr. Chii-Dong Lin (Kansas State University) will visit for a 4-month period also beginning in September 1986. Independently, we have arranged for Prof. R. S. Berry of the Department of Chemistry of the University of Chicago to hold a continuing joint appointment with (the University and) the Argonne Physics (and Chemistry) Divisions. Prof. Berry and his students will spend time, distributed over a year, at Argonne interacting with our programs.

## XI. ATOMIC PHYSICS AT ATLAS

The new atomic physics beamline at ATLAS was completed and ready for experiments in late 1985. The beamline components are designed to provide two target areas: the first, midway along the beamline (where access into an adjoining laboratory space provides the possibility for a crossed laser-beam/fast ion-beam interaction geometry); and a second larger area at the end of the beamline.

There is an atomic spectroscopy target chamber equipped with a 2.2-meter grazing-incidence spectrometer (a VUV spectrometer can also be made available here). A general-purpose chamber will follow the spectrometer target chamber, in front of a well-shielded beam dump. An existing McPherson hemispherical spectrometer will be installed for high-resolution electron spectroscopy. It will be equipped with a position-sensitive channel plate detector in its focal plane.

A large 90° selection magnet is planned to be installed at the end of the beamline. Its principal purpose will be to provide the possibility of coincidence type measurements between the projectile charge state as measured with a position-sensitive detector in the final magnet focal plane and other channels of collision systems (e.g. photons, x-rays, secondary electrons and recoil ions).

During the first running period after the full ATLAS facility became operational, several atomic physics experiments were scheduled and/or run. Some of the highlights include:



- a. Doppler-free Auger Electron Spectroscopy from Ne-like and Na-like High-Z Atoms (H. G. Berry, L. Curtis,\* R. Haar,\* E. P. Kanter, R. Schectman,\* and D. Schneider†)

We have begun a series of measurements to study the level structures of high-Z Ne-like and Na-like ions. In the first experiments beams of 220-MeV  $\text{Ni}^{17+}$  and  $\text{Ni}^{10+}$  were excited in ion-atom collisions with argon and helium gas targets. The resultant LMM Auger electrons were measured at 0 degrees with a tandem parallel-plate electrostatic spectrometer. Because of the high beam velocity, this technique leads to a large kinematic expansion of the projectile frame electron energy spectrum when measured in the laboratory. These first tests were extremely promising.

The purpose of these experiments is to test fundamental atomic structure theory and models regarding the dynamic excitation processes in highly-ionized multi-electron systems. Measurements of the level structure of highly-stripped heavy ions provide important tests of relativistic many-body problems. Comparisons with theory in many-body systems are most meaningful for ions with a nearly closed shell where the fewest number of configurations are needed to generate accurate relativistic wavefunctions. To date most of the work has been done, both experimentally and theoretically near the closed K-shell. Recently, however, the fluorine-like, neon-like, and sodium-like systems have received a great deal of attention in moderately-ionized ( $Z < 42$ ) systems. There is a need for more experiments to extend these measurements and to study nonradiative decay processes as well. These measurements complement ongoing x-ray spectroscopic studies and yield information regarding branching ratios, etc. This work also complements the existing theoretical effort in the vicinity of the closed shell. Furthermore, these systems are of direct interest to those who deal with high-temperature plasmas, since closed-shell systems persist over a wide range of temperatures and densities.

---

\*University of Toledo, Toledo, Ohio.

†Hahn-Meitner Institute, Berlin, W. Germany.

b. Recoil Gas Spectroscopy (H. G. Berry, L. Engström, A. E. Livingston,\* and K. Galvez\*)

Highly-charged recoil ions at low lab energies (a few eV) are formed in collisions with highly-charged heavy ions. Recent experiments at GSI, Orsay, ALICE, and at Oxford (Tandem) have shown rich photon spectra arising from all charge states of recoil neon ions. Most relevant to this research was the observation of the  $2s^3S - 2p^3P$  transition in two-electron neon.

We have made an initial search of the argon recoil spectrum for transitions in the 3- to 6-electron argon (see Figs. XI-1 and XI-2). The principal goal was the observation of calibration wavelengths in the argon spectrum, and an analysis of the excited-state distributions. To compare with a standard beam-foil measurement such as we have made previously, this technique has one principal advantage: the Doppler broadening and Doppler shifting of the measured spectra are reduced close to zero. The principal disadvantage is the large increase in fluorescence from lower-charged recoil ions. We find that such spectral blending is a severe problem in the argon spectrum.

Precision wavelength measurements will test new recent calculations (Goldman and Drake, to be published) of QED effects in 2-electron systems, and our own calculations in 3- and 4-electron systems.

---

\*University of Notre Dame, South Bend, Indiana.

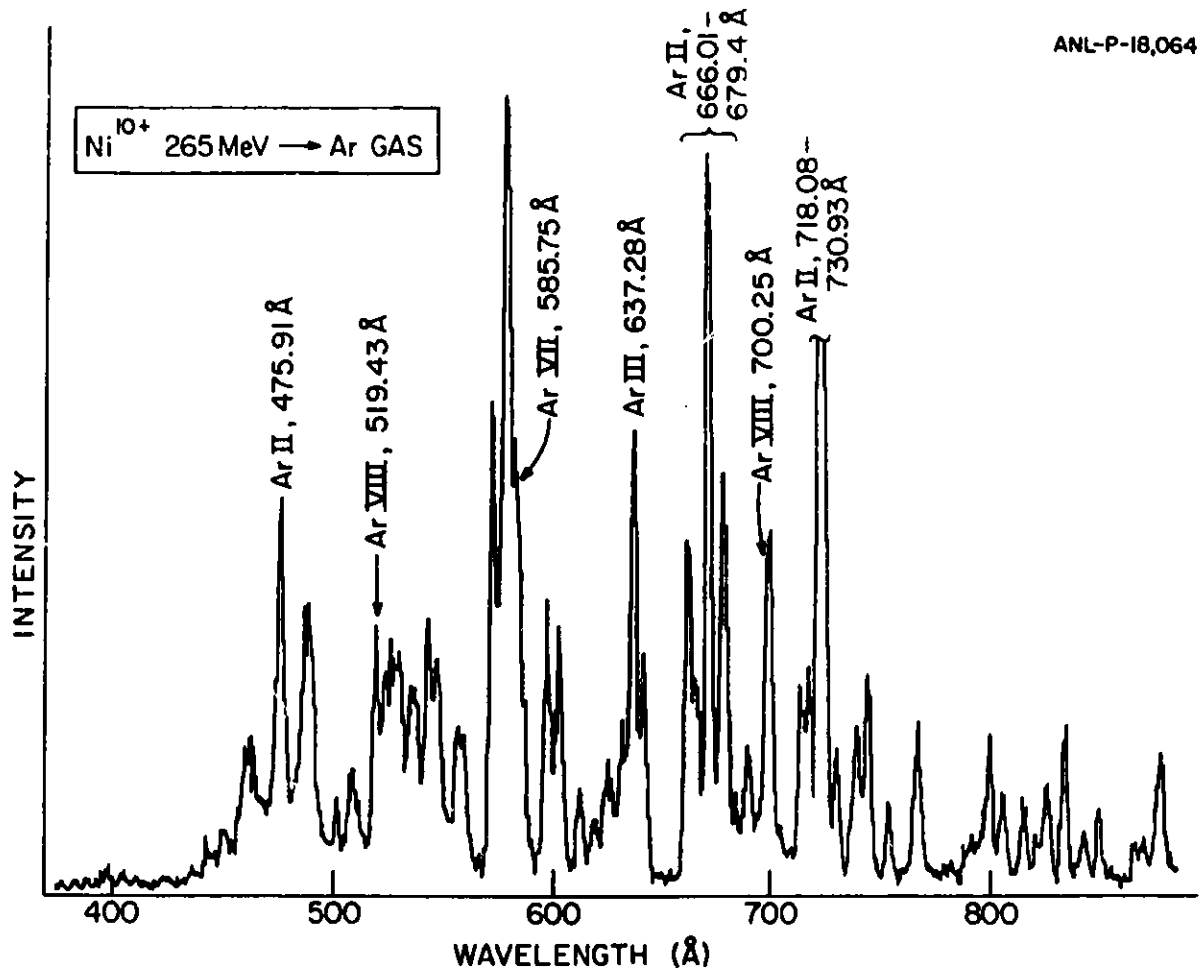


Figure XI-1. Spectrum of argon gas excited by a 265-MeV nickel beam.

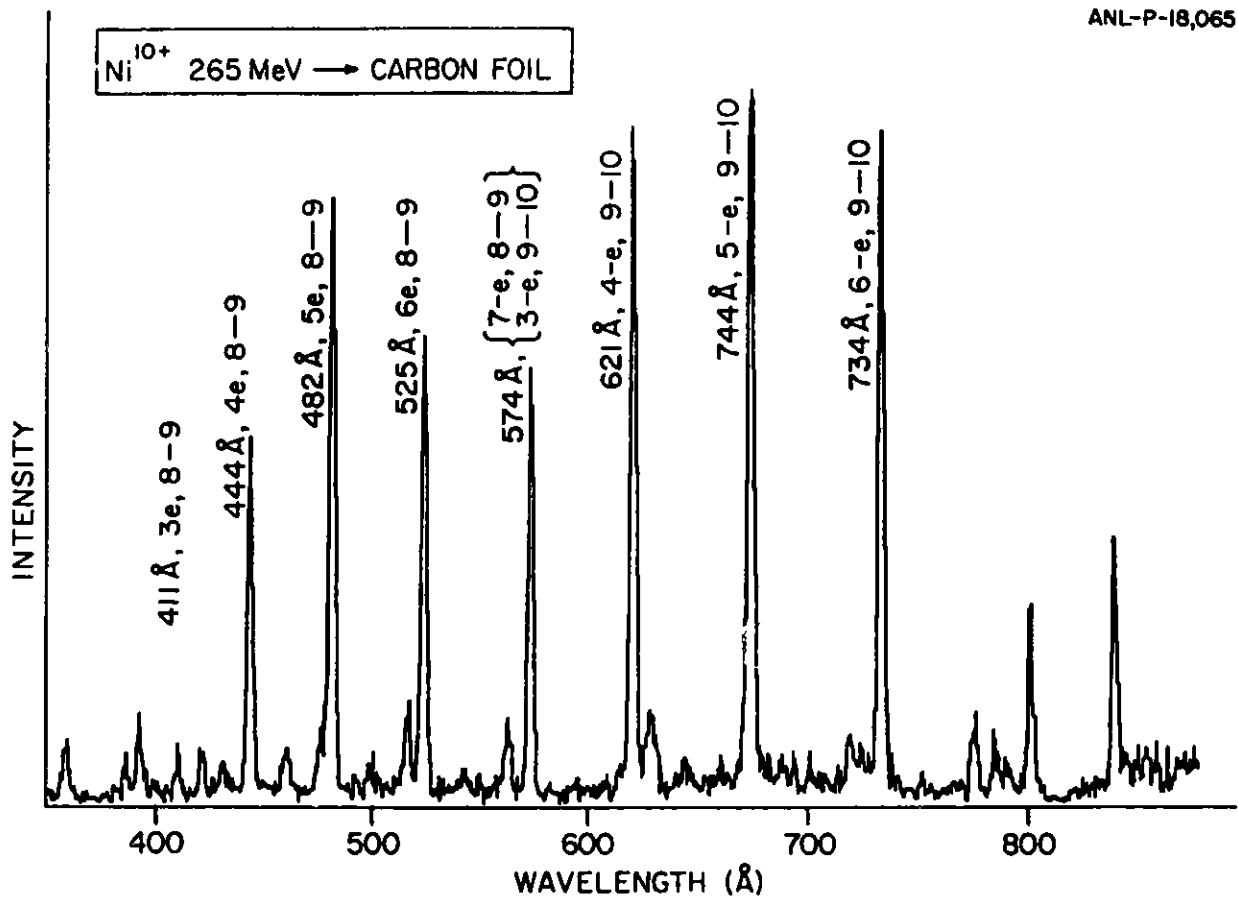


Figure XI-2. Beam-foil spectrum of 265-MeV nickel.

- c. Heavy-ion-induced Desorption of Molecules (D. S. Gemmell, J. E. Hunt,\* E. P. Kanter, W. Koenig, W. Kutschera, R. C. Pardo, and B. J. Zabransky)

The first studies of ion-induced desorption of molecular ions of large organic molecules were performed in 1974 using fission fragments from  $^{252}\text{Cf}$ . This led to the establishment of an analytical technique known as  $^{252}\text{Cf}$  plasma desorption mass spectrometry ( $^{252}\text{Cf}$ -PDMS). A surprising feature found in  $^{252}\text{Cf}$ -PDMS is the relatively high probability for desorption of ionic forms with masses equal to or close to that of the entire adsorbed species. The mass spectrum, which also includes species arising from fragmentation, provides valuable information on the molecular weight and structure of many important molecules for which alternative methods are difficult or non-existent.  $^{252}\text{Cf}$ -PDMS has extended the mass range for mass spectroscopy up to about 25,000. There are very strong incentives for extending the range much higher--up to  $\sim 500,000$  may be possible. An extension up to just 50,000 would bring a host of enzymes, proteins, polymers, and many other compounds of scientific and industrial significance within the scope of mass spectrometry. To extend the attainable range of masses, a careful study of the mechanisms involved in PDMS is needed. Furthermore, such a study is of intrinsic scientific interest--at present very little is understood about the process by which the passage of a fast heavy ion can lead to the desorption of a large and complex organic molecule.

We have initiated at ATLAS a study of the phenomenon through use of pulses of monoenergetic heavy-ion beams in well-established charge states. Related studies have already been undertaken at tandem accelerators in Uppsala and Erlangen involving, however, either lower-mass heavy ions or, with one exception, lower incident charges. From these studies the desorption rate for relatively light molecules was found to be a function of the electronic stopping power [ $-(dE/dx) \propto (q^2/v^2)$ ] where  $q$  is the charge state of the incident heavy ions and  $v$  is its velocity. Both linear and quadratic dependences on the stopping power have been observed depending on the molecular species that was desorbed as well as on its polarity. The quadratic dependence is suggestive of a higher-order process. The dependence on the charge of the incident ion indicates that the energy transfer leading to

---

\*Chemistry Division, ANL.

desorption occurs in a thin atomic layer at the surface of the sample before charge equilibration has occurred. The charge  $q$  determines the "brightness" of the track, while  $v$  determines the interaction distance. For very massive molecules the increase of the desorption yield with the "brightness" appears to be much larger than for lighter molecules. Moreover, very interesting multiplicity distributions of fragment ions are found in coincidence with the desorbed heavy molecules. These throw light on the energy transfer in the desorption process. With ATLAS it is now possible to use much heavier ions as well as higher charge states than was possible up to now to study systematically the desorption process. This may lead to an extension of PDMS to a considerably higher mass range than attainable with the techniques mentioned above.

There is good reason to extend these measurements to ATLAS since there are strong indications that the probability for desorbing very massive molecular ions increases as one goes to high-energy high-Z projectiles.

In our first run at ATLAS, we used single pulses of  $^{58}\text{Ni}$  ions accelerated to 300 MeV in the booster linac. The primary aim in these initial experiments was to demonstrate a "proof of principle". We showed that we can in fact achieve single pulses  $<0.5$  nsec in duration, with a repetition rate of 5.8 kHz, and that we can measure time-of-flight spectra for desorbed ions. Those tests used targets of Zn octylethyl porphine, polyethylene, glycol 400, polystyrene, and CsI. For the first target, the yield of molecular ions (molecular weight = 597) was found to be 0.1 per incident Ni ion. We now plan to proceed to explore the dependence of the desorption probability upon such parameters as projectile velocity and charge state, substrate properties, etc. We plan to use a beam of 400-MeV  $^{127}\text{I}$  ions in order to begin to understand the dependence of the desorption probability on projectile mass.

d. Resonant Transfer and Excitation for Highly-charged Ions

(K. H. Berkner,\* E. M. Bernstein,† M. W. Clark,† W. G. Graham,‡, E. P. Kanter, and J. A. Tanis†)

The overall goal of this research is to probe fundamental atomic interactions in ion-atom collisions by correlating projectile charge-changing events with x-ray emission. Experimentally, this work is carried out by measuring coincidences between x rays (emitted from the projectile and/or target) and the outgoing projectile charge state of interest.

Resonant transfer and excitation (RTE) occurs when capture of a bound target electron is accompanied by simultaneous excitation of the projectile followed by de-excitation via photon emission. This process is analogous to dielectronic recombination (DR) in which the captured electron is initially free instead of bound. RTE and DR proceed via an inverse Auger transition and, hence, are resonant for projectile velocities (in the rest frame of the electron) corresponding to the allowed Auger electron energies. For both RTE and DR many intermediate resonance states are possible, each one corresponding to an allowed Auger transition. Experimentally, observation of a resonant behavior in the x-ray yield associated with capture identifies the RTE mechanism. A formal theoretical treatment of simultaneous charge transfer and excitation in ion-atom collisions has been developed by Feagin, Briggs and Reeves.

DR has been identified as a potential energy-loss mechanism in magnetically confined nuclear fusion plasmas since impurity ions (such as C, O, Fe, etc.) in the plasma can recombine by this mechanism. Hence, DR has been the subject of intense experimental and theoretical investigations. Measurement of cross sections for DR has proven to be a formidable task since either crossed-beam or merged-beam techniques are required and only recently have laboratory measurements of this important fundamental process become available.

---

\*Lawrence Berkeley Laboratory, Berkeley, California.

†Western Michigan University, Kalamazoo, Michigan.

‡The New University of Ulster, Ulster, N. Ireland.

Measurements of RTE indicate that this process closely approximates dielectronic recombination and it appears likely that RTE can be used as a benchmark in testing theoretical calculations of DR cross sections particularly for highly ionized ions. Since RTE can be measured in collisions with static targets, merged or crossed beam techniques are not required. To date DR has been measured only for low charge-state ions (singly-, doubly-charged, etc.) ions while RTE has been measured for high charge states (lithium-like, beryllium-like, etc.)

It is of considerable interest to extend these RTE measurements to heavier ions, from both fundamental and applied points of view. Calculations predict that the structure in the RTE maximum will become more pronounced as  $Z$  increases and that the two maxima which to date are barely resolved, will separate more widely, thereby allowing a more detailed comparison with theory. For molecular hydrogen targets the maxima should become narrower due to the smaller electron momentum distribution in  $H_2$  compared to He. Measurement of RTE (or DR) for iron ions in particular is of interest from the applied point of view since iron is likely to be found as a contaminant in tokamak fusion plasmas. These RTE measurements for iron can only be performed using ATLAS since this is the only accelerator in the United States which can provide sufficiently high energy for the iron ions as well as the required energy and charge-state variability. In our first test experiments at ATLAS we excited 550-MeV  $Ni^{25+}$  ions in a He gas cell and observed both K- and L-x-rays in coincidence with the charge-state-analyzed projectile ions. These experiments used a 2-dimensional position-sensitive low-pressure Breskin gas counter to detect the ions. Because of the high-count-rate capabilities of this detector, we were able, for the first time, to study both the charge-changing and non-charge-changing components of the x-ray spectrum. Furthermore, this setup will allow us to study the impact-parameter dependence of the RTE process.



e. Radiation Chemistry Studies with Heavy Ions (J. A. Laverne\* and R. H. Schuler\*)

Radiation chemical reactions in water and aqueous solutions induced by heavy ions differ from those produced by fast electrons. The local density of radicals and other reactive intermediates within the heavy-ion track can be very high and radical recombination can compete effectively with diffusion into the bulk medium. Heavy-ion track structure and its effect on radiolytic processes can be elucidated by examining the dependence of the yields of radiolytic products on particle energy, charge, linear energy transfer ( $LET = -dE/dx$ ) and local energy density. Extensive studies have been performed on water with heavy ions of up to  $\sim 30$  MeV using the facilities of the Notre Dame Nuclear Structure Laboratory. However, in order to understand track processes in more detail it is important to extend these studies to a variety of more energetic heavy ions having lower LETs. Preliminary studies on the production of  $HO_2\cdot$  from ferrous sulfate-cupric sulfate solutions have been successfully performed using carbon ions of up to 100 MeV produced by ATLAS. These experiments are important because of the increased usage of heavy ions in radiation biology and medical therapy.

Irradiations will be performed using the existing techniques developed at the Notre Dame heavy-ion facility and duplicated in the preliminary studies at ATLAS. The particles are passed through a window assembly consisting of 6.4-mm diameter beam-defining aperture, an electron suppression tube and a  $\sim 4$  mg/cm<sup>2</sup> titanium exit window and into a pyrex sample cell with  $\sim 5$  mg/cm<sup>2</sup> mica window. The beam is stopped in the sample cell and the total current is monitored with absolute doses determined from the particle energy and integrated beam current. High-energy resolution,  $<0.1\%$ , and accurate beam energies are necessary. Beam currents are kept low ( $\sim 2$  pA) to avoid dose rate effects and completely stripped ions are used to avoid an ambiguity in current measurements. The production of oxygen, which in the ferrous-cupric system is equal to the yield of  $HO_2\cdot$ , is measured by bubbling helium through the sample cell and into a Hersch electrolytic cell; the output of the latter is proportional to the oxygen concentration.

---

\*University of Notre Dame, South Bend, Indiana.

Extensive studies have been performed at Notre Dame on the production of  $\text{HO}_2^\bullet$  in the radiolysis of ferrous sulfate-cupric sulfate solutions with  $^1\text{H}$ ,  $^4\text{He}$ ,  $^7\text{Li}$ ,  $^9\text{Be}$ ,  $^{11}\text{B}$  and  $^{12}\text{C}$  ions of a few to  $\sim 30$  MeV initial ion energy. As the particle energy increases the differential yields decrease and, for the lighter ions, approaches the limiting fast electron yield. This observed decrease in yield with increasing particle energy is less pronounced than for  $\text{H}_2$  production from benzene, suggesting that the production of  $\text{HO}_2^\bullet$  is less dependent on the initial local energy density in the particle track. Experiments at Notre Dame are limited to  $\sim 30$  MeV initial ion energy because of instrumental limitations and the fact that considerable energy is lost in the window assembly. Preliminary experiments with carbon ions at ATLAS have extended the ion energy to  $\sim 100$  MeV. At this energy the LET of a carbon ion is comparable to that of a helium ion at its Bragg peak. In this system diffusion of intermediates is important and LET becomes a valid parameter to describe radiolytic processes in the track core. Further experiments with carbon ions up to  $\sim 300$  MeV, where the LET drops to  $\sim 5$  eV/Å, are necessary. These results and experiments with other ions will provide a more comprehensive picture of the radiation chemistry of water. All work will be closely correlated to experimental and theoretical studies currently being carried out at the Notre Dame Radiation Laboratory.

f. Accelerator Development (C. L. Cocke,\* T. J. Gray,\* R. C. Pardo,  
P. Richard,\* K. Shepard and V. Needham\*)

Tests were performed to demonstrate the feasibility of using the ATLAS linac in an accel/decel mode to provide slow highly-charged ions. In these tests a beam of bare 36-MeV oxygen ions was produced by the Argonne FN tandem and injected into the booster linac using nine  $\beta = 0.06$  and three  $\beta = 0.105$  resonators. The beam was decelerated to 5.6 MeV with approximately 40% transmission. The emergent beam measured 3 mm (FWHM) at a distance of 4 meters beyond the linac exit. Those tests proved that the operation of such a linac in the deceleration mode is quite feasible and that it is possible, by appropriate phase and field selection, to decelerate through the zeroes in the universal transit time factor curves. This was a crucial demonstration for the project at Kansas State University to build such a deceleration device. In conjunction with this project, several KSU staff members spent extended periods at ANL this year to gather experience in the fabrication and testing of Argonne-type split-ring resonators.

---

\*Kansas State University, Manhattan, Kansas.

### STAFF MEMBERS OF THE PHYSICS DIVISION

Listed below are the permanent staff of the Physics Division for the year ending 31 March 1986. The program heading indicates only the individual's current primary activity.

#### EXPERIMENTAL NUCLEAR PHYSICS

- \*Irshad Ahmad, Ph.D., University of California, 1966
- †Jack Aron, B.S., Fenn College, 1955
- \*Birger B. Back, Ph.D., University of Copenhagen, 1974
- \*\*R. Russell Betts, Ph.D., University of Pennsylvania, 1972
- ‡Lowell M. Bollinger, Ph.D., Cornell University, 1951
- Cary N. Davids, Ph.D., California Institute of Technology, 1967
- §Melvin S. Freedman, Ph.D., University of Chicago, 1942
- Stuart J. Freedman, Ph.D., University of California, 1972
- Donald F. Geesaman, Ph.D., State University of New York, Stony Brook, 1976
- ¶Bruce G. Glagola, Ph.D., University of Maryland, 1978
- Michael Green, Ph.D., Indiana University, 1983
- ||Walter F. Henning, Ph.D., Technical University, Munich, 1968
- Roy J. Holt, Ph.D., Yale University, 1972
- Harold E. Jackson, Jr., Ph.D., Cornell University, 1959
- Robert V. F. Janssens, Ph.D., Université Catholique de Louvain, Belgium, 1978
- \*Sheldon B. Kaufman, Ph.D., University of Chicago, 1953
- Teng Lek Khoo, Ph.D., McMaster University, 1972
- Dennis G. Kovar, Ph.D., Yale University, 1971
- ††Walter Kutschera, Ph.D., University of Graz, Austria, 1965

---

\*Transferred from Chemistry Division on October 1, 1985.

†Special Term Appointee as of January 6, 1986.

\*\*Transferred from Chemistry Division on October 1, 1985. Temporarily on leave at the University of Oxford, England until July 1, 1986.

‡In charge of tandem-superconducting linac operations and the ATLAS project.

§Resident Associate Guest Appointee.

¶ATLAS User Liaison Physicist.

||Joint appointment with the University of Chicago.

††Temporarily assigned to the University of Munich, W. Germany (September 1985 - September 1986)

- \*Alexander Langsdorf, Jr., Ph.D., Massachusetts Inst. of Technology, 1937  
 \*Frank J. Lynch, B. S., University of Chicago, 1944  
   Thomas Moog, B.A., Princeton University, 1975  
   James Napolitano, Ph.D., Stanford University, 1982  
   Richard C. Pardo, Ph.D., University of Texas, 1976  
   Karl Ernst Rehm, Ph.D., Technical University, Munich, 1973  
 \*G. Roy Ringo, Ph.D., University of Chicago, 1940  
 †Stephen J. Sanders, Ph.D., Yale University, 1977  
 ‡John P. Schiffer, Ph.D., Yale University, 1954  
   Kenneth W. Shepard, Ph.D., Stanford University, 1970  
 \*George E. Thomas, B.A., Illinois Wesleyan, 1943  
 †Flemming Videbaek, Ph.D., University of Copenhagen, 1974  
   Lester C. Welch, Ph.D., University of Southern California, 1970  
 †Bruce D. Wilkins, Ph.D., University of California, 1962  
 §Jan L. Yntema, Ph.D., Free University of Amsterdam, 1952  
   Benjamin Zeidman, Ph.D., Washington University, 1957

#### THEORETICAL NUCLEAR PHYSICS

- ¶Arnold R. Bodmer, Ph.D., Manchester University, 1953  
   Fritz Coester, Ph.D., University of Zurich, 1944  
 †Richard R. Chasman, Ph.D., University of California 1959  
   Henning Esbensen, Ph.D., University of Aarhus, 1977  
 †Dieter Kurath, Ph.D., University of Chicago, 1951  
   Stephen Laudowne, Ph.D., Carnegie-Mellon University, 1970  
   Tsung-Shung Harry Lee, Ph.D., University of Pittsburgh, 1973  
 †James E. Monahan, Ph.D., St. Louis University, 1951

---

\*Special Term Appointee.

†Transferred from Chemistry Division on October 1, 1985.

‡Associate Director of the Physics Division. Joint appointment with the University of Chicago.

§Retired February 28, 1986. Reappointed as a Special Term Appointee.

¶Transferred full time to the University of Illinois at Chicago

Circle on September 30, 1985. Reappointed as a Resident Associate Guest.

‡Resident Associate Guest Appointee.

\*Vijay Pandharipande, Ph.D., University of Bombay, 1969  
 Murray Peshkin, Ph.D., Cornell University, 1951  
 Steven C. Pieper, Ph.D., University of Illinois, 1970  
 Robert B. Wiringa, Ph.D., University of Illinois, 1978

#### ATOMIC AND MOLECULAR PHYSICS

Joseph Berkowitz, Ph.D., Harvard University, 1955  
 H. Gordon Berry, Ph.D., University of Wisconsin, 1967  
 William J. Childs, Ph.D., University of Michigan, 1956  
 †Donald S. Gemmell, Ph.D., Australian National University, 1960  
 Leonard S. Goodman, Ph.D., University of Chicago, 1952  
 Elliot P. Kanter, Ph.D., Rutgers University, 1977  
 ‡Wolfgang Koenig, Ph.D., University of Marburg, 1979  
 §Gilbert J. Perlow, Ph.D., University of Chicago, 1940  
 Zeev Vager, Ph.D. Weizmann Institute of Science, 1962  
 Linda Young, Ph.D., University of California, Berkeley, 1981

#### ADMINISTRATIVE STAFF

¶Richard E. Combs, M.B.A., Lewis University, 1981  
 ¶James R. Specht, A.A.S., DeVry Technical Institute, 1964

---

\*Special Term Appointee.

†Director of the Physics Division.

‡Left the Physics Division in November 1985.

§Retired February 27, 1986. Reappointed as a Resident Associate Guest.

Joint appointment as Editor of Applied Physics Letters.

¶Assistant Director of the Physics Division.

**TEMPORARY APPOINTMENTS**

Postdoctoral Appointees

- Christian Beck (from Centre National de la Recherche Scientifique, France):  
Nuclear physics research at ATLAS.  
(July 1985-- )
- Georg H. Both (from University of Cologne, Germany):  
Accelerator-based atomic physics.  
(September 1985-- )
- Hyuck Cho (from University of Arizona, Tucson, Arizona):  
Photoionization studies.  
(November 1985-- )
- Bronislaw K. Dichter (from Yale University, New Haven, CT)  
Experimental heavy-ion research.  
(October 1985-- )
- Lars Engstrom (from University of Lund, Sweden):  
Accelerator-based atomic physics.  
(September 1984-- )
- Aurel Faibis (from Weizmann Institute of Science, Rehovoth, Israel):  
Structure of molecular ions and interactions of atoms with thin solid  
foils as revealed in fast ion - target collisions.  
(September 1983--September 1985)
- Stephen T. Gibson (from University of Adelaide, Australia):  
UV laser photodissociation of molecular ions and photoionization spectra  
of molecular ions.  
(September 1984--January 1986)
- Romain Holzmann (from University of Louvain, Belgium):  
Gamma-ray spectroscopy of high-spin states.  
(September 1984-- )
- John A. Johnstone (from Los Alamos National Laboratory, New Mexico):  
Coulomb modifications in the  $\pi$  single-particle potential.  
(November 1984-- )
- Joerg G. Keller (from the University of Darmstadt, W. Germany):  
Nuclear physics at ATLAS.  
(October 1985-- )
- Kaidee Lee (from University of Minnesota, Minneapolis, Minnesota):  
Photoionization, photoelectron, and photofragmentation studies.  
(November 1984-- )
- Kevin T. Lesko (from the University of Washington, Seattle, Washington):  
Heavy ion nuclear physics and weak interaction physics.  
(June 1983--July 1985)

Wen Chao Ma (Vanderbilt University, Nashville, Tennessee):  
Heavy ion nuclear physics research.  
(January 1986-- )

Peter Seidl (from Los Alamos National Laboratory, Los Alamos, N.M.):  
Electroproduction of the delta and tensor polarization of the deuteron.  
(September 1985--March 1986)

Amarjit Sen (from the University of Western Ontario, Canada):  
Laser-ion beam studies.  
(June 1985-- )

Adriaan M. Van Den Berg (from the University of Groningen, The Netherlands):  
Experimental nuclear physics using heavy ions.  
(September 1983--June 1985)

Michael Vineyard (Florida State University, Tallahassee, Florida):  
Experimental nuclear physics using heavy ions.  
(January 1984-- )

Tzu-Fang Wang (Yale University, New Haven, Connecticut):  
Heavy ion research at ATLAS.  
(February 1986-- )

Long-Term Visitors (at Argonne more than 4 months)

Isaac D. Abella (University of Chicago, Chicago, Illinois):  
Laser interaction of fast ion beams.  
(October 1983-- )

Colston Chandler (University of New Mexico, Albuquerque, New Mexico):  
N-body quantum scattering theory in two-Hilbert spaces - theory and  
practice of approximations.  
(August 1984--June 1985)

Charlotte Froese-Fischer (Vanderbilt University, Nashville, Tennessee):  
Studies of properties of atomic states.  
(January 1986-- )

Tom J. Gray (Kansas State University, Manhattan, Kansas):  
Linac development.  
(February--July 1985)

Jayant Kumar (University of Minnesota, Minneapolis, Minnesota):  
Laser spectroscopy on radioactive atoms  
(August 1983--August 1985)

\*Harry J. Lipkin (Weizmann Institute of Science, Rehovot, Israel):  
Investigation of current problems in hadron spectroscopy.  
(July 1985-- )

---

\*1985-86 Argonne Fellow.



- Zhenhao Liu (Beijung University, Beijing, Peoples Republic of China):  
Heavy-ion research at ATLAS.  
(April 1985-- )
- Eisuke Minehara (Japan Atomic Energy Research Institute, Tokyo):  
Linac development.  
(February 1985-- )
- William R. Phillips (University of Manchester, England):  
Heavy-ion research at ATLAS.  
(October 1985-- )
- Rolf H. Siemssen (University of Groningen, The Netherlands):  
Investigations of nucleus-nucleus collisions.  
(September 1984--August 1985)
- Yasunori Yamazaki (Tokyo Institute of Technology, Tokyo, Japan):  
Molecular-ion studies.  
(April--August 1985)
- Yun-Yan Zhou (Institute of Modern Physics, Academia Sinica, Lanzhou,  
People's Republic of China): DAPHNE data-acquisition system.  
(September 1985-- )

#### Resident Graduate Students

- Philip W. Arcuni (University of Chicago, Chicago, Illinois): Electron  
spectroscopy of ion-atom collisions. (October 1981--October 1985)
- David T. Baran (Northwestern University, Evanston, Illinois): Medium-energy  
nuclear physics studies. (June 1985-- )
- Jordan B. Camp (University of Chicago, Chicago, Illinois): Weak  
interactions. (October 1982-- )
- Christopher Fasano (University of Chicago, Chicago, Illinois): Quark  
effects in nuclei. (October 1985-- )
- Miles A. Finn (University of Minnesota, Minneapolis, Minnesota):  
On-line laser spectroscopy of radioactive atoms using the  
superconducting linac. (April 1981--October 1985)
- Michael A. Kroupa (University of Chicago, Chicago, Illinois): Search  
for magnetic monopoles using a plastic scintillator array.  
(July 1982-- )
- Frank L. H. Wolfs (University of Chicago, Chicago, Illinois):  
Research in heavy-ion physics. (September 1983-- )

Short-Term Visitors (at Argonne less than 4 months)A. Faculty

- Morris Algranati (Weizmann Institute of Science, Rehovot, Israel):  
Molecular-ion computer documentation. (November 1985)
- Daniel Ashery (Tel Aviv University, Tel Aviv, Israel): Study of pion  
absorption in  $^3\text{He}$ . (May--June 1985)
- Patrick J. Cooney (Millersville State College, Millersville,  
Pennsylvania): Studies of the interaction of fast-moving ions with  
matter.  
(June--July 1985)
- Mark Drigert (University of Notre Dame, South Bend, Indiana): Gamma-ray  
facility for ATLAS. (June--August 1985)
- Hans Enling (GSI, Darmstadt, W. Germany): Nuclear structure studies.  
(November 1985-- )
- Edward L. Hohman (York Community High School, Elmhurst, Illinois):  
Summer high-school student coordinator.  
(June--August 1985)
- Jui Qing Liang (Shanxi University, People's Republic of China):  
Study of the Aharonov-Bohm effect.  
(October 1985--January 1986)
- Charles F. Maguire (Vanderbilt University, Nashville, Tennessee):  
Nuclear research at ATLAS.  
(June--August 1985)
- Ady Mann (The Technion, Haifa, Israel): Molecular-ion studies.  
(June--August 1985)
- Hugh McManus (Michigan State University, E. Lansing, Michigan):  
Pion production and absorption studies.  
(June--August 1985)
- Itzhak Plesser (Weizmann Institute of Science, Rehovot, Israel):  
Molecular-ion studies.  
(October--November 1985)
- Wayne N. Polyzou (University of Iowa, Iowa City, Iowa):  
Relativistic quantum mechanics.  
(May--June 1985)
- Ove Poulsen (University of Aarhus, Aarhus, Denmark):  
Atomic structure measurements using fast-beam laser spectroscopy.  
(May--June 1985)

Francis Prosser (University of Kansas, Lawrence, Kansas):  
Heavy-ion studies at ATLAS  
(June-July 1985)

David Radford (Chalk River Nuclear Laboratory, Canada):  
Studies of high spin on the yrast line.  
(January--February 1986)

Branko Ruscic (Rudjer Boskovic Institute, Zagreb, Yugoslavia):  
Photoionization of atoms and small radicals.  
(June--August 1985)

Ralph E. Segel (Northwestern University, Evanston, Illinois):  
Pion absorption  
(August--September 1985)

Peter B. Treacy (Australian National University, Canberra, Australia):  
Heavy-ion research at ATLAS.  
(August--September 1985)

#### B. Graduate Students

Tomas E. A. Brage (Vanderbilt University, Nashville, Tennessee):  
Hyperfine interactions.  
(January 1986-- )

Ping-Lin Chung (University of Iowa, Iowa City, Iowa):  
Deuteron form factors for high-momentum states.  
(July 1985)

Ulrik Leif Nielsen (University of Aarhus, Aarhus, Denmark):  
Construction of small collinear fast-beam laser interaction facility  
(June--August 1985)

#### Undergraduate Students

Samuel G. Armato III (University of Chicago, Chicago, Illinois):  
(June--August 1985)

Diane Beaty (University of Notre Dame):  
(May--July 1985)

Daniel Boyer (Illinois State University, Normal, Illinois):  
(January 1986-- )

Daniel J. Ciarlette (Lewis University, Lockport, Illinois):  
(October 1985-- )

Thomas Coleman (College of St. Francis, Joliet, Illinois):  
(September 1985-- )

David Dryer (Lewis University, Lockport, Illinois):  
(March--May 1985)

- Robert J. Foley (DePauw University, Greencastle, Indiana):  
(June--August 1985)
- David Hinds (University of Chicago, Chicago, Illinois):  
June--September 1985)
- Regina Hoffman (Lewis University, Lockport, Illinois):  
November 1985--March 1986)
- Andrew Konstantaras (Grinnell College, Grinnell, Iowa):  
(September--December 1985)
- Donna Loucks (College of St. Francis, Joliet, Illinois):  
(June 1984--July 1985)
- Maureen Madden (Lewis University, Lockport, Illinois):  
(March--August 1985)
- Christopher Merrill (Illinois Institute of Technology, Chicago, Illinois).  
(January 1984--June 1985)
- Craig Meyers (University of Illinois, Urbana, Illinois):  
(June--August 1985)
- Kevin O'Grady (Depaul University, Chicago, Illinois):  
(September--December 1985)
- Michael O'Keefe (Lewis University, Lockport, Illinois):  
(November 1984-- )
- Margaret McParland (Midwest College of Engineering, Lombard, Illinois):  
(November 1985-- )
- Bonnie Pewitt (University of Kentucky, Lexington, Kentucky):  
(May--August 1985)
- Paul Reimer (Bethel College, North Newton, Kansas):  
(January 1986-- )
- Nadine Roy (Lewis University, Lockport, Illinois):  
(December 1984--August 1985)
- Eric Sather (University of Chicago, Chicago, Illinois):  
(June--August 1985)
- Anthony Schlinsog (Andrews University, Berrien Springs, Michigan):  
(September--December 1985)
- Stuart Schmidt (Lewis University, Lockport, Illinois):  
(December 1984--August 1985)
- Peter Sobol (Purdue University, W. Lafayette, Indiana):  
(June--August 1985)

James Stewart (University of Michigan, Flint, Michigan):  
(May--August 1985)

John J. Stewart (Lewis University, Lockport, Illinois):  
(August 1983--January 1986)

John Sweetser (Cornell University, Ithaca, New York):  
(June--August 1985)

Kenneth J. Wasniewski (Lewis University, Lockport, Illinois).  
(September 1983--September 1985)

#### TECHNICAL AND ENGINEERING STAFF

Ralph Benaroya

Peter J. Billquist

John M. Bogaty

\*Patric K. Den Hartog

William F. Evans

Joseph Falout

Jack T. Goral

John P. Greene

Ray E. Harden

†Dale J. Henderson

#Donald V. Hulet

James M. Joswick

Raymond B. Kickert

Gary W. Klimczak

Robert Kowalczyk

Charles A. Kurtz

†Paul Markovich

Bruce G. Nardi

James E. Nelson

Walter Ray, Jr.

§Bruce J. Zabransky

Gary P. Zinkann

---

\*Supervisor of tandem-superconducting linac operations.

†Transferred from Chemistry Division on October 1, 1985.

#Transferred from EES Division on March 10, 1986.

§In charge of Dynamitron accelerator operations.

PUBLICATIONS FROM 1 APRIL 1985 THROUGH 31 MARCH 1986

The list of "journal articles and book chapters," is classified by topic; the arrangement is approximately that followed in the Table of Contents of this Annual Review. The "reports at meetings" include abstracts, summaries, and full texts in volumes of proceedings; they are listed chronologically.

JOURNAL ARTICLES AND BOOK CHAPTERS

MEDIUM-ENERGY

Tensor Polarization in Pion-Deuteron Elastic Scattering

E. Ungricht, W. S. Freeman, D. F. Geesaman, R. J. Holt, J. R. Specht,  
B. Ziedman, E. J. Stephenson, J. D. Moses, M. Farkhondeh, S. Gilad, and  
R. P. Redwine

Phys. Rev. C 31, 934 (March 1985)

Prospect for Observation of Polarization in Electron-Deuteron Elastic Scattering at High Momentum Transfer

R. J. Holt, M. C. Green, L. Young, R. S. Kowalczyk, D. F. Geesaman,  
B. Ziedman, L. S. Goodman and J. Napolitano

Proc. of Conference on Nuclear Physics with Electromagnetic Probes,  
11th Europys. Conf. Paris, France, 1-5 July 1985,  
Nucl. Phys. A446, 389-391 (1985)

Prospects for a Deuterium Internal Target, Tensor Polarized by Optical Pumping-Spin Exchange

M. C. Green

Nuclear Physics with Stored, Cooled Beams

Proc. 1984 IUCF Workshop, McCormick's Creek, IN, 14-17 October 1984,  
(AIP Conf. Proc. No. 128 (1985) ed. P. Schwandt and H. O. Meyer)  
p. 268-276

Tensor Polarization in Pion-Deuteron Elastic Scattering

R. J. Holt

Proceedings of the 17th LAMPF Users Group Meeting, Los Alamos, NM  
7-8 November 1983, Report LA-10080-C (April 1984) ed. K. Ruminer and  
B. Talley p. 76-85

Measurement of the  $^{16}\text{N}(2^-, \text{g.s.}) \rightarrow ^{16}\text{O}^+(\text{g.s.}) + e^- + \bar{\nu}_e$  Beta Decay Branching Ratio

Alexandra R. Heath and Gerald T. Garvey

Phys. Rev. C 31, 2190 (1985)

E2 Strength of the Lowest Resonances in  $^6\text{Li}(\alpha, \gamma)$ : Collective Effects in the 1p Shell

J. E. Nelson, J. Napolitano and S. J. Freedman

Phys. Rev. C 31, 2295 (June 1985)

New Experiments with Free Neutrons

Stuart J. Freedman

Physics Today 38(1), S-42 (1985)

Emission of  $^3\text{He}$  and  $^4\text{He}$  in Reactions of 70- and 160-MeV  $\pi^\pm$  Mesons with Ag  
 S. B. Kaufman, D. B. Wilkins, D. J. Henderson, R. E. L. Green,  
 R. G. Korteling and G. W. Butler  
 Phys. Rev. C 32, 1977 (1985)

Complexity and Understanding

Roy Ringo

Physics Today (Letters) Dec. 1985, p. 15

#### HEAVY-ION

Complete Fusion and Quasifission in Reactions Between Heavy Ions

B. Back

Phys. Rev. C 31, 2104 (1985)

High-Sensitivity Alpha-Particle and Electron Spectroscopy

Irshad Ahmad

Nucl. Instrum. Methods A242, 395 (1986)

One-Neutron Transfer in Ni-Ni Interactions Below the Barrier

J. Wiggins, R. Brooks, M. Beckerman, S. B. Gazes, L. Grodzins,

A. P. Smith S. G. Steadman, Y. Xiao and F. Videbaek

Phys. Rev. C 31, 1315 (1985)

One- and Two-Neutron Transfer Reactions with  $^{14}\text{C}$

F. Videbaek, O. Hansen, B. S. Nilsson, E. R. Flynn and J. C. Peng

Nucl. Phys. A433, 441 (1985)

Characteristic Time for Mass Asymmetry Relaxation in Quasi-Fission Reactions

W. Q. Shen, J. Albinski, R. Bock, A. Gobbi, S. Gralla, K. D. Hidenbrand,

N. Herrmann, J. Kuzminski, W. R. J. Muller, H. Stelzer, J. Toke,

B. B. Back, S. Bjornholm, S. P. Sorensen, A. Olmi and G. Guarino

Europhys. Lett. 1, 113 (1986)

Angular Distributions in Heavy-Ion-Induced Fission

B. B. Back, R. R. Betts, J. E. Gindler, B. D. Wilkins, S. Saini,

M. B. Tsang, C. K. Gelbke, W. G. Lynch, M. A. McMahan and P. A. Baisden

Phys. Rev. 32, 195 (1985)

Quasi-elastic Nucleon Transfer and the Heavy-Ion Interaction Potential

A. M. Van Den Berg, W. Henning, I. L. Lee, K. T. Lesko, K. E. Rehm,

J. P. Schiffer, G. S. F. Stephans and F. L. H. Wolfs

Phys. Rev. Lett. 56, 572 (1986)

Spectroscopy of the Heavy-Ion Transfer Reactions  $^{48}\text{Ca}(^{28}\text{Si}, ^{27}\text{Al})^{49}\text{Sc}$

S. D. Hoath, G. C. Morrison, J. M. Nelson, F. Videbaek, P. D. Bond,

Ole Hansen, M. J. Levine, C. E. Thorn and W. Trautmann

Phys. Letts. B154, 33 (1985)

Total Gamma-Ray Spectrum in  $^{153}\text{Ho}$ : From the Yrast Line into the Continuum

D. C. Radford, I. Ahmad, R. Holzmann, R. V. F. Janssens, T. L. Khoo,

M. L. Drigert, U. Garg and H. Helppi

Phys. Rev. Lett. 55, 1727 (1985)

Nuclear Structure Effects in the Feeding of Yrast States of Gd, Dy and Er Nuclei

J. Borggreen, G. Sletten, S. Bjornholm, J. Pederson, R. V. F. Janssens, I. Ahmad, P. Chowdhury, T. L. Khoo, Y. H. Chung and P. J. Daly  
Nuc. Phys. A443, 120 (1985)

Two-Proton Neutron-Hole Yrast Excitations in  $^{147}_{66}\text{Dy}_{81}$

R. Broda, P. J. Daly, Z. W. Grabowski, H. Helppi, M. Kortelahti, J. McNeill, R. V. F. Janssens, R. D. Lawson, D. C. Radford and J. Blomqvist

Z. Phys. A - Atoms and Nuclei 321, 287 (1985)

Feeding Times of High-Spin States in  $^{152,154}\text{Dy}$ : Probes of Nuclear Structure Above the Yrast Line

F. Azgue, H. Enling, E. Grosse, C. Michel, R. S. Simon, W. Spreng, H. J. Wollersheim, T. L. Khoo, P. Chowdhury, D. Frekers, R. V. F. Janssens, A. Pakkanen, P. J. Daly, M. Kortelahti, D. Schwalm and G. Seiler-Clark

Nucl. Phys. A439, 573 (1985)

Transfer Cross Sections for  $^{58}\text{Ni} + ^{58}\text{Ni}$  and  $^{58}\text{Ni} + ^{64}\text{Ni}$  in the Vicinity of the Fusion Barrier

K. E. Rehm, F. L. H. Wolfs, A. M. van den Berg and W. Henning

Phys. Rev. Lett. 55, 280 (1985)

Energy Dependence of the Cross Sections for the  $^{24}\text{Mg}(^{16}\text{O}, ^{12}\text{C})^{28}\text{Si}(\text{g.s.})$  Reaction

S. J. Sanders, H. Ernst, W. Henning, C. Jachcinski, D. G. Kovar, J. P. Schiffer and J. Barrette

Phys. Rev. C. 31, 1775 (May 1985)

Influence of Nucleon Fermi Motion on Incomplete Fusion

G. S. F. Stephans, D. G. Kovar, R. V. F. Janssens, G. Rosner, H. Ikezoe, B. Wilkins, D. Henderson, K. T. Lesko, J. J. Kolata, C. K. Gelbke, B. V. Jacak, Z. M. Koenig, G. D. Westfall, A. Szanto de Toledo, E. M. Szanto and P. L. Gonthier

Phys. Lett. 161B, 60 (1985)

Cross Section Balance in the  $^{14}\text{N} + ^{159}\text{Tb}$  Reactions and the Origin of Fast Alpha Particles

R. H. Siemssen, G. J. Balster, H. W. Wilschut, P. D. Bond, P. C. N. Crouzen, P. B. Goldhoorn, Han Shukui and K. Sujkowski

Phys. Lett. 161B, 261 (1985)

Fission and Particle Decay of Cold Compound Nuclei with High Angular Momentum

K. T. Lesko, W. Henning, K. E. Rehm, G. Rosner, J. P. Schiffer, G. S. F. Stephans, B. Ziedman, and W. Freeman

Phys. Rev. Lett. 55, 803 (1985)

$^{13}\text{B} + ^{13}\text{C}$  and  $^{11}\text{B} + ^{12}\text{C}$  Reactions from 4 to 9 MeV/Nucleon

J. F. Mateja, A. D. Frawley, D. G. Kovar, D. Henderson, H. Ikezoe, R. V. F. Janssens, G. Rosner, G. S. F. Stephans, B. Wilkins, K. T. Lesko, and M. F. Vineyard

Phys. Rev. C 31, 867 (March 1985)



Spontaneous  $^{14}\text{C}$  Emission from  $^{223}\text{Ra}$ 

W. Kutschera, I. Ahmad, S. G. Armato III, A. M. Freidman,  
J. E. Gindler, W. Henning, T. Ishii, M. Paul and K. E. Rehm  
Phys. Rev. C 32, 2036 (1985)

## Could There be an Ordered Condensed State in Beams of Fully Stripped Heavy Ions?

J. P. Schiffer and P. Kienle  
Z. Phys. A - Atoms and Nuclei 321, 181 (1985)

## The Use of Neutral Cs Vapor Flow in a Negative-ion Sputter Source

J. L. Yntema and P. J. Billquist  
Nucl. Instrum. Methods A234, 401 (1985)

## Evaluation of Target Purity Using Various Vacuum Systems

G. E. Thomas, K. E. Rehm and G. W. Klimczak  
Nuclear Targets, Proc. of the 12th World Conf. of the Int. Nucl.  
Target Dev. Soc., Antwerp, Belgium, 25-28 Sept. 1984 (North-Holland-  
Amsterdam 1985) ed. J. van Audenhove and J. Pauwels  
Nucl. Instr. Methods, A236, 658-661 (1985)

## THEORY

## Nuclear Effects in Deep-Inelastic Lepton Scattering

Edmond L. Berger and F. Coester  
Phys. Rev. D 32, 1071 (1985)

## Brueckner-Bethe and Variational Calculations of Nuclear Matter

B. D. Day and R. B. Wiringa  
Phys. Rev. C 32, 1057 (1985)

Theory of Mesonic and Dibaryonic Excitations in the  $\pi\text{NN}$  Scattering System:  
Derivation of the  $^1\text{NN}$  Scattering Equations

T.-S. H. Lee and A. Matsuyama  
Phys. Rev. C 32, 516 (1985)

Validity of the Coupled-Channel Method for the Study of Delta Excitation in  
Intermediate-Energy NN Scattering

T.-S. H. Lee and A. Matsuyama  
Phys. Rev. C 32, 1986 (1985)

Mechanism of the  $^3\text{He}(\pi, pn)$  Reaction

T.-S. H. Lee  
Phys. Rev. C 31, 2163 (1985)

## Study of the Two-Nucleon Mechanism of Pion Absorption in Nuclei

K. Ohta, M. Thies and T.-S. H. Lee  
Ann. Phys. 163, 420 (1985)

Pion Scattering to  $4^-$  States in  $^{14}\text{C}$ 

D. B. Holtkamp, S. J. Seestrom-Morris, D. Dehnhard, S. J. Greene,  
S. J. Harvey, D. Kurath and J. A. Carr  
Phys. Rev. C 31, 957 (1985)

## The Classical Limit of the Surface Response in Fermi Liquids

G. Bertsch and H. Esbensen  
Phys. Lett. 161B, 248 (1985)

Delta Excitations in Heavy Nuclei Induced by ( $^3\text{He},t$ ) and ( $p,n$ ) Reactions

H. Esbensen and T.-S. H. Lee  
Phys. Rev. C 32, 1966 (1985)

Calculation of the Complete Reaction Cross Section for  $^{16}\text{O} + ^{208}\text{Pb}$  Near the Coulomb Barrier

S. C. Pieper, M. J. Rhoades-Brown and S. Landowne  
Phys. Lett. 162B, 43 (1985)

Pair Distributions and Energy-Density Functionals for Liquid  $^4\text{He}$  Drops

S. C. Pieper, R. B. Wiringa and V. R. Pandharipande  
Phys. Rev. B. 32, 3341 (1985)

Coulomb Effects and Charge Symmetry Breaking for the  $A = 4$  Hypernuclei

A. R. Bodmer and Q. N. Usmani  
Phys. Rev. C 31, 1400 (1985)

## Clues to QCD Dynamics from Flavor Dependence of Nucleon Spin-Flip Transition

Harry J. Lipkin  
Phys. Rev. Lett. 53, 2075 (1984)

Calculation of the ( $\Delta$ -h,p-h) Landau Parameter  $g_{\Delta}^{\prime}$  from a Many-Body Hamiltonian Including  $\pi$  and  $\Delta$  Degrees of Freedom

H. Sagawa, T.-S. H. Lee and K. Ohta  
Phys. Rev. C 33, 629 (1986)

Momentum Distribution in  $A = 3$  and 4 Nuclei

R. Schiavilla, V. R. Pandharipande and R. B. Wiringa  
Nucl. Phys. A449, 219 (1986)

## Relativistic Effects in Three-Body Bound States

W. Glockle, T.-S. H. Lee and F. Coester  
Phys. Rev. C 33, 709 (1986)

## Coulomb Polarization Effects in Low Energy P-D Elastic Scattering

G. Y. Bencze and C. Chandler  
Phys. Lett. 163B, 21 (1985)

Shell-Model Studies in  $^{89}\text{Nb}$ 

A. Amusa  
Z. Phys. A322, 567 (1985)

## ATOMIC AND MOLECULAR

Photoionization Mass Spectrometric Study and Ab Initio Calculations of Ionization and Bonding in P-H Compounds; Heats of Formation, Bond Energies, and the  ${}^3B_1-{}^1A_1$  Separation in  $Ph_2^+$

J. Berkowitz, L. A. Curtiss, S. T. Gibson, J. P. Greene, G. L. Hillhouse and J. A. Pople

J. Chem. Phys. 84(1), 375 (1985)

Photoionization of the Amidogen Radical

S. T. Gibson, J. P. Greene and J. Berkowitz

J. Chem. Phys. 83, 4319 (1985)

Photoionization of Atomic Bromine

B. Ruscic, J. P. Greene and J. Berkowitz

J. Phys. B: At. Mol. Phys 17, 1503 (1984)

Ab Initio Calculation of  $4f^N6s^2$  Hyperfine Structure in Neutral Rare-Earth Atoms

K. T. Cheng and W. J. Childs

Phys. Rev. A 31, 2775 (1985)

Electric-Dipole Moments in CaI and CaF by Molecular-Beam Laser-rf Double-Resonance Study of Stark Splittings

W. J. Childs, G. L. Goodman and L. S. Goodman

J. Mol. Spec. 115, 215 (1986)

Emission-Angle-Dependent Post-Collision Interaction

P. W. Arcuni

Phys. Rev. A 33, 105 (1986)

Lifetime Measurements of Core-Excited Quartet Levels in NaI

L. Engstrom, L. Young, L. P. Somerville and H. G. Berry

Phys. Rev. A 32, 1468 (1985)

The Electronic Polarization Induced in Solids Traversed by Fast Ions

Donald S. Gemmell and Zeev Vager

From Treatise on Heavy-Ion Science, Vol. 6, ed. D. Allan Bromley (Plenum Publishing Corp., 1985) pp. 243-284

Charge-State Distribution of Nitrogen Ions Resulting from the Foil-Induced Dissociation of 4.2-MeV  $N_2^+$  Ions

D. Maor, P. J. Cooney, A. Faibis, E. P. Kanter, W. Koenig and

B. Zabransky

Phys. Rev. A 32, 105 (July 1985)

PUBLISHED REPORTS AT MEETINGS

Proceedings of the SNEAP Meeting, Rochester, N.Y., October 3-5, 1983  
University of Rochester Report, ed. by Terry Lund, Eileen Pullara, Yvonne Zaccaria and Clint Cross

Argonne LINAC Status Report  
Richard C. Pardo  
p. 301-311

Argonne Computer Control System for Post-Accelerator ATLAS  
Richard C. Pardo  
p. 341-353

Heavy-Ion Energy Determination From a Post Accelerator ATLAS - Linac  
Richard C. Pardo  
p. 354-362

Competition Between Rotational and Aligned-Particle High-Spin Excitation in  $^{153,154}\text{Dy}$   
A. Pakkanen, M. Kortelahti, R. Broda, Y. H. Chung, P. J. Daly, S. R. Faber, Z. Grabowski, H. Helppi, J. McNeill, J. Wilson, T. L. Khoo, I. Ahmad, J. Borggreen, P. Chowdhury, H. Emling, R. V. F. Janssens and W. Kühn  
Proc. of the 5th Nordic Meeting on Nuclear Physics, Jyväskylä, Finland, 12-16 March 1984 ISEN 951-679-170-0-1985, p. 325-334

Proceedings of the Second Workshop on RF-Superconductivity, Geneva, Switzerland, 23-27 July 1984, Cern Report, ed. H. Lengeler (Nov. 1984)

Status of RF Superconductivity at Argonne National Laboratory  
K. W. Shepard  
p. 9-24

Long Term Operation of Niobium Superconducting Resonators in the Argonne Heavy-Ion Linac  
K. W. Shepard  
p. 447-454

A Soap Opera - The Sad Tale of the Quark  
H. J. Lipkin  
The Quark Structure of Matter, Proceedings of the Yukon Advanced Study Institute, Whitehorse, Yukon, Canada, 12-26 August 1984, ed. N. Isgur, G. Karl, P. J. O'Donnell (World Scientific), 1985  
p. 108-144

Development of Superconducting Niobium Accelerating Structures for Heavy Ions  
K. W. Shepard, S. Takeuchi and G. P. Zinkann  
Proceedings of the Applied Superconductivity Conference, San Diego, 10-13 September 1984 IEEE Trans. Magn. Mag-21, 146-148 (1985).

## Fusion and Limiting Mechanisms

D. G. Kovar

Fundamental Problems in Heavy-Ion Collisions, Proc. of the 5th Adriatic International Conf. on Nuclear Physics, Hvar, Croatia, 24-29 Sept. 1984 (World Scientific Pub. Co., Pte. Ltd. 1984) ed. N. Cindro, W. Greiner and R. Caplar pp. 185-204

## Evaluation of Target Purity Using Various Vacuum Systems

G. E. Thomas, K. E. Rehm and G. W. Klimczak

Nuclear Targets, Proc. of the 12th World Conf. on the Int. Nucl. Target Dev. Soc. Antwerp, Belgium, 25-28 Sept. 1984. (North-Holland-Amsterdam 1985) ed. J. van Audenhove and J. Pauwels  
Nucl. Instr. Methods A236, 658-661 (1985)

## In-Beam Tests of an Air-Core Superconducting-Solenoid Particle Spectrometer

R. Stern, F. Becchetti, T. Casey, J. Janecke, P. Lister, D. Kovar,

R. Janssens, R. Pardo, M. Vineyard and J. J. Kolata

Abst. for Conf. on Instrumentation of Heavy-Ion Nuclear Research, ORNL, 22-24 October 1984, Conf. 841005--Absts., p. 95-97

## DAPHNE...A Parallel Multiprocessor Data-Acquisition System for Nuclear Physics

L. C. Welch

IEEE Trans. Nucl. Sci. NS-32, 238-243 (1985), Proc. of the Nuclear and Plasma Science Symposium, Orlando, FL October 29 - Nov. 2, 1984

## Proc. of the Eighth Int. Conf. on the Application of Accelerators in Research and Industry, Denton, TX. 12-14 Nov. 1984, (North-Holland, 1985)

ed. J. L. Duggan, I. L. Morgan, J. A. Martin

Nucl. Instrum. Methods B10/11, (1985)

## Final-Charge-State-Dependence in the Production of Foil-Excited Heavy Rydberg Atoms

E. P. Kanter, W. Koenig, A. Faibis and B. J. Zabransky

p. 36-38

## Electron Emission Following Fast Ion Impact on Thin Solid Targets

D. Schneider, H. Kudo and E. Kanter

p. 113-115

## A Multiparticle 3D Imaging Technique to Study the Structure of Molecular Ions

W. Koenig, A. Faibis, E. P. Kanter, Z. Vager and B. J. Zabransky

p. 295-265

## Proposed Ion-Atom Collision Facility at Kansas State University

C. L. Cocke, P. Richard, J. S. Eck and R. C. Pardo

p. 838-842

## Unified Approach to Pion Absorption and Double-Charge-Exchange Reactions

T.-S. H. Lee

Proc. of the LAMPF Workshop on Pion Double Charge Exchange, LASL, 10-12 January 1985, LASL Report LA-10550-C, ed. H. W. Baer and M. J. Leitch, 1985, p. 347-355

International Workshop XIII on Gross Properties of Nuclei and Nuclear Excitations, Hirschegg, Kleinwalsertal, Austria, 14-19 January 1985, Report ISSN 0720-8715, ed. Hans Feldmeier

Reaction Studies Near the Barrier for Medium Heavy Systems: Ni + Sn  
W. Henning  
p.23-25

Spontaneous Emission of  $^{14}\text{C}$  from  $^{223}\text{Ra}$   
W. Kutschera, I. Ahmad, S. G. Armato III, A. M. Friedman, J. E. Gindler, W. Henning, T. Ishii, M. Paul and K. E. Rehm  
p. 241

Deep-Inelastic Lepton Scattering by Nuclei: The Pion-Exchange Model  
F. Coester and E. L. Berger  
Proceedings of the Conference on Hadronic Probes and Nuclear Interactions, Arizona State University 11-14 March 1985. AIP New York 1985, ed. Joseph R. Comfort, William R. Gibbs, and Barry G. Ritchie.  
AIP Conf. Proc. 133, 184-191 (1985)

Superconducting Linacs--Some Recent Developments  
L. M. Bollinger  
Proc. of the Fourth International Conference on Electrostatic Accelerator Technology and Associated Boosters, Buenos Aires, Argentina, Apr. 15-19, 1985. (North-Holland 1986) ed. E. Ventura and P. Thieberger, pp. 246-258.  
Nucl. Instru. Methods A244, 246-258 (1986)

Spring Meeting of the American Physical Society, Crystal City, VA, 24-27 April 1985

Measurement of the Energy Dependent Asymmetry in the Beta Decay of  $^8\text{Li}$   
R. A. Bigelow, P. A. Quin, S. J. Freedman and J. Napolitano  
BAPS 30 (4), 701 (1985)

Study of Cross Section Systematics in the System  $^{58}\text{Ni} + \text{Asn}$   
W. Henning, A. Van Den Berg, K. T. Lesko, K. E. Rehm, J. P. Schiffer, G. S. F. Stephans and F. Wolfs  
BAPS 30 (4), 707 (1985)

Quasielastic Processes in the  $^{28}\text{Si} + ^{40}\text{Ca}$  Reaction at 8 MeV/A  
M. F. Vineyard, D. G. Kovar, G. S. F. Stephans, K. E. Rehm, G. Rosner, H. Ikezoe, J. J. Kolata and R. Vojtech  
BAPS 30 (4), 708 (1985)

Study of Quasielastic Transfer Reactions for  $^{58}\text{Ni} + \text{Asm}$  Systems  
A. M. Van Den Berg, K. E. Rehm, D. G. Kovar, W. Kutschera, and G. S. F. Stephans  
BAPS 30 (4), 732 (1985)

Study of Transfer Reactions for the Systems  $^{58}\text{Ni} + ^{58}\text{Ni}$  and  $^{58}\text{Ni} + ^{64}\text{Ni}$  in the Vicinity of the Fusion Barrier

K. E. Rehm, F. Wolfs, A. M. Van Den Berg and W. Henning  
BAPS 30 (4), 733 (1985)

Projectile Breakup of 15-35 MeV/A  $^{14}\text{N}$

G. S. F. Stephans, D. G. Kovar, R. V. F. Janssens, C. K. Gelbke,  
B. V. Jacak, W. Koenig and G. D. Westfall  
BAPS 30 (4), 746 (1985)

Lifetime Measurements in  $^{184}\text{Pt}$ : Evidence for "Intruder" States?

U. Garg, A. Chaudhury, M. W. Drigert, E. G. Funk, J. W. Mihelich,  
D. L. Radford, H. Helppi, R. Holzmann, R. V. F. Janssens, T. L. Khoo  
and A. M. Van den Berg  
BAPS 30 (4), 762 (1985)

Total  $\gamma$ -ray Spectrum from  $^{153}\text{Ho}$  Measured with Compton-Suppressed Spectrometers

R. Holzmann, D. C. Radford, I. Ahmad, R. V. F. Janssens and T. L. Khoo  
BAPS 30 (4), 761 (1985)

Spontaneous Decay of  $^{223}\text{Ra}$  by  $^{14}\text{C}$  Emission

W. Kutschera, I. Ahmad, S. G. Armato III, A. M. Freidman, J. E. Gindler,  
W. Henning, T. Ishii, M. Paul and K. E. Rehm  
BAPS 30 (4), 777 (1985)

Proceedings of the Workshop on Some Aspects of Autoionization in Atoms and Small Molecules, ANL-PHY-85-3, November 1985, May 2-3, 1985, Argonne National Laboratory, Argonne, Illinois

Mechanisms of Autoionization in Atoms Inferred from Recent Experiments

J. Berkowitz  
p. 15-30

Distortion of He\*\* Emission Lines after Fast-Ion Collisions

P. W. Arcuni  
p. 233-240

1985 Particle Accelerator Conference, Vancouver, B. C. Canada, 13-16 May 1985

A Camac-Based Intelligent Subsystem for ATLAS. Example Application:  
Cryogenic Monitoring and Control

R. C. Pardo, Y. Kawarasaki and K. Wasniewski  
IEEE Trans. Nucl. Sci. NS-32 (5), 2017-2019 (1985)

A Superconducting Heavy Ion Injector Linac

K. W. Shepard  
IEEE Trans. Nucl. Sci. NS-32 (5), 3574-3577 (1985)

Atomic Physics Program Contractor's Workshop, 13-14 May 1985, Chapel Hill, N.C., Book of Abstracts

Photoionization, Photoelectron Spectroscopy and UV-Laser Photodissociation  
J. Berkowitz, S. Gibson, J. P. Greene and K. Lee  
pp. 19-21

Interactions of Fast Atomic and Molecular Ions with Matter  
A. Faibis, E. P. Kanter, W. Koenig, Z. Vager and D. S. Gemmell  
pp. 39-41

Fast Ion Spectroscopy  
H. G. Berry, L. Young, L. Engstrom, L. P. Somerville and P. W. Arcuni  
pp. 48-50

Electric Dipole Moment of CaI ( $X\Sigma^{2+}$ ) by Molecular-Beam, Laser-rf Double Resonance  
W. J. Childs and L. S. Goodman  
pp. 51-53

The Fourth Conference on Real-time Computer Applications in Nuclear and Particle Physics, Chicago, Illinois, 20-24 May 1985  
IEEE Trans. Nuc. Sci. NS-32, (1985)

DAPHNE... The Design of a Parallel Multiprocessor Data-Acquisition System  
R. T. Daly, T. H. Mood and L. C. Welch  
1379-1383

DAPHNE... A Parallel Multiprocessor Data-Acquisition System-Software  
L. C. Welch, R. T. Daly, D. Loucks, T. H. Moog and J. Stewart  
p. 1405-1408

Proceedings of the Symposium on Electromagnetic Properties of High Spin States, Stockholm 29-31 May 1985, Report AFI 85, ed. I. Bergstrom

Information on Continuum States from Feeding Times and Total  $\gamma$  spectra Measured with BGO Suppressed Detectors  
T. L. Khoo, I. Ahmad, P. Chowdhury, D. Frekers, R. Holzmann, R. V. F. Janssens, D. C. Radford, F. Azguez, H. Emling, M. W. Drigert, U. Garg, H. Helppi, A. Pakkanan, P. J. Daly and M. Kortelahti  
Paper #9 Tuesday pp. 1-12

Suppression of Neutron Emission in Heavy-Ion Induced Fusion Reactions: Entrance Channel Effect and/or Superdeformed Shapes?  
R. V. F. Janssens, R. Holzmann, W. Henning, T. L. Khoo, K. T. Lesko, D. C. Radford, G. S. F. Stephans, A.M. Van den Berg, W. Kuhn, V. Metag, A. Ruckelshausen, D. Habs, H. Groger, R. Repnow, S. Hlavac, R. S. Simon, G. Duchin, R. Freeman, B. Haas, F. Haas and R.M. Ronningen  
Paper #16 Thursday pp. 1-6



16th Annual Meeting of the Division of Electron and Atomic Physics, American Physical Society, Norman, OK, 29-31 May 1985

Angle-dependent Post-collision Interaction

Philip Arcuni

Bull. Am. Phys. Soc. 30, 847 (1985)

Charge State Distributions of Nitrogen Ions Resulting from the Foil-induced Dissociation of 4.2 MeV  $N_2^+$  Ions

P. J. Cooney, A. Faibis, E. P. Kanter, W. Koenig, D. Maor and  
B. J. Zabransky

Bull. Am. Phys. Soc. 30, 861 (1985)

The  $1s2s^3S-1s2p^3P$  Fine Structure Transitions in Helium-like Titanium ( $Ti^{20+}$ )

E. J. Galvez, A. E. Livingston, A. J. Mazure, H. G. Berry,  
L. P. Somerville and J. E. Hardis

Bull. Am. Phys. Soc. 30, 859 (1985)

Lifetime Measurements of Core-Excited Quartet Levels in Na

L. Engstrom, L. Young, L. P. Somerville and H. G. Berry

Bull. Am. Phys. Soc. 30, 879 (1985)

Electric Dipole Moments of the  $X\Gamma^{2+}$  Ground States of CaI and CaF by Molecular-beam Laser-rf Double Resonances

W. J. Childs and L. S. Goodman

Bull. Am. Phys. Soc. 30, 879 (1985)

Recent Wavelength Measurements in 2- and 3-electron Systems

H. G. Berry

Proc. Atomic Theory Workshop on Relativistic and QED Effects in Heavy Atoms, Gaithersburg, MD. 23-24 May 1985, ed. Hugh P. Kelly and Yong-Ki Kim, AIP Conference Proceedings 136 (1985) pp. 94-99

Mechanisms of Autoionization Inferred from Recent Experiments

J. Berkowitz

33rd Ann. Conf. on Mass Spectrometry and Allied Topics, San Diego, CA 26-31 May 1985, Book of Abstracts, p. 15

Report of the Internal Target Working Group

R. J. Holt

Proc. of CEBAF/SURA 1985 Summer Workshop, Newport News, VA, 3-7 June 1985, ed. Hall Crannell and Franz Gross, CEBAF Report December 1985, p. 45-56

Deep Inelastic Muon Scattering with Hadron Detection

D. F. Geesaman and M. C. Green

Proc. of CEBAF/SURA 1985 Summer Workshop, Newport News, VA, 3-7 June 1985, ed. Hall Crannell and Franz Gross, CEBAF Report December 1985, p. 222-236

## Relativistic Multiple Scattering Theories

F. Coester

Proc. of the International Symposium on Medium Energy Nucleon and Antinucleon Scattering, Bad Honnef, W. G. , 18-21 June 1985, Springer-Verlag 1985, ed. H. V. van Geramb  
Lecture Notes in Physics 243, 377-390 (1985)

Fourteenth International Conference on the Physics of Electronic and Atomic Collisions, Palo Alto, CA, 24-30 July 1985. Book of Abstracts of Contributed Papers, ed. M. J. Coggiola, D. L. Huestis, R. P. Saxon

Anomalies in the Final-Charge-State Dependence of Foil-Excited, Fast Heavy Rydberg Atoms

W. Koenig, A. Faibis, E. P. Kanter, J. Sokolov, B. J. Zabransky, and Z. Vager  
p. 457

A Detection System to Study the Stereochemistry of Molecular Ions

A. Faibis, W. Koenig, E. P. Kanter, Z. Vager and B. J. Zabransky  
p. 660

Energy Dissipation in Heavy Systems: The Transition from Quasielastic to Deep-Inelastic Scattering

K. E. Rehm, A. van den Berg, J. J. Kolata, D. G. Kovar, W. Kutschera, G. Rosner, G. S. F. Sephans, J. L. Yntema and L. L. Lee  
Proc. 1984 INS-RIKEN International Symposium on Heavy Ion Physics, Mt. Fuji, 27-31 Aug. 1985, ed. S. Kubono, M. Ishihara, M. Ichimura  
Suppl. J. Phys. Soc. Japan 54, 410-421 (1985)

Nuclear Structure and Reactions Studied with the Darmstadt-Heidelberg Crystal Ball

V. Metag, R. D. Fischer, G. Koch, W. Kühn, r. Muhlshans, R. Novotny, A. Ruckelshausen, H. Stroher, D. Habs, H. J. Henrich, W. Hennerici, R. Repnow, H. Groger, R. Kroth, D. Schwalm, S. Hlavac, W. Reisdorf, R. S. Simon, R. V. F. Janssens, T. L. Khoo, A. Lazzarini, H. Gemmeke, D. Konnerth, W. Dunnweber, W. Hering, W. Trautmann, W. Trombik, D. Freeman, B. Haas and F. Hass  
Proc. 1984 INS-RIKEN International Symposium on Heavy Ion Physics, Mt. Fuji, 27-31 Aug. 1985, ed. S. Kubono, M. Ishihara, M. Ichimura  
Suppl. J. Phys. Soc. Japan 54, 439-455 (1985)

Bond Energies of Nitrogen and Phosphorous Hydrides and Fluorides

J. Berkowitz, S. T. Gibson, J. P. Greene, O. M. Neskovic and B. Ruscic  
Abstract for the Int. Symp. on Applications of Mathematical Concepts to Chemistry, Dubrovnik, Croatia, Yugoslavia, 2-5 Sept. 1985, Book of Abstracts

Autoionization in Molecules - A Path Toward Better Understanding

J. Berkowitz, B. Ruscic, S. T. Gibson and J. P. Greene  
Abstract for the Int. Symp. on Applications of Mathematical Concepts to Chemistry, Dubrovnik, Croatia, Yugoslavia, 2-5 Sept. 1985, Book of Abstracts

## Photoionization Mass Spectrometry of Transient Species

S. T. Gibson, J. Berkowitz and J. P. Greene

190th Am. Chem. Soc. Meeting, Chicago, IL 8-13 September 1985,  
Book of Abstracts ACS ISBN 8412-0927-8, Div. Phys. Chem. #50

American Physical Society Meeting, Asilomar, CA, 28-30 October 1985

## Use of an Enge Split-pole Spectrograph as a Gasfilled Magnetic Separator

W. Henning, M. Paul, W. Kutschera, K. E. Rehm and R. H. Siemssen

BAPS 30, 1249 (1985)Elastic Scattering and Total Reaction Cross Sections for  $^{58}\text{Ni} + \text{Asn}$ F. L. H. Wolfs, A. van den Berg, W. Henning, K. E. Rehm, J. P. Schiffer,  
R. H. Siemssen and W. S. FreemanBAPS 30, 1279 (1985)Coincidences Between Heavy ( $A \geq 12$ ) Reaction Products from  $^{28}\text{Si} + ^{28}\text{Si}$  at  
9 MeV/AJ. Hinnefeld, J. Kolata, D. Henderson, R. Janssens, D. Kovar, K. Lesko,  
S. Sanders, G. Stephans, M. Vineyard, B. Wilkins, F. Prosser and  
V. ReinertBAPS 30, 1246 (1985)Fusion-evaporation Cross Sections for  $^{24}\text{Mg} + ^{24}\text{Mg}$  at  $5 < E_{\text{lab}} < 9$  MeV/AF. W. Prosser, S. V. Reinert, D. G. Kovar, G. Rosner, G. S. F. Stephans,  
J. J. Kolata, A. Szanto de Toledo and E. SzantoBAPS 30, 1279 (1985)Quasielastic Processes in the  $^{28,30}\text{Si} + ^{206,208}\text{Pb}$  Reactions at 6 MeV/A and  
8 MeV/AA. R. Vojtech, J. Kolata, K. E. Rehm, D. Kovar, G. Stephans, G. Rosner  
and H. IkezoeBAPS 30, 1280 (1985)Effects of  $\pi\pi$  Correlation in  $\pi\text{N}$  Scattering

John A. Johnstone and T.-S. Harry Lee

BAPS 30, 1260 (1985)

## Performance of a Large Bragg-Curve Spectrometer

M. F. Vineyard, D. Henderson, D. G. Kovar and B. Wilkins

BAPS 30, 1250 (1985)Proximity Effects in the Alpha Emission from Deep-inelastic Collisions of 280-  
MeV  $^{32}\text{S}$  with  $^{58}\text{Ni}$ P. L. Gonthier, R. Ramaker, R. Kryger, D. Mogridge, M. Kort, K. Price,  
D. Kovar, M. Vineyard, G. Stephans, B. Wilkins and A. Van den BergBAPS 30, 1281 (1985)Analysis of Transfer Reactions for the System  $^{48}\text{Ti} + ^{208}\text{Pb}$  Within a Random  
Walk Model

K. E. Rehm

BAPS 30, 1280 (1985)

Electron Spectrum Following Fission of  $^{252}\text{Cf}$

D. Wark, J. Camp and G. Garvey

BAPS 30, 1272 (1985)

Strange Quark Mass in a Chiral SU(3) Bag Model

John A. Johnstone

BAPS 30, 1260 (1985)

1985 Southeastern Sectional APS Meeting, Athens, GA, 2-4 December 1985

Calibration of Relative Pulse Height vs. Energy for NaI(Tl) Light Charged Particle Spectrometers

C. F. Maguire, D. G. Kovar, C. Beck, C. N. Davids, D. Henderson,

M. F. Vineyard, F. W. Prosser, S. V. Reinert and J. J. Kolata

Bull. Am. Phys. Soc. 30, 1769 (1985)

Opportunities in Nuclear Physics with Internal Targets in Electron Storage Rings

R. J. Holt

Bull. Am. Phys. Soc. 30, 1772 (1985)

#### Informal Reports

Dissipative Heavy-ion Collisions

Hans H. Feldmeier

Lecture series delivered at Argonne during October and November 1984.

Report No. ANL-PHY-85-2

Proceedings of the Workshop on Some Aspects of Autoionization in Atoms and Small Molecules

ed. H. G. Berry, J. Berkowitz, and R. S. Berry

ANL Report No. ANL-PHY-85-3. Meeting held May 2-3, 1985

Distribution for ANL-86-22Internal:

Ahmad, I.	Green, M. C.	Pewitt, E. G.
Avery, R.	Henderson, D. J.	Pieper, S. C.
Back, B. B.	Holt, R. J.	Rehm, K. E.
Baran, D.	Huberman, E.	Ringo, G. R.
Berkowitz, J.	Inokuti, M.	Sanders, S. J.
Berry, H. G.	Jackson, H. E.	Schiffer, J. P.
Betts, R. R.	Janssens, R. V. F.	Segel, R. E.
Bodmer, A. R.	Kanter, E. P.	Sen, A.
Bollinger, L. M.	Kaufman, S. B.	Shepard, K. W.
Camp, J.	Khoo, T.-L.	Smither, R. K.
Chasman, R. R.	Klotz, C. E.	Springer, R. W.
Childs, W. J.	Kovar, D. G.	Steinberg, E. P.
Cissel, D. W.	Krisciunas, A. B. (12)	Tack, L.
Coester, F.	Kroupa, M.	Thayer, K. J. (63)
Combs, R. E.	Kurath, D.	Till, C. E.
Davids, C. N.	Kutschera, W.	Vager, Z.
Dehmer, P. M.	Landowne, S.	Videbaek, F.
Den Hartog, P. K.	Langsdorf, A.	Welch, L. C.
Derrick, M.	LeSage, L. G.	Wilkins, B. D.
Diebold, R. E.	Lee, K.	Wiringa, R. A.
Dunford, R. W.	Lee, T.-S. H.	Wolfs, F. J. L.
Esbensen, H.	Lewis, R. A.	Yntema, J. L.
Fasano, C.	Lynch, F. J.	Young, L.
Fradin, F. Y.	Messina, P.	Zabransky, B. J.
Freedman, M. S.	Monahan, J. E.	Zeidman, B.
Freedman, S. J.	Moog, T.	ANL Contract File
Geesaman, D. F.	Napolitano, J. J.	ANL Libraries
Gemmell, D. S.	Pardo, R. C.	ANL Patent Dept.
Glagola, B.	Perlow, G. J.	TIS Files (6)
Goodman, L. S.	Peshkin, M.	

External:

DOE-TIC, for distribution per UC-34 in TID-4500 Report (81)  
 Manager, Chicago Operations Office, DOE  
 Physics Division Review Committee:

- F. Calaprice, Princeton U.
- J. W. Cronin, U. Chicago
- W. Happer, Jr., Princeton U.
- H. P. Kelly, U. Virginia
- A. K. Kerman, Massachusetts Inst. Technology
- P. Kienle, GSI
- S. E. Koonin, California Inst. Technology
- S. R. Nagel, U. Chicago
- P. Paul, State U. of New York, Stony Brook

Y. Abe, Kyoto U., Japan  
 A. Abragam, CEN Saclay, France  
 E. G. Adelberger, U. Washington  
 K. W. Allen, Oxford U., England  
 O. Almen, Chalmers U. Technology, Gothenburg, Sweden  
 J. Alster, Tel-Aviv U., Ramat Aviv, Israel  
 A. Amusa, U. Ife, Ile-Ofe, Nigeria  
 G. Anagnostatos, Aghia Paraskevi-Attikis, Athens, Greece  
 N. Anantaraman, VEC Laboratory, Calcutta, India  
 J. U. Anderson, U. Aarhus, Denmark  
 D. Ashery, Tel Aviv U., Israel  
 S. Aziz, Indiana U.  
 P. J. Ball, Nuclear Enterprises Ltd., Edinburgh, Scotland  
 J. B. Ball, Oak Ridge National Lab.  
 E. Barnard, Atomic Energy Board, Pretoria, South Africa  
 G. B. Beard, Wayne State U.  
 B. Bederson, New York U.  
 I. Bergstrom, Nobelinstitut fur Fysik, Stockholm, Sweden  
 K. Bethge, U. Frankfurt, Germany  
 M. R. Bhiday, U. Poona, India  
 C. H. Blanchard, U. Wisconsin, Madison  
 A. E. Blaugrund, Weizmann Inst. of Science, Rehovot, Israel  
 J. Blok, Free U., Amsterdam, The Netherlands  
 H. E. Blosser, Michigan State U.  
 R. Bock, GSI, Darmstadt, Germany  
 A. Bohr, Inst. Theoretical Physics, Copenhagen, Denmark  
 J. Borggreen, Niels Bohr Inst., Roskilde, Denmark  
 R. L. Boudrie, Los Alamos National Lab.  
 T. J. Bowles, Los Alamos National Lab.  
 A. J. F. Boyle, U. Western Australia, Nedland, Western Australia  
 D. Branford, U. of Edinburgh, Edinburgh, Scotland  
 M. Braun, Research Inst. of Physics, Stockholm, Sweden  
 D. A. Bromley, Yale U.  
 F. D. Brooks, U. Cape Town, Rondebosch, Cape, S. Africa  
 G. E. Brown, State U. of New York, Stony Brook  
 D. L. Bushnell, Northern Illinois U.  
 P. Caruthers, Los Alamos National Lab.  
 P. Catillion, CEN Saclay, France  
 J. Cerny, Lawrence Berkeley Lab.  
 L. T. Chadderton, Clayton, Victoria, Australia  
 S. Chakravarti, Jadavpur U., Calcutta, India  
 L. Chan, Chicago, IL  
 C. Chandler, U. New Mexico  
 A. Chatterjee, Bhabha Atomic Research Centre, Bombay, India  
 A. Chaudhury, U. Notre Dame  
 K. T. Cheng, Lawrence Livermore National Lab.  
 G. F. Chew, Lawrence Berkeley Lab.  
 P. Chowdhury, Reactor Research Centre, Tamil Madu, India  
 C. J. Christensen, Danis AEC, Roskilde, Denmark  
 P.-L. Chung, U. Iowa  
 W. A. Chupka, Yale U.  
 J. W. Clark, Washington U.  
 C. M. Class, Rice U.  
 T. B. Clegg, U. North Carolina

C. Coceva, ENEA, Centro "E. Clementel", Bologna, Italy  
C. L. Cocke, Kansas State U.  
S. Cohen, Speakeasy Computing Corp., Chicago, IL  
D. R. Cok, Eastman Kodak Research Labs., Rochester, NY  
P. J. Cooney, Millersville State College, Millersville, PA  
B. Crasemann, U. Oregon  
J. Cseh, Inst. Nucl. Rsch., Hungarian Ady. Sci., Debrecen Hungary  
N. Cue, State U. of New York, Albany  
S. E. Darden, U. Notre Dame  
J. A. Davies, Chalk River Nuclear Labs.  
D. Dazhao, Beijing, China  
R. Deslattes, National Bureau of Standards, Washington, DC  
R. M. DeVries, Los Alamos National Lab.  
P. T. Debevec, U. Illinois  
D. Dehnhard, U. Minnesota  
J. Delaunay, CEN Saclay, France  
H. de Waard, Rijksuniversiteit, Groningen, The Netherlands  
B. Donnally, Lake Forest College, Lake Forest, IL  
T. R. Donoghue, Ohio State U.  
M. Drigert, U. Notre Dame  
A. K. Edwards, U. Georgia  
H. Ehrhardt, U. Kaiserslautern, Germany  
Y. Eisen, SOREQ Nuclear Center, Yavne, Israel  
F. ElBedewi, Atomic Energy Establishment, Dokky, Cairo, Egypt  
M. ElNadi, Cairo U., Egypt  
J. H. D. Eland, U. Oxford, England  
A. J. Elwyn, Fermi National Accelerator Lab.  
H. Emling, GSI, Darmstadt, Germany  
L. Engstrom, U. Lund, Sweden  
G. N. Epstein, Massachusetts Inst. Technology  
J. R. Erskine, Div. Nuclear Physics, USDOE  
H. C. Evans, Queens U., Kingston, Ontario, Canada  
A. Faibis, Weizmann Inst. of Science, Rehovot, Israel  
L. C. Feldman, AT&T Bell Laboratories, Murray Hill, NJ  
H. Feldmeier, GSI, Darmstadt, Germany  
A. T. G. Ferguson, Atomic Energy Research Establishment, Berks., England  
B. Filippone, California Inst. Technology  
A. A. Forster, Tech. U. Munich, Garching, Germany  
H. T. Fortune, U. Pennsylvania  
J. L. Fowler, Oak Ridge National Lab.  
J. D. Fox, Florida State U.  
D. Frekers, TRIUMF, Vancouver, BC, Canada  
F. Fujimoto, U. Tokyo, Japan  
C. A. Gagliardi, Texas A&M U.  
N. Gangas, U. Ioannina, Greece  
U. Garg, U. Notre Dame  
G. T. Garvey, Los Alamos National Lab.  
H.-U. Gersch, Zfk Rossendorf, Democratic Republic of Germany  
S. T. Gibson, Australian National U., Canberra, Australia  
S. Gil, Tandem-CNEA, Buenos Aires, Argentina  
P. Gilles, U. Kansas  
N. K. Glendenning, Lawrence Berkeley Lab.  
P. F. A. Goudsmit, SIN, Villigen, Switzerland  
H. E. Gove, U. Rochester

T. J. Gray, Kansas State U.  
 K.-O. Groeneveld, U. Frankfurt, Germany  
 E. E. Gross, Office of High Energy and Nuclear Physics, DOE  
 H. Grunder, CEBAF  
 Y. Gu, Fudan U., Shanghai, China  
 D. Habs, Max-Planck Inst. fur Kernphysik, Heidelberg, Germany  
 W. Haeberli, U. Wisconsin, Madison  
 I. Halpern, U. Washington  
 M. Hamermesh, U. Minnesota  
 J. W. Hammer, Inst. Strahlenphysik, Stuttgart, Germany  
 I. Hamouda, Atomic Energy Establishment, Cairo, Egypt  
 S. S. Hanna, Stanford U.  
 A. O. Hanson, U. of Illinois  
 J. C. Hardy, Chalk River Nuclear Lab., Ontario, Canada  
 M. A. Harith, Cairo U., Cairo, Egypt  
 B. G. Harvey, Lawrence Berkeley Lab.  
 M. Hasan, Northern Illinois U.  
 J. Hattula, U. Jyvaskyla, Finland  
 D. L. Hendrie, Office of High Energy and Nuclear Physics, USDOE  
 E. M. Henley, U. Washington  
 W. Henning, GSI, Darmstadt, Germany  
 R. G. Herb, National Electrostatics Corp., Middleton, WI  
 W. H. A. Hesselink, van de Vriji U., De Boelelaan, The Netherlands  
 K. Hida, U. Tokyo, Japan  
 R. E. Holland, Downers Grove, IL  
 H. Hotop, U. Kaiserslautern, Germany  
 V. W. Hughes, Yale U.  
 J. R. Huizenga, U. of Rochester  
 H. Ikezoe, JAERI, Tokai Rsch. Establishment, Ibaraki-ken, Japan  
 M. Inghram, U. Chicago  
 D. R. Inglis, U. Massachusetts  
 M. Ismail, Bhabha Atomic Research Centre, Calcutta, India  
 K. Iwantani, Hiroshima U., Japan  
 C. E. Johnson, U. Liverpool, Liverpool, Merseyside, England  
 G. Jonkers, Free U., Amsterdam, The Netherlands  
 P. B. Kahn, State University of New York at Stony Brook  
 A. J. Kalnay, IVIC, Caracas, Venezuela  
 M. Karls, U. Wisconsin, Milwaukee  
 K. Katori, U. Tsukuba, Ibaraki, Japan  
 M. Kawai, Kyushu U., Fukuoka, Japan  
 B. D. Keister, Carnegie-Mellon U.  
 H. P. Kelly, U. Virginia  
 J. C. Kelly, U. New South Wales, Kensington, Australia  
 T. J. Kennett, McMaster U., Hamilton, Ontario, Canada  
 A. K. Kerman, Massachusetts Inst. Technology  
 S. Ketudat, Chulalongkorn U., Bangkok, Thailand  
 E. Klemt, U. Heidelberg, Germany  
 W. Kleppinger, Rutgers U.  
 H.-J. Körner, Tech. U. Munchen, Germany  
 W. Koenig, GSI, Darmstadt, Germany  
 J. J. Kolata, U. Notre Dame  
 N. Koller, Rutgers U.  
 S. E. Koonin, California Inst. Technology  
 W. Kühn, U. Giessen, Germany  
 H. G. Kümmel, Ruhr U., Bochum, Germany



K. Kubodera, Sophia U., Tokyo, Japan  
 H. Kudo, U. Tsukuba, Ibaraki, Japan  
 D. Kusno, U. Indonesia, Jakarta, Indonesia  
 R. O. Lane, Ohio U.  
 J. Last, U. Heidelberg, Germany  
 R. M. Laszewski, U. Illinois  
 A. H. Laufer, Office of Basic Energy Sciences, USDOE  
 K. V. Laurikainen, Siltavuorenpenger 20, Helsinki, Finland  
 S. M. Lee, U. Tsukuba, Ibaraki, Japan  
 L. L. Lee, Jr., State U. of New York, Stony Brook  
 K. T. Lesko, Lawrence Berkeley Lab.  
 S. Levenson, Bell Communications Research, Red Bank, NJ  
 J. S. Lilley, Daresbury Lab., Warrington, England  
 Z. Liu, U. Arizona  
 A. E. Livingston, U. Notre Dame  
 L. F. Long, U. Notre Dame  
 H. O. Lutz, U. Bielefeld, Germany  
 J. Maa, National Tsing-Hua U., Hsinchu, Taiwan, China  
 J. H. Macek, U. Nebraska  
 M. H. Macfarlane, Indiana U.  
 R. Madey, Kent State U.  
 M. R. Maier, Michigan State U.  
 M. Mando, Physics Inst. U. Largo Enrich Fermi, Firenze, Italy  
 A. Mann, Technion, Haifa, Israel  
 D. Maor, Technion, Haifa, Israel  
 R. Marianelli, Office of Basic Energy Sciences, USDOE  
 A. Marinov, The Hebrew U. Jerusalem, Israel  
 N. Marquardt, Ruhr U., Bochum, Germany  
 J. V. Martinez, Office Basic Energy Sciences, USDOE  
 C. Mayer-Böricke, Kernforschungsanlage Juelich, Germany  
 T. Mayer-Kuckuk, U. Bonn, Germany  
 L. McGraner, Ohio State U.  
 R. D. McKeown, California Inst. Technology  
 W. R. McMurray, Southern U. Nuclear Inst., Faure, South Africa  
 G. K. Mehta, Indian Inst. Technology, Kanpur, India  
 E. Merzbacher, U. North Carolina  
 W. E. Meyerhof, Stanford U.  
 A. Michaudon, CEA, Centre d'Etudes de Bruyeres le Chatel, Montrouge, France  
 D. W. Mingay, Atomic Energy Board, Pretoria, South Africa  
 M. Minster, Tel-Aviv U., Israel  
 C. F. Moore, U. Texas, Austin  
 F. P. Mooring, Glen Ellyn, IL  
 G. C. Morrison, U. Birmingham, England  
 U. B. Mosel, U. Giessen, Germany  
 B. R. Mottelson, Inst. Theoretical Physics, Copenhagen, Denmark  
 A. Müller-Arnke, Inst. für Kernphysik der Tech. Hochschule, Darmstadt, Germany  
 C. Müller-Roth, U. Munich, Germany  
 K. Nakai, National Lab. for High Energy Physics, Ibaraki-ken, Japan  
 H. Narumi, U. Hiroshima, Japan  
 N. Nath, Kurukshetra U., India  
 Q. O. Navarro, Phillippine Atomic Energy Comm., Zuezon City, Philippines  
 J. Negele, Massachusetts Inst. Technology  
 G. C. Neilson, U. Alberta, Edmonton, Canada  
 J. O. Newton, Australian National U., Canberra, Australia

U. Nielson, U. Aarhus, Denmark  
H. Nifenecker, Centre d'Etudes Nucleaires, Grenoble, France  
J. A. Nolen, Jr., Michigan State U.  
R. Novotny, U. Giessen, Germany  
H. Ohnuma, Tokyo Inst. Tech., Japan  
T. R. Ophel, Australian National Lab., Canberra, Australia  
O. Osberghaus, U. Freiburg, Germany  
A. Osman, Cairo U., Egypt  
V. R. Pandharipande, U. Illinois  
S. P. Pandya, Physical Research Lab., Navrangpura, Ahmedabad, India  
W. K. H. Panofsky, Stanford U.  
M. Paul, Hebrew U. Jerusalem, Israel  
J. Pochodzalla, Michigan State U.  
J.-C. Poizat, U. Claude Bernard, Villeurbanne, France  
A. Poletti, U. Auckland, New Zealand  
R. E. Pollock, Indiana U.  
J. A. Pople, Carnegie-Mellon U.  
W. Potzel, Tech. U. Munich, Germany  
O. Poulsen, U. Aarhus, Denmark  
R. S. Preston, Northern Illinois U.  
F. W. Prosser, Jr., U. Kansas  
N. G. Puttaswamy, Bangalore U., India  
S. Raboy, Harpur College, State U. of New York, Binghamton  
D. Radford, Chalk River Nuclear Lab., Ontario, Canada  
J. Rafelski, U. Capetown, Rondebosch, Cape, South Africa  
J. L. Rainwater, Columbia U.  
I. Ramarao, Tata Inst. Fundamental Research, Bombay, India  
D. Reitmann, Faure, South Africa  
J. M. Remillieux, U. Claude Bernard, Villeurbanne, France  
M. Rhoades-Brown, State U. of New York, Stony Brook  
P. Richard, Kansas State U.  
A. Richter, Inst. fur Kernphysik, Tech. Hochschule, Darmstadt, Germany  
R. Ritchie, Oak Ridge National Lab.  
R. G. H. Robertson, Los Alamos National Lab.  
B. Rosner, Technion, Haifa, Israel  
G. Rosner, Tech. U. Munchen, Garching, Germany  
B. Ruscic, Rugjer Boskovic Inst., Zagreb, Yugoslavia  
N. Ryde, Chalmers U. Technology, Gothenburg, Sweden  
O. Sala, Instituto de Fisica da USP, Sao Paulo, Brazil  
N. P. Samios, Brookhaven National Lab.  
A. Saplakoglu, Ankara Nucl. Rsch. & Training Center, Besevler/Ankara, Turkey  
R. P. Scharenberg, Purdue U.  
R. M. Schectman, U. Toledo  
D. Schneider, Hahn-Meitner Inst., Berlin, Germany  
O. W. B. Schult, KFA Julich, Germany  
A. Schwarzschild, Brookhaven National Lab.  
R. E. Segel, Northwestern U.  
P. Seidl, Lawrence Berkeley Lab.  
J. P. F. Sellschop, U. of the Witwatersrand, Johannesburg, South Africa  
K. K. Seth, Northwestern U.  
S. M. Shafroth, U. North Carolina  
C.-M. Shen, National Tsing Hua U., Taiwan, China  
A. P. Shukla, Indian Inst. Technology, Kanpur, India  
R. Shyan, GSI, Darmstadt, Germany

R. H. Siemssen, KVI, U. Groningen, The Netherlands  
 C. Signorini, Inst. di Fisica, Via Marzola, Padova, Italy  
 C. P. Slichter, U. Illinois  
 P. C. Sood, Banaras Hindu U., Varanasi, India  
 P. Sperr, Hochschule d. Bundeswehr Munchen, Neubiberg, Germany  
 J. Speth, Inst. fur Kernphysik, Julich, Germany  
 H. E. Stanton, Oak Lawn, IL  
 N. Stein, Los Alamos National Lab.  
 G. S. F. Stephans, Massachusetts Inst. Technology  
 E. J. Stephenson, Indiana U.  
 M. F. Steuer, U. Georgia  
 J. Stoltzfus, Beloit College  
 U. Strohmusch, I. Institut Exp. Physik, Zyklotron, Hamburg, Germany  
 H. Stroher, U. Giessen, Germany  
 T. Takemasa, Saga U., Japan  
 S. Takeuchi, JAERI, Ibaraki-ken, Japan  
 J. A. Tanis, Western Michigan U.  
 L. J. Tassie, Australian National U., Canberra, Australia  
 G. E. Thomas, El Paso, IL  
 W. J. Thompson, Office of High Energy and Nuclear Physics, USDOE  
 E. W. Titterton, Australian National U., Canberra, Australia  
 C. C. Trail, Brooklyn College  
 P. B. Treacy, Australian National U., Canberra, Australia  
 P.-K. Tseng, National Taiwan U., China  
 A. F. Tulinov, Moscow State U., USSR  
 E. Ungricht, Spectrospin AG, Fallandek, Switzerland  
 R. Vandenbosch, U. Washington  
 G. van Middelkoop, Vrije U., Amsterdam, The Netherlands  
 H. Verheul, Natuurkundig Lab., Amsterdam, The Netherlands  
 A. Vermeer, U. Utrecht, The Netherlands  
 J. Vervier, Universite Catholique de Louvain, Louvain-la-Neuve, Belgium  
 S. E. Vigdor, Indiana U.  
 E. Vogt, TRIUMF, Vancouver, BC, Canada  
 D. von Ehrenstein, U. Bremen, Germany  
 S. Wagner, Physikalisch-Technische Bundesanstalt, Germany  
 J. D. Walecka, CEBAF  
 T. P. Wangler, Los Alamos National Lab.  
 R. L. Watson, Texas A&M U.  
 A. Weinreb, Hebrew U., Jerusalem, Israel  
 V. Weisskopf, Massachusetts Inst. Technology  
 W. R. Wharton, Carnegie Mellon U.  
 M. G. White, Princeton U.  
 E. P. Wigner, Princeton U.  
 J. F. Williams, Queens U., North Ireland, Great Britain  
 C. S. Wu, Columbia U.  
 J. J. Wynne, IBM, Yorktown Heights, NY  
 D. Youngblood, Texas A&M U.  
 D. Zajfman, Technion-Inst. Technology, Haifa, Israel  
 W. Zipper, Silesian U., Katowice, Poland  
 W. Zych, Warsaw Tech. U., Poland

Library, U. Wien, Zentralbibliothek der Physikalischen Inst., Wien,  
AUSTRIA

Inst. voor Theo. Fysica, Katholieke Universiteit Leuven, Heverlee, BELGIUM

Library, Central Bureau of Nuclear Measurements, EURATOM, Geel, BELGIUM

Nuclear Physics Library, U. Sao Paulo, Dept. de Fisica Nuclear, Sao Paulo,  
S.P., BRAZIL

Library, U. Federal de Pernambuco, Departamento de Fisica, Recife, PE, BRAZIL

Divisao de Estudos Avancados, CTA/IAE, Sao Jose dos Campos, BRAZIL

Institut Central de Fisica, U. Brasilia, Brasilia, D.F., BRAZIL

Tech. Info. Services, Ford Aerospace and Comm. Corp., Newport Beach,  
CALIFORNIA

Dept. of Physics, California State U., Los Angeles, CALIFORNIA

Preprint Library, McGill University, Montreal, Quebec, CANADA

Physics Department, U. Alberta, Nuclear Research Centre, Edmonton, Alberta,  
CANADA

Facultad de Ciencias, U. Chile, Departamento de Fisica, Santiago, CHILE

Physics Department, U. Denver, Denver, COLORADO

Library, U. COLORADO Nuclear Physics Laboratory, Boulder, COLORADO

Physics Library, Catholic U. of America, Keane Physics Research Center,  
Washington, DC

The Library, Niels Bohr Institute, Copenhagen, DENMARK

Librarian, U.K.A.E.A., Culham Lab., Abingdon, Oxon, ENGLAND

Dept. of Physics, Schuster Lab., The University, Manchester, ENGLAND

Library, U. Sussex, Brighton, ENGLAND

Departmental Library, U. College London, Dept. of Physics & Astronomy, London  
WCI, ENGLAND

Info. Officer, Sci. Rsch. Council, Daresbury Laboratory, Daresbury,  
Warrington, ENGLAND

Library, Laboratoire Souterrain de Modane, Modane, FRANCE

Secretariat Anneaux de Collisions, Laboratoire de l'Acc. Lin., de l'Universite  
de Paris-Sud, Orsay, FRANCE

Bibliotheque, Institut de Phys. Nucl., Div. de Phys. Theor., Orsay Cedex,  
FRANCE

Librarian, Institut des Sciences Nucleaires, IN 2 P 3, Grenoble Cedex, FRANCE

Lab. de Physique, C.N.R.S., Nucl. et de Phys. des Accelerateurs, Strasbourg,  
Cedex, FRANCE

Preprint Library, C.R.N., Laboratoire P.N.T., Strasbourg Cedex, FRANCE

Bibliotheque D.Ph.T., CEA Saclay, Orme des Merisiers, Gif-sur-Yvette, FRANCE

Preprint Library, CNRS-Luminy-Case, Centre de Phys. Theorique, Marseille  
Cedex, FRANCE

Library, Physik-Department, Technischen Universitat Munchen, Garching, GERMANY

Librarian, U. Munich, Sektion Physik, Garching, GERMANY

Library, U. Munich, Sektion Physik, Garching, GERMANY

Bibliothek, Gesellschaft fur Schwerionenforschung mbH, Darmstadt, GERMANY

Librarian, Deutsches Elektronen-Synchrotron, Bibliothek, Hamburg,  
Notkestieg 1, GERMANY

Library, Bibliotheek V. UY. Natuurkunde, Amsterdam-Zuid, HOLLAND

Physics Library, IIT Research Institute, Chicago, ILLINOIS

Physics Department, U. ILLINOIS at Chicago Circle, Chicago, ILLINOIS

North Branch, Chemist's Laboratories, Downers Grove, ILLINOIS

Post Graduate Dept. of Physics, U. Kashmir, Amarsingh Bagh, Hazratbal,  
Srinagar, INDIA

Librarian, Bhabha Atomic Research Centre, Bidhan Nagar, Calcutta, INDIA

Cyclotron Project, Indiana U., Bloomington, INDIANA

Preprint Library, U. Indonesia, Physics Dept., Jakarta, INDONESIA  
 Dept. of Physics, U. Mosul, Mosul, IRAQ  
 Physics Library, Weizmann Institute of Science, Rehovot, ISRAEL  
 Physics Preprint Library, U. Negev, Beer-Sheva, ISRAEL  
 Theoretical Physics Department, Hebrew University, Jerusalem, ISRAEL  
 Istituto di Fisica, dell Universita Catania, ITALY  
 Inst. Naz. di Fisica Nucleaire, Sezione di Pisa, Pisa, ITALY  
 Segreteria Techica, Laboratorio delle Radiazioni, Istituto Superiore di  
 Sanita, Roma, ITALY  
 Preprint Library, Istituto di Fisica Sperimentale, Politecnico di Torino,  
 Torino, ITALY  
 Preprint Librarian, Istituto di Fisica, Torino, ITALY  
 Dept. of Nuclear Engineering, Tohoku U., Sendai, JAPAN  
 High Energy Physics Laboratory, U. Tokyo, Faculty of Science, Bunkyo,  
 Tokyo, JAPAN  
 Meson Science Laboratory, U. Tokyo, Faculty of Science, Hongo, Bunkyo-ku,  
 Tokyo, JAPAN  
 The Library, U. Tokyo, Institute for Nuclear Study, Midori-Cho, Tanashi,  
 Tokyo, JAPAN  
 Librarian, RIKEN, Cyclotron Laboratory, Wako-shi, Saitama, JAPAN  
 The Preprint Center, Nagoya U.. Dept. of Physics, Nagoya, JAPAN  
 Preprint Library, Korea U., Physics Department, Seoul, KOREA  
 Library, Korean Atomic Energy Res. Inst., Cheongryang, Seoul, KOREA  
 Librarian, Louisiana State U., Dept. of Physics & Astronomy, Baton Rouge,  
 LOUISIANA  
 Director, Louisiana State U., Nuclear Science Center, Baton Rouge, LOUISIANA  
 Phys. Reading Room, Massachusetts Inst. Technology, Cambridge, MASSACHUSETTS  
 Physica Department Library, Dentro de Inv. y de Est. Avanzados, Inst. Polit.  
 Nac., Mexico D.F. MEXICO  
 Preprint Library, Instituto de Fisica, Theoretical Physics Group, Mexico D.F.,  
 MEXICO  
 Librarian, Michigan State U., Cyclotron Lab., E. Lansing, MICHIGAN  
 The Library, U. Mississippi, Documents Department, University, MISSISSIPPI  
 Library, Koninklijke Nederlandse Akademie van Wetenschappen, Amsterdam,  
 NETHERLANDS  
 Library, Kloveniersburgwal 29, GC Amsterdam, NETHERLANDS  
 Serial Records Section, Dartmouth College Library, Hanover, NEW HAMPSHIRE  
 Phys. Preprint Library, Institute for Advanced Study, Princeton, NEW JERSEY  
 Physics/Optics/Astronomy Library, U. Rochester, Rochester, NEW YORK  
 Serials Department, Cornell U. Libraries, Ithaca, NEW YORK  
 Physics Department, Brooklyn College, Brooklyn, NEW YORK  
 Physics Library, U. Cincinnati, Cincinnati, OHIO  
 Library ANLPDQ, Chemical Abstracts Service, Columbus, OHIO  
 Library, Chemical Abstracts Service, Columbus, OHIO  
 Olive Kettering Library, Antioch College, Yellow Springs, OHIO  
 Library, Pakistan Institute of Nuclear Science and Technology, Rawalpindi,  
 PAKISTAN  
 Dept. of Physics, Quaid-e-Azam University, Islamabad, PAKISTAN  
 Preprint Library, Lab. de Fisica de Engenharia Nucleares, Servico de Fisica,  
 Sacavem, PORTUGAL  
 Library, U. din Timisoara, Biblioteca Centrala Universitari, R.S., ROMANIA  
 Preprint Library, High Energy Lab., Inst. Physics and Nuclear Engrg.,  
 Bucharest, ROMANIA  
 Library, Tandem Accelerator Lab., Uppsala, SWEDEN

D. U. Fen Fakültesi, Diyarbakir U., Fizik Bölümü, Diyarbakir, TURKEY  
Department of Physics, U. Central de Venezuela, Facultad de Ciencias, Caracas,  
VENEZUELA

Commander, U.S. Army Nuclear and Chemical Agency, Springfield, VIRGINIA  
Physics Library, U. Wisconsin-Madison, Madison, WISCONSIN  
Physics Department, Marquette University, Milwaukee, WISCONSIN